THE UNIVERSITY *of* EDINBURGH

Advanced ultrasound-assisted removal of organic pollutants in water: from piezocatalysis to sono-adsorption

Franziska Bößl

THE UNIVERSITY *of* EDINBURGH

Thesis submitted for the degree of

Doctor of Philosophy

The University of Edinburgh

2023

Declaration

I declare that the thesis has been composed by myself and that the work has not be submitted for any other degree or professional qualification. I confirm that the work submitted is my own and I am the first author of all publications that make up five chapters of this PhD thesis. My contribution and those of the other authors to this work have been explicitly indicated below. In all these publications, my contribution as defined by the Contributor Roles Taxonomy (CRediT) was conceptualisation, methodology, validation, formal analysis, investigation, data curation, writing – original draft and visualisation. With the exception of my supervisor, Ignacio Tudela, the contribution of all co-authors to these publications were resource provision, investigation (supporting), writing – review & editing (supporting). I confirm that appropriate credit has been given within this thesis where reference has been made to the work of others.

The work presented in Chapter 1 was previously published in *Current Opinion in Green and Sustainable Chemistry* as *Piezocatalysis: Can catalysts really dance?* by **F. Bößl** and **I. Tudela**. This study was conceived by all the authors. I carried out conceptualisation, methodology, investigation, writing - original draft and visualisation.

The work presented in Chapter 2 was previously published in *Chemical Engineering Journal Advances* as *Piezocatalytic degradation of pollutants in water: Importance of catalyst size, poling and excitation mode* by **F. Bößl**, T. P. Comyn, P. I. Cowin, F. R. García-García and **I. Tudela**. This study was primarily conceived by myself and my supervisor, with the support of all other co-authors. My CRediT contribution was conceptualisation, methodology, validation, formal analysis, investigation, data curation, writing – original draft and visualisation.

The work presented in Chapter 3 was previously published in *Chemical Engineering Journal Advances* as *Effect of frequency and power on the piezocatalytic and sonochemical degradation of dyes in water* by **F. Bößl**, V. C. Menzel, E. Chatzisymeon, T. P. Comyn, P.

Cowin, A. J. Cobley and **I. Tudela**. This study was primarily conceived by myself and my supervisor, with the support of all other co-authors. My CRediT contribution was conceptualisation, methodology, validation, formal analysis, investigation, data curation, writing – original draft and visualisation.

The work presented in Chapter 4 was previously published in *Electrochimica Acta* as *Importance of energy band theory and screening charge effect in piezo-electrocatalytical processes* by **F. Bößl**, V. C. Menzel, K. Jeronimo, A. Arora, Y. Zhang, T. P. Comyn, P. Cowin, C. Kirk, N. Robertson and **I. Tudela**. This study was primarily conceived by myself and my supervisor, with the support of all other co-authors. My CRediT contribution was conceptualisation, methodology, validation, formal analysis, investigation, data curation, writing – original draft and visualisation.

The work presented in Chapter 5 was previously published in *Ultrasonic Sonochemistry* as *Synergistic sono-adsorption and adsorption-enhanced sonochemical degradation of dyes in water by additive manufactured PVDF-based materials* by **F. Bößl**, S. Brandani, V. C. Menzel, M. Rhodes, M. S. Tovar-Oliva, C. Kirk and **I. Tudela**. This study was primarily conceived by myself, my supervisor and Professor Brandani, with the support of all other co-authors. My CRediT contribution was conceptualisation, methodology, validation, formal analysis, investigation, data curation, writing – original draft and visualisation.

Franziska Bößl
29th November 2023

Abstract

Piezocatalysis is a novel concept in the field of catalysis that aims to develop environmentally friendly catalytic processes independent of energy sources such as light and electricity by utilising prevalent mechanical vibrations like wind and tides. The present work aimed to fully understand the fundamentals of piezocatalysis by investigating the suggested mechanisms and rigorously implementing thorough control experiments to separate 'true' piezocatalytic activity from other phenomena that may also occur at the same time when using ultrasound.

The first part of this work used theoretical and experimental approaches to investigate the concept of piezocatalysis. Potassium bismuth titanate-bismuth ferrite lead titanate (BF-KBT-PT) ceramics were used as catalysts to understand the effect of piezocatalyst size, poling/unpoling, and excitation mode on the degradation of Rhodamine B (RhB) in water. The results showed that whilst poling had a significant effect on the degradation of RhB, piezocatalysis is a more complex combination of different phenomena simultaneously contributing to the overall degradation of RhB.

The second part of this work investigated the effect of ultrasonic frequency and power on the piezocatalytic degradation of RhB. Different experimental set-ups with operating frequencies ranging of 20 kHz to 1 MHz and adjustable powers were used. The results revealed that, at lower ultrasonic frequencies (<100 kHz) and moderate acoustic powers, mechanical effects from acoustic cavitation had a positive effect on the piezocatalytical generation of radicals, enhancing the overall degradation of Rhodamine B. However, the sonochemical formation of radicals remained a significant contributor to the overall degradation. At higher frequencies (>100 kHz), though, the chemical effects from acoustic cavitation became so dominant that no piezocatalytical contribution to the degradation of RhB was noticed, leading to the question of whether piezocatalysts are necessary when optimising sonication parameters such as frequency and power can achieve fast degradation kinetic constant rates of 0.037 min^{-1}.

To further understand how piezocatalysis works, the third part of this study investigated the importance of the energy band theory mechanism by using three different piezocatalysts with varying energy band gaps and piezoelectric properties. Besides BF-KBT-PT, other materials such as zinc oxide and barium titanate were used to degrade RhB under the excitation of combined ultrasound and mechanical agitation. The results indicated that both energy band theory and screening charge effects may play important roles in the piezocatalytic contribution to the overall degradation process, as the piezocatalyst most likely to generate radicals via both mechanisms (poled $BaTiO_3$) achieved the best overall dye degradation.

Based on previous results, the final part of this study investigated the potential of PVDF-composite materials for a more environmentally friendly removal of pollutants from water. A bulky and easy-to-recover piezocatalyst was developed using additive manufacturing. The results showed that PVDF-$BaTiO_3$ piezocatalysts behaved significantly different compared to $BaTiO_3$, indicating another ultrasound assisted phenomenon taking place. Additional experiments with non-piezoelectric PVDF revealed a possible contribution of sono-adsorption to the overall removal of RhB. In this context, a phenomenological model was developed, which for the first time accounted for the physico-chemical phenomena present during ultrasound-assisted adsorption. This study therefore provides insight on the occurrence of another concurrent phenomenon in piezocatalysis, in addition to demonstrating a new approach for additively manufacturing simple-to-recover PVDF-based catalysts.

In conclusion, this work provided evidence that piezocatalysis may indeed exist, but also that it is a far more complex process than what has initially been assumed in the literature. The importance of conducting thorough control experiments has been emphasized to better understand the role of other ultrasound-assisted phenomena simultaneously occurring during sonication for piezocatalysis.

Lay Summary

Piezocatalysis is a promising area of research that could pave the way for innovative environmental catalytic processes aiming to be independent of common energy sources such as light or electricity. In the first part of this study, a theoretical and experimental approach was used to investigate the effects of different factors on the piezocatalytic degradation of a dye, rhodamine B (RhB). Whilst the theoretical and experimental results revealed an apparently contradicting effect of piezocatalyst size, poling clearly showed a significant impact on the degradation of the dye.

In the second part, different experimental set-ups with operating frequencies ranging from 20 kHz to 1 MHz were used to investigate the effect of ultrasonic frequency and power on the piezocatalytic process. The results showed that mechanical effects caused by acoustic cavitation, which are more common at lower ultrasonic frequencies (<100 kHz), considerably enhanced the piezocatalytic degradation of RhB. However, at higher ultrasonic frequencies (>100 kHz) chemical effects derived from the acoustic field are more dominant leading to a remarkable sonochemical degradation of RhB. This raised the question of whether a piezocatalyst was actually necessary since optimising sonication parameters such as frequency and power may be sufficient enough to fully degrade organic pollutants such as dyes.

The third part of this study, used three different piezoelectric materials as catalysts to investigate the ‘true’ mechanism behind piezocatalysis. The results showed that both mechanisms suggested in the literature may be important for the overall piezocatalytic process, as the catalyst that could potentially degrade RhB via both mechanisms showed the best overall degradation of RhB.

In the last part of this work, a PVDF-based, bulky and easy to recover catalyst was developed using additive manufacturing. The results revealed another ultrasound related phenomenon contributing to the overall removal RhB when using PVDF-based catalysts. Additional

experiments with non-piezoelectric PVDF revealed the great potential of additive manufactured PVDF for complete dye removal within a few minutes.

This work highlighted the complexity of the novel piezocatalytic process and emphasised the importance of other phenomena beyond piezoelectric polarisation for piezocatalytic research.

Acknowledgements

First and foremost, I would like to express my sincere gratitude and appreciation to my only supervisor, Nacho, for his unwavering support, especially during the challenging times our research group encountered. His guidance and encouragement have been invaluable, providing me with the strength and resilience to overcome obstacles and stay focused on our goals. I am truly grateful for his continuous support, both academically and personally. Thank you for your unwavering commitment and guidance during challenging times.

I am also deeply thankful to all collaborators whose valuable insights and assistance have enriched the outcomes of this PhD project. Their willingness to share their knowledge and engage in constructive discussions have been invaluable in enhancing the quality of this research project. A special thanks goes to Tim Comyn and Peter Cowin for providing BF-KBT-PT and their broad experience and help with piezoelectricity related queries. I would like to extend my sincere thanks to Professor Neil Robertson, Dr Caroline Kirk, Ayushi Arora, Yishu Zhang and Mathilda Rhodes from the School of Chemistry for their fruitful discussions and support with material characterisation. I also want to express my deepest gratitude to Professor Stefano Brandani for his invaluable contributions to our unforeseen findings on adsorption-related phenomena.

Last but not least, my sincere thank goes to my group members Valentin and Mayra, with whom I have shared both rewarding and challenging moments. I would like to express my appreciation for their strength and resilience they have demonstrated, as our entire group navigated through difficult circumstances together. Throughout our research journey we expected the university not only to be a supportive and respectful but also a safe place, as outlined in its policies. We believed that the values of dignity and respect would be upheld creating a positive atmosphere where everyone feels valued and treated with fairness. Unfortunately, we had to face incidents, often hidden beneath the surface, causing emotional

distress and affecting our ability to work in a supportive and nurturing environment. It is disheartening to reflect on these challenges, as they highlight the need for greater awareness. There have been times when communication and accountability of those in charge fell short when it came to addressing reported concerns. Despite encountering these unfortunate challenges, we managed to persevere and maintain our focus on our research. While these experiences were undoubtedly difficult, they have also provided us opportunities for personal growth and a deeper understanding of the importance of a supportive, respectful and safe work environment.

Dissemination

Publications directly related to this PhD thesis

Journal articles

1. **Franziska Bößl**, Ignacio Tudela*, Piezocatalysis: Can catalysts really dance?, Current Opinion in Green and Sustainable Chemistry, Volume 32, 2021, 100537, https://doi.org/10.1016/j.cogsc.2021.100537.
2. **Franziska Bößl***, Tim P. Comyn, Peter I. Cowin, Francisco R. García-García, Ignacio Tudela*, Piezocatalytic degradation of pollutants in water: Importance of catalyst size, poling and excitation mode, Chemical Engineering Journal Advances, Volume 7, 2021, 100133, https://doi.org/10.1016/j.ceja.2021.100133.
3. **Franziska Bößl***, Valentin C. Menzel, Efthalia Chatzisymeon, Tim P. Comyn, Peter Cowin, Andrew J. Cobley, Ignacio Tudela*, Effect of frequency and power on the piezocatalytic and sonochemical degradation of dyes in water, Chemical Engineering Journal Advances, Volume 14, 2023, 100477, https://doi.org/10.1016/j.ceja.2023.100477.
4. **Franziska Bößl***, Valentin C. Menzel, Karina Jeronimo, Ayushi Arora, Yishu Zhang, Tim P. Comyn, Peter Cowin, Caroline Kirk, Neil Robertson, Ignacio Tudela*, Importance of energy band theory and screening charge effect in piezo-electrocatalytical processes, Electrochimica Acta, Volume 462, 2023, 142730, https://doi.org/10.1016/j.electacta.2023.142730.
5. **Franziska Bößl***, Stefano Brandani, Valentin C. Menzel, Matilda Rhodes, Mayra S. Tovar-Oliva, Caroline Kirk, Ignacio Tudela*, Synergistic sono-adsorption and adsorption-enhanced sonochemical degradation of dyes in water by additive manufactured PVDF-based materials, Ultrasonics Sonochemistry, Volume 100, 2023, 106602, https://doi.org/10.1016/j.ultsonch.2023.106602.

*denotes corresponding author

Conference presentations

1. **Franziska Bößl**, Ignacio Tudela, Piezo-electrocatalysis – magic or science?, Electrochemistry Northwest 2020 (online), Manchester (UK), 1st July, 2020.

   Award: Selected as one of the best oral presentations to participate in RSC Electrochem 2021.

2. **Franziska Bößl**, Ignacio Tudela, Piezo-electrocatalysis – is that a thing?, RSC Butler Meeting (online), Newcastle (UK), 1st September, 2020.

   Award: Best oral presentation in general electrochemistry

3. **Franziska Bößl**, Ignacio Tudela, Piezocatalytic degradation of RhB: importance of catalyst size, poling and excitation mode, UoE School of Engineering PGR Conference (online), Edinburgh (UK), 16th April, 2021.

4. **Franziska Bößl**, Ignacio Tudela, Piezo-electrocatalytic mechanisms from an electrochemical point of view, SCI Electrochemistry Postgraduate Conference (online), Manchester (UK), 10th-11th June, 2021.

5. **Franziska Bößl**, Ignacio Tudela Piezo-electrocatalysis: how does it work?, RSC Electrochem 2021 (online), UK, 2021.

6. **Franziska Bößl**, Ignacio Tudela, Piezo-electrocatalytic Degradation of Rhodamine B in Water: Experimental and Theoretical Prospects, 240th ECS Meeting (online), Orlando (Florida, USA), 10th-14th, 2021.

7. **Franziska Bößl**, Valentin C. Menzel, Mayra S. Tovar-Oliva, Efthalia Chatzisymeon, Ignacio Tudela, The effect of acoustic power at low frequency ultrasound on the piezo-electrocatalytic and sonochemical degradation of pollutants in water, RSC Electrochem 2022, Edinburgh (UK), 4th-6th September, 2022.

Other publications during PhD

Journal articles

1. Valentin C. Menzel*, Xuerui Yi, **Franziska Bößl**, Caroline Kirk, Neil Robertson, Ignacio Tudela*, Additive manufacturing of polyaniline electrodes for electrochemical applications, Additive Manufacturing, Volume 54, 2022, 102710, https://doi.org/10.1016/j.addma.2022.102710.

*denotes corresponding author

Conference presentations

1. Mayra S. Tovar-Oliva, **Franziska Bößl**, Valentin C. Menzel, Ignacio Tudela. Electrodeposition of Cu-based catalysts for CO_2 conversion, SCI Electrochemistry Postgraduate Conference, Loughborough (UK), 25th May, 2022.
2. Valentin C. Menzel , Xuerui Yi, **Franziska Bößl** , Caroline Kirk, Neil Robertson, Ignacio Tudela, 3D Printing Highly Conductive Polyaniline Based Electrodes for Electrochemical Applications, RSC Electrochem 2022, Edinburgh (UK), 4th-6th September, 2022.
3. Mayra S. Tovar-Oliva, Valentin C. Menzel, Luis Navarro-Tovar, **Franziska Bößl**, Ignacio Tudela, Electrodeposition of uniformly distributed Cu-based catalysts of gas diffusion electrodes for the electrochemical conversion of CO_2, RSC Electrochem 2022, Edinburgh (UK), 4th-6th September, 2022.

Table of Contents

Table of Contents XII

List of Abbreviations XIV

1 Introduction and Literature review 1

1.1 Background 1

1.2 Conventional methods for waste water treatment 2

1.3 Piezocatalytic treatment of waste water 9

1.4 Literature review highlights and conclusions 10

1.5 Problem statement and motivation 12

1.6 Objectives of the research project 12

1.7 References 14

2 Importance of catalyst size, poling and excitation mode 32

2.1 Introduction 32

2.2 Discussion highlights and conclusions 33

2.3 References 35

3 Effect of frequency and power on the piezocatalytic and sonochemical process 51

3.1 Introduction 51

3.2 Discussion highlights and conclusions 52

3.3 References 54

4 Importance of energy band theory and screening charge effect 70

4.1 Introduction 71

4.2 Discussion highlights and conclusions 71

4.3 References 73

5 Additive manufactured PVDF-based materials for piezocatalytic and sono-adsorption removal of pollutants 87

5.1 Introduction 87

5.2 Discussion highlights and conclusions 88

5.3 References 90

6 Overall conclusions and future work 107

6.1 Overall conclusions 107

6.2 Future work 109

6.3 References 111

Appendix 113

Chapter 2 Supplementary Material 114

List of Abbreviations

AA	Acetic acid
AM	Additive manufacturing
$BaTiO_3$	Barium titanate
BET	Brunauer-Emmett-Teller theory
BF-KBT-PT	Potassium bismuth titanate-bismuth fer- rite lead titanate
BQ	Benzoquinone
CB	Conduction band
CBM	Conduction band minimum
DE	Degradation efficiency
DFT	Density-functional theory
d_{ij}	Piezoelectric charge constants
EDS	Energy dispersive X-ray spectrometer
EDTA	Ethylenediaminetetraacetic acid
FEM	Finite element method
FIB-SEM	Focused ion beam-scanning electron microscopy
MA	Mechanical agitation
P	Poled
PVDF	Polyvinylidene fluoride
RhB	Rhodamine B
SHE	Standard hydrogen electrode
TA	Terephthalic acid
TEP	Triethyl phosphate
UP	Unpoled
US	Ultrasound
US+MA	Ultrasound and mechanical agitation
UV-Vis	Ultraviolet–visible spectroscopy
UV-Vis DRS	Ultraviolet–visible diffuse reflectance spectroscopy
VB	Valence band
VBM	Valence band maximum
XPS	X-ray photoelectron spectrometry
XRD	X-ray diffraction
XRPD	X-ray powder diffraction
ZnO	Zinc oxide

1 Introduction and Literature review

1.1 Background

Industrialisation has been a driving factor for the progress and development of human society. It has facilitated the growth of advanced technologies, health care and modern infrastructure that have undeniably improved the quality of living for billions of people around the world. However, all these advances have also led to substantial environmental issues including water, air and soil pollution caused by the accumulation of organic and inorganic toxic compounds [1-5]. These pollutants do not only endanger the delicate balance of the ecosystem but also pose a significant threat to human health [6-9]. Among these pollutants, the discharge of wastewater containing dyes has emerged as a pressing environmental concern due to the persistence, toxicity and colour of dyes [10-13].

Dye wastewater primarily originates from the textile, paper and dye industries due to their extensive use of synthetic dyes in production processes. The discharge of dyes into water bodies can disrupt the balance of the aquatic ecosystems by obstructing light penetration leading to detrimental effects on aquatic life such as decreased photosynthesis and the potential for eutrophication [14]. Furthermore, dyes are known to pose a substantial risk to both human and animal well-being due to being toxic, mutagenic and carcinogenic. The ecological consequences of these hazards highlight the critical need to address the issue of dye discharge and develop sustainable wastewater treatment methods.

To address the issues of water pollution various wastewater treatment techniques have been developed. Among these are conventional methods such as biodegradation [15] and physical adsorption[16] as well as other established processes using electrochemical treatment [17] or membrane separation [18]. Although all of these techniques have demonstrated their potential in wastewater treatment, they also have limitations, such as low efficiency, high cost or reliance on external energy sources such as light or electricity. Therefore, it is crucial to further develop

these techniques but also to explore new concepts for wastewater treatment that are not only environmentally friendly and economically feasible but also highly effective in addressing environmental concerns.

1.2 Conventional methods for waste water treatment

When dealing with dye-contaminated wastewater conventional treatment methods typically revolve around three key objectives: decomposition, degradation and mineralisation the organic pollutant [19-22]. In general, these processes involve breaking down organic dyes into less harmful or non-toxic compounds, ideally into inorganic substances like carbon dioxide and water.

Dye decomposition is often referred to the initial stage in the treatment of wastewater. It involves breaking down the complex organic dye molecules into simpler organic compounds through oxidation, reduction, hydrolysis or photolysis. Dye decomposition aims to reduce the colour and toxicity of the wastewater but can sometimes also lead to intermediate products that are more toxic than the parent dye [20, 22].

Dye degradation is a more advanced treatment stage that aims to reduce the dye and its intermediate products to simpler, less harmful substances. This process typically relies on the use of advanced oxidation processes to break down the dye molecules further [20, 22].

Dye mineralisation represents the most advanced stage in wastewater treatment where the dye molecules are converted into simple, inorganic compounds like carbon dioxide, water and inorganic ions [19, 21]. Achieving complete mineralisation is particularly challenging due to the complex structures of many dyes. However, the complete mineralisation can lead to carbon dioxide, which on the one hand is a less toxic compound than most dye compounds but on the other hand well-known to contribute to greenhouse gas emissions. Hence, it becomes imperative to explore additional process steps when carbon dioxide is generated during

wastewater treatment. The implementation of carbon capture and utilisation technologies should be considered as a means to efficiently manage and mitigate carbon dioxide emissions within the wastewater treatment process. This becomes particularly important when considering the application of a wastewater technology on an industrial level.

1.2.1 Adsorption

Adsorption processes are widely used for dye wastewater treatment and involve the attachment of dye molecules onto the surface of a solid material, known as an adsorbent. Adsorption is extensively utilised for the treatment of dye wastewater owing to its remarkable efficacy in the removal of both colour and pollutants from industrial effluents. This is addressing the needs of from industries such as textiles, leather, and paper [23-25]. Over the years, various materials have been tested and used as adsorbents, including activated carbon, zeolites, clay minerals, and certain polymers. The choice of adsorbent depends on factors such as the type of dye, cost, and availability [23-25].

Adsorption processes can be categorised based on whether the interactions between dye molecules and the adsorbent surface are of a physical or chemical nature. Depending on the type of adsorption common mechanisms include electrostatic attractions, van der Waals forces and chemical bonding.

Extensive research has been conducted on adsorption processes across various reactor designs such as batch and continuous reactors [23-25]. In batch processes the contaminated water interacts with the adsorbent and after reaching equilibrium the treated water and adsorbent materials undergo separation. In continuous processes a steady flow of wastewater passes through a fixed bed of adsorbent enabling uninterrupted and ongoing treatment. The efficiency of adsorption is influenced by several factors such as contact time, temperature or pH as well as initial dye concentration [23].

Variations in contact time can both positively and negatively impact the adsorptive removal of dyes. Once equilibrium is reached between the active sites of the adsorbent and the dye molecules further contact time does not influence adsorption. Positive effects on adsorption occur with increased contact time until equilibrium is achieved. However, extended reaction times can adversely affect the economic efficiency of treatment processes by increasing energy requirements [23, 26-28].

Temperature significantly impacts dye adsorption and serves as a key indicator of whether the adsorption process is endothermic or exothermic. In exothermic processes, the adsorption capacity decreases with rising temperature while in endothermic processes it increases with temperature elevation. The treatment temperature also plays a significant factor in influencing the economic cost of the adsorptive removal of dyes from wastewater [23, 29].

The solution pH is also crucial in the adsorption of dye from contaminated water. It was reported that changes in pH can influence reactions between dye molecules and adsorbents attributed to alterations in the ionisation level and surface charge of the adsorbent. In general, a low pH favours the adsorption of anionic dyes whilst a high pH favours the adsorption of cationic dyes [23, 25, 30, 31].

The initial dye concentration significantly influences adsorption phenomena. While an increase in initial dye concentration has positive effects up to a certain point, as the increased tendency of adsorption for high levels of dye contaminants is directly linked to the available active sites on the adsorbent's surface [23, 25, 32]. The enhanced adsorption capacity is initially boosted by unsaturated active sites but as the adsorbent surface becomes saturated there is a substantial reduction in dye adsorption.

In conclusion, while adsorption processes offer a promising solution for dye wastewater treatment several challenges remain. As highlighted process parameters such as pH, initial dye concentration, temperature and contact time play crucial roles in the efficacy of adsorption and therefore necessitating thorough consideration and optimisation. This is inevitable for real-world applications, particularly in mixed pollutant systems, that require further exploration to

meet wastewater treatment requirements, as the limited selectivity of adsorbents pose a significant challenge potential competition of the targeted dyes with other ions in wastewater [23-25]. Another major challenge lies in the development of cost-effective and efficient regeneration methods that are viable for long-term operation [23-25]. In this regard, the stability of adsorbents also needs to be considered as another a key parameter determining their suitability for practical application. Additionally, cost analysis remains a critical concern due to limited information available. Establishing a comprehensive life cycle cost analysis, especially during the regeneration progress remains essential for a thorough understanding of the economic aspects of adsorptive dye removal. However, the main limitation of adsorption for dye wastewater is its exclusive removal of contaminants without degrading, decomposing or mineralising the pollutants. Consequently, additional processes are required to address this aspect.

1.2.2 Photocatalysis

Photocatalyis is a well-known concept that aims to harness the energy from light to drive chemical reactions. The prominence of photocatalysis trying to utilise light for chemical reactions, has increased significantly due to its ability to mineralise recalcitrant organics instead of merely transforming them into another phase [33-35]. The mineralisation of recalcitrant organic pollutants positions photocatalysis as a promising alternative to existing water treatment technologies such as adsorption. So far, photocatalysis has already shown promising results in removing various water contaminants including hazardous pesticides, drugs or dyes and with this showcasing the versatility of the photocatalytic process in waste water treatment [33-35]. However, to enhance the feasibility of photocatalysis as a commercial water treatment technology, several challenges must be addressed. These challenges range from catalyst development, reactor design to process optimisation and energy consumption [33].

To overcome these limitations and enhance the efficiency of photocatalysis researchers have undertaken extensive efforts in modifying traditional photocatalysts. One strategy involves the introduction of doping agents into the bulk photocatalyst and with this trying to alter the electron transfer and narrowing the band gap [33-35]. This modification also facilitated an improved absorption of visible light addressing one of the primary shortcomings of conventional photocatalysts. Furthermore, the fabrication of hybrid photocatalysts due to the incorporation of semiconductors has shown promise in preventing charge recombination [33-35]. This approach ensures that photo-generated electrons and holes flow in the desired directions optimising their participation in photocatalytic reactions.

The transition from laboratory-scale research to industrial applications comes with its own set of challenges. The design and configuration of photocatalytic reactors play a pivotal role in determining the overall performance of the photocatalytic process [33, 36, 37]. Over the years, the majority of tested photocatalytic reactors have remained at the lab scale due to various limitations encountered during the design phase. One significant obstacle is the low concentration of pollutants in real-world wastewater resulting in slow photodegradation rates. The prolonged reaction times required to completely decompose trace amounts of pollutants may hinder the practical feasibility of large-scale implementation [33, 36].

Besides this, the configuration of the reactor itself is a critical consideration with distinctions between suspended and fixed bed catalysts influencing the overall performance of the photocatalytic system [36, 38-40]. Depending on the reactor both natural sunlight and artificial light sources for the activation of photocatalysts can be used[36, 40]. While natural sunlight can be inconsistent and weather-dependent, artificial light is a more stable energy source. However, the use of artificial light comes with its own challenges such as higher energy consumption and the need for cooling systems to control elevated temperatures resulting from prolonged exposure to high-intensity light [36, 40, 41].

Based on the challenges discussed, it becomes evident that while photocatalysis holds immense promise, unlocking its full potential requires further research to be fully implemented

as a wastewater treatment technique at larger scale. It is therefore also worth exploring other wastewater treatment methods.

1.2.3 Electrochemical waste water treatment

In the field of wastewater treatment electrochemical methods have also gained much attention as a promising solution for tackling recalcitrant pollutants. Utilising electrical energy to initiate chemical reactions enables these methods to eliminate recalcitrant contaminants from water [42-44]. The growing attention towards electrochemical wastewater techniques stems from their potential to efficiently and selectively remove pollutants making them an interesting option for environmental remediation [42-44]. Over the years, extensive research efforts were made on various electrochemical techniques for wastewater treatment. Among these, electrocoagulation and electrochemical oxidation have emerged as the most investigated methods [42-44].

Electrocoagulation involves the in-situ generation of coagulants by dissolving aluminium or iron ions from respective electrodes [43, 45]. These electrochemical reactions occur at the anode, while hydrogen is generated at the cathode. The electrocoagulation process is usually carried out in either a mono-polar or bi-polar electrode arrangement. The generated aluminium or iron ions act as highly efficient coagulants for flocculating particulates. In particular, hydrolysed aluminium ions can from extensive networks of Al-O-Al-OH, allowing for the chemical adsorption of pollutants in the treated solution [43, 45]. The electrodes are commonly made of either in plate form using aluminium or iron or they can even be composed of packed scraps such as milling or steel turnings [43].

The advantages of electrocoagulation encompass a high efficiency in removing pollutants, relatively low initial costs due to the potential utilisation of scraps from milling or steel turnings, small treatment set-ups, as well as a complete automation of the treatment process. However, there are also some limitations of this wastewater treatment method due to high energy

consumptions which can significantly impact the operational costs as well as metal residues introduced into the water by the electrodes [42, 43].

Electrochemical oxidation for wastewater treatment is a process tries to utilise electric current to induce oxidation reactions leading to the removal of pollutants from wastewater. To achieve this, electrodes are immersed in the wastewater and an electric potential is applied to drive electrochemical reactions. The use of electrochemical oxidation for wastewater treatment dates back to the 19th century when the electrochemical decomposition of cyanide was first reported [46]. Since then, research has primarily focused on enhancing the efficiency of oxidising various pollutants on diverse electrodes, improving the electrocatalytic activity and stability of electrode materials as well as investigating factors influencing the process performance to elucidate the mechanisms and kinetics of pollutant degradation [42, 43]. While experimental investigations have predominantly focused on the impact of anodic electrode materials there was limited research on the influence of cathodic materials [42, 43].

The electrochemical oxidation process offers similar advantages for wastewater treatment as electrocoagulation such as a high efficiency in removing a variety of pollutants. However, challenges such as energy consumption, electrode maintenance or unwanted side reactions when implementing this technology.

In conclusion, electrochemical treatment of dye wastewater holds great promise based on their high degradation efficiency that make these methods attractive for industrial applications. However, challenges such as energy consumption or achieving high selectivity for dye molecules amidst the complex matrix of pollutants remain. Ensuring that electrochemical processes selectively target the dyes without causing unintended degradation of non-target compounds is an area of ongoing research. Similarly, the high energy requirements can impact the economic feasibility of large-scale applications. Research efforts are directed towards optimising the energy efficiency of electrochemical systems to make them more sustainable.

1.3 Piezocatalytic treatment of waste water

Over the last decade a new technology has demonstrated potential for wastewater treatment by degrading organic pollutants such as dyes, pharmaceuticals and pesticides. This new technology aims to take advantage of the piezoelectric effect. The piezoelectric effect is a well-known physical phenomenon in which some materials generate an electric charge in response to applied mechanical stress. This unique ability of piezoelectric materials to generate electric charge originates from their non-centrosymmetric crystalline structure, distinguishing them from other non-piezoelectric materials [47]. The piezoelectric effect has been widely used in applications such as sensors, actuators, and nanogenerators [48]. However, it was not until the discovery of the piezoelectrochemical effect by Hong et al. in 2010 that the piezoelectric effect was utilised in catalysis, leading to the emergence of piezocatalysis [49]. Utilising the piezoelectric effect provides piezocatalysis the unique advantage to harness mechanical vibrations to induce catalytic activity and with this reducing the dependency on factors such as light or electricity [50].

The current emphasis in piezocatalysis research has primarily revolved around the development of piezoelectric materials with catalytic properties [51-54]. In this regard, the subsequent literature review published in Current Opinion in Green and Sustainable Chemistry tried to identify some overlooked aspects in piezocatalytic research by delving into related research fields such as piezoelectricity, sonochemistry and electrochemistry. The review aimed to draw attention to important factors frequently omitted in piezocatalysis but could have the potential to considerably improve the piezocatalytic performance. Particular attention was paid to key factors such as the mechanical field, applied frequency or redox potentials and how they could influence the piezocatalytic process.

1.3.1 Literature review highlights and conclusions

Over the last decade, remarkable advancements have been made towards the development of piezocatalytic systems for wastewater treatment. Research efforts in this field have mainly concentrated around the development and fabrication of piezocatalytic materials for the degradation of organic pollutants, with a particular emphasis on dyes, or water splitting [53, 55-59]. The piezoelectric materials, commonly referred to as piezocatalysts, are typically suspended in aqueous solutions and activated by a mechanical field. This mechanical field is usually generated by commercial high-power ultrasonic systems that operate within the frequency range of 20-40 kHz [53, 60-62]. These high-power ultrasonic systems generate mechanical waves within the designated frequency range and with this ultimately stimulating the piezocatalysts. As a result, the mechanical energy from the ultrasonic waves is converted into the desired chemical reactions due to the piezoelectric polarisation of the piezocatalyst, making this method a promising approach for wastewater treatment.

Despite the promising potential piezocatalysis has, there are a several challenges that must be overcome before piezocatalytic processes can be widely implemented in the wastewater treatment industry. As highlighted in the literature review published in Current Opinion in Green and Sustainable Chemistry, one of the main challenges is to fully understand the mechanism driving the piezocatalytic process. In the case of ultrasound-assisted piezocatalysis, it is crucial to understand the complex interactions between the piezocatalyst, acoustic field and the targeted contaminants in order to optimise the piezocatalytic efficiency.

Another critical aspect in optimising piezocatalytic systems is to achieve a high catalytic activity while minimising the energy consumption. In this regard, it is important to systematically investigate various parameters such as the piezocatalysts properties, the strength and frequency of the acoustic field, the reactor design and operating conditions. The combination of a systematic experimental approach with advanced simulations could help to optimise the

parameters influencing piezocatalytic systems to maximise the degradation efficiency of organic pollutants while minimising the energy requirements.

Moreover, the scalability of piezocatalytic technology for the treatment of larger volumes of wastewater is another important factor that must not be underestimated. Given the well-documented challenges in transferring sonochemical effects from one scale to another [63-67], it is crucial to carefully assess whether piezocatalysis can be applied on an industrial scale. Scaling up the piezocatalytic process without compromising its efficiency and reliability will therefore require enhanced engineering and design considerations.

Based on these valuable insights into the current state of piezocatalysis it can be concluded that it is imperative to address the highlighted challenges and limitations of piezocatalysis in order to transition.

Drawing from the valuable insights of this literature review it becomes evident that addressing the challenges and limitations of piezocatalysis is imperative for the transition of a theoretical concept to practical applications or even commercialisation. For the transition of the piezocatalytic concept into a commercially viable technology, that can be embraced by industries on a larger scale, a multifaceted approach is needed.

Furthermore, a direct comparison between the emerging piezocatalytic concept and other well-established wastewater treatment methods, such as photocatalysis, proves challenging. This is primarily attributed to a substantial difference in their respective developmental stages. Piezocatalysis is currently in its conceptual phase focused on exploring its underlying mechanisms, yet it lacks vital data regarding economic feasibility, the cost of catalyst preparation and post-treatment. Consequently, a thorough comparison with established wastewater treatment methods faces hindrances, emphasising the need for further advancements and research in the area of piezocatalysis before meaningful comparisons can be drawn.

1.4 Problem statement and motivation

The treatment of wastewater remains a pressing global challenge, with conventional methods often proving to be both expensive and energy-intensive and occasionally even have adverse environmental and health impacts. While piezocatalysis has emerged as another promising technique, existing research has yet to comprehensively address the underlying piezocatalytic mechanisms, optimise piezocatalytic efficiency as well as to evaluate the scalability of ultrasound-assisted piezocatalytic systems. These research gaps hinder the full realisation of piezocatalysis as a sustainable and effective technique for large-scale, commercial wastewater treatment.

Therefore, this PhD project is motivated by the pressing need to address the current limitations in piezocatalytic research and with this tries to unlock the potential of piezocatalysis as an innovative approach to wastewater treatment. By thoroughly investigating the underlying mechanisms, optimising process parameters and considering the scalability of ultrasound-assisted piezocatalysis, this research aspires to determine the potential of piezocatalysis as a sustainable and efficient wastewater treatment technology. The findings will not only enhance the understanding of this innovative technology but will also offer practical solutions for making larger-scale wastewater treatment more efficient, energy-saving, and environmentally friendly.

1.5 Objectives of the research project

This PhD project aims to investigate the potential of piezocatalysis as a sustainable and efficient wastewater treatment technology. The main objectives of this project are:

- Investigating the underlying mechanisms of the piezocatalytic process, with a specific emphasis on fully understanding the complex interactions between the piezocatalyst,

acoustic field and targeted contaminants in ultrasound-assisted piezocatalysis. To achieve this, a combination of systematic experimental studies and advanced simulations will be employed to gain insights into the fundamental mechanisms and explore the factors that influence the piezocatalytic efficiency. Furthermore, larger-scale reactors will be utilised in order to obtain valuable insights into challenges and opportunities of implementing piezocatalyis in real-world applications.

- Optimising piezocatalytic systems for enhanced catalytic activity while trying to minimise the required energy consumption. To achieve this, parameters such as frequency and power of the acoustic field, operating conditions as well as the piezocatalyst properties will be systematically investigated.
- Investigating other potential piezocatalytic mechanisms aiming to provide a deeper understanding of the ‘true’ mechanism behind piezocatalysis by evaluating the performance of different piezocatalyst materials.
- Development of a piezocatalyst that incorporates beneficial characteristics identified in the previous chapters aiming to enhance the piezocatalytic activity while minimizing potential secondary pollution caused by micro-sized catalyst particles.

By accomplishing these objectives, this PhD project aims to contribute to the advancement of piezocatalysis as a sustainable and effective technique for wastewater treatment. The findings will provide valuable insights into the underlying mechanisms, process optimisation strategies as well as scalability considerations of ultrasound-assisted piezocatalytic systems. These insights will play a pivotal role in paving the way for the development of efficient, energy-saving and environmentally friendly wastewater treatment solutions at a larger scale.

1.6 References

[1] M.S. El-Shahawi, A. Hamza, A.S. Bashammakh, W.T. Al-Saggaf

An overview on the accumulation, distribution, transformations, toxicity and analytical methods for the monitoring of persistent organic pollutants

Talanta, 80 (5) (2010), 1587-97, 10.1016/j.talanta.2009.09.055

[2] E.A.H. Pilon-Smits, J.L. Freeman

Environmental cleanup using plants: biotechnological advances and ecological considerations

Frontiers in Ecology and the Environment, 4 (4) (2006), 203-210, 10.1890/1540-9295(2006)004[0203:Ecupba]2.0.Co;2

[3] R. Soni, S. Bhardwaj, D.P. Shukla

Chapter 14 - Various water-treatment technologies for inorganic contaminants: current status and future aspects

in: P. Devi, P. Singh, S.K. Kansal (Eds.),Inorganic Pollutants in Water, Elsevier2020, pp. 273-295

[4] K.L. Wasewar, S. Singh, S.K. Kansal

Chapter 13 - Process intensification of treatment of inorganic water pollutants

in: P. Devi, P. Singh, S.K. Kansal (Eds.),Inorganic Pollutants in Water, Elsevier2020, pp. 245-271

[5] N. Sharma, A.S. Sodhi, N. Batra

Basic Concepts in Environmental Biotechnology, CRC Press, Boca Raton, 2021

[6] B. Lellis, C.Z. Fávaro-Polonio, J.A. Pamphile, J.C. Polonio

Effects of textile dyes on health and the environment and bioremediation potential of living organisms

Biotechnology Research and Innovation, 3 (2) (2019), 275-290, 10.1016/j.biori.2019.09.001

[7] P. Mudu, B. Terracini, M. Martuzzi

Human health in areas with industrial contamination, World Health Organization. Regional Office for Europe, Copenhagen, 2014

[8] K. Remoundou, P. Koundouri

Environmental effects on public health: an economic perspective

Int J Environ Res Public Health, 6 (8) (2009), 2160-78, 10.3390/ijerph6082160

[9] S. Sharma, S. Chatterjee

Microplastic pollution, a threat to marine ecosystem and human health: a short review

Environ Sci Pollut Res Int, 24 (27) (2017), 21530-21547, 10.1007/s11356-017-9910-8

[10] R. Al-Tohamy, S.S. Ali, F. Li, K.M. Okasha, Y.A. Mahmoud, T. Elsamahy, H. Jiao, Y. Fu, J. Sun

A critical review on the treatment of dye-containing wastewater: Ecotoxicological and health concerns of textile dyes and possible remediation approaches for environmental safety

Ecotoxicol Environ Saf, 231 (2022), 113160, 10.1016/j.ecoenv.2021.113160

[11] D.A. Yaseen, M. Scholz

Textile dye wastewater characteristics and constituents of synthetic effluents: a critical review

International Journal of Environmental Science and Technology, 16 (2) (2018), 1193-1226, 10.1007/s13762-018-2130-z

[12] A. Tkaczyk, K. Mitrowska, A. Posyniak

Synthetic organic dyes as contaminants of the aquatic environment and their implications for ecosystems: A review

Sci Total Environ, 717 (2020), 137222, 10.1016/j.scitotenv.2020.137222

[13] M. Davarazar, M. Kamali, C. Venâncio, A. Gabriel, T.M. Aminabhavi, I. Lopes

Activation of persulfate using copper oxide nanoparticles for the degradation of Rhodamine B containing effluents: Degradation efficiency and ecotoxicological studies

Chemical Engineering Journal, 453 (2023), 10.1016/j.cej.2022.139799

[14] M. Berradi, R. Hsissou, M. Khudhair, M. Assouag, O. Cherkaoui, A. El Bachiri, A. El Harfi

Textile finishing dyes and their impact on aquatic environs

Heliyon, 5 (11) (2019), e02711, 10.1016/j.heliyon.2019.e02711

[15] Z.H. Liu, Y. Kanjo, S. Mizutani

Removal mechanisms for endocrine disrupting compounds (EDCs) in wastewater treatment - physical means, biodegradation, and chemical advanced oxidation: a review

Sci Total Environ, 407 (2) (2009), 731-48, 10.1016/j.scitotenv.2008.08.039

[16] G. Crini, E. Lichtfouse, L.D. Wilson, N. Morin-Crini

Conventional and non-conventional adsorbents for wastewater treatment

Environmental Chemistry Letters, 17 (1) (2018), 195-213, 10.1007/s10311-018-0786-8

[17] Y. Feng, L. Yang, J. Liu, B.E. Logan

Electrochemical technologies for wastewater treatment and resource reclamation

Environmental Science: Water Research & Technology, 2 (5) (2016), 800-831, 10.1039/c5ew00289c

[18] C. Fonseca Couto, L.C. Lange, M.C. Santos Amaral

A critical review on membrane separation processes applied to remove pharmaceutically active compounds from water and wastewater

Journal of Water Process Engineering, 26 (2018), 156-175, 10.1016/j.jwpe.2018.10.010

[19] J.S. Knapp, K.C.A. Bromley-Challoner

Recalcitrant organic compounds

Handbook of Water and Wastewater Microbiology2003, pp. 559-595

[20] E. Kudlek

Decomposition of Contaminants of Emerging Concern in Advanced Oxidation Processes

Water, 10 (7) (2018), 10.3390/w10070955

[21] E.S. Mouele, J.O. Tijani, O.O. Fatoba, L.F. Petrik

Degradation of organic pollutants and microorganisms from wastewater using different dielectric barrier discharge configurations--a critical review

Environ Sci Pollut Res Int, 22 (23) (2015), 18345-62, 10.1007/s11356-015-5386-6

[22] A. Saravanan, P. Senthil Kumar, S. Jeevanantham, S. Karishma, B. Tajsabreen, P.R. Yaashikaa, B. Reshma

Effective water/wastewater treatment methodologies for toxic pollutants removal: Processes and applications towards sustainable development

Chemosphere, 280 (2021), 130595, 10.1016/j.chemosphere.2021.130595

[23] S. Dutta, B. Gupta, S.K. Srivastava, A.K. Gupta

Recent advances on the removal of dyes from wastewater using various adsorbents: a critical review

Materials Advances, 2 (14) (2021), 4497-4531, 10.1039/d1ma00354b

[24] D. Lan, H. Zhu, J. Zhang, S. Li, Q. Chen, C. Wang, T. Wu, M. Xu

Adsorptive removal of organic dyes via porous materials for wastewater treatment in recent decades: A review on species, mechanisms and perspectives

Chemosphere, 293 (2022), 133464, 10.1016/j.chemosphere.2021.133464

[25] Y. Zhou, J. Lu, Y. Zhou, Y. Liu

Recent advances for dyes removal using novel adsorbents: A review

Environ Pollut, 252 (Pt A) (2019), 352-365, 10.1016/j.envpol.2019.05.072

[26] V. Katheresan, J. Kansedo, S.Y. Lau

Efficiency of various recent wastewater dye removal methods: A review

Journal of Environmental Chemical Engineering, 6 (4) (2018), 4676-4697, 10.1016/j.jece.2018.06.060

[27] T.A. Khan, M. Nazir

Enhanced adsorptive removal of a model acid dye bromothymol blue from aqueous solution using magnetic chitosan-bamboo sawdust composite: Batch and column studies

Environmental Progress & Sustainable Energy, 34 (5) (2015), 1444-1454, 10.1002/ep.12147

[28] Z. Li, Y. Sun, J. Xing, Y. Xing, A. Meng

One step synthesis of Co/Cr-codoped ZnO nanoparticle with superb adsorption properties for various anionic organic pollutants and its regeneration

J Hazard Mater, 352 (2018), 204-214, 10.1016/j.jhazmat.2018.03.049

[29] A. Ofomaja, Y. Ho

Equilibrium sorption of anionic dye from aqueous solution by palm kernel fibre as sorbent

Dyes and Pigments, 74 (1) (2007), 60-66, 10.1016/j.dyepig.2006.01.014

[30] E. Daneshvar, M.S. Sohrabi, M. Kousha, A. Bhatnagar, B. Aliakbarian, A. Converti, A.-C. Norrström

Shrimp shell as an efficient bioadsorbent for Acid Blue 25 dye removal from aqueous solution

Journal of the Taiwan Institute of Chemical Engineers, 45 (6) (2014), 2926-2934, 10.1016/j.jtice.2014.09.019

[31] M.A.M. Salleh, D.K. Mahmoud, W.A.W.A. Karim, A. Idris

Cationic and anionic dye adsorption by agricultural solid wastes: A comprehensive review

Desalination, 280 (1-3) (2011), 1-13, 10.1016/j.desal.2011.07.019

[32] Z. Eren, F.N. Acar

Adsorption of Reactive Black 5 from an aqueous solution: equilibrium and kinetic studies

Desalination, 194 (1-3) (2006), 1-10, 10.1016/j.desal.2005.10.022

[33] M.N. Chong, B. Jin, C.W. Chow, C. Saint

Recent developments in photocatalytic water treatment technology: a review

Water Res, 44 (10) (2010), 2997-3027, 10.1016/j.watres.2010.02.039

[34] H. Kumari, Sonia, Suman, R. Ranga, S. Chahal, S. Devi, S. Sharma, S. Kumar, P. Kumar, S. Kumar, A. Kumar, R. Parmar

A Review on Photocatalysis Used For Wastewater Treatment: Dye Degradation

Water Air Soil Pollut, 234 (6) (2023), 349, 10.1007/s11270-023-06359-9

[35] M. Saeed, M. Muneer, A.U. Haq, N. Akram

Photocatalysis: an effective tool for photodegradation of dyes-a review

Environ Sci Pollut Res Int, 29 (1) (2022), 293-311, 10.1007/s11356-021-16389-7

[36] Z. Kuspanov, B. Bakbolat, A. Baimenov, A. Issadykov, M. Yeleuov, C. Daulbayev

Photocatalysts for a sustainable future: Innovations in large-scale environmental and energy applications

Sci Total Environ, 885 (2023), 163914, 10.1016/j.scitotenv.2023.163914

[37] I. Muñoz, J. Rieradevall, F. Torrades, J. Peral, X. Domènech

Environmental assessment of different solar driven advanced oxidation processes

Solar Energy, 79 (4) (2005), 369-375, 10.1016/j.solener.2005.02.014

[38] R.J. Braham, A.T. Harris

Review of Major Design and Scale-up Considerations for Solar Photocatalytic Reactors

Industrial & Engineering Chemistry Research, 48 (19) (2009), 8890-8905, 10.1021/ie900859z

[39] C. McCullagh, N. Skillen, M. Adams, P.K.J. Robertson

Photocatalytic reactors for environmental remediation: a review

Journal of Chemical Technology & Biotechnology, 86 (8) (2011), 1002-1017, 10.1002/jctb.2650

[40] K.P. Sundar, S. Kanmani

Progression of Photocatalytic reactors and it's comparison: A Review

Chemical Engineering Research and Design, 154 (2020), 135-150, 10.1016/j.cherd.2019.11.035

[41] O.M. Alfano, D. Bahnemann, A.E. Cassano, R. Dillert, R. Goslich

Photocatalysis in water environments using artificial and solar light

Catalysis Today, 58 (2-3) (2000), 199-230, 10.1016/s0920-5861(00)00252-2

[42] E. Brillas, C.A. Martínez-Huitle

Decontamination of wastewaters containing synthetic organic dyes by electrochemical methods. An updated review

Applied Catalysis B: Environmental, 166-167 (2015), 603-643, 10.1016/j.apcatb.2014.11.016

[43] G. Chen

Electrochemical technologies in wastewater treatment

Separation and Purification Technology, 38 (1) (2004), 11-41, 10.1016/j.seppur.2003.10.006

[44] D.K. Sarfo, A. Kaur, D.L. Marshall, A.P. O'Mullane

Electrochemical degradation and mineralisation of organic dyes in aqueous nitrate solutions

Chemosphere, 316 (2023), 137821, 10.1016/j.chemosphere.2023.137821

[45] F. Shen, X. Chen, P. Gao, G. Chen

Electrochemical removal of fluoride ions from industrial wastewater

Chemical Engineering Science, 58 (3-6) (2003), 987-993, 10.1016/s0009-2509(02)00639-5

[46] A.T. Kuhn

Electrolytic decomposition of cyanides, phenols and thiocyanates in effluent streams—a literature review

Journal of Applied Chemistry and Biotechnology, 21 (2) (2007), 29-34, 10.1002/jctb.5020210201

[47] R. Lay, G.S. Deijs, J. Malmstrom

The intrinsic piezoelectric properties of materials - a review with a focus on biological materials

RSC Adv, 11 (49) (2021), 30657-30673, 10.1039/d1ra03557f

[48] S.R. Anton, H.A. Sodano

A review of power harvesting using piezoelectric materials (2003–2006)

Smart Materials and Structures, 16 (3) (2007), R1-R21, 10.1088/0964-1726/16/3/r01

[49] K.-S. Hong, H. Xu, H. Konishi, X. Li

Direct Water Splitting Through Vibrating Piezoelectric Microfibers in Water

The Journal of Physical Chemistry Letters, 1 (6) (2010), 997-1002, 10.1021/jz100027t

[50] Z. Liang, C.-F. Yan, S. Rtimi, J. Bandara

Piezoelectric materials for catalytic/photocatalytic removal of pollutants: Recent advances and outlook

Applied Catalysis B: Environmental, 241 (2019), 256-269, 10.1016/j.apcatb.2018.09.028

[51] J. Dai, N. Shao, S. Zhang, Z. Zhao, Y. Long, S. Zhao, S. Li, C. Zhao, Z. Zhang, W. Liu

Enhanced Piezocatalytic Activity of $Sr_{0.5}Ba_{0.5}Nb_2O_6$ Nanostructures by Engineering Surface Oxygen Vacancies and Self-Generated Heterojunctions

ACS Appl Mater Interfaces, 13 (6) (2021), 7259-7267, 10.1021/acsami.0c21202

[52] B. Yuan, J. Wu, N. Qin, E. Lin, Z. Kang, D. Bao

Sm-doped $Pb(Mg_{1/3}Nb_{2/3})O_3$-$xPbTiO_3$ piezocatalyst: Exploring the relationship between piezoelectric property and piezocatalytic activity

Applied Materials Today, 17 (2019), 183-192, 10.1016/j.apmt.2019.07.015

[53] X. Zhou, B. Shen, J. Zhai, N. Hedin

Reactive Oxygenated Species Generated on Iodide-Doped $BiVO_4$/$BaTiO_3$ Heterostructures with Ag/Cu Nanoparticles by Coupled Piezophototronic Effect and Plasmonic Excitation

Advanced Functional Materials, 31 (13) (2021), 10.1002/adfm.202009594

[54] A. Zhang, Z. Liu, B. Xie, J. Lu, K. Guo, S. Ke, L. Shu, H. Fan

Vibration catalysis of eco-friendly $Na_{0.5}K_{0.5}NbO_3$-based piezoelectric: An efficient phase boundary catalyst

Applied Catalysis B: Environmental, 279 (2020), 10.1016/j.apcatb.2020.119353

[55] E. Lin, Z. Kang, J. Wu, R. Huang, N. Qin, D. Bao

$BaTiO_3$ nanocubes/cuboids with selectively deposited Ag nanoparticles: Efficient piezocatalytic degradation and mechanism

Applied Catalysis B: Environmental, 285 (2021), 10.1016/j.apcatb.2020.119823

[56] L. Chen, Y. Jia, J. Zhao, J. Ma, Z. Wu, G. Yuan, X. Cui

Strong piezocatalysis in barium titanate/carbon hybrid nanocomposites for dye wastewater decomposition

J Colloid Interface Sci, 586 (2021), 758-765, 10.1016/j.jcis.2020.10.145

[57] Y.T. Lin, S.N. Lai, J.M. Wu

Simultaneous Piezoelectrocatalytic Hydrogen-Evolution and Degradation of Water Pollutants by Quartz Microrods@Few-Layered MoS_2 Hierarchical Heterostructures

Adv Mater, 32 (34) (2020), e2002875, 10.1002/adma.202002875

[58] P.T. Thuy Phuong, Y. Zhang, N. Gathercole, H. Khanbareh, N.P. Hoang Duy, X. Zhou, D. Zhang, K. Zhou, S. Dunn, C. Bowen

Demonstration of Enhanced Piezo-Catalysis for Hydrogen Generation and Water Treatment at the Ferroelectric Curie Temperature

iScience, 23 (5) (2020), 101095, 10.1016/j.isci.2020.101095

[59] W. Feng, J. Yuan, L. Zhang, W. Hu, Z. Wu, X. Wang, X. Huang, P. Liu, S. Zhang

Atomically thin ZnS nanosheets: Facile synthesis and superior piezocatalytic H_2 production from pure H_2O

Applied Catalysis B: Environmental, 277 (2020), 10.1016/j.apcatb.2020.119250

[60] D. Liu, C. Jin, F. Shan, J. He, F. Wang

Synthesizing $BaTiO_3$ Nanostructures to Explore Morphological Influence, Kinetics, and Mechanism of Piezocatalytic Dye Degradation

ACS Appl Mater Interfaces, 12 (15) (2020), 17443-17451, 10.1021/acsami.9b23351

[61] J. Ling, K. Wang, Z. Wang, H. Huang, G. Zhang

Enhanced piezoelectric-induced catalysis of $SrTiO_3$ nanocrystal with well-defined facets under ultrasonic vibration

Ultrason Sonochem, 61 (2020), 104819, 10.1016/j.ultsonch.2019.104819

[62] S. Lan, Y. Chen, L. Zeng, H. Ji, W. Liu, M. Zhu

Piezo-activation of peroxymonosulfate for benzothiazole removal in water

J Hazard Mater, 393 (2020), 122448, 10.1016/j.jhazmat.2020.122448

[63] N. Gondrexon, V. Renaudin, C. Petrier, P. Boldo, A. Bernis, Y. Gonthier

Degradation of pentachlorophenol aqueous solutions using a continuous flow ultrasonic reactor: experimental performance and modelling

Ultrason Sonochem, 5 (4) (1999), 125-31, 10.1016/s1350-4177(98)00041-8

[64] O. Louisnard, J. Gonzalez-Garcia, I. Tudela, J. Klima, V. Saez, Y. Vargas-Hernandez

FEM simulation of a sono-reactor accounting for vibrations of the boundaries

Ultrason Sonochem, 16 (2) (2009), 250-9, 10.1016/j.ultsonch.2008.07.008

[65] P.R. Gogate, V.S. Sutkar, A.B. Pandit

Sonochemical reactors: Important design and scale up considerations with a special emphasis on heterogeneous systems

Chemical Engineering Journal, 166 (3) (2011), 1066-1082, 10.1016/j.cej.2010.11.069

[66] P.R. Gogate, A.B. Pandit

Sonochemical reactors: scale up aspects

Ultrason Sonochem, 11 (3-4) (2004), 105-17, 10.1016/j.ultsonch.2004.01.005

[67] S. Manickam, M. Ashokkumar

Cavitation: A Novel Energy-Efficient Technique for the Generation of Nanomaterials (1st ed.), Jenny Stanford Publishing, New York, 2014

Available online at www.sciencedirect.com

ScienceDirect

Current Opinion in
Green and Sustainable Chemistry

Piezocatalysis: Can catalysts really dance?

Franziska Bößl and Ignacio Tudela

Piezocatalysis is an emerging area of research that has the potential to enable new green advances in catalytic processes independent of energy sources such as light or electricity. However, research has mainly focused on the development of piezoelectric materials that exhibit certain catalytic behaviour, rather than on elucidating the fundamentals behind this new catalytic phenomenon. This review aims to highlight overseen aspects in piezocatalysis research that are common practice in other research areas such as general piezoelectricity, sonochemistry and electrochemistry. Factors that are generally overlooked but that would have a critical impact on piezocatalysis such as the nature of the mechanic field, its frequency and the redox potentials of the reactions involved will be briefly discussed.

Addresses
Edinburgh Electrochemical Engineering Group (e3 Group), Institute for Materials and Processes, School of Engineering, The University of Edinburgh, Edinburgh, EH9 3FB, UK

Corresponding author: Tudela, Ignacio ( )

Current Opinion in Green and Sustainable Chemistry 2021, **32:**100537

This review comes from a themed issue on **Special Issue Young Ideas in Green and Sustainable Catalysis (2022)**

Edited by **Emilia Paone**

Available online 21 July 2021

For complete overview of the section, please refer the article collection - Special Issue Young Ideas in Green and Sustainable Catalysis (2022)

https://doi.org/10.1016/j.cogsc.2021.100537

Introduction

In recent years, piezoelectric materials have been reported to exhibit catalytic activity for the removal of organic pollutants in water [1–19], water splitting [10,20–25] and bacterial disinfection [26–30] as a result of their piezoelectric response. This emerging new catalytic phenomenon, known as 'piezocatalysis' or 'piezo-electrocatalysis', takes advantage of the piezoelectric effect to convert mechanical energy into electricity that is used for electrochemical reactions. The types of mechanical vibration piezocatalysis ultimately aims to use are in the form of natural motion such as wind or waves, but could also be redundant vibrations in industrial systems. Owing to this, piezocatalysis is considered as a promising green catalytic process independent of energy sources such as light or electricity [31]. Research in this field has mainly focused on enhancing piezocatalytic efficiency by modifying piezoelectric materials to be used as piezocatalysts rather than elucidating the fundamentals behind the observed catalytic phenomenon [1,4,6,16,20,24,32]. However, elucidating the main factors influencing piezocatalytic processes is still an ongoing task, leaving piezocatalytic processes far from being fully understood. Understanding and applying the fundamental principles and common practices from well-established research areas such as piezoelectricity, electrochemistry and sonochemistry is necessary to fully exploit the promising potential piezocatalysis has as a green and sustainable catalysis. Unfortunately, this is still not the norm in current piezocatalysis research.

Physico-chemical mechanisms

The piezocatalytic reaction mechanisms proposed so far are analogous to those in electro- and photo-catalysis [4,9,10,12,13,16–18,20,21], although in this case the driving force would be the piezoelectric response of the material. Researchers initially settled on a mechanism explaining piezocatalysis by a 'bulk' polarisation (Figure 1a) [3,5,7,12,18,33] where external stresses, mainly caused by an acoustic field, cause deformation and charge separation resulting in a 'top-to-bottom' potential difference that enables redox reactions to occur at different locations within the piezocatalyst surface. Negative charges (e^-) react with dissolved oxygen and produce superoxide radicals ($^{\bullet}O_2^-$) in negatively charged regions of the surface, whereas hydroxyl radicals are said to be formed by positive charges (h^+) and hydroxide ions.

- Reduction: $O_2 + e^- \rightarrow {}^{\bullet}O_2^-$ (−0.33 V vs SHE) [34]
- Oxidation: $OH^- + h^+ \rightarrow {}^{\bullet}OH$ (+1.89 V vs SHE) [35]

As deduced from the reduction potentials stated above, a minimum potential difference of 2.22 V between those regions, which would effectively behave as 'cathodes' and 'anodes' in any electrochemical device, is required for those reactions to occur (and that is without accounting for other factors such as kinetic and concentration overpotentials that would further increase said potential difference). However, FEM simulations of piezocatalysts [6,8,18–20,23,31,36,37] clearly indicate that this 'top-to-bottom' electric potential difference is unlikely to be larger than the minimum required for the redox reactions suggested above. This means that other physico-chemical phenomena that could potentially cause such reactions must be considered.

Another phenomenon that could explain piezocatalytic activity is the occurrence of localised piezoelectric activity resulting in localised superficial polarisation (Figure 1b). This localised piezoelectric response could lead to large electric potential differences within micro- and nano-structured surface features of piezocatalysts, which is why it may be an important factor driving piezocatalytic processes [31]. Nevertheless, research on micro- and nanoscale piezoelectricity is still in its infancy [38], and more progress is required to better understand this phenomenon.

Other potential explanations behind piezocatalysis reside on the effect that piezoelectric properties of the catalyst may have on its valence and conduction band, favouring the redox reactions of interest under ultrasound [4,6,8,17,19,21,23]. This is indeed very similar to what researchers in the sonochemistry community would call sonocatalysis (Figure 1c), which generally occurs in semiconductor materials under sonication [39]. Most piezocatalysts are fabricated from semiconductor materials that could lead to a possible contribution of sonocatalysis in the observed catalytic

Figure 1

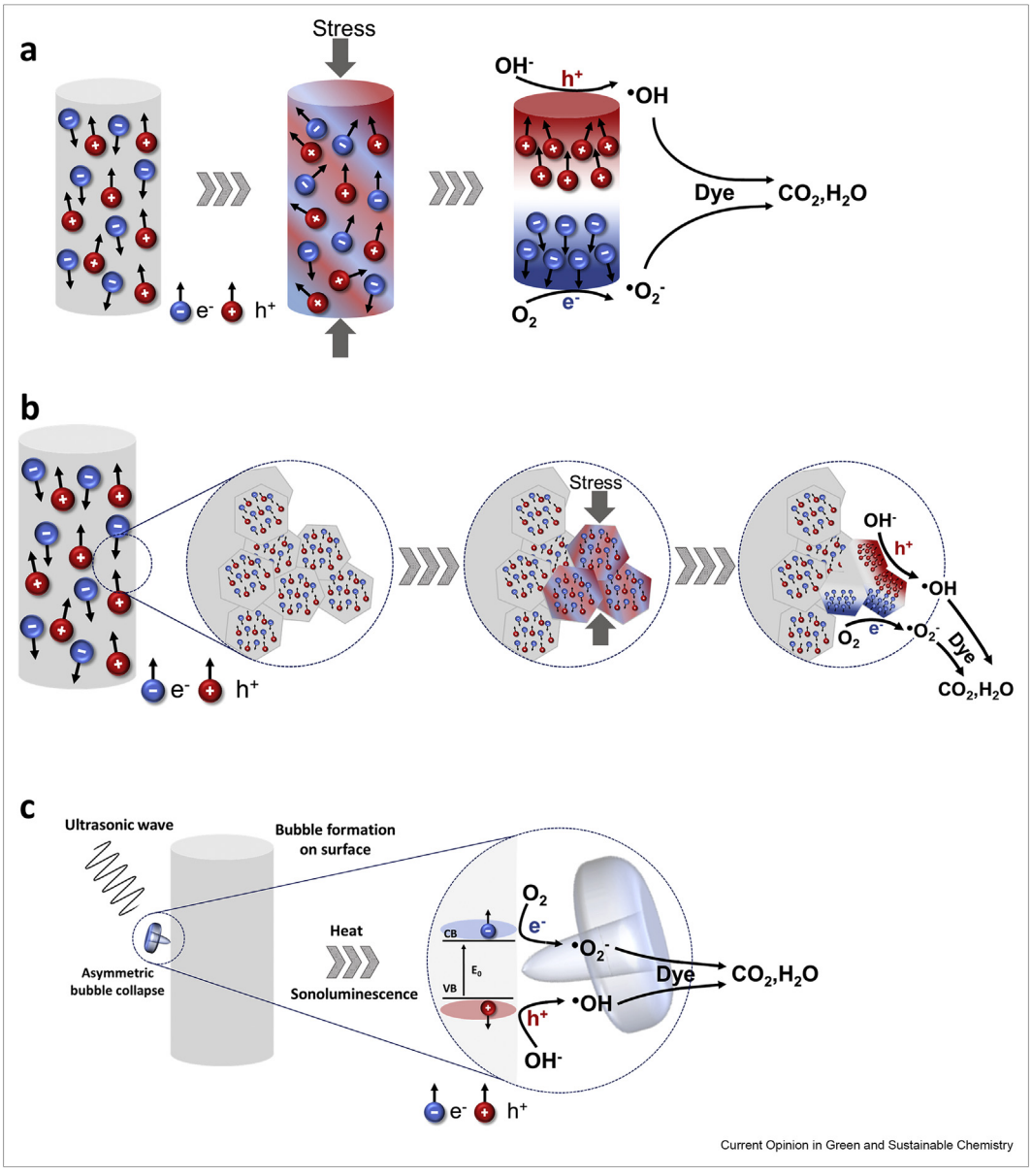

Illustration of different types of piezocatalytic mechanisms: **(a)** 'top-to-bottom' electric potential difference due to bulk polarisation of a piezocatalyst under stress; **(b)** electric potential difference due to localised polarisation within micro-and nano-structured features of piezocatalysts; **(c)** valence band (VB) and conduction band (CB) in semiconductor materials in presence of cavitating bubbles under ultrasound (i.e., sonocatalysis).

activities, which would be enhanced in those cases where the catalyst is made of a piezoelectric material [31]. Besides this, sonochemistry is intrinsically connected to piezocatalysis when using ultrasound. It is widely known that sonication on its own can form $^{\bullet}OH$ and $^{\bullet}O_2^-$ radicals [40,41]. Therefore, sonochemistry should never be neglected as it could play an important role in observed catalytic processes assumed to only be piezocatalytic in nature. For this reason, it is strongly suggested to conduct appropriate blank experiments (e.g. presence/absence of ultrasound, catalyst and radical scavengers) to better distinguish between radicals evolving on the piezocatalyst surface due to its piezoelectric response and those created by sonication [31]. In general, radical scavenger experiments (Figure 2e) are not only limited to $^{\bullet}OH$ and $^{\bullet}O_2^-$ radicals [4] but also to 'non-radicalary species' such as h^+ and e^-, hence why they are very useful to determine which physico-chemical phenomena may be causing the observed catalytic activity [31].

Piezocatalysts

Material, size and geometry

Generally, a piezocatalyst is a piezoelectric material (or composite) that converts mechanical stresses into charges that drive redox reactions. For this reason, it can also be described as a miniaturised electrochemical device that combines power source and electrodes. Many piezocatalysts are based on barium titanate ($BaTiO_3$) [3,5,7,11–13,17–19,26,33,36,42] (Figure 2d), polyvinylidene difluoride (PVDF) [14,27,32,43] or zinc oxide (ZnO) [8,44,45]. A wide range of piezocatalyst shapes (Figure 2a–c) has been reported [11,19,23,33], with some studies suggesting that fibres/wires exhibit enhanced piezocatalytic activity compared with particles/spheres [19,33], while others suggest the use of thin sheets aiming at the same purpose [23].

Regardless of material and shape, the theoretical piezoelectric output of any piezoelectric particle is directly proportional to its size, as suggested by the following equation [46]:

$$V_p = \frac{d_{ij}\sigma_j w_i}{\varepsilon_0 \varepsilon_{r,i}} \quad (1)$$

where V_p is the piezoelectric open-circuit potential, σ_j is the applied stress in j direction, d_{ij} is the piezoelectric charge coefficient, w_i is the length of the piezocatalyst in i direction of polarisation, $\varepsilon_{r,i}$ is the relative permittivity in the i dimension and ε_0 represents the electrical permittivity of free space. In addition, the larger the particle is, the lower the resonance frequency generally is for any piezoelectric material, as indicated by the equations included in Table 1, which are derived from the relationship between frequency constant N_i and resonance frequency f_r for different particle geometries [47]. If one assumed that the 'top-to-bottom' potential difference caused by bulk polarisation was the dominant mechanism in piezocatalysis (as many of the studies in the literature do [3,5,7,12,18,33]), the goal should be to achieve the largest piezoelectric output possible at the frequency close to that of the application (e.g. tens of kHz, depending on the ultrasonic system used to 'excite' the piezocatalysts). However, that would require particles well within the micron scale (tens or hundreds of microns [31]), perhaps even millimetres. Unfortunately, though, most of the research on piezocatalysis has been conducted on catalysts within the submicron scale [1,3,5,7,9,11,14,15,18,19,23,25,32,33,48]. Moreover, no study has so far really attempted to shed some light on the potential effect of frequency on this novel catalytic process, even though the operation of piezocatalysts at frequencies closer to their resonance frequency would indeed result in a significantly greater 'bulk' polarisation (hence a larger 'top-to-bottom' potential difference). These are factors that have not really been considered by the research community to date but that should be explored in the near future to better understand how piezocatalysis fundamentally works and its link with basic piezoelectricity.

Piezoelectric properties

The piezoelectric nature of any material can be defined by a series of piezoelectric coefficients or parameters. Piezoelectric charge constants d_{ij} (e.g. d_{11} or d_{33} part of a 6×6 matrix) or dielectric constants ε_{ij}^{T} (e.g. ε_{11}^{T}, ε_{22}^{T} or ε_{33}^{T} part of a 3×3 matrix) are among the best indicators of the potential performance of any given piezoelectric material and should be of significant interest for piezocatalysis. Very rarely in piezocatalysis research, piezoelectric coefficients are defined to indicate the piezoelectric nature (or lack of) of piezocatalysts [23,27,31]. However, although the vast majority of research in this field recognises piezoelectric phenomena as the source of the catalytic activity of piezocatalysts, no significant information (e.g. piezoelectric charge constants, dielectric constants or electrochemical coupling factors) is generally found about the 'true' piezoelectric nature of a piezocatalyst in most of the studies available in the literature. Some studies do present workaround methods based on chemical and/or physical measurements to shed some light on the 'true' piezoelectric nature of piezocatalysts [2,6,7,9,19,23,24,33,49], but those methods are not standardised and are difficult to replicate.

The lack of information on piezoelectric coefficients or performance from piezocatalysts means that their 'true' piezoelectric nature can only be hypothesised (more details about this can be found in the following subsection on 'Poling'). One of the challenges is that, although piezoelectric charge coefficients are well

Figure 2

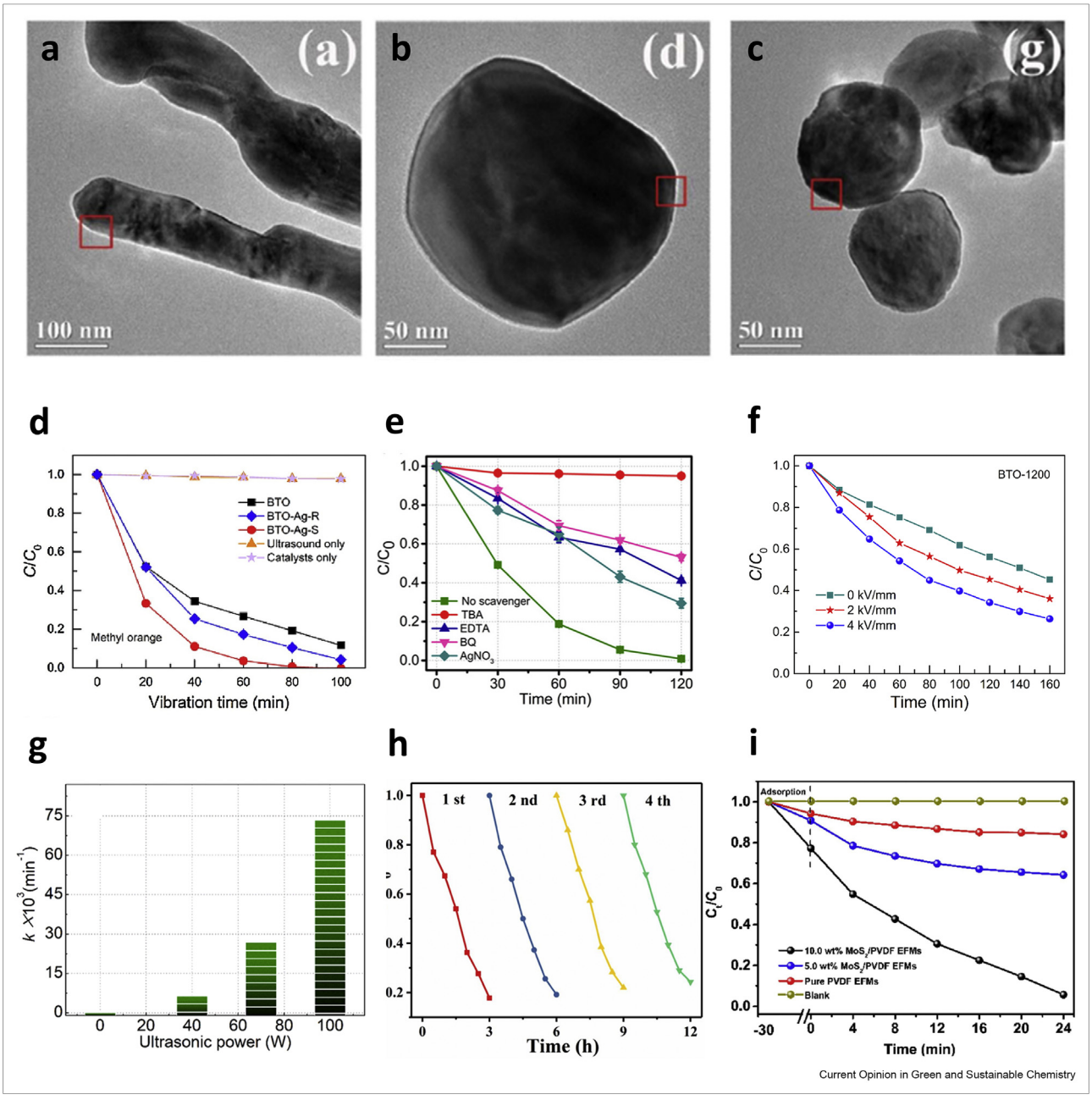

Examples of catalysts, degradation curves and kinetic rates from current piezocatalysis research: **(a–c)** TEM images of hydrothermal $BaTiO_3$ nanowires, hydrothermal $BaTiO_3$ nanoparticles and commercial $BaTiO_3$ nanoparticles, respectively. Reprinted from the study by Wu et al [19], Copyright 2018, with permission from Elsevier. **(d)** Piezocatalytic degradation of methyl orange in water in the presence of $BaTiO_3$ nanoparticles (BTO), randomly Ag-deposited $BaTiO_3$ nanocrystals (BTO-Ag-R) and selectively Ag-deposited $BaTiO_3$ nanocrystals (BTO-Ag-S). Reprinted from the study by Lin et al [3], Copyright 2020, with permission from Elsevier. **(e)** Piezocatalytic degradation of RhB in the presence of various radical scavengers: disodium ethylene diamine tetra-acetate dehydrate (EDTA), tert-butyl alcohol (TBA), benzoquinone (BQ) and $AgNO_3$. Reprinted in part with permission from Dai et al [4], Copyright 2021 American Chemical Society. **(f)** Piezocatalytic degradation of methyl orange by BaTiO3 nanoparticles calcined at 1200 °C and poled at different voltages. Reprinted with permission from Wu et al [18], Copyright 2018 American Chemical Society. **(g)** Effect of ultrasonic power on piezocatalytic degradation of RhB. Reprinted in part with permission from Liu et al [33], Copyright 2020 American Chemical Society. **(h)** Cycle experiments for the piezocatalytic degradation of RhB by $SrTiO_3$. Reprinted from the study by Ling et al [9], Copyright 2020, with permission from Elsevier. **(i)** Piezocatalytic degradation of oxytetracycline solution over exfoliated multi-flaw MoS_2/PVDF electrospun fibre membranes with different MoS_2 content. Please note that it is not clear whether adsorption/desorption equilibrium was achieved prior to the piezocatalytic experiments. Reprinted from the study by Ma et al [49], Copyright 2021, with permission from Elsevier.

Table 1

Relationship between frequency constant N_i (N_L = longitudinal mode frequency constant; N_T = thickness mode frequency constant; N_P = radial mode frequency constant) and resonance frequency f_r for different shapes.

Shape	Polarisation direction	Voltage field	Mode of vibration: displacement	Frequency constant N_i
Plate				$N_L = f_r l$
				$N_L = f_r w$
				$N_T = f_r h$
Disc				$N_P = 2 f_r r$
				$N_T = f_r h$
Bar				$N_L = f_r l$
Rod				$N_L = f_r l$

defined for bulk materials and films, the same coefficients may not necessarily translate to powdered samples of the same material. Unfortunately, current measurement techniques for piezoelectric coefficients are devised for either thin films or bulk materials and might not be entirely suitable for widely used nanoscale piezocatalysts [50]. Therefore, developing appropriate measurement techniques for micron and nanoscale piezocatalysts is necessary to better understand how piezoelectric piezocatalysts function.

Poling

The need to conduct a 'poling' process (i.e. alignment of randomly oriented Weiss domains through the application of a strong electric field at high temperatures below the Curie point of the material) to improve the piezoelectric coefficients of any material and enhance its piezoelectric behaviour is a widely known practice in the development of piezoelectric applications [51]. However, it has received relatively low attention from most of the piezocatalysis research community, even though some studies have clearly demonstrated that greater poling voltages result in a significantly enhanced piezocatalytic performance [14,16,18,42,52] (Figure 2f). Poling is not only important to improve a piezocatalytic process; the comparison of poled and unpoled piezocatalysts of the same material also allows researchers to better distinguish whether an observed catalytic activity is 'true' piezocatalysis or may be caused by other catalytic phenomena such as sonocatalysis [31]. For this reason, comparison with unpoled and poled version of the same material should be conducted more often to better understand the causes (i.e. physico-chemical mechanisms) of the observed piezocatalytic activity.

Other factors

Catalyst reusability is of high economic interest and an important aspect to be considered in piezocatalysis research (Figure 2h), which is why several studies report good reusability of piezocatalysts with no significant changes in the observed catalytic activity [2,4,6,9,13,14,16,26]. Another factor that must be considered when evaluating the catalytic activity of piezocatalysts is the material's adsorbent nature. Reaching adsorption–desorption equilibrium of the reactant by stirring piezocatalysts in the target solution is a widely reported approach in piezocatalysis [1,4,6,32,33,52]. However, it is not often clear to conclude whether that equilibrium has been reached in many piezocatalysis studies (Figure 2i) [49,53]. Reaching adsorption–desorption equilibrium prior to the catalytic process is important to separate adsorption from pure piezocatalytical activity, as adsorption onto the piezocatalyst could significantly distort some of the research findings reported (e.g. reaction rate constants). To avoid this, research in this field should ensure that adsorption–desorption equilibrium is reached prior to any experimental run and that the adsorption and porous nature of the material is properly characterised (e.g. BET analysis [31]).

Piezocatalyst excitation

Ultrasound, generally at 20–40 kHz by means of a commercial ultrasonic horn or bath, is the most common way to 'excite' piezocatalysts [1,4–6,8,9,11,12,17–19,21,22,25,33]. However, as hinted in Section 3.1, these frequencies may not be the optimum ones to operate at if one considers the resonance frequency (f_r) of piezocatalysts. Furthermore, the acoustic pressure in ultrasonic probes/baths operating at 20–40 kHz does not generally exceed 2 bar [54], which might not be sufficient to exert adequate stress on piezocatalysts to experience large enough potentials for the previously suggested redox reactions. Some studies have suggested that piezocatalyst polarisation is enhanced by collapsing cavitation bubbles with pressures up to 10^8 Pa [8,19,20,37,43]. However, if acoustic cavitation under ultrasound was the only method to achieve the required piezocatalyst polarisation, the applicability of piezocatalysis would be significantly restricted to systems where acoustic cavitation could be induced by ultrasound. Therefore, other excitation methods should be considered in future research to shed more light on the 'real-world' potential of piezocatalysis.

Ultrasound is still very useful to better understand the main factors influencing piezocatalysis. Nevertheless, the use of ultrasound requires a thorough consideration

of important aspects from sonochemistry research such as the acoustic field, acoustic power or temperature control, as further explained in the following subsections.

Acoustic field

Control and reproducibility of the acoustic field should be a critical aspect when using sonication to excite piezocatalysts, as its nature strongly affects the occurrence of acoustic cavitation and related physico-chemical phenomena [41,55]. Moreover, a better control and understanding of the acoustic field can enable its modulation to enhance piezocatalytic activity [31]. For this, it is important to accurately define and control setup variables such as reactor position within the ultrasonic bath (or location of ultrasonic horn within reactor), degassing of water, combination of ultrasound with other agitation methods, etc. However, this is not currently the norm in piezocatalysis research, although it is well known in sonochemistry research that such factors have a significant effect. These factors should be considered when designing experimental setups and procedures in piezocatalysis.

Ultrasonic power

The effect of applied power on piezocatalytic activity (Figure 2g) has been demonstrated by several studies [9,15,33]. However, higher electrical power applied to the transducers used in either ultrasonic baths or horns does not necessarily translate to greater acoustic power in the reaction environment [56]. For that reason, it is recommended to calorimetrically calibrate the ultrasonic system to determine the 'real' acoustic power [57] by dividing the measured power by either the sonication volume (W cm^{-3}) or the emitter surface area of the ultrasonic source (W cm^{-2}). This procedure would also help to understand the energy requirements and discuss benefits and disadvantages prior to scaling-up [58].

Temperature

Continuous sonication generally leads to a significant increase in temperature. Some studies tried to address this challenge by replacing the water in the ultrasonic bath or adding ice cubes/water during the experiment [12,17,32,59,60]. However, these approaches would significantly disturb the acoustic field, potentially affecting the reliability and reproducibility of the research. A thorough temperature control such as those used in sonochemistry [31] is therefore necessary in piezocatalysis research to not only avoid any contribution of pyrocatalysis [22,48] but also achieve and maintain a stable acoustic field.

Conclusions

Piezocatalysis indeed has the potential to become a 'green and sustainable' catalytic process, but only when the fundamental principles from piezoelectricity, electrochemistry and sonochemistry are considered and applied to fully understand how this new concept in catalysis works. For that to happen, research on piezocatalysis will not only need to adopt some of the practices of other fields such as piezoelectricity or sonochemistry but also address some of the challenges (e.g., better understanding of micro- and nano-scale piezoelectric phenomena) mentioned in this review.

Declaration of competing interest

The authors declare that they have no known competing financial interests or personal relationships that could have appeared to influence the work reported in this paper.

References

Papers of particular interest, published within the period of review, have been highlighted as:

* of special interest
** of outstanding interest

1. Zhou X, Shen B, Zhai J, Hedin N: **Reactive oxygenated species generated on iodide-doped $BiVO_4$/$BaTiO_3$ heterostructures with Ag/Cu nanoparticles by coupled piezophototronic effect and plasmonic excitation**. *Adv Funct Mater* 2021:202009594. https://doi.org/10.1002/adfm.202009594.

2. Peng F, Yin R, Liao Y, Xie X, Sun J, Xia D, He C: **Kinetics and mechanisms of enhanced degradation of ibuprofen by piezocatalytic activation of persulfate**. *Chem Eng J* 2020, **392**: 123818. https://doi.org/10.1016/j.cej.2019.123818.

3. Lin E, Kang Z, Wu J, Huang R, Qin N, Bao D: **$BaTiO_3$ nanocubes/cuboids with selectively deposited Ag nanoparticles: efficient piezocatalytic degradation and mechanism**. *Appl Catal, B* 2021, **285**:119823. https://doi.org/10.1016/j.apcatb.2020.119823.

4. Dai J, Shao N, Zhang S, Zhao Z, Long Y, Zhao S, Li S, Zhao C, Zhang Z, Liu W: **Enhanced piezocatalytic activity of $Sr_{0.5}Ba_{0.5}Nb_2O_6$ nanostructures by engineering surface oxygen vacancies and self-generated heterojunctions**. *ACS Appl Mater Interfaces* 2021, **13**:7259–7267. https://doi.org/10.1021/acsami.0c21202.

5. Chen L, Jia Y, Zhao J, Ma J, Wu Z, Yuan G, Cui X: **Strong piezocatalysis in barium titanate/carbon hybrid nanocomposites for dye wastewater decomposition**. *J Colloid Interface Sci* 2021, **586**:758–765. https://doi.org/10.1016/j.jcis.2020.10.145.

6. Zhang A, Liu Z, Xie B, Lu J, Guo K, Ke S, Shu L, Fan H: **Vibration catalysis of eco-friendly $Na_{0.5}K_{0.5}NbO_3$-based piezoelectric: an efficient phase boundary catalyst**. *Appl Catal, B* 2020, **279**: 119353. https://doi.org/10.1016/j.apcatb.2020.119353.

7. Wang P, Li X, Fan S, Chen X, Qin M, Long D, Tadé MO, Liu S: **Impact of oxygen vacancy occupancy on piezo-catalytic activity of $BaTiO_3$ nanobelt**. *Appl Catal, B* 2020, **279**:119340. https://doi.org/10.1016/j.apcatb.2020.119340.

8. Ning X, Hao A, Cao Y, Hu J, Xie J, Jia D: **Effective promoting piezocatalytic property of zinc oxide for degradation of organic pollutants and insight into piezocatalytic mechanism**. *J Colloid Interface Sci* 2020, **577**:290–299. https://doi.org/10.1016/j.jcis.2020.05.082.

9. Ling J, Wang K, Wang Z, Huang H, Zhang G: **Enhanced piezoelectric-induced catalysis of $SrTiO_3$ nanocrystal with well-defined facets under ultrasonic vibration**. *Ultrason Sonochem* 2020, **61**:104819. https://doi.org/10.1016/j.ultsonch.2019.104819.

10. Lin YT, Lai SN, Wu JM: **Simultaneous piezoelectrocatalytic hydrogen-evolution and degradation of water pollutants by**

quartz Microrods@Few-layered MoS_2 hierarchical heterostructures. *Adv Mater* 2020, **32**, e2002875. https://doi.org/10.1002/adma.202002875.

11. Lin E, Qin N, Wu J, Yuan B, Kang Z, Bao D: **$BaTiO_3$ nanosheets and caps grown on TiO_2 nanorod arrays as thin-film catalysts for piezocatalytic applications**. *ACS Appl Mater Interfaces* 2020, **12**:14005–14015. https://doi.org/10.1021/acsami.0c00962.

12. Lan S, Chen Y, Zeng L, Ji H, Liu W, Zhu M: **Piezo-activation of peroxymonosulfate for benzothiazole removal in water**. *J Hazard Mater* 2020, **393**:122448. https://doi.org/10.1016/j.jhazmat.2020.122448.

13. Biswas A, Saha S, Pal S, Jana NR: **TiO_2-Templated $BaTiO_3$ nanorod as a piezocatalyst for generating wireless cellular stress**. *ACS Appl Mater Interfaces* 2020, **12**:48363–48370. https://doi.org/10.1021/acsami.0c14965.

14. Bagchi B, Hoque NA, Janowicz N, Das S, Tiwari MK: **Re-useable self-poled piezoelectric/piezocatalytic films with exceptional energy harvesting and water remediation capability**. *Nano Energy* 2020, **78**:105339. https://doi.org/10.1016/j.nanoen.2020.105339.

15. ** Amiri O, Salar K, Othman P, Rasul T, Faiq D, Saadat M: **Purification of wastewater by the piezo-catalyst effect of $PbTiO_3$ nanostructures under ultrasonic vibration**. *J Hazard Mater* 2020, **394**:122514. https://doi.org/10.1016/j.jhazmat.2020.122514.
Several factors influencing the piezocatalytic degradation of organic contaminants in water was investigated. Experiments with different ultrasonic powers showed typical sonochemical effects of lower degradation efficiencies at high ultrasonic powers due to acoustic decoupling and bubble coalescence.

16. ** Yuan B, Wu J, Qin N, Lin E, Kang Z, Bao D: **Sm-doped $Pb(Mg_{1/3}Nb_{2/3})O_{3-x}PbTiO_3$ piezocatalyst: exploring the relationship between piezoelectric property and piezocatalytic activity**. *Appl Mater Today* 2019, **17**:183–192. https://doi.org/10.1016/j.apmt.2019.07.015.
This study mainly focused on the influence of piezoelectric properties (including poling) on the piezocatalytic performance via composition arrangement. The maximal piezocatalytic activity was achieved with a composition at the materials morphotropic phase boundary where the piezoelectric coefficient also reached its maximum.

17. Qian W, Zhao K, Zhang D, Bowen CR, Wang Y, Yang Y: **Piezoelectric material-polymer composite porous foam for efficient dye degradation via the piezo-catalytic effect**. *ACS Appl Mater Interfaces* 2019, **11**:27862–27869. https://doi.org/10.1021/acsami.9b07857.

18. * Wu J, Xu Q, Lin E, Yuan B, Qin N, Thatikonda SK, Bao D: **Insights into the role of ferroelectric polarization in piezocatalysis of nanocrystalline $BaTiO_3$**. *ACS Appl Mater Interfaces* 2018, **10**:17842–17849. https://doi.org/10.1021/acsami.8b01991.
One of the first studies considering the effect of poling on piezocatalytic activity. It was shown that poling $BaTiO_3$ piezocatalysts can significantly enhance the piezocatalytic activity.

19. Wu J, Qin N, Bao D: **Effective enhancement of piezocatalytic activity of $BaTiO_3$ nanowires under ultrasonic vibration**. *Nano Energy* 2018, **45**:44–51. https://doi.org/10.1016/j.nanoen.2017.12.034.

20. Huang X, Lei R, Yuan J, Gao F, Jiang C, Feng W, Zhuang J, Liu P: **Insight into the piezo-photo coupling effect of $PbTiO_3$/CdS composites for piezo-photocatalytic hydrogen production**. *Appl Catal, B* 2021, **282**:119586. https://doi.org/10.1016/j.apcatb.2020.119586.

21. Xu X, Xiao L, Wu Z, Jia Y, Ye X, Wang F, Yuan B, Yu Y, Huang H, Zou G: **Harvesting vibration energy to piezo-catalytically generate hydrogen through Bi_2WO_6 layered-perovskite**. *Nano Energy* 2020, **78**:105351. https://doi.org/10.1016/j.nanoen.2020.105351.

22. ** Thuy Phuong PT, Zhang Y, Gathercole N, Khanbareh H, Hoang Duy NP, Zhou X, Zhang D, Zhou K, Dunn S, Bowen C: **Demonstration of enhanced piezo-catalysis for hydrogen generation and water treatment at the ferroelectric Curie temperature**. *iScience* 2020, **23**:101095. https://doi.org/10.1016/j.isci.2020.101095.
This study investigated ferroelectric polarisation due to an applied stress or temperature change for both piezo- and pyrocatalytic H_2 generation and wastewater treatment. Experimental evidence for enhanced piezocatalytic water splitting and Rhodamine B degradation via excitation at the catalysts' Curie temperature T_c. One of few studies that considered a systematic experimental set-up and approach similar to that widely accepted in sonochemistry.

23. Feng W, Yuan J, Zhang L, Hu W, Wu Z, Wang X, Huang X, Liu P, Zhang S: **Atomically thin ZnS nanosheets: facile synthesis and superior piezocatalytic H_2 production from pure H_2O**. *Appl Catal, B* 2020, **277**:119250. https://doi.org/10.1016/j.apcatb.2020.119250.

24. Feng W, Yuan J, Gao F, Weng B, Hu W, Lei Y, Huang X, Yang L, Shen J, Xu D, *et al.*: **Piezopotential-driven simulated electrocatalytic nanosystem of ultrasmall MoC quantum dots encapsulated in ultrathin N-doped graphene vesicles for superhigh H_2 production from pure water**. *Nano Energy* 2020, **75**:104990. https://doi.org/10.1016/j.nanoen.2020.104990.

25. Wang YC, Wu JM: **Effect of controlled oxygen vacancy on H_2-production through the piezocatalysis and piezophototronics of ferroelectric R3C $ZnSnO_3$ nanowires**. *Adv Funct Mater* 2019, **30**:1907619. https://doi.org/10.1002/adfm.201907619.

26. Xia D, Tang Z, Wang Y, Yin R, He H, Xie X, Sun J, He C, Wong PK, Zhang G: **Piezo-catalytic persulfate activation system for water advanced disinfection: process efficiency and inactivation mechanisms**. *Chem Eng J* 2020, **400**:125894. https://doi.org/10.1016/j.cej.2020.125894.

27. Vatlin IS, Chernozem RV, Timin AS, Chernova AP, Plotnikov EV, Mukhortova YR, Surmeneva MA, Surmenev RA: **Bacteriostatic effect of piezoelectric poly-3-hydroxybutyrate and polyvinylidene fluoride polymer films under ultrasound treatment**. *Polymers (Basel)* 2020, **12**:12010240. https://doi.org/10.3390/polym12010240.

28. Sharma M, Vaish R: **Vibration energy harvesting for degradation of dye and bacterial cells using cement-based $Ba_{0.85}Ca_{0.15}Zr_{0.1}Ti_{0.90}O_3$ composites**. *Mater Today Commun* 2020, **25**. https://doi.org/10.1016/j.mtcomm.2020.101592.

29. Sharma M, Singh VP, Kumar S, Vaish R: **Multicatalytic behavior of $Ba_{0.85}Ca_{0.15}Ti_{0.9}$ $Zr_{0.1}O_3$ ceramics for pharmaceutical/dye/bacterial treatments**. *J Appl Phys* 2020, **127**:135103. https://doi.org/10.1063/1.5141813.

30. Sharma M, Singh G, Vaish R: **Dye degradation and bacterial disinfection using multicatalytic $BaZr_{0.02}Ti_{0.98}O_3$ ceramics**. *J Am Ceram Soc* 2020, **103**:4774–4784. https://doi.org/10.1111/jace.17171.

31. * Bößl F, Comyn TP, Cowin PI, García-García FR, Tudela I: **Piezocatalytic degradation of pollutants in water: importance of catalyst size, poling and excitation mode**. *Chem Eng J Adv* 2021, **7**:100133. https://doi.org/10.1016/j.ceja.2021.100133.
This study sheds some light on controversial situations surrounding piezocatalysis research. The effect of piezocatalyst size, piezocatalyst poling/unpoling and agitation mode on aqeuous Rhodamine B is investigated by both experimental and theoretical approaches. Results highlight the importance of sonochemistry, sonocatalysis and electrochemistry for piezocatalysis research.

32. Raju TD, Veeralingam S, Badhulika S: **Polyvinylidene fluoride/$ZnSnO_3$ nanocube/Co_3O_4 nanoparticle thermoplastic composites for ultrasound-assisted piezo-catalytic dye degradation**. *ACS Appl Nano Materials* 2020, **3**:4777–4787. https://doi.org/10.1021/acsanm.0c00771.

33. * Liu D, Jin C, Shan F, He J, Wang F: **Synthesizing $BaTiO_3$ nanostructures to explore morphological influence, kinetics, and mechanism of piezocatalytic dye degradation**. *ACS Appl Mater Interfaces* 2020, **12**:17443–17451. https://doi.org/10.1021/acsami.9b23351.
In this work, three morphologies of $BaTiO_3$ piezocatalysts (nanocubes, nanofibers and nanoparticles) were investigated regarding their piezocatalytic efficiency for dye degradation. Nanofibers exhibited a higher piezocatalytic degradation performance attributed to a larger specific surface area, fine crystal size, and easier deformation due to their aspect ratio.

34. Koppenol WH, Stanbury DM, Bounds PL: **Electrode potentials of partially reduced oxygen species, from dioxygen to water**. *Free Radic Biol Med* 2010, **49**:317–322. https://doi.org/10.1016/j.freeradbiomed.2010.04.011.

35. Sharma VK: **Oxidation of inorganic contaminants by ferrates (VI, V, and IV)–kinetics and mechanisms: a review**. *J Environ Manag* 2011, **92**:1051–1073. https://doi.org/10.1016/j.jenvman.2010.11.026.

36. Zhu P, Chen Y, Shi J: **Piezocatalytic tumor therapy by ultrasound-triggered and $BaTiO_3$ -mediated piezoelectricity**. *Adv Mater* 2020, **32**, e2001976. https://doi.org/10.1002/adma.202001976.

37. Zhou X, Yan F, Wu S, Shen B, Zeng H, Zhai J: **Remarkable piezophoto coupling catalysis behavior of $BiO_X/BaTiO_3$ (X = Cl, Br, $Cl_{0.166}Br_{0.834}$) piezoelectric composites**. *Small* 2020, **16**, e2001573. https://doi.org/10.1002/smll.202001573.

38. Zhang J, Wang C, Bowen C: **Piezoelectric effects and electromechanical theories at the nanoscale**. *Nanoscale* 2014, **6**:13314–13327. https://doi.org/10.1039/c4nr03756a.

39. Qiu P, Park B, Choi J, Thokchom B, Pandit AB, Khim J: **A review on heterogeneous sonocatalyst for treatment of organic pollutants in aqueous phase based on catalytic mechanism**. *Ultrason Sonochem* 2018, **45**:29–49. https://doi.org/10.1016/j.ultsonch.2018.03.003.

40. Hayyan M, Hashim MA, AlNashef IM: **Superoxide ion: generation and chemical implications**. *Chem Rev* 2016, **116**:3029–3085. https://doi.org/10.1021/acs.chemrev.5b00407.

41. González-García J, Sáez V, Tudela I, Díez-Garcia MI, Deseada Esclapez M, Louisnard O: **Sonochemical treatment of water polluted by chlorinated organocompounds. A review**. *Water* 2010, **2**:28–74. https://doi.org/10.3390/w2010028.

42. Sharma M, Vaish R, Ibrahim SM: **Effect of poling condition on piezocatalysis activity of $BaTiO_3$-cement composites**. *Mater Lett* 2020, **280**:128583. https://doi.org/10.1016/j.matlet.2020.128583.

43. Tu S, Guo Y, Zhang Y, Hu C, Zhang T, Ma T, Huang H: **Piezocatalysis and piezo-photocatalysis: catalysts classification and modification strategy, reaction mechanism, and practical application**. *Adv Funct Mater* 2020, **30**:2005158. https://doi.org/10.1002/adfm.202005158.

44. Nie Q, Xie Y, Ma J, Wang J, Zhang G: **High piezo–catalytic activity of ZnO/Al_2O_3 nanosheets utilizing ultrasonic energy for wastewater treatment**. *J Clean Prod* 2020, **242**:118532. https://doi.org/10.1016/j.jclepro.2019.118532.

45. Laurenti M, Garino N, Canavese G, Hernandez S, Cauda V: **Piezo- and photocatalytic activity of ferroelectric ZnO:Sb thin films for the efficient degradation of rhodamine-beta dye pollutant**. *ACS Appl Mater Interfaces* 2020, **12**:25798–25808. https://doi.org/10.1021/acsami.0c03787.

46. Qian W, Yang W, Zhang Y, Bowen CR, Yang Y: **Piezoelectric materials for controlling electro-chemical processes**. *Nano-Micro Lett* 2020, **12**:149. https://doi.org/10.1007/s40820-020-00489-z.

47. Arnau A, Soares D: **Fundamentals of piezoelectricity**. In *Piezoelectric transducers and applications*. Edited by Vives AA, Ed, Berlin, Heidelberg: Springer; 2009:1–37.

48. You H, Ma X, Wu Z, Fei L, Chen X, Yang J, Liu Y, Jia Y, Li H, Wang F, *et al.*: **Piezoelectrically/pyroelectrically-driven vibration/cold-hot energy harvesting for mechano-/pyro- bi-catalytic dye decomposition of $NaNbO_3$ nanofibers**. *Nano Energy* 2018, **52**:351–359. https://doi.org/10.1016/j.nanoen.2018.08.004.

49. Ma W, Yao B, Zhang W, He Y, Yu Y, Niu J: **Fabrication of PVDF-based piezocatalytic active membrane with enhanced oxytetracycline degradation efficiency through embedding few-layer E-MoS2 nanosheets**. *Chem Eng J* 2021, **415**:129000. https://doi.org/10.1016/j.cej.2021.129000.

50. Abdollahi A, Domingo N, Arias I, Catalan G: **Converse flexoelectricity yields large piezoresponse force microscopy signals in non-piezoelectric materials**. *Nat Commun* 2019, **10**:1266. https://doi.org/10.1038/s41467-019-09266-y.

51. Martínez-Ayuso G, Friswell MI, Haddad Khodaparast H, Roscow JI, Bowen CR: **Electric field distribution in porous piezoelectric materials during polarization**. *Acta Mater* 2019, **173**:332–341. https://doi.org/10.1016/j.actamat.2019.04.021.

52. Wang Y, Wen X, Jia Y, Huang M, Wang F, Zhang X, Bai Y, Yuan G, Wang Y: **Piezo-catalysis for nondestructive tooth whitening**. *Nat Commun* 2020, **11**:1328. https://doi.org/10.1038/s41467-020-15015-3.

53. Cheng T, Gao W, Gao H, Wang S, Yi Z, Wang X, Yang H: **Piezocatalytic degradation of methylene blue, tetrabromobisphenol A and tetracycline hydrochloride using Bi4Ti3O12 with different morphologies**. *Mater Res Bull* 2021, **141**:111350. https://doi.org/10.1016/j.materresbull.2021.111350.

54. Yasui K: **Influence of ultrasonic frequency on multibubble sonoluminescence**. *J Acoust Soc Am* 2002, **112**:1405–1413. https://doi.org/10.1121/1.1502898.

55. Tudela I, Saez V, Esclapez MD, Diez-Garcia MI, Bonete P, Gonzalez-Garcia J: **Simulation of the spatial distribution of the acoustic pressure in sonochemical reactors with numerical methods: a review**. *Ultrason Sonochem* 2014, **21**:909–919. https://doi.org/10.1016/j.ultsonch.2013.11.012.

56. Tudela I, Zhang Y, Pal M, Kerr I, Cobley AJ: **Ultrasound-assisted electrodeposition of composite coatings with particles**. *Surf Coating Technol* 2014, **259**:363–373. https://doi.org/10.1016/j.surfcoat.2014.06.023.

57. Contamine RF, Wilhelm AM, Berlan J, Delmas H: **Power measurement in sonochemistry**. *Ultrason Sonochem* 1995, **2**:S43–S47. https://doi.org/10.1016/1350-4177(94)00010-p.

58. Neppolian B, Ashokkumar M, Tudela I, González-García J: **Hybrid sonochemical treatment of contaminated wastewater: sonophotochemical and sonoelectrochemical approaches. Part I: description of the techniques**. In *Advances in water treatment and pollution prevention*. Edited by Sharma SK, Sanghi R, Eds, London: Springer; 2012:267–302.

59. Singh G, Sharma M, Vaish R: **Transparent ferroelectric glass–ceramics for wastewater treatment by piezocatalysis**. *Commun Mater* 2020, **1**. https://doi.org/10.1038/s43246-020-00101-2.

60. Shi J, Zeng W, Dai Z, Wang L, Wang Q, Lin S, Xiong Y, Yang S, Shang S, Chen W, *et al.*: **Piezocatalytic foam for highly efficient degradation of aqueous organics**. *Small Sci* 2020, **1**:2000011. https://doi.org/10.1002/smsc.202000011.

2 Importance of catalyst size, poling and excitation mode

2.1 Introduction

As discussed in the previous chapter, the majority of studies available in the literature used ultrasound for the excitation of piezocatalysts without considering a systematic approach in their experimental set-ups and procedures [1-5]. So far, small reactors with little information on the location or depth within the ultrasonic bath have been used [1-3, 5, 6], even though such information is essential to control and ensure reproducibility of the acoustic field. Besides this, other factors such as temperature control and calorimetric calibrations that are also critical for the reproducibility and comparability of results are often not considered.

Therefore, the present study aimed to understand the effect of catalyst size, poling and excitation mode on the piezocatalytic process, and it tried to do so by using a new theoretical and experimental approach that systematically took into account all the issues previously pointed out. A Finite Element Model (FEM) was developed to simulate the piezoelectric polarisation of freely suspended particles under ultrasound. The experimental approach followed common practice and knowledge from sonochemistry, involving a precise control of reaction temperature, acoustic power, reactor size and position within the ultrasonic bath. In addition to this, it was decided to move away from the small-scale ultrasonic reactors currently used in piezocatalytic research since sonochemistry experts have recognised that larger-scale ultrasonic reactors differ significantly from those used at laboratory scale [7-11]. Given this intrinsic problem with ultrasound-assisted research, it is difficult to transfer sonochemical effects from one reactor to another. A good example of this is a study on the sonoelectrochemical degradation of trichloroacetic acid, where no significant contributions of ultrasound were observed in the smaller scale reactor, but a remarkable effect was noticed at a larger pre-pilot reactor [12]. While in this particular case the contribution of ultrasound was beneficial for the overall process, the opposite may be true in piezocatalytic research.

Significant piezocatalytic activity has been reported when using small scale reactors (<100 mL) with very low sonochemical contributions. However, due to the complexity of scaling up ultrasound-assisted processes, similar observations of piezocatalytic activity at larger scale may not be as straightforward. It is therefore essential to conduct piezocatalytic research using larger scale reactors in order to assess the potential of piezocatalysis as a new ecologically friendly technology. It was therefore decided to us a 1000 mL reactor for this study.

To also minimise the impact of other potential factors such as adsorption as well as ensuring a true piezoelectric nature of the used catalyst, a commercially available piezoelectric material, potassium bismuth titanate-bismuth ferrite lead titanate (BF-KBT-PT), was selected as the piezocatalyst for this study. BF-KBT-PT was a preferred choice due to its high piezoelectric properties (d_{33} and d_{31} values of 100 pC/N and −40 pC/N) as well as exhibiting high coercive stress [13, 14]. Due to this high coercive stress BF-KBT-PT is able to maintain the piezoelectric effect even after undergoing stress-inducing processes such as grinding and sieving into fine particles, allowing for an easy and cost-effective preparation of the piezocataysts. Besides this, BF-KBT-PT is a very dense solid with no porosity and poor adsorbent behaviour, ensuring that any degradation in RhB was due to either piezocatalytic or sonochemical/sonocatalytical effects and not due to dye adsorption onto the catalyst.

2.2 Discussion highlights and conclusions

The present study demonstrated that piezocatalysis is a more complex phenomenon than previously assumed in the literature and emphasised on the importance of thorough control experiments to better distinguish between simultaneously occurring ultrasound-assisted phenomena.

The developed FEM model with freely suspended particles overcomes the unrealistic assumption of fixed and grounded particles in previously reported FEM simulations [3, 15, 16].

Even though, this new FEM model is more realistic than those previously reported in the literature, it still has some limitations e.g. perfectly smooth surfaces with no roughness, use of linear acoustics and 2D geometries. Nevertheless, the FEM simulations indicated that the generation of superoxide and hydroxyl radicals via the suggested redox reactions is unlikely to occur from ‘bulk’ piezoelectric polarisation of BF-KBT-PT catalysts. However, the experimental results using BF-KBT-PT catalysts did not only show RhB degradation but also confirmed the participation of superoxide and hydroxyl in the radicalary degradation. The results for the effect of catalyst size also challenged the concept of 'bulk' piezoelectric polarisation since the best overall RhB degradation was achieved with the smallest piezocatalyst. This indicates that localised piezoelectric polarisation at micro- and nano features at the catalyst surface may be more important for the piezocatalytic process.

One of the most significant aspects of this research was the utilisation of a larger-scale reactor (1000 mL). While the experimental findings did demonstrate some piezocatalytic activity, it was far less than the sonochemical contribution to the overall RhB degradation. This is in contrast to most of the work on piezocatalysis available in the literature, which showed strong piezocatalytic activity with minimal sonochemical effects in small-scale reactors (<100 mL) [1-6]. However, the experimental results in this study are consistent with previous sonochemical studies conducted on a larger scale [17], highlighting the potential implications of scaling up the piezocatalytic process for future industrial applications.

Nevertheless, further research is needed to fully elucidate the piezocatalytic phenomenon and its driving factors. One reason why the used piezocatalysts might not have achieved a sufficient ‘bulk’ polarisation could be the operating frequency and power of the ultrasonic source used in this study. It is widely assumed that piezoelectric materials achieve a better piezoelectric response when operated close to their resonance frequency. Similarly, sonochemical effects are also known to depend on the operating frequency and power [18-21]. It is therefore essential from both sonochemical and piezoelectric point of view to systematically evaluate the effect of ultrasonic frequency and power on the piezocatalytic process.

To gain a deeper understanding of the research outcomes and their significance, all results and a more comprehensive discussion can be found in *Piezocatalytic degradation of pollutants in water: Importance of catalyst size, poling and excitation mode* published in *Chemical Engineering Journal Advances*, which constitutes Chapter 2 of this thesis.

2.3 References

[1] D. Liu, Y. Song, Z. Xin, G. Liu, C. Jin, F. Shan

High-piezocatalytic performance of eco-friendly $(Bi_{1/2}Na_{1/2})TiO_3$-based nanofibers by electrospinning

Nano Energy, 65 (2019), 10.1016/j.nanoen.2019.104024

[2] F. Peng, R. Yin, Y. Liao, X. Xie, J. Sun, D. Xia, C. He

Kinetics and mechanisms of enhanced degradation of ibuprofen by piezo-catalytic activation of persulfate

Chemical Engineering Journal, 392 (2020), 10.1016/j.cej.2019.123818

[3] J. Wu, N. Qin, D. Bao

Effective enhancement of piezocatalytic activity of $BaTiO_3$ nanowires under ultrasonic vibration

Nano Energy, 45 (2018), 44-51, 10.1016/j.nanoen.2017.12.034

[4] J. Wu, Q. Xu, E. Lin, B. Yuan, N. Qin, S.K. Thatikonda, D. Bao

Insights into the Role of Ferroelectric Polarization in Piezocatalysis of Nanocrystalline $BaTiO_3$

ACS Appl Mater Interfaces, 10 (21) (2018), 17842-17849, 10.1021/acsami.8b01991

[5] D. Xia, Z. Tang, Y. Wang, R. Yin, H. He, X. Xie, J. Sun, C. He, P.K. Wong, G. Zhang

Piezo-catalytic persulfate activation system for water advanced disinfection: Process efficiency and inactivation mechanisms

Chemical Engineering Journal, 400 (2020), 10.1016/j.cej.2020.125894

[6] S. Masimukku, Y.-C. Hu, Z.-H. Lin, S.-W. Chan, T.-M. Chou, J.M. Wu

High efficient degradation of dye molecules by PDMS embedded abundant single-layer tungsten disulfide and their antibacterial performance

Nano Energy, 46 (2018), 338-346, 10.1016/j.nanoen.2018.02.008

[7] N. Gondrexon, V. Renaudin, C. Petrier, P. Boldo, A. Bernis, Y. Gonthier

Degradation of pentachlorophenol aqueous solutions using a continuous flow ultrasonic reactor: experimental performance and modelling

Ultrason Sonochem, 5 (4) (1999), 125-31, 10.1016/s1350-4177(98)00041-8

[8] G. Cravotto, P. Cintas

Power ultrasound in organic synthesis: moving cavitational chemistry from academia to innovative and large-scale applications

Chem Soc Rev, 35 (2) (2006), 180-96, 10.1039/b503848k

[9] P.R. Gogate, V.S. Sutkar, A.B. Pandit

Sonochemical reactors: Important design and scale up considerations with a special emphasis on heterogeneous systems

Chemical Engineering Journal, 166 (3) (2011), 1066-1082, 10.1016/j.cej.2010.11.069

[10] P.R. Gogate, A.B. Pandit

Sonochemical reactors: scale up aspects

Ultrason Sonochem, 11 (3-4) (2004), 105-17, 10.1016/j.ultsonch.2004.01.005

[11] S. Manickam, M. Ashokkumar

Cavitation: A Novel Energy-Efficient Technique for the Generation of Nanomaterials (1st ed.), Jenny Stanford Publishing, New York, 2014

[12] M.D. Esclapez, V. Saez, D. Milan-Yanez, I. Tudela, O. Louisnard, J. Gonzalez-Garcia

Sonoelectrochemical treatment of water polluted with trichloroacetic acid: from sonovoltammetry to pre-pilot plant scale

Ultrason Sonochem, 17 (6) (2010), 1010-20, 10.1016/j.ultsonch.2009.11.009

[13] J. Bennett, A.J. Bell, T.J. Stevenson, T.P. Comyn

Tailoring the structure and piezoelectric properties of $BiFeO_3$-$(K_{0.5}Bi_{0.5})TiO_3$–$PbTiO_3$ ceramics for high temperature applications

Applied Physics Letters, 103 (15) (2013), 10.1063/1.4824652

[14] T. Stevenson, D.G. Martin, P.I. Cowin, A. Blumfield, A.J. Bell, T.P. Comyn, P.M. Weaver

Piezoelectric materials for high temperature transducers and actuators

Journal of Materials Science: Materials in Electronics, 26 (12) (2015), 9256-9267, 10.1007/s10854-015-3629-4

[15] C. Jin, D. Liu, J. Hu, Y. Wang, Q. Zhang, L. Lv, F. Zhuge

The role of microstructure in piezocatalytic degradation of organic dye pollutants in wastewater

Nano Energy, 59 (2019), 372-379, 10.1016/j.nanoen.2019.02.047

[16] D. Yu, Z. Liu, J. Zhang, S. Li, Z. Zhao, L. Zhu, W. Liu, Y. Lin, H. Liu, Z. Zhang

Enhanced catalytic performance by multi-field coupling in $KNbO_3$ nanostructures: Piezo-photocatalytic and ferro-photoelectrochemical effects

Nano Energy, 58 (2019), 695-705, 10.1016/j.nanoen.2019.01.095

[17] O. Louisnard, J. Gonzalez-Garcia, I. Tudela, J. Klima, V. Saez, Y. Vargas-Hernandez

FEM simulation of a sono-reactor accounting for vibrations of the boundaries

Ultrason Sonochem, 16 (2) (2009), 250-9, 10.1016/j.ultsonch.2008.07.008

[18] R.J. Wood, J. Lee, M.J. Bussemaker

A parametric review of sonochemistry: Control and augmentation of sonochemical activity in aqueous solutions

Ultrason Sonochem, 38 (2017), 351-370, 10.1016/j.ultsonch.2017.03.030

[19] Z. Eren, N.H. Ince

Sonolytic and sonocatalytic degradation of azo dyes by low and high frequency ultrasound

J Hazard Mater, 177 (1-3) (2010), 1019-24, 10.1016/j.jhazmat.2010.01.021

[20] M.H. Abdurahman, A.Z. Abdullah, N.F. Shoparwe

A comprehensive review on sonocatalytic, photocatalytic, and sonophotocatalytic processes for the degradation of antibiotics in water: Synergistic mechanism and degradation pathway

Chemical Engineering Journal, 413 (2021), 10.1016/j.cej.2020.127412

[21] E.A. Serna-Galvis, J. Lee, F. Hernández, A.M. Botero-Coy, R.A. Torres-Palma

Sonochemical Advanced Oxidation Processes for the Removal of Pharmaceuticals in Wastewater Effluents

Removal and Degradation of Pharmaceutically Active Compounds in Wastewater Treatment2020, pp. 349-381

Chemical Engineering Journal Advances 7 (2021) 100133

Contents lists available at ScienceDirect

Chemical Engineering Journal Advances

journal homepage: www.elsevier.com/locate/ceja

Piezocatalytic degradation of pollutants in water: Importance of catalyst size, poling and excitation mode

Franziska Bößl[a,b,*], Tim P. Comyn[c], Peter I. Cowin[c], Francisco R. García-García[b], Ignacio Tudela[a,b,*]

[a] Edinburgh Electrochemical Engineering Group (e^3 Group), The University of Edinburgh, Edinburgh EH9 3FB, UK
[b] Institute for Materials and Processes, School of Engineering, The University of Edinburgh, Edinburgh EH9 3FB, UK
[c] Ionix Advanced Technologies Ltd., 3M Buckley Innovation Centre, Firth Street, Huddersfield HD1 3BD, UK

ARTICLE INFO

Keywords:
Piezocatalysis
Sonocatalysis
Sonochemistry
Ultrasonic vibration
Dye degradation
Piezoelectric materials

ABSTRACT

Piezocatalysis is a promising area of research that would enable new advances in environmental catalytic processes independent of energy sources such as light or electricity. To shed more light on this field, theoretical and experimental studies were conducted using poled and unpoled BF-KBT-PT ceramics as catalysts in order to investigate the effect that piezocatalyst size, piezocatalyst poling/unpoling and agitation mode have on the degradation of a dye, Rhodamine *B* (RhB), in water. While an apparently contradictory trend in the theoretical and experimental results was observed in relation to piezocatalyst size, poling indeed had a significant effect on the degradation of RhB, indicating that a complex combination of different phenomena such as 'top-to-bottom' electric potential difference due to 'bulk' piezoelectric polarisation, nanoscale piezoelectric response and sonocatalysis may result in the overall catalytic degradation of RhB. However, the greatest contribution to the degradation of the dye would come from sonochemistry, as ultrasound in absence of a catalyst already achieved a remarkable degradation of RhB. This study therefore demonstrates the complexity of piezocatalysis, and why other phenomena besides bulk piezoelectric polarisation of catalysts must be taken into account in piezocatalysis research.

1. Introduction

Piezocatalysis is a new research area within the broad field of catalysis that has attracted significant attention in recent years, as it would take advantage of the polarisation developed by a piezoelectric material, subjected to an applied mechanical stress, to conduct redox reactions at the surface of said piezoelectric material in order to remove recalcitrant pollutants from water [1–3]. Piezocatalysis therefore has a strong potential as a new green catalysis area where redundant system vibrations (e.g. mechanical vibrations of exhaust systems or chemical reactors) could be used not only to enhance well established catalytic phenomena such as photocatalysis, but also open the gate to new catalytic routes independent of energy sources such as light or electricity. A good example of this is the research conducted is the removal of dyes in aqueous solutions with suspended piezocatalysts, which were 'polarised' by ultrasonic irradiation [4–7].

For piezocatalysis to reach its potential, an efficient use of mechanical energy (e.g. acoustic field) to reduce the activation energy of the chemical reactions of interest must take place. To achieve this, one must fully understand the physico-chemical factors behind it, and account for all the other physical and chemical phenomena that could also influence the overall catalytic process. One of this factors would be the piezoelectric behaviour of the material, which would require the understanding of the effect of poling or unpoling [8,9]. However, only a few studies have slightly considered the poled/unpoled nature of piezocatalysts in the past [5,10–12], even though it is clear that poling (or the lack of) should be a factor that would significantly contribute to a better understanding of how piezocatalysis works and whether other phenomena besides piezoelectricity may also be important.

The general trend in piezocatalysis has been to assume that the piezocatalytic degradation of dyes originates from redox reactions caused by 'top-to-bottom' electric potential difference experienced by the piezocatalyst particles under an ultrasonic field [5,13–15]. According to some of the basic principles of piezoelectricity [16–19], piezocatalysts should experience a 'top-to-bottom' electric potential difference according to the following equation under a certain external stress (in this case, an acoustic wave):

$$V_p = \frac{d_{ij}\sigma_j w_i}{\varepsilon_0 \varepsilon_{r,i}} \quad (1)$$

where V_p is the piezoelectric open-circuit potential, σ_j is the applied stress in j direction, d_{ij} is the piezoelectric charge coefficient, w_i the length of the piezocatalyst in i direction of polarisation, $\varepsilon_{r,i}$ is the relative

* Corresponding authors.
E-mail addresses: (F. Bößl), (I. Tudela).

https://doi.org/10.1016/j.ceja.2021.100133
Received 19 January 2021; Received in revised form 31 May 2021; Accepted 1 June 2021

permittivity in i dimension and ε_0 represents the electrical permittivity of free space. Eq. (1) predicts that, the larger the particle, the greater the 'top-to-bottom' electric field it experiences. However, the vast majority of research in this field has focused on exploring nano-scale piezocatalysts [1,7,13,20,21], when it is clear that the 'top-to-bottom' electric potential difference should increase if using piezocatalysts with larger sizes.

Nearly all of the published studies make use of ultrasonic baths to 'excite' piezocatalysts by setting an ultrasonic field within the treated aqueous solutions [5,6,21–23]. However, most of these studies did not follow a systematic approach towards the design of the experimental set-up and procedures:

- Use of small 'reactors' (e.g. <100 mL beakers or vials containing the solutions to be treated, which generally consist of water containing a dye and the piezocatalyst of choice) with little to no information regarding location and depth within the ultrasonic bath and whether that exact same location was used in all experiments [5,6,21–24]. It is well known in the field of sonochemistry that the presence and location of any object will have a strong effect on the acoustic field within an ultrasonic bath [25], hence why it is extremely important to control it accurately.
- Lack of consideration for factors such as temperature control during ultrasonication or ultrasonic power calibration [5,6,21–24,26,27]. Again, it is well known in the field of sonochemistry that these factors are critical to effectively characterise any type of 'sonoreactor' [28] and ensure reproducibility and comparability of research.

To shed some light on this apparently controversial situation surrounding piezocatalysis research, the present study tackles those issues previously mentioned by investigating the effect that piezocatalyst size, piezocatalyst poling/unpoling and agitation mode have on the degradation of a dye (RhB) in water, and it does so both theoretically and experimentally:

- Theoretically, by conducting Finite Elements Method (FEM) simulations of the polarisation of suspended piezocatalysts in an ultrasonically irradiated aqueous solution under realistic conditions.
- Experimentally, by taking a systematic approach where aspects such as reactor size and location within the ultrasonic bath, its ultrasonic power and temperature are strictly controlled.

The results here presented demonstrate that the catalytic degradation of RhB was not only caused by the 'top-to-bottom' electric potential difference due to the 'bulk' polarisation experienced by the piezocatalyst, as phenomena such as nanoscale piezoelectricity on micro- and nano-structured surfaces and sonocatalysis would also occur in both poled and unpoled piezocatalysts. Moreover, another phenomenon such as sonochemistry made a significant contribution to the degradation of the dye, demonstrating the complexity of the overall degradation process and highlighting why other phenomena must be taken into account when studying piezocatalysis.

2. Materials and methods

2.1. Catalysts

A commercially available piezoelectric material for high temperature piezoelectric applications, potassium bismuth titanate-bismuth ferrite lead titanate (BF-KBT-PT), was used to fabricate the catalysts for this study. BF-KBT-PT, which was supplied by Ionix Advanced Technologies Ltd., was synthesised by conventional solid-state synthesis following the same approach previously described by the authors [29,30]. Whereas other piezoelectric materials such as lead zirconate titanate (PZT) can readily become unpoled and lose its bulk piezoelectric properties as a result of applied stress [31], the high coercive stress of BF-KBT-PT piezoelectric ceramics allows for the maintenance of the piezoelectric effect, even after grinding into small particles.

Two types of this piezoelectric material were considered in order to verify whether any catalytic activity observed could be attributed to 'top-to-bottom' electric potential differences caused by bulk polarisation of the piezocatalysts (i.e. what has widely considered as the general mechanism behind piezocatalysis) or any other phenomena (e.g. sonochemistry, sonocatalysis):

i Poled BF-KBT-PT, which did exhibit a 'true' bulk piezoelectric behaviour (d_{33} and d_{31} values of 100 pC/N and −40 pC/N, respectively).
ii Unpoled BF-KBT-PT, which did not experience any bulk piezoelectricity at all (d_{33} and d_{31} values of 0 pC/N).

Both poled (P) and unpoled (UP) BF-KBT-PT catalysts were prepared from poled and unpoled piezoceramics discs of the same material. The only difference between the poled and unpoled BF-KBT-PT piezoceramics discs was that the unpoled piezoceramic discs were depoled at a temperature above the Curie point. The BF-KBT-PT piezoceramic disc were first broken down into small pieces by hammering, and then manually ground into fine particles with a pestle and mortar. The fine particles were then sieved to obtain four different particle size distributions in order to study any potential effect of piezocatalyst size on the performance of the degradation process: (i) <63 μm (P63 and UP63), (ii) 63–125 μm (P125), (iii) 125–250 μm (P250) and (iv) 250–500 μm (P500).

The existence of the piezoelectric effect in ground, poled, materials, was proven empirically with a Berlincourt metre (APC International) by aligning the unelectroded particles in the metre in various orientations (e.g. -35, −42, −47 or +143 pC/N). The unpoled materials displayed zero piezoelectric output (0 pC/N) in the Berlincourt metre using the same method. The crystalline structure of poled and unpoled BF-KBT-PT catalysts was determined by X-ray diffraction (XRD, Bruker D8) with Cu Kα radiation. The surface structure and composition was determined by focused ion beam-scanning electron microscopy (FIB-SEM, Zeiss Gemini 2 crossbeam 550) with an energy dispersive X-ray spectrometer (EDS).

2.2. FEM simulations

Previous studies in the literature have unrealistically assumed that piezocatalysts were fixed and grounded under single forces defined in some of the solid boundaries of the piezocatalyst [23,32–34]. For this reason, a new FEM model was developed to theoretically evaluate the polarisation experienced by the poled piezocatalysts in a liquid being irradiated with ultrasound.

The new FEM model couples the acoustic field in the liquid with the vibration of a single piezocatalytic particle and its piezoelectric response using COMSOL Multiphysics 5.5. In the model, the piezocatalyst remains 'freely' suspended in the liquid to better reflect the real conditions under which piezocatalysts have been ultrasonically irradiated in all the experimental studies found in the literature. A detailed explanation of the physics implemented in the model, boundary conditions and piezocatalyst properties can be found in the Supplementary Material.

Although the FEM simulations here presented are significantly more realistic than those previously published in the literature [20,23,32,34], they still have some simplifications that should be pointed out:

i 2D geometries (instead of 3D)
ii Use of linear acoustics: the acoustic field inside an ultrasonic bath is non-linear due to the existence of cavitation. Not accounting for asymmetrical collapses near the surface may overlook localised high pressures result in high-degree of localised polarisation. Wu et al. tried to account for this phenomenon in their FEM simulations to a certain extent [23].
iii Perfectly smooth surfaces with no roughness.

Nevertheless, we must point out that these simplifications should not result in significant quantitative and qualitative differences between the simulated and *real* 'top-to-bottom' electric potential difference experienced by the particles.

2.3. Experimental set-up

All experiments were conducted in a 1000 mL beaker containing a 5 mg L^{-1} RhB aqueous solution and immersed in an ultrasonic bath (Ultrawave QS12) with an operating frequency of 32–38 kHz (Fig. S4a in Supplementary Material). The beaker was placed in the centre of the ultrasonic bath with a controlled depth (4 cm) and constant water level to ensure the reproducibility of the results. The temperature of the ultrasonic bath was controlled by a circulating water cooling system immersed in the bath to maintain the temperature of the RhB solution at 30 ± 2 °C. In those experiments where mechanical agitation was introduced, an overhead stirrer (SciQuip Basic 20) was used at 200 rpm to keep the poled and unpoled BF-KBT-PT catalysts suspended in the solution. The ultrasonic bath operating at full power was calibrated following the standard calorimetric method widely used in sonochemistry research [35]; the ultrasonic power was 12.2 ± 0.4 W L^{-1} in absence of mechanical agitation, and 14.3 ± 0.7 W L^{-1} in the presence of mechanical agitation when using the overhead stirrer. Prior to each experiment, the water in the ultrasonic bath was thoroughly degassed for 60 min to ensure a reproducible acoustic field inside the bath.

120 min\ blank (i.e. no catalyst) and piezocatalytic RhB degradation experiments were conducted under three different excitation methods: (i) mechanical agitation (MA) at 200 rpm, (ii) ultrasound at 12.2 ± 0.4 W L^{-1} (US), and (iii) the combination of mechanical agitation at 200 rpm and ultrasound at 14.3 ± 0.7 W L^{-1} (US + MA). In each experiment, 3 mL samples of the RhB aqueous solution were taken every 10 min with a 0.22 μm PTFE-syringe-filter. Each sample was then analysed by a UV-vis spectrophotometer (Shimadzu UV-3600 Plus) at the characteristic wavelength of 554 nm (Fig. S4b in Supplementary Material). For the catalytic RhB degradation experiments, 1 g of either poled (P) or unpoled (UP) BF-KBT-PT catalysts particles with different sizes (P63, UP63, P125, P250 and P500) were added to the RhB aqueous solution, which was stirred at 200 rpm for 30 min to ensure adsorption-desorption equilibrium was reached prior to every experiment (no changes were observed in the concentration of RhB due to adsorption on the catalysts in all cases). The non-porous, poor adsorbent nature of the material used here (see Supplementary Material for nitrogen adsorption isotherm analysis) was extremely important, as it ensured that the decrease in RhB concentration during piezocatalytic experiments was due to either piezocatalytical or sonochemical/sonocatalytical phenomena and not due to dye adsorption onto the catalyst. This is a rather controversial situation in other piezocatalysis studies where there was clear adsorption of the targeted pollutant onto the surface of the catalyst without definite proof of reaching adsorption equilibrium [24,36,37], which could potentially distort the results reported.

To further explore and confirm the importance of radicalary degradation routes on piezocatalysts, additional experiments were conducted with/without the smallest poled BF-KBT-PT piezocatalysts (P63) under combined ultrasound and mechanical agitation (US + MA) in the presence of several radical and charge scavengers: terephthalic acid (TA) 99.5%, benzoquinone (BQ) 99% and ethylenediaminetetraacetic acid (EDTA) disodium salt dihydrate 99%, all of them from ACROS Organics. TA, BQ and EDTA were selected due to their role as chemical traps for $^{\bullet}OH$ [38], $^{\bullet}O_2^-$ [39] and h^+ [40], respectively. The concentration of scavengers added was 10 mM for TA, 0.15 mM for BQ and 2 mM for EDTA.

3. Results

3.1. Effect of piezocatalyst size

As stated earlier, Eq. (1) predicts that, the larger the particle, the greater the 'top-to-bottom' electric field it experiences. This was confirmed by FEM simulations (Fig. 1; clips of the simulations are available as Supplementary Material) of four different poled BF-KBT-PT piezocatalysts with particle sizes analogous to piezocatalysts that were used in our subsequent experiments (P500, P250, P125 and P63). The largest simulated particle, with a height of 500 μm (Fig. 1a), achieved the greatest 'top-to-bottom' electric potential difference of 0.66 V. The smaller particles with heights of 250 μm (Fig. 1b), 125 μm (Fig. 1c) and 63 μm (Fig. 1d) experienced a 'top-to-bottom' potential difference of up to 0.33 V, 0.17 V and 0.08 V, respectively.

Following these FEM simulations, one would expect to observe the greatest degradation of RhB when the largest poled BF-KBT-PT piezocatalyst (P500) was used, and to that end, experiments with four different piezocatalyst sizes (P500, P250, P125 and P63) were conducted to confirm this. Prior to this though, a thorough characterisation was conducted in all the different poled BF-KBT-PT piezocatalysts to ensure that the main differential factor in all piezocatalysts was the size, hence ensuring a 'true' like-for-like comparison. FIB-SEM analysis was conducted to observe any potential differences in terms of size and shape (Fig. 2a–d) as well as surface structure (Fig. 2e–h), revealing that there was no significant difference between the different piezocatalytic particles except for their size: the poled BF-KBT-PT piezocatalysts generally presented a cuboid morphology with clearly distinguishable sizes of <63 μm (P63), 63–125 μm (P125), 125–250 μm (P250) and 250–500 μm (P500). EDS spectra (Fig. 4i–l) confirmed an identical composition for all the poled BF-KBT-PT piezocatalysts. XRD analysis (Fig. 4m) was conducted to evaluate the phase structure of the piezocatalysts. The BF-KBT-PT material used in this study exhibited peak splitting across most of the reflections (especially in the case of (110) planes), indicating phase co-existence [29]. Minor peak splitting in the {200} family characteristic of tetragonal materials was also observed, whereas no peak splitting was observed in the {111} phase, confirming that lattice distortion of the rhombohedral phase was negligible [29]. One noticeable characteristic in the XRD spectra for the different particles was the intensity of the peaks, which diminished as the particle size increased. However, the relative heights of the peaks were identical, confirming the virtually identical perovskite structure of the poled BF-KBT-PT piezocatalysts, where no visible secondary phase was observed [29]. The difference in intensity originated from the larger particles, which resulted in a rougher sample surface when conducting powder diffraction analysis. In summary, except for particle size, all the poled BF-KBT-PT piezocatalysts used in this part of the study were identical. Therefore, any potential differences observed in their piezocatalytic performance should primarily relate to their size.

The RhB degradation experiments (Fig. 3) conducted under combined ultrasound/mechanical agitation revealed that, whereas there was a slight trend of enhanced RhB degradation after 120 min with an increase in particle size (P500 piezocatalysts achieved an overall RhB degradation of around 85%, whilst P250 achieved 83% and P125 roughly 81%), the highest RhB degradation after 120 min was in fact achieved with the smallest piezocatalyst (P63 overall RhB degradation of nearly 90%). This did not only contradict the FEM simulations, but also raised the question of whether the increase in RhB degradation observed when using the poled BF-KBT-PT catalysts was primarily caused by piezocatalysis as it currently stands (i.e. 'top-to-bottom' electric potential difference caused by the bulk piezoelectric response of the piezocatalytic particle), or whether other catalytic phenomena may have a significant effect. To shed some light on this, it was decided to evaluate the effect of piezocatalyst poling/unpoling and agitation mode.

3.2. Effect of piezocatalyst poling/unpoling and excitation mode

To better understand the apparently contradicting results observed in the experiments conducted to investigate the effect of piezocatalyst size, it was decided to continue working with the smallest piezocatalyst (particle size of <63 μm), as it was the poled piezocatalyst (P63) that unexpectedly yielded the highest degradation of RhB. In this case though, the experiments would be compared with its equivalent in unpoled form (UP63). UP63 particles should experience negligible bulk polarisation due to the cancellation of dipoles oriented in different di-

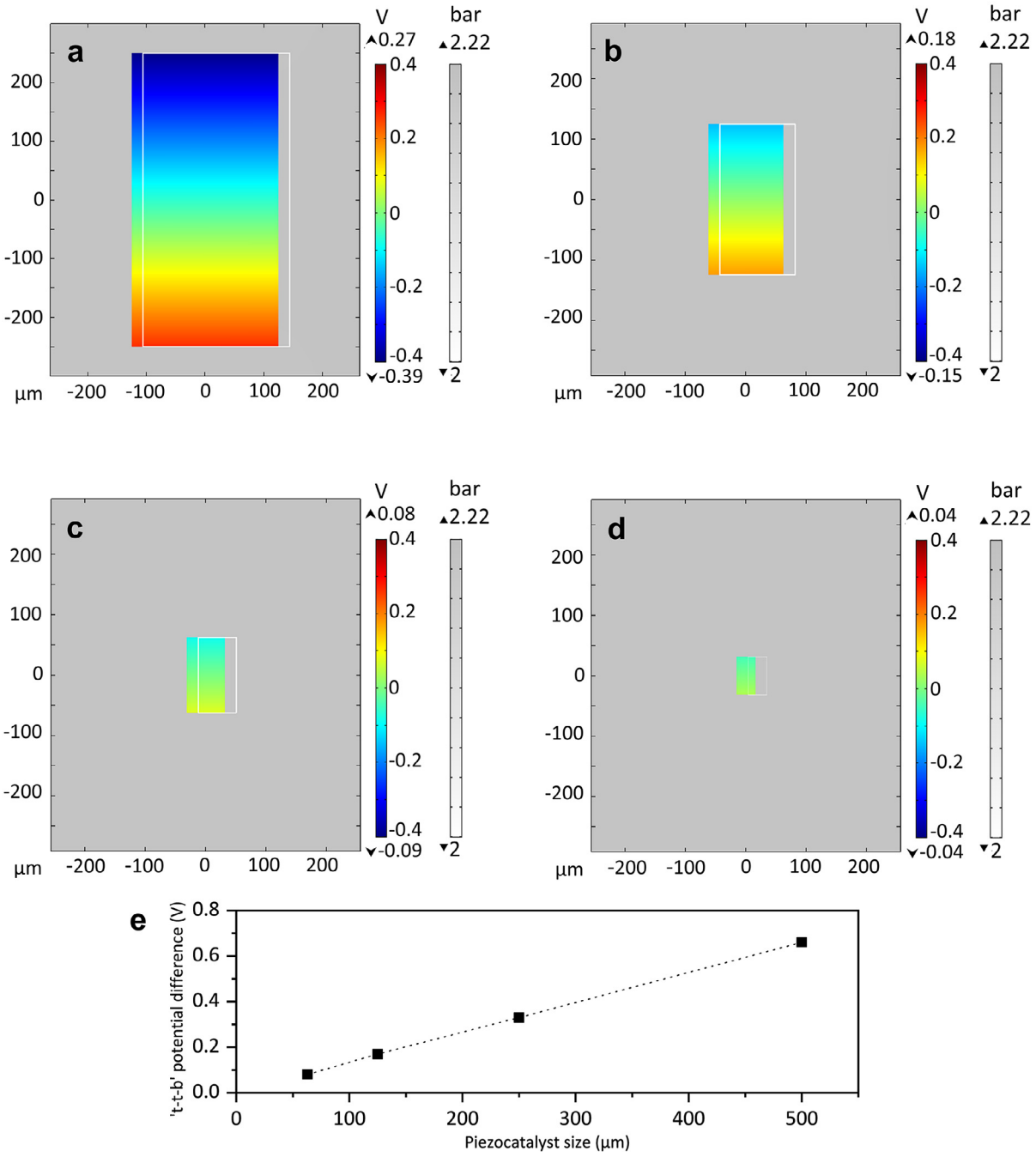

Fig. 1. FEM simulations of poled BF-KBT-PT catalysts suspended in a liquid (water) where an acoustic field (35 kHz) has been established: (a) particle size of 500 μm, (b) particle size of 250 μm, (c) particle size of 125 μm and (d) particle size of 63 μm, (e) 'top-to-bottom' ('t-t-b')potential difference as a function of piezocatalyst size.

rections, hence why no 'top-to-bottom' electric potential difference leading to piezocatalytic degradation of RhB should be observed; otherwise, it would be a clear indication that other phenomena might be at play. Prior to this though, a thorough characterisation was conducted on the UP63 catalysts to confirm that the main differential factor in this case was their piezoelectric nature, while the rest of the characteristics (i.e. surface structure, size and morphology) remained the same. Both poled and unpoled BF-KBT-PT particles (P63 and UP63) presented a cuboid morphology with sizes of <63 μm (Fig. 4a,b). No differences in terms of surface structure (Fig. 4c,d) nor material composition (Fig. 4e,f) were also observed, whereas only a minor difference was noticed in the XRD spectra, which was the intensity of the signal recorded for the UP63 catalysts (Fig. 4g). Nevertheless, that difference in signal could be attributed to the unpoled nature of the UP63 particles; the relative height of the peaks in the UP63 samples was the same as that of the peaks in the P63 samples, indicating that both UP63 and P63 presented the same phase structure. These results again confirmed that, with the exception of their poled/unpoled nature (i.e. piezoelectric/non-piezoelectric, respectively), both P63 and UP63 catalysts were identical, hence ensuring a like-for-like comparison.

Fig. 5 displays the normalised concentration of RhB during different degradation experiments conducted in presence/absence of poled (P63) and unpoled (UP63) BF-KBT-PT catalysts under different agitation modes. Under mechanical agitation in absence of ultrasound, no RhB

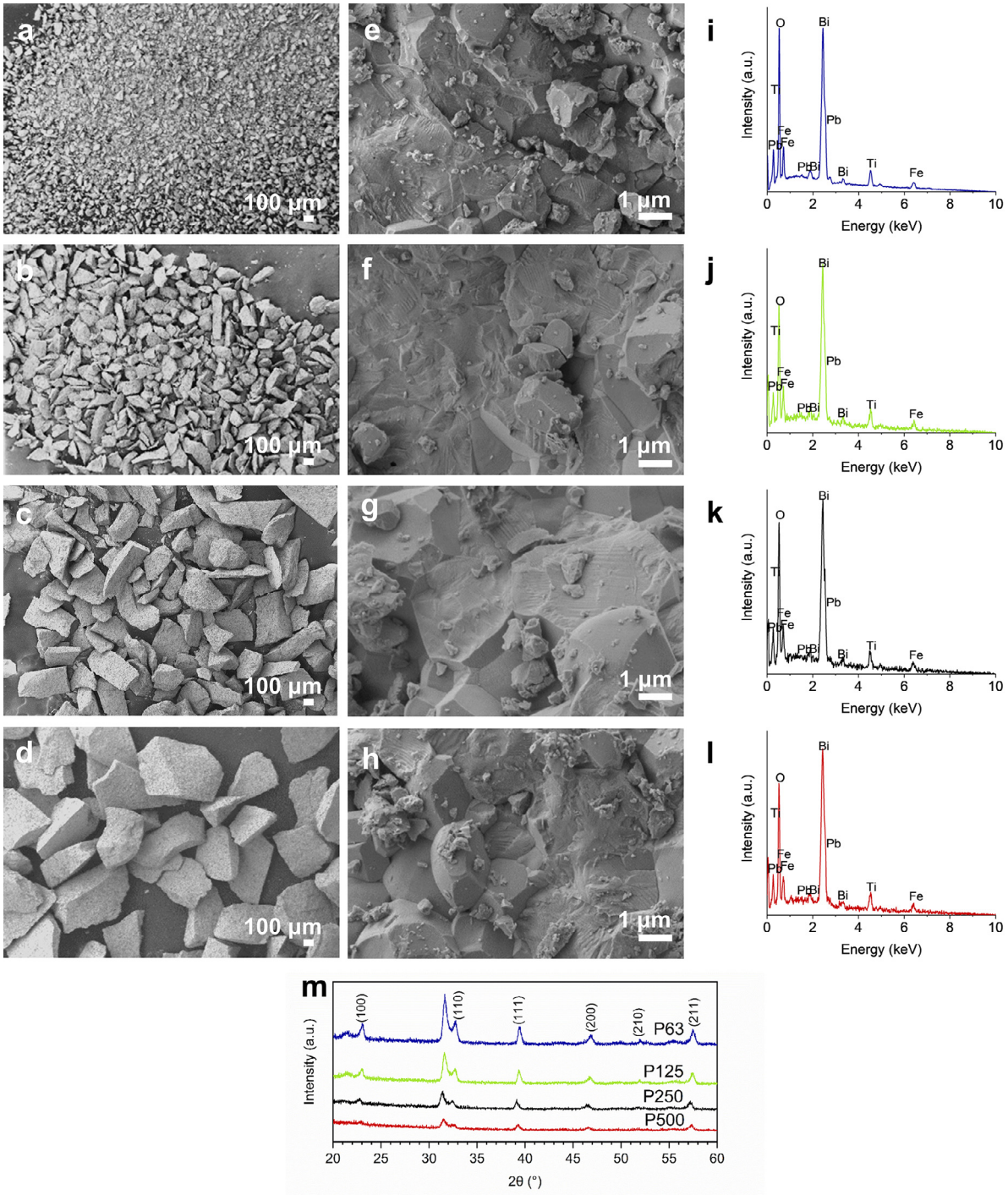

Fig. 2. FIB-SEM (a–h), EDS (i–l) and XRD analysis (m) of poled BF-KBT-PT piezocatalysts with different sizes: P63 (<63 µm), P125 (63–125 µm), P250 (125–250 µm) and P500 (250–500 µm). Size and shape of P63 (a), P125 (b), P250 (c) and P500 (d); surface structure of P63 (e), P125 (f), P250 (g) and P500 (h); composition analysis of P63 (i), P125 (j), P250 (k) and P500 (l); phase analysis of P63, P125, P250 and P500 (m).

degradation was observed, whether or not the catalysts were present in the solution (MA, P63 MA and UP63 MA). The introduction of ultrasound changed this, as RhB degradation was clearly observed in all cases, although the results varied significantly depending on the presence/absence of mechanical agitation and/or piezocatalysts.

Under ultrasound on its own (US), a nearly 30% degradation of RhB was achieved after 120 min. Further addition of the unpoled BF-KBT-PT catalyst (UP63 US) had no significant effect on the removal of RhB. However, the addition of the poled BF-KBT-PT catalyst (P63 US) did have an effect, enhancing the degradation of RhB up to 35%. A far more significant effect was observed when mechanical agitation was added to ultrasound. In absence of BF-KBT-PT catalysts, the combination of ultrasound and mechanical agitation alone (US + MA) resulted in a remarkable degradation of RhB of about 80%. This was further enhanced by the addition of the poled BF-KBT-PT piezocatalyst, resulting in a degradation of nearly 90% of the RhB in the treated solutions (P63 US + MA). However, the more interesting results were observed with the addition of the unpoled BF-KBT-PT catalyst (UP63 US + MA): whereas no significant enhancement in the degradation of RhB was observed at the end of the experiments compared to the same condition in absence of cata-

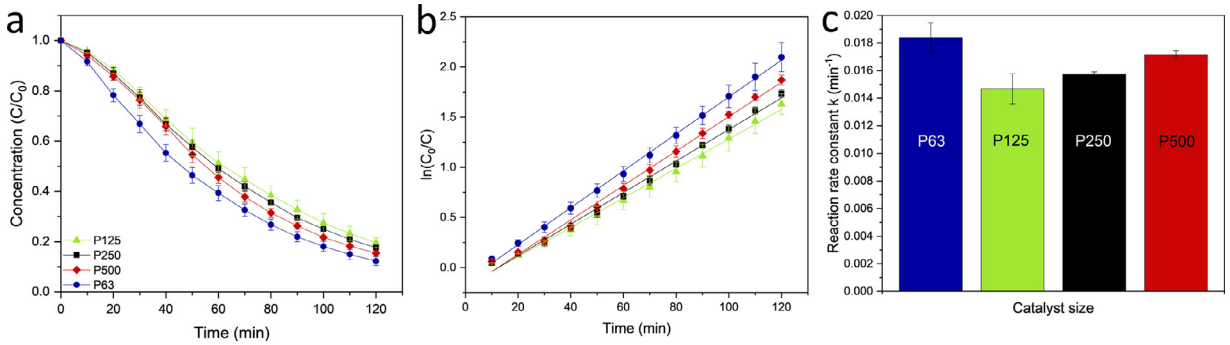

Fig. 3. RhB degradation experiments under combined ultrasound/mechanical agitation in presence of poled BF-KBT-PT catalysts with difference sizes: P63 (<63 μm), P125 (63–125 μm), P250 (125–250 μm) and P500 (250–500 μm): (a) Evolution of C/C_0 vs reaction time, (b) pseudo first-order linear fit of $\ln(C_0/C)$ vs reaction time, (c) pseudo first-order degradation reaction rate constants.

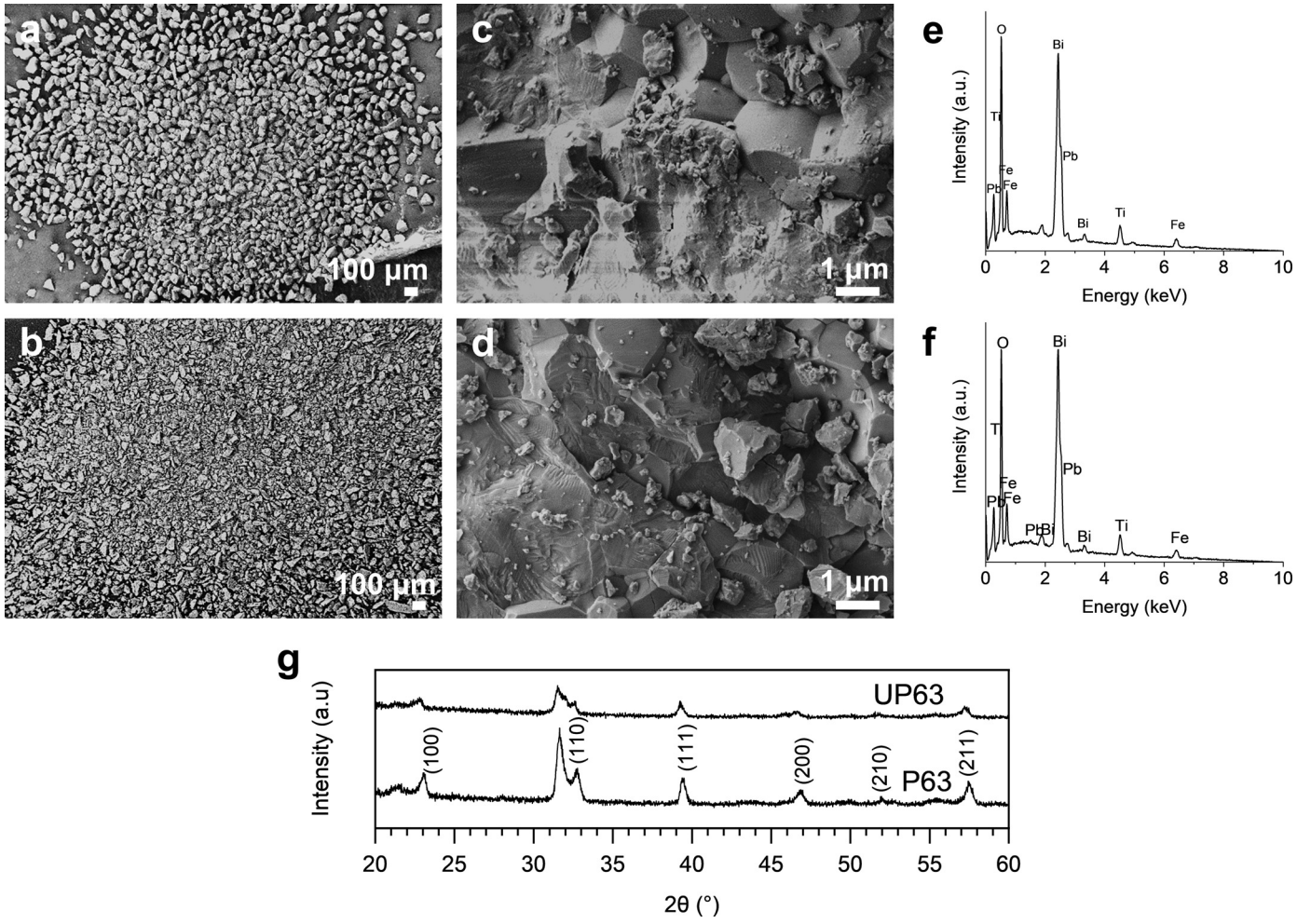

Fig. 4. FIB-SEM (a–d), EDS (e–f) and XRD analysis (g) of unpoled and poled BF-KBT-PT catalysts (P63 and UP63, respectively) with sizes of <63 μm. Size and shape of UP63 (a) and P63 (b); surface structure of UP63 (c) and P63 (d); composition analysis of UP63 (e) and P63 (f); phase analysis of UP63 and P63 (g).

lysts (US + MA), there was a clear effect of the presence of the unpoled material during the first 80 min.

3.3. Influence of radical and charge scavengers

Additional experiments in the presence of several radical and charge scavengers (TA, BQ and EDTA) were conducted under combined mechanical agitation and ultrasound (US + MA) in presence/absence of poled piezocatalysts (P63) to confirm the importance of radicalary degradation routes in the degradation of RhB (Fig. 6).

TA had a significant hindering effect on the degradation of RhB, both in presence and absence of piezocatalysts (Fig. 6a–c), demonstrating the importance of $^{\bullet}$OH radicals in the degradation of RhB. Nevertheless, RhB degradation was still lower under combined ultrasound and mechanical agitation on its own (53%) than in the presence of the P63 piezocatalyst (62%), indicating that the generation of $^{\bullet}$OH radicals was higher in presence of the P63 piezocatalysts.

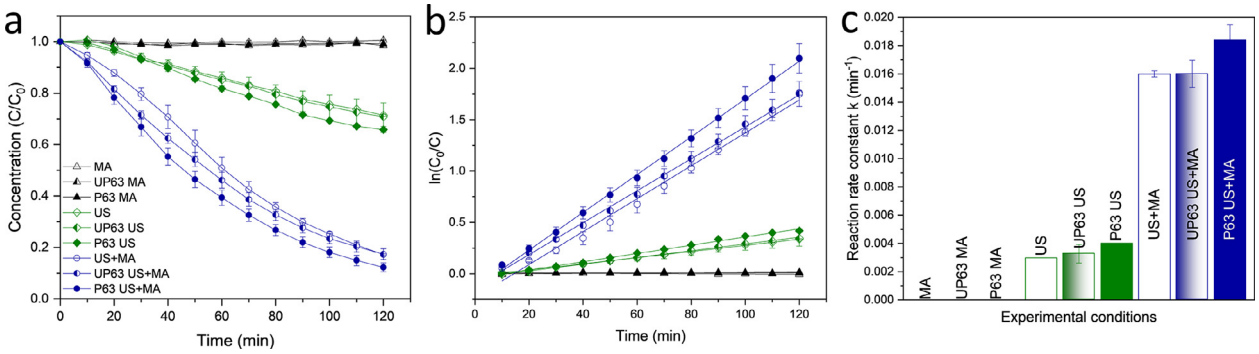

Fig. 5. RhB degradation experiments in absence/presence of poled and unpoled BF-KBT PT catalysts (P63 and UP63, respectively) with sizes of <63 μm under different excitation methods: mechanical agitation (MA), ultrasound (US) and combined ultrasound/mechanical agitation (US + MA): (a) Evolution of C/C_0 vs reaction time, (b) pseudo first-order linear fit of $\ln(C_0/C)$ vs reaction time, (c) pseudo first-order degradation reaction rate constants.

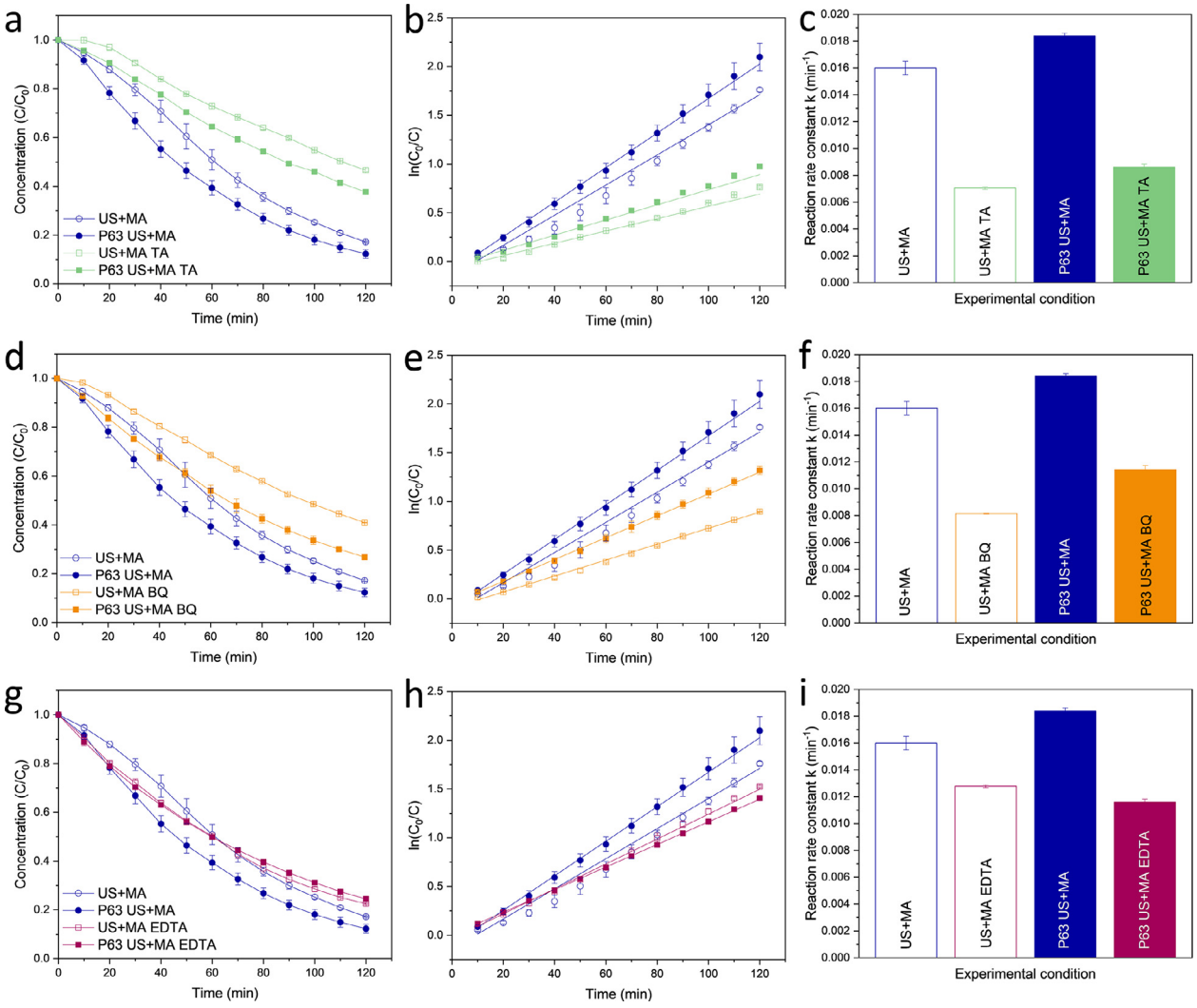

Fig. 6. RhB degradation experiments in absence/presence of poled BF-KBT-PT catalysts with sizes of <63 μm (P63) under combined ultrasound/mechanical agitation (US + MA) in presence of different radical scavengers: (a) evolution of C/C_0 vs reaction time, (b) pseudo first-order linear fit of $\ln(C_0/C)$ vs reaction time, (c) pseudo first-order degradation reaction rate constants in presence of terephthalic acid (TA); (d) evolution of C/C_0 vs reaction time, (e) pseudo first-order linear fit of $\ln(C_0/C)$ vs reaction time, (f) pseudo first-order degradation reaction rate constants in presence of benzoquinone (BQ); (g) evolution of C/C_0 vs reaction time, (h) pseudo first-order linear fit of ln (C_0/C) vs reaction time, (i) pseudo first-order degradation reaction rate constants in presence of ethylenediaminetetraacetic acid (EDTA).

Similar observations were made in the case of BQ (Fig. 6d–f): a significant reduction of RhB was noticed in both cases, confirming the important role of $^{\bullet}O_2^-$ radicals in the process. In addition, RhB degradation in absence of piezocatalysts (59%) was again lower than that in presence of the P63 piezocatalysts (73%), suggesting that the formation of $^{\bullet}O_2^-$ radicals was again greater in presence of the P63 piezocatalysts.

EDTA also inhibited the degradation of RhB (Fig. 6g–i), but not as much as TA and BQ. The slight decrease in degradation under combined ultrasound and mechanical agitation on its own (77%) was lower due to the potential interaction of EDTA with the sonochemical formation of radicals [41]. However, the decrease in RhB degradation in presence of P63 piezocatalysts was slightly more pronounced (75%), confirming the importance of the h^+ degradation route in the presence of piezocatalysts.

4. Discussion

The complex and apparently contradicting results here presented highlight the complexity of the phenomena taking place. To start the analysis and discussion of the results, one should first consider the reaction mechanisms that could explain the piezocatalytic degradation of RhB in water. According to many of the studies in the literature, such process would be based on redox degradation of RhB by $^{\bullet}OH$ and $^{\bullet}O_2^-$ radicals, which would be generated by the following redox reactions originating from the 'top-to-bottom' electric potential difference experienced by the piezocatalyst particles (Fig. 7a) [5,18,42,43]:

- Oxidation: $OH^- + h^+ \rightarrow {}^{\bullet}OH$
- Reduction: $O_2 + e^- \rightarrow {}^{\bullet}O_2^-$

What most of the published piezocatalysis research omits is that the reduction potential of said oxidation reaction is +1.89 V vs SHE (standard hydrogen electrode) [44], whereas the reduction potential of the reduction reaction is −0.33 V vs SHE [45] (only a few papers on piezocatalysis extend their discussion to redox potentials [4,10,23,46]; these will be further discussed later in this section). This means that, from a strict electrochemical point of view, a minimum electrochemical potential difference of 2.22 V between those areas where the reduction and oxidation reactions are taking place is required for those reactions to occur (and that is excluding other electrochemical factors such as kinetic and concentration overpotentials, as well as ohmic losses that may be quite significant in semiconductor materials such as those generally used in piezocatalysis research). When compared with this electrochemical potential difference of 2.22 V, the FEM simulations here presented (Fig. 1) clearly indicate that none of the poled piezocatalysts used in this study should experience a 'top-to-bottom' electric potential difference high enough to lead to the redox reactions previously mentioned (Fig. 7a). This is not just an observation that can be made from the FEM simulations here included, as it can also be made from nearly all those studies available in the literature that include other FEM models with less realistic assumption [5,20,23,34,47]. Moreover, the piezocatalysts that achieved the highest RhB degradation had the smallest particles size of all the sizes studied, clearly confirming that whereas 'top-to-bottom' electric potential differences experienced by the piezocatalyst particles under an ultrasonic field are not enough to cause the degradation of the dye on its own, other mechanisms that may be maximised when reducing the particle size must have a role on the overall degradation process.

One of those other mechanisms would be related to nanoscale piezoelectricity occurring at micro- and nano-structured features of surfaces, which could potentially result in the superficial, localised polarisation of particles [48], leading to a nanoscale piezoelectric response at the surface in both poled and even unpoled materials [49,50]. Unpoled $LiNbO_3$ piezocatalytic particles are a good example [11]: each particle has different multi-domains, with each of them presenting its own polarisation field; even though their net polarisation is still negligible due to cancellation with opposite polarisation fields in other domains, it still generated a localised piezoelectric effect leading to the piezocatalytic degradation of a dye. All of the poled and unpoled BF-KBT-PT catalysts used in this study presented the same micro- and nano-structured surface (Figs. 2e–h, 4c-d), where BF-KBT-PT grains were clearly discernible. In this situation, the nanoscale piezoelectric response would be expected to occur; its influence in the piezocatalytic degradation of RhB would be stronger in the smallest particles due to their greater geometrical surface area/volume ratio, as observed for the P63 particles (Fig. 3). This nanoscale piezoelectric response caused in micro- and nano-structured features of catalysts with multi-domains could lead to large electric potential differences within the surface of the piezocatalysts (Fig. 7b), which would explain why nano-piezocatalysts used in previous studies that should not experience a high degree of "top-to-bottom' electric potential difference seemed to have some piezocatalytic response [7,21–23,27,46].

Superficial potential differences caused by nanoscale piezoelectric response instead of (or combined with) 'top-to-bottom' electric potential differences may explain to some extent the results obtained in Figs. 5 and 7, but there is at least another potential mechanism that should be considered. This is where it is worth considering the research by Bao and co-workers on several piezocatalytic materials such as $BaTiO_3$ [5] and related materials [4,5,23,46] or $BiFeO_3/TiO_2$ [10]. Whereas the authors initially proposed a mechanism purely based on the 'top-to-bottom' electric potential differences [5] that, according to their own FEM simulations, should not be large enough to drive redox reactions in opposite sides of the catalyst, they later moved to a piezocatalytic redox mechanism based on the catalyst valence band (VB) and conduction band (CB) that would favour the reaction of interest under ultrasound [4,10,23,46]. This is in essence what researchers in the sonochemistry community would call sonocatalysis (Fig. 7c), where cavitating bubbles generated by ultrasound would asymmetrically collapse nearby the surface of semiconductor particles. This collapse would result in sonoluminescence and/or thermal phenomena leading to electron-hole pairs with the potential to generate $^{\bullet}OH$ and $^{\bullet}O_2^-$ radicals at theCB and VB, respectively, of semiconductor materials [51,52]. Any piezoelectric material such as the poled and unpoled BF-KBT-PT catalysts used in this study (or other piezoelectric materials such as PZT) can be described as a semiconductor material, which means that the vast majority of piezocatalysis research conducted until now has indeed been based on semiconductor materials under ultrasound. Therefore, sonocatalysis is inherently related to piezocatalysis, and must be properly considered as part of the discussion.

To recap the previous paragraphs, it could be said that the overall catalytic degradation of RhB occurring in the experiments conducted in this study (and, in extension, in all previous piezocatalysis research) relies on the following phenomena: (i) 'top-to-bottom' electric potential difference caused by the bulk polarisation of the piezocatalyst (Fig. 7a), (ii) superficial electric potential differences caused by the nanoscale piezoelectric response on micro- and nano-structured features of the catalyst surface (Fig. 7b), and (iii) sonocatalysis (Fig. 7c), with the suggested redox reaction routes strongly supported by the scavenger experiments conducted (Fig. 6). Both nanoscale piezoelectric response and sonocatalysis would occur, to some extent, in all the catalysts used in this study, whether they were poled or unpoled. This would explain the clear effect observed in the presence of the unpoled catalyst during the first 80 min of experiments under combined ultrasound and mechanical agitation (Fig. 5, UP63 US + MA); it would also explain why the smallest poled piezocatalyst (P63) yielded the highest degradation of RhB under combined ultrasound and mechanical agitation (Fig. 4, P63 US + MA), as the smallest particles with the greatest geometrical surface area/volume ratio would benefit the most from both nanoscale piezoelectric response and sonocatalysis. Even though the unpoled catalysts would still experience some piezocatalytic effect, the poling nature of the material still is important, particularly for the sonocatalytic mechanism, as the larger electric potential difference experienced by the P63 particles would help electrons and holes in the conduction band to migrate easier and faster to the surface of the catalyst [10]. 'Top-to-bottom'

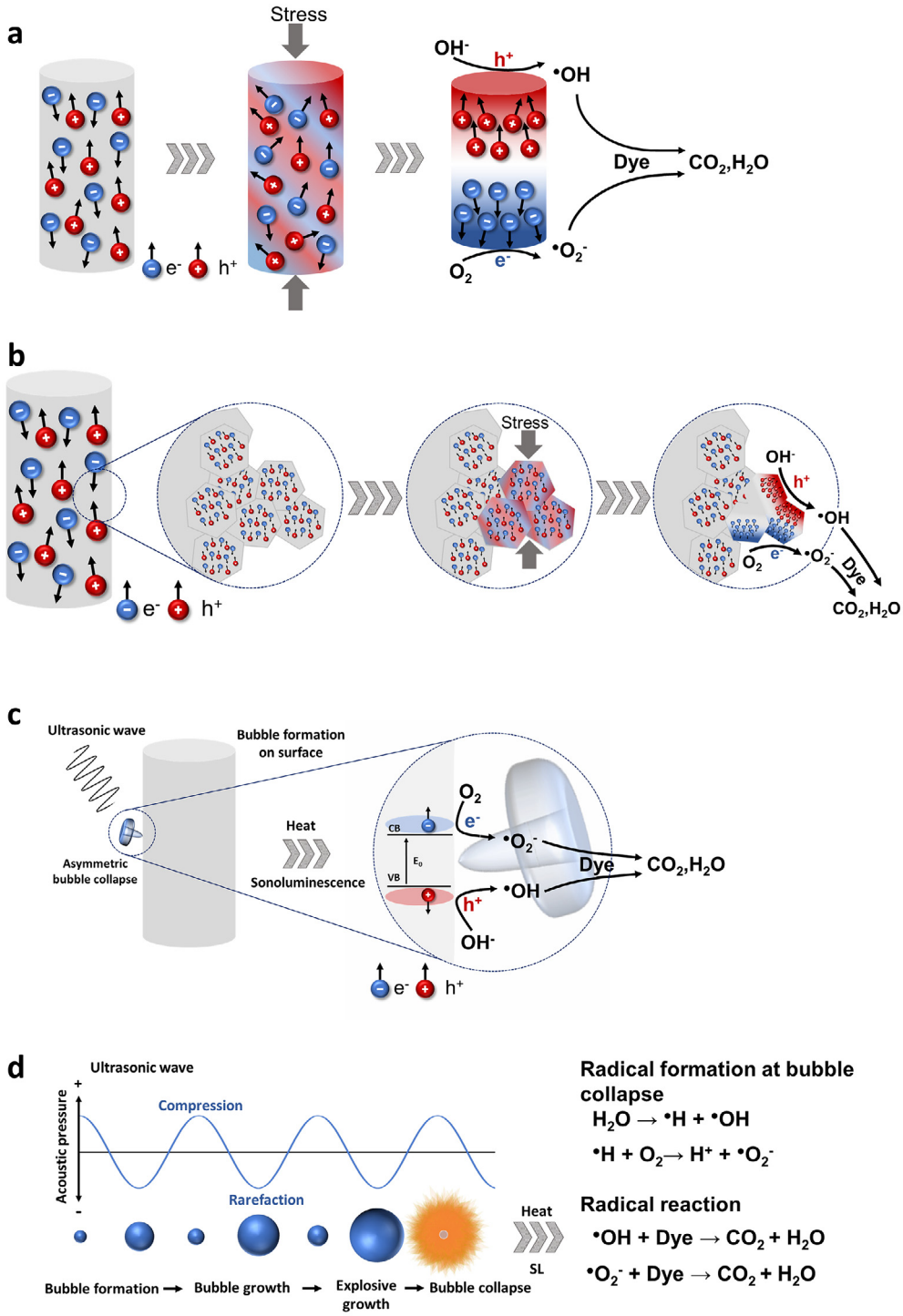

Fig. 7. Illustration of the different mechanisms for the overall piezocatalytic degradation of dyes: (a) 'top-to-bottom' electric potential difference due to bulk polarisation of a piezoelectric particle under stress; (b) electric potential difference due to localised polarisation within micro- and nano-structured features of poled/unpoled particles; (c) valence band and conduction band in semiconductor materials in presence of cavitating bubbles under ultrasound (i.e. sonocatalysis); (d) bubble formation, growth and collapse under ultrasound and resulting chemical processes (i.e. sonochemistry).

electric potential difference caused by bulk polarisation therefore contributes in an indirect way to the sonocatalytic mechanism; it is therefore still worth taking it into account as part of the overall catalytic degradation process, otherwise it would not be possible to observe the slight trend in RhB degradation for the larger poled particles (P500, P250 and P125) under combined ultrasound and mechanical agitation (Fig. 5); nevertheless, its contribution is minor compared to the other phenomena. It is also worth mentioning here that, besides bulk polarisation, nanoscale piezoelectric response and sonocatalysis, another phenomenon that could also contribute to the catalytic degradation of RhB is pyrocatalysis [53]; however, it is unlikely that neither the poled or unpoled BF-KBT-PT particles experienced any pyroelectric response in this study due to the temperature control implemented into the experimental set-up to precisely avoid such effects during the experiments.

By now, it should be clear that piezocatalysis is far more complicated than what it seemed in previous research, and the combination of different phenomena (i.e. 'top-to-bottom' bulk polarisation, nanoscale piezoelectric response at the surface, sonocatalysis) may be rather complex, even when studying like-for-like materials such as those in this study. But even this would still miss the most significant contribution to the degradation of RhB, sonochemistry, which is based on the occurrence of acoustic cavitation when a liquid is ultrasonically irradiated. Cavitat-

Table 1
Comparison of pseudo first-order reaction rate constants for RhB degradation from this work with other studies available in the literature. US: ultrasound; MA: mechanical agitation.

Piezocatalyst	Set up	Frequency [kHz]	Acoustic power (Electric input power)	Rate constant [min^{-1}]	Ref
–	US	32–38	12.2 ± 0.4 W L^{-1} (200 W)	0.003	this study
BF-KBT-PT (P63)	US	32–38	12.2 ± 0.4 W L^{-1} (200 W)	0.004	this study
–	US + MA	32–38 200 rpm	14.3 ± 0.7 W L^{-1} (200 W)	0.016	this study
BF-KBT-PT (P63)	US + MA	32–38 200 rpm	14.3 ± 0.7 W L^{-1} (200 W)	0.018	this study
BiOCl	US	40	N/A (120 W)	0.003	[59]
$SrTiO_3$	US	40	N/A (300 W)	0.009	[7]
$(Bi_{1/2}Na_{1/2})TiO_3$	US	40	N/A (100 W)	0.012	[6]
$BaTiO_3$	US	40	N/A (400 W)	0.041	[60]
$BaTiO_3$ (BTO-800, 4kV)	US	40	N/A (80 W)	0.009	[5]
$Ba_{0.8}Sr_{0.2}TiO_3$	US	40	~0.1 W cm^{-2} (80 W)	0.013	[4]
$K_{0.5}Na_{0.5}NbO_3$	US	40	N/A (180 W)	0.019	[61]
MoS_2-PVDF	US	–	N/A (100 W)	0.210	[12]
$KNbO_3$	US	40	N/A (110 W)	0.003	[34]
Cl-ZnO	US	40	3.86 W cm^{-2} (100 W)	0.007	[26]

ing bubbles violently collapse after reaching a certain size; as a result, temperatures and pressures in the order of 5000 K and 1000 atm, respectively, are reached at the centre of the bubble, driving forward a wide variety of physico-chemical phenomena such as the generation of high-energy species (radicals) from the solvent [57] (Fig. 7d). The presence of ultrasound, even in the absence of catalysts, had the most remarkable effect on the degradation of RhB (Fig. 5, US and US + MA). The results here presented are in fact fairly similar to those previously reported in the literature [54] outlining that significant dye degradation may be achieved sonochemically without the additional presence of catalysts. As demonstrated by the experiments with scavengers (Fig. 6), both $^{\bullet}OH$ and $^{\bullet}O_2^-$ radicals are also produced by sonochemistry [55,56] when the ultrasonic power is high enough. Unfortunately, many previous studies where ultrasound was used to 'excite' piezocatalysts did not include any blank experiments in absence of piezocatalysts to discard any potential contribution of sonochemistry to the degradation process [6,11,12,17,33,47]. Therefore, this study not only confirms that sonochemistry should always be taken into account (it can actually provide the main contribution to the degradation process under certain conditions such as those in this study), but also that its role can be rather complex: in the present study, the combination of ultrasound and mechanical agitation resulted in higher degradation due to enhanced cavitation activity, as demonstrated by the calorimetric calibration conducted in both cases (the ultrasonic power in the reactor was 12.2 ± 0.4 W L^{-1} under ultrasound on its own and 14.3 ± 0.7 W L^{-1} under combined ultrasound and mechanical agitation). The reason for this would be the synergistic effect that combining ultrasound and mechanical agitation has on the acoustic field, as well as the increase of air in the solution [54].

The acoustic field (and potential sonochemical phenomena derived from it) is therefore a critical aspect of piezocatalysis when using ultrasound to excite piezocatalysts, and even small localised variations in the acoustic field may have apparently 'contradicting' effects in the results. For example, solid particles (e.g. piezocatalysts) in a liquid irradiated by ultrasound could act as a 'barrier' for the propagation of the acoustic waves [58], resulting in a small decrease of cavitational activity. A direct indication of this would be the experiments conducted with EDTA (Fig. 6g–i), where the lower degradation achieved in presence of the P63 piezocatalyst strongly suggests that 'pure' sonochemical degradation of RhB was slightly decreased when solids were present. This detrimental effect would be even more obvious in the experiments conducted with some of the intermediate size particles (e.g. P125 in Fig. 3), were RhB degradation was even lower than under combined ultrasound and mechanical agitation on its own (US + MA in Fig. 5), as they are neither small enough to benefit from geometrical surface area/volume ratio (which is critical for both nanoscale piezoelectricity and sonocatalytic phenomena), nor large enough to benefit from greater 'top-to-bottom' electric potential difference (which would indirectly contribute to sonocatalysis). To better highlight the importance of the acoustic field, Table 1 displays some of the results from this study with those from the literature. Compared to those previous studies on piezocatalytic degradation of RhB, the material used in the present work, BF-KBT-PT, was not developed for piezocatalytic purposes. Even so, the highest pseudo first-order reaction rate constant achieved with this material was significantly higher than most of the values previously reported for piezocatalysts that were specifically developed in this regard. The combination of ultrasound and mechanical agitation significantly enhanced RhB degradation kinetics, even with no presence of a catalyst. Table 1 therefore highlights the great opportunity that understanding the acoustic field brings to further enhance piezocatalytic processes.

5. Conclusion

The present study has tried to shed more light onto what piezocatalysis may be, and whether other catalytic phenomena besides 'top-to-bottom' electric field difference cause by bulk polarisation should be factored in piezocatalysis research. The theoretical FEM simulations and experimental RhB degradation results obtained for BF-KBT-PT material in its poled and unpoled versions demonstrate that piezocatalysis under an ultrasonic field would be a combination of different phenomena beyond bulk polarisation, as nano-piezoelectric response of micro- and nano-structured features in the surface of the catalysts, as well as sonocatalysis, could also influence the overall catalytic process. Moreover, sonochemistry made the greatest contribution to the degradation of RhB, demonstrating that ultrasound, especially when combined with mechanical agitation, could already achieve a high degree of dye degradation in absence of piezocatalysts.

In summary, the present study demonstrates that piezocatalysis may indeed exist, but it is far more complex than what previous studies may have suggested. For this reason, it is necessary to conduct thorough blank experiments and maintain a better control of the conditions under which those experiments take place (e.g. confirmation of (non-)piezoelectric nature of catalysts, constant temperature, reproducible ultrasonic field, etc.), which unfortunately may not be the norm in current piezocatalysis research. We therefore hope that some of the approaches and practices followed in this study are implemented in future piezocatalysis research to continue with the development of this promising area of catalysis.

Declaration of Competing Interest

The authors have no known competing financial interests or personal relationships that could have appeared to influence the work reported in this paper.

Acknowledgements

F.B. and I.T. would like to thank the University of Edinburgh for funding this research through its Start Up fund. The authors would also like to thank Dr James Cumby and Dr Thomas Glenn at the University of Edinburgh for their kind support in XRD and FIB-SEM analysis, respectively.

Supplementary materials

Supplementary material associated with this article can be found, in the online version, at doi:10.1016/j.ceja.2021.100133.

References

[1] O. Amiri, K. Salar, P. Othman, T. Rasul, D. Faiq, M. Saadat, Purification of wastewater by the piezo-catalyst effect of PbTiO3 nanostructures under ultrasonic vibration, J. Hazard. Mater. 394 (2020) 122514, doi:10.1016/j.jhazmat.2020.122514.

[2] S. Lan, Y. Chen, L. Zeng, H. Ji, W. Liu, M. Zhu, Piezo-activation of peroxymonosulfate for benzothiazole removal in water, J. Hazard. Mater. 393 (2020) 122448, doi:10.1016/j.jhazmat.2020.122448.

[3] C. Zhang, W. Fei, H. Wang, N. Li, D. Chen, Q. Xu, H. Li, J. He, J. Lu, p-n Heterojunction of BiOI/ZnO nanorod arrays for piezo-photocatalytic degradation of bisphenol A in water, J. Hazard. Mater. 399 (2020) 123109, doi:10.1016/j.jhazmat.2020.123109.

[4] B. Yuan, J. Wu, N. Qin, E. Lin, D. Bao, Enhanced piezocatalytic performance of (Ba,Sr)TiO_3 nanowires to degrade organic pollutants, ACS Appl. Nano Mater. 1 (2018) 5119–5127, doi:10.1021/acsanm.8b01206.

[5] J. Wu, Q. Xu, E. Lin, B. Yuan, N. Qin, S.K. Thatikonda, D. Bao, Insights into the role of ferroelectric polarization in piezocatalysis of nanocrystalline $BaTiO_3$, ACS Appl. Mater. Interfaces 10 (2018) 17842–17849, doi:10.1021/acsami.8b01991.

[6] D. Liu, Y. Song, Z. Xin, G. Liu, C. Jin, F. Shan, High-piezocatalytic performance of eco-friendly ($Bi_{1/2}Na_{1/2}$)TiO_3-based nanofibers by electrospinning, Nano Energy 65 (2019) 104024, doi:10.1016/j.nanoen.2019.104024.

[7] J. Ling, K. Wang, Z. Wang, H. Huang, G. Zhang, Enhanced piezoelectric-induced catalysis of $SrTiO_3$ nanocrystal with well-defined facets under ultrasonic vibration, Ultrason. Sonochem. 61 (2020) 104819, doi:10.1016/j.ultsonch.2019.104819.

[8] N.K. James, T. Comyn, D. Hall, L. Daniel, A. Kleppe, S. van der Zwaag, W.A. Groen, Analysis of the state of poling of lead zirconate titanate (PZT) particles in a Zn-ionomer composite, Ferroelectrics 493 (2016) 139–150, doi:10.1080/00150193.2016.1134033.

[9] C.R. Bowen, A.C. Dent, R. Stevens, M.G. Cain, A. Avent, A new method to determine the un-poled elastic properties of ferroelectric materials, Sci. Technol. Adv. Mater. 18 (2017) 264–272, doi:10.1080/14686996.2017.1302274.

[10] B. Yuan, J. Wu, N. Qin, E. Lin, Z. Kang, D. Bao, Sm-doped Pb($Mg_{1/3}Nb_{2/3}$)O_3-x$PbTiO_3$ piezocatalyst: exploring the relationship between piezoelectric property and piezocatalytic activity, Appl. Mater. Today 17 (2019) 183–192, doi:10.1016/j.apmt.2019.07.015.

[11] G. Singh, M. Sharma, R. Vaish, Exploring the piezocatalytic dye degradation capability of lithium niobate, Adv. Powder Technol. 31 (2020) 1771–1775, doi:10.1016/j.apt.2020.01.031.

[12] B. Bagchi, N.A. Hoque, N. Janowicz, S. Das, M.K. Tiwari, *Re*-usable self-poled piezoelectric/piezocatalytic films with exceptional energy harvesting and water remediation capability, Nano Energy 78 (2020) 105339, doi:10.1016/j.nanoen.2020.105339.

[13] E. Lin, Z. Kang, J. Wu, R. Huang, N. Qin, D. Bao, BaTiO3 nanocubes/cuboids with selectively deposited Ag nanoparticles: efficient piezocatalytic degradation and mechanism, Appl. Catal. B. Environ. 285 (2021) 119823, doi:10.1016/j.apcatb.2020.119823.

[14] D. Liu, C. Jin, F. Shan, J. He, F. Wang, Synthesizing $BaTiO_3$ nanostructures to explore morphological influence, kinetics, and mechanism of piezocatalytic dye degradation, ACS Appl. Mater. Interfaces 12 (2020) 17443–17451, doi:10.1021/acsami.9b23351.

[15] P. Wang, X. Li, S. Fan, X. Chen, M. Qin, D. Long, M.O. Tadé, S. Liu, Impact of oxygen vacancy occupancy on piezo-catalytic activity of $BaTiO_3$ nanobelt, Appl. Catal. B. Environ. 279 (2020) 119340, doi:10.1016/j.apcatb.2020.119340.

[16] M.B. Starr, X. Wang, Fundamental analysis of piezocatalysis process on the surfaces of strained piezoelectric materials, Sci. Rep. 3 (2013) 2160, doi:10.1038/srep02160.

[17] J.M. Wu, W.E. Chang, Y.T. Chang, C.K. Chang, Piezo-catalytic effect on the enhancement of the ultra-high degradation activity in the dark by single- and few-layers MoS_2 Nanoflowers, Adv. Mater. 28 (2016) 3718–3725, doi:10.1002/adma.201505785.

[18] Y. Feng, L. Ling, Y. Wang, Z. Xu, F. Cao, H. Li, Z. Bian, Engineering spherical lead zirconate titanate to explore the essence of piezo-catalysis, Nano Energy 40 (2017) 481–486, doi:10.1016/j.nanoen.2017.08.058.

[19] W. Qian, W. Yang, Y. Zhang, C.R. Bowen, Y. Yang, Piezoelectric materials for controlling electro-chemical processes, Nano-Micro Lett. 12 (2020) 90, doi:10.1007/s40820-020-00489-z.

[20] W. Feng, J. Yuan, L. Zhang, W. Hu, Z. Wu, X. Wang, X. Huang, P. Liu, S. Zhang, Atomically thin ZnS nanosheets: facile synthesis and superior piezocatalytic H_2 production from pure H_2O, Appl. Catal. B Environ. 277 (2020) 119250, doi:10.1016/j.apcatb.2020.119250.

[21] F. Peng, R. Yin, Y. Liao, X. Xie, J. Sun, D. Xia, C. He, Kinetics and mechanisms of enhanced degradation of ibuprofen by piezo-catalytic activation of persulfate, Chem. Eng. J. 392 (2020) 123818, doi:10.1016/j.cej.2019.123818.

[22] D. Xia, Z. Tang, Y. Wang, R. Yin, H. He, X. Xie, J. Sun, C. He, P.K. Wong, G. Zhang, Piezo-catalytic persulfate activation system for water advanced disinfection: process efficiency and inactivation mechanisms, Chem. Eng. Journal 400 (2020) 125894, doi:10.1016/j.cej.2020.125894.

[23] J. Wu, N. Qin, D. Bao, Effective enhancement of piezocatalytic activity of $BaTiO_3$ nanowires under ultrasonic vibration, Nano Energy 45 (2018) 44–51, doi:10.1016/j.nanoen.2017.12.034.

[24] S. Masimukku, Y.C. Hu, Z.H. Lin, S.W. Chan, T.M. Chou, J.M. Wu, High efficient degradation of dye molecules by PDMS embedded abundant single-layer tungsten disulfide and their antibacterial performance, Nano Energy 46 (2018) 338–346, doi:10.1016/j.nanoen.2018.02.008.

[25] Y. Liu, T. Yamabuchi, T. Yoshizawa, S. Hirobayashi, Finite element simulation of coupled vibration modes in an ultrasonic cleaning tub: effect of the presence of a washing object, Acoust. Sci. Technol. 12 (2005) 59–65.

[26] J. Yuan, X. Huang, L. Zhang, F. Gao, R. Lei, C. Jiang, W. Feng, P. Liu, Tuning piezoelectric field for optimizing the coupling effect of piezo-photocatalysis, Appl. Catal. B Environ. 278 (2020) 119291, doi:10.1016/j.apcatb.2020.119291.

[27] M.H. Wu, J.T. Lee, Y.J. Chung, M. Srinivaas, J.M. Wu, Ultrahigh efficient degradation activity of single- and few-layered $MoSe_2$ nanoflowers in dark by piezo-catalyst effect, Nano Energy 40 (2017) 369–375, doi:10.1016/j.nanoen.2017.08.042.

[28] V. Sáez, A. Frías-Ferrer, J. Iniesta, J. González-García, A. Aldaz, E. Riera, Characterization of a 20kHz sonoreactor. Part I: analysis of mechanical effects by classical and numerical methods, Ultrason. Sonochem. 12 (2005) 59–65, doi:10.1016/j.ultsonch.2004.06.011.

[29] J. Bennett, A.J. Bell, T.J. Stevenson, T.P. Comyn, Tailoring the structure and piezoelectric properties of $BiFeO_3$ -($K_{0.5}Bi_{0.5}$)TiO_3 –$PbTiO_3$ ceramics for high temperature applications, Appl. Phys. Lett. 103 (2013) 152901, doi:10.1063/1.4824652.

[30] T. Stevenson, D.G. Martin, P.I. Cowin, A. Blumfield, A.J. Bell, T.P. Comyn, P.M. Weaver, Piezoelectric materials for high temperature transducers and actuators, J. Mater. Sci. Mater. Electron. 26 (2015) 9256–9267, doi:10.1007/s10854-015-3629-4.

[31] Q.M. Zhang, J. Zhao, Electromechanical properties of lead zirconate titanate piezoceramics under the influence of mechanical stresses, IEEE Trans. Ultrason. Ferroelectr. Freq. Control 46 (1999) 1518–1526, doi:10.1109/58.808876.

[32] C. Jin, D. Liu, J. Hu, Y. Wang, Q. Zhang, L. Lv, F. Zhuge, The role of microstructure in piezocatalytic degradation of organic dye pollutants in wastewater, Nano Energy 59 (2019) 372–379, doi:10.1016/j.nanoen.2019.02.047.

[33] R. Su, H.A. Hsain, M. Wu, D. Zhang, X. Hu, Z. Wang, X. Wang, F.T. Li, X. Chen, L. Zhu, Y. Yang, Y. Yang, X. Lou, S.J. Pennycook, Nano-ferroelectric for high efficiency overall water splitting under ultrasonic vibration, Angew. Chem. Int. Ed. Engl. 58 (2019) 15076–15081, doi:10.1002/anie.201907695.

[34] D. Yu, Z. Liu, J. Zhang, S. Li, Z. Zhao, L. Zhu, W. Liu, Y. Lin, H. Liu, Z. Zhang, Enhanced catalytic performance by multi-field coupling in $KNbO_3$ nanostructures: piezo-photocatalytic and ferro-photoelectrochemical effects, Nano Energy 58 (2019) 695–705, doi:10.1016/j.nanoen.2019.01.095.

[35] R.F. Contamine, A.M. Wilhelm, J. Berlan, H. Delmas, Power measurement in sonochemistry, Ultrason. Sonochem. 2 (1995) S43–S47, doi:10.1016/1350-4177(94)00010-P.

[36] T. Cheng, W. Gao, H. Gao, S. Wang, Z. Yi, X. Wang, H. Yang, Piezocatalytic degradation of methylene blue, tetrabromobisphenol A and tetracycline hydrochloride using Bi4Ti3O12 with different morphologies, Mater. Res. Bull. 141 (2021) 111350, doi:10.1016/j.materresbull.2021.111350.

[37] W. Ma, B. Yao, W. Zhang, Y. He, Y. Yu, J. Niu, Fabrication of PVDF-based piezocatalytic active membrane with enhanced oxytetracycline degradation efficiency through embedding few-layer E-MoS2 nanosheets, Chem. Eng. J. 415 (2021) 129000, doi:10.1016/j.cej.2021.129000.

[38] N. Wang, L. Zhu, M. Wang, D. Wang, H. Tang, Sono-enhanced degradation of dye pollutants with the use of H_2O_2 activated by Fe_3O_4 magnetic nanoparticles as peroxidase mimetic, Ultrason. Sonochem. 17 (2010) 78–83, doi:10.1016/j.ultsonch.2009.06.014.

[39] J.M. Monteagudo, H. El-Taliawy, A. Durán, G. Caro, K. Bester, Sono-activated persulfate oxidation of diclofenac: degradation, kinetics, pathway and contribution of the different radicals involved, J. Hazard. Mater. 357 (2018) 457–465, doi:10.1016/j.jhazmat.2018.06.031.

[40] S. Farhadi, F. Siadatnasab, A. Khataee, Ultrasound-assisted degradation of organic dyes over magnetic $CoFe_2O_4$@ZnS core-shell nanocomposite, Ultrason. Sonochem. 37 (2017) 298–309, doi:10.1016/j.ultsonch.2017.01.019.

[41] L. Parizot, T. Chave, M.E. Galvez, H. Dutilleul, P. Da Costa, S.I. Nikitenko, Sonocatalytic oxidation of EDTA in aqueous solutions over noble metal-free Co3O4/TiO2 catalyst, Appl. Catal. B Environ. 241 (2019) 570–577, doi:10.1016/j.apcatb.2018.09.001.

[42] K.S. Hong, H. Xu, H. Konishi, X. Li, Piezoelectrochemical effect: a new mechanism for azo dye decolorization in aqueous solution through vibrating piezoelectric microfibers, J. Phys. Chem. C 116 (2012) 13045–13051, doi:10.1021/jp211455z.

[43] M.B. Starr, J. Shi, X. Wang , Piezopotential-driven redox reactions at the surface of piezoelectric materials, Angew. Chem. Int. Ed. Engl. 51 (2012) 5962–5966, doi:10.1002/anie.201201424.

[44] V.K. Sharma, Oxidation of inorganic contaminants by ferrates (VI, V, and IV)–kinetics and mechanisms: a review, J. Environ. Manag. 92 (2011) 1051–1073, doi:10.1016/j.jenvman.2010.11.026.
[45] W.H. Koppenol, D.M. Stanbury, P.L. Bounds, Electrode potentials of partially reduced oxygen species, from dioxygen to water, Free Radic. Biol. Med. 49 (2010) 317–322, doi:10.1016/j.freeradbiomed.2010.04.011.
[46] E. Lin, J. Wu, N. Qin, B. Yuan, Z. Kang, D. Bao, Enhanced piezocatalytic, photocatalytic and piezo-/photocatalytic performance of diphasic $Ba_{1-x}Ca_xTiO_3$ nanowires near a solubility limit, Catal. Sci. Technol. 9 (2019) 6863–6874, doi:10.1039/C9CY01713E.
[47] H. Li, Y. Sang, S. Chang, X. Huang, Y. Zhang, R. Yang, H. Jiang, H. Liu, Z.L. Wang, Enhanced ferroelectric-nanocrystal-based hybrid photocatalysis by ultrasonic-wave-generated piezophototronic effect, Nano Lett. 15 (2015) 2372–2379, doi:10.1021/nl504630j.
[48] J. Zhang, C. Wang, C. Bowen, Piezoelectric effects and electromechanical theories at the nanoscale, Nanoscale 6 (2014) 13314–13327, doi:10.1039/C4NR03756A.
[49] M. Zelisko, Y. Hanlumyuang, S. Yang, Y. Liu, C. Lei, J. Li, P.M. Ajayan, P. Sharma, Anomalous piezoelectricity in two-dimensional graphene nitride nanosheets, Nat. Commun. 5 (2014) 4284, doi:10.1038/ncomms5284.
[50] S. Dai, M. Gharbi, P. Sharma, H.S. Park, Surface piezoelectricity: size effects in nanostructures and the emergence of piezoelectricity in non-piezoelectric materials, J. Appl. Phys. 110 (2011) 104305, doi:10.1063/1.3660431.
[51] P. Qiu, B. Park, J. Choi, B. Thokchom, A.B. Pandit, J. Khim, A review on heterogeneous sonocatalyst for treatment of organic pollutants in aqueous phase based on catalytic mechanism, Ultrason. Sonochem. 45 (2018) 29–49, doi:10.1016/j.ultsonch.2018.03.003.
[52] X. Chen, J. Dai, G. Shi, L. Li, G. Wang, H. Yang, Sonocatalytic degradation of Rhodamine B catalyzed by β-Bi_2O_3 particles under ultrasonic irradiation, Ultrason. Sonochem. 29 (2016) 172–177, doi:10.1016/j.ultsonch.2015.08.010.
[53] J. Wu, N. Qin, B. Yuan, E. Lin, D. Bao, Enhanced pyroelectric catalysis of $BaTiO_3$ nanowires for utilizing waste heat in pollution treatment, ACS Appl. Mater. Interfaces 10 (2018) 37963–37973, doi:10.1021/acsami.8b11158.
[54] X. Zhang, C. Hao, C. Ma, Z. Shen, J. Guo, R. Sun, Studied on sonocatalytic degradation of Rhodamine B in aqueous solution, Ultrason. Sonochem. 58 (2019) 104691, doi:10.1016/j.ultsonch.2019.104691.
[55] M. Hayyan, M.A. Hashim, I.M. AlNashef, Superoxide ion: generation and chemical implications, Chem. Rev. 116 (2016) 3029–3085, doi:10.1021/acs.chemrev.5b00407.
[56] T. Kondo, V. Mišík, P. Riesz, Sonochemistry of cytochrome c. Evidence for superoxide formation by ultrasound in argon-saturated aqueous solution, Ultrason. Sonochem. 3 (1996) S193–S199, doi:10.1016/S1350-4177(96)00025-9.
[57] J. González-García, V. Sáez, I. Tudela, M.I. Díez-Garcia, M. Deseada Esclapez, O. Louisnard, Sonochemical treatment of water polluted by chlorinated organocompounds. A review, Water 2 (2010) 28–74 (Basel), doi:10.3390/w2010028.
[58] P.R. Gogate, M. Sivakumar, A.B. Pandit, Destruction of Rhodamine B using novel sonochemical reactor with capacity of 7.5 l, Sep. Purif. Technol. 34 (2004) 13–24, doi:10.1016/S1383-5866(03)00170-9.
[59] M. Ismail, Z. Wu, L. Zhang, J. Ma, Y. Jia, Y. Hu, Y. Wang, High-efficient synergy of piezocatalysis and photocatalysis in bismuth oxychloride nanomaterial for dye decomposition, Chemosphere 228 (2019) 212–218, doi:10.1016/j.chemosphere.2019.04.121.
[60] W. Qian, K. Zhao, D. Zhang, C.R. Bowen, Y. Wang, Y. Yang, Piezoelectric material-polymer composite porous foam for efficient dye degradation via the piezo-catalytic effect, ACS Appl. Mater. Interfaces 11 (2019) 27862–27869, doi:10.1021/acsami.9b07857.
[61] A. Zhang, Z. Liu, X. Geng, W. Song, J. Lu, B. Xie, S. Ke, L. Shu, Ultrasonic vibration driven piezocatalytic activity of lead-free K0.5Na0.5NbO3 materials, Ceram. Int. 45 (2019) 22486–22492, doi:10.1016/j.ceramint.2019.07.271.

3 Effect of frequency and power on the piezocatalytic and sonochemical process

3.1 Introduction

The results in the previous chapter showed that piezocatalysis may indeed exist, but it is a more complex process that involves several ultrasound-assisted phenomena taking place simultaneously. It was also indicated that ‘bulk’ piezoelectric polarisation was unlikely to be sufficient to achieve a large enough electrical potential for the required redox reactions to generate superoxide and hydroxyl radicals. Similar to the majority of piezocatalytic research, the study used a common excitation frequency of around 40 kHz [1-4]. However, this operating frequency might have been far away from the piezocatalysts’ resonance frequency or the global frequency of the operating system, where a piezoelectric material should exhibit a more pronounced piezoelectric response [5, 6].

In order to confirm the viability of the proposed piezocatalytic mechanism based on ‘bulk’ piezoelectric polarisation, it is essential to investigate the effect of different ultrasonic frequencies on the piezocatalytic process. If ‘bulk’ piezoelectric polarisation is an important factor in the piezocatalytic process an enhancement in the overall catalytic activity should be achieved with a piezocatalyst excited close to its resonance frequency or the global operating frequency of the system.

As it was also highlighted in Chapter 2, other phenomena such as sonochemistry and sonocatalysis are simultaneously occurring when studying piezocatalysis under ultrasound. The occurrence of these phenomena can be attributed to acoustic cavitation which is greatly affected by factors such as ultrasonic frequency and power. Therefore, the objective of this study is to evaluate and understand the impact of ultrasonic frequency and power on the piezocatalytic and sonochemical process, in order to determine whether ‘bulk’ piezoelectric polarisation is a key factor in the overall piezocatalytic process.

For this purpose, a variety of ultrasonic set-ups was used to cover a wide range of operating frequencies from 20 kHz to 1 MHz. To address an intrinsic issue of ultrasound-related studies where small variations in the set-up geometry can lead to significant differences of the acoustic field [5-10], the widely accepted calorimetric method for the estimation of the acoustic power [11, 12] was applied to ensure the comparability of the different ultrasonic systems used in this study. The effect of ultrasonic frequency on the piezocatalytic and sonochemical process was compared with an acoustic power of 10−12 W L^{-1} due to the maximum acoustic power of the ultrasonic bath (operating at 32−38 kHz) being 12.2±0.4 W L^{-1}. Therefore, several calorimetric calibrations at different electrical power outputs had to be conducted for each set-up and frequency to determine acoustic powers close enough of to that of the ultrasonic bath.

3.2 Discussion highlight and conclusions

The present study evaluated the effect of ultrasonic frequency and power on the piezocatalytic and sonocatalytic process. The results suggested that mechanical effects (i.e. shock waves, micro-jetting and asymmetric bubble collapse) dominating at lower ultrasonic frequencies (<100 kHz) could cause a localised piezoelectric response that is more significant for piezocatalytic research than ‘bulk’ piezoelectric polarisation resulting from an excitation close to resonance frequency. FIB-SEM analysis demonstrated the severe impact of asymmetric bubble collapse on the surface of the piezocatalyst, highlighting the potential for a strong local piezoelectric response in these regions.

The study also demonstrated that an increase in acoustic power resulted in an enhanced sonochemical degradation of RhB at both low and high ultrasonic frequencies. However, for the piezocatalytic process, an increased acoustic power did not necessarily led to a more pronounced piezocatalytic contribution. At lower ultrasonic frequencies this can be attributed to the behaviour and distribution of cavitation bubbles where upper and lower power thresholds

influence the cavitation activity. When the acoustic power is below the lower threshold, the acoustic field is too weak to initiate bubble formation, resulting in lower sonochemical and piezocatalytic degradation. In between the upper and lower limits, elevated negative pressures during the rarefaction followed by higher pressures in the compression phase result in a more violent bubble collapse that seems to be beneficial for the piezocatalytic response. However, excessive acoustic power leads to an increase in bubble coalescence, degassing, and liquid agitation [13, 14], which caused a progressively detrimental impact on the mechanical effects that influencing the piezocatalytic contribution.

It can therefore be concluded, that low frequency ultrasound with moderate acoustic powers is favourable to maximise the piezocatalytic degradation route by a localised piezoelectric response rather than aiming for ‘bulk’ piezoelectric polarisation. However, high acoustic powers combined with high ultrasonic frequencies would be beneficial for the sonochemical degradation without the need to add a piezocatalyst. Nevertheless, if piezocatalysis is dependent on an acoustic cavitation-induced localised piezoelectric response, real-world and industrial applications would be significantly limited. It is therefore crucial to explore other potential mechanisms that could also drive piezocatalytic processes.

In this regard, another potential mechanism that has been proposed over recent years to explain piezocatalysis is the energy band theory [15]. In this mechanism, energy band gap and levels play an important role for the piezocatalytic process. The energy band gap of BF-KBT-PT had not been considered until this point, as it should not have influenced the original proposed mechanism for piezocatalysis. However, if the energy band theory is a more suitable mechanism for piezocatalysis, the energy band gap and levels of BF-KBT-PT could indeed be a limiting factor for the piezocatalytic contributions of BF-KBT-PT.

To gain a deeper understanding of the research outcomes and their significance, all results and a more comprehensive discussion can be found in *Effect of frequency and power on the piezocatalytic and sonochemical degradation of dyes in water* published in *Chemical Engineering Journal Advances*, which constitutes Chapter 3 of this thesis.

3.3 References

[1] A. Zhang, Z. Liu, B. Xie, J. Lu, K. Guo, S. Ke, L. Shu, H. Fan

Vibration catalysis of eco-friendly $Na_{0.5}K_{0.5}NbO_3$-based piezoelectric: An efficient phase boundary catalyst

Applied Catalysis B: Environmental, 279 (2020), 10.1016/j.apcatb.2020.119353

[2] H. Kalhori, A.H. Youssef, A. Ruediger, A. Pignolet

Competing contributions to the catalytic activity of barium titanate nanoparticles in the decomposition of organic pollutants

Journal of Environmental Chemical Engineering, 10 (6) (2022), 10.1016/j.jece.2022.108571

[3] W. Ma, M. Lv, F. Cao, Z. Fang, Y. Feng, G. Zhang, Y. Yang, H. Liu

Synthesis and characterization of ZnO-GO composites with their piezoelectric catalytic and antibacterial properties

Journal of Environmental Chemical Engineering, 10 (3) (2022), 10.1016/j.jece.2022.107840

[4] E. Lin, N. Qin, J. Wu, B. Yuan, Z. Kang, D. Bao

$BaTiO_3$ Nanosheets and Caps Grown on TiO_2 Nanorod Arrays as Thin-Film Catalysts for Piezocatalytic Applications

ACS Appl Mater Interfaces, 12 (12) (2020), 14005-14015, 10.1021/acsami.0c00962

[5] I. Tudela, V. Sáez, M.D. Esclapez, P. Bonete, H. Harzali, F. Baillon, J. González-García, O. Louisnard

Study of the influence of transducer-electrode and electrode-wall gaps on the acoustic field inside a sonoelectrochemical reactor by FEM simulations

Chemical Engineering Journal, 171 (1) (2011), 81-91, 10.1016/j.cej.2011.03.064

[6] O. Louisnard, J. Gonzalez-Garcia, I. Tudela, J. Klima, V. Saez, Y. Vargas-Hernandez

FEM simulation of a sono-reactor accounting for vibrations of the boundaries

Ultrason Sonochem, 16 (2) (2009), 250-9, 10.1016/j.ultsonch.2008.07.008

[7] J. González-García, V. Sáez, I. Tudela, M.I. Díez-Garcia, M. Deseada Esclapez, O. Louisnard

Sonochemical Treatment of Water Polluted by Chlorinated Organocompounds. A Review

Water, 2 (1) (2010), 28-74, 10.3390/w2010028

[8] I. Tudela, Y. Zhang, M. Pal, I. Kerr, A.J. Cobley

Ultrasound-assisted electrodeposition of composite coatings with particles

Surface and Coatings Technology, 259 (2014), 363-373, 10.1016/j.surfcoat.2014.06.023

[9] J. Klima, A. Frias-Ferrer, J. Gonzalez-Garcia, J. Ludvik, V. Saez, J. Iniesta

Optimisation of 20 kHz sonoreactor geometry on the basis of numerical simulation of local ultrasonic intensity and qualitative comparison with experimental results

Ultrason Sonochem, 14 (1) (2007), 19-28, 10.1016/j.ultsonch.2006.01.001

[10] I. Tudela, V. Saez, M.D. Esclapez, M.I. Diez-Garcia, P. Bonete, J. Gonzalez-Garcia

Simulation of the spatial distribution of the acoustic pressure in sonochemical reactors with numerical methods: a review

Ultrason Sonochem, 21 (3) (2014), 909-19, 10.1016/j.ultsonch.2013.11.012

[11] R.F. Contamine, A.M. Wilhelm, J. Berlan, H. Delmas

Power measurement in sonochemistry

Ultrasonics Sonochemistry, 2 (1) (1995), S43-S47, 10.1016/1350-4177(94)00010-p

[12] T. Kimura, T. Sakamoto, J.-M. Leveque, H. Sohmiya, M. Fujita, S. Ikeda, T. Ando

Standardization of ultrasonic power for sonochemical reaction

Ultrasonics Sonochemistry, 3 (3) (1996), S157-S161, 10.1016/s1350-4177(96)00021-1

[13] R.J. Wood, J. Lee, M.J. Bussemaker

A parametric review of sonochemistry: Control and augmentation of sonochemical activity in aqueous solutions

Ultrason Sonochem, 38 (2017), 351-370, 10.1016/j.ultsonch.2017.03.030

[14] E.A. Serna-Galvis, J. Lee, F. Hernández, A.M. Botero-Coy, R.A. Torres-Palma

Sonochemical Advanced Oxidation Processes for the Removal of Pharmaceuticals in Wastewater Effluents

Removal and Degradation of Pharmaceutically Active Compounds in Wastewater Treatment2020, pp. 349-381

[15] K. Wang, C. Han, J. Li, J. Qiu, J. Sunarso, S. Liu

The Mechanism of Piezocatalysis: Energy Band Theory or Screening Charge Effect?

Angew Chem Int Ed Engl, 61 (6) (2022), e202110429, 10.1002/anie.202110429

Chemical Engineering Journal Advances 14 (2023) 100477

Contents lists available at ScienceDirect

Chemical Engineering Journal Advances

journal homepage: www.sciencedirect.com/journal/chemical-engineering-journal-advances

Effect of frequency and power on the piezocatalytic and sonochemical degradation of dyes in water

Franziska Bößl [a,*], Valentin C. Menzel [a], Efthalia Chatzisymeon [b], Tim P. Comyn [c], Peter Cowin [c], Andrew J. Cobley [d], Ignacio Tudela [a,*]

[a] School of Engineering, Institute for Materials and Processes, Edinburgh Electrochemical Engineering Group (e3 Group), The University of Edinburgh, Sanderson Building, Robert Stevenson Road, Edinburgh, EH9 3FB, United Kingdom
[b] School of Engineering, Institute for Infrastructure and Environment, The University of Edinburgh, William Rankine Building, Thomas Bayes Road, Edinburgh, EH9 3JL, United Kingdom
[c] Ionix Advanced Technologies Ltd., 3M Buckley Innovation Centre, Firth Street, Huddersfield, HD1 3BD, United Kingdom
[d] Functional Materials and Chemistry Research Group, Research Centre for Manufacturing and Materials, Institute of Clean Growth and Future Mobility, Coventry University, Beresford Avenue, Coventry, CV6 5LZ, United Kingdom

ARTICLE INFO

Keywords:
Piezocatalysis
Sonochemistry
Dye degradation
Cavitation
Ultrasonic frequency
Ultrasonic power

ABSTRACT

For the very first time, the effect of frequency on the piezocatalytic degradation of dyes has been systematically evaluated. To achieve this, a combination of systems and experimental setups operating at different ultrasonic frequencies ranging from 20 kHz up to 1 MHz were used. In addition, the effect of ultrasonic power was investigated at a low ultrasonic frequency of 20 kHz and higher ultrasonic frequency of 576 kHz to shed more light into the controversial discussion surrounding the 'true' mechanisms behind piezocatalysis. The results revealed that mechanical effects derived from acoustic cavitation, predominant at lower ultrasonic frequencies (<100 kHz), indeed enhanced the piezocatalytic degradation of the dye, Rhodamine B, to some extent (from 53% to 64% RhB degradation after 2 h). However, it was again demonstrated that sonochemical production of radicals remains a significant contributor for the overall degradation of the dye. Moreover, at higher ultrasonic frequencies (>100 kHz), the chemical effects derived from acoustic cavitation were so remarkable, that it raised the question of whether a piezocatalyst is really necessary when the optimisation of frequency and power may be enough for sonochemistry to fully degrade organic pollutants at a fast rate (pseudo first-order degradation reaction rate constant up to 0.037 min^{-1}).

1. Introduction

Piezocatalysis is a new concept in the field of catalysis that has attracted much attention in recent years. This novel area of research is considered a promising development within catalysis due to the potential use of renewable and prevalent vibrations such as those from wind or tides that could make catalytic reactions independent from energy sources like electricity and light [1–8]. Piezocatalysis aims to take advantage of piezoelectric materials that have the ability to generate an electrical response while being strained or stressed by an external force. This external force is commonly applied by a mechanical field (i.e. acoustic field generated by ultrasound) [5-7,9-16] surrounding the piezoelectric materials, leading to redox reactions occurring over the surface of such materials (i.e. piezocatalyst).

Despite numerous reports on piezocatalytic processes [4,7,11-15, 17-22], the mechanism of piezocatalysis remains controversial [1,23]. In recent years, two very different potential mechanisms have been suggested for piezocatalysis [1-4,21-24]. On the one hand, researchers have considered energy band theory analogous to photocatalysis, where redox reactions occurring at the surface of piezocatalysts are determined by the energy band levels from the valence and conduction bands. On the other hand, researchers have referred to more classical piezoelectricity (either bulk or localised piezoelectric polarisation) where the piezoelectric potential is the driving force of chemical reactions at the piezocatalyst surface.

If bulk piezoelectric polarisation resulting from the piezoelectric potential was the dominant mechanism behind piezocatalysis (Fig. 1a), achieving the maximum piezoelectric polarisation within a

* Corresponding author.
E-mail addresses: (F. Bößl), (I. Tudela).

https://doi.org/10.1016/j.ceja.2023.100477

Available online 4 March 2023

piezocatalyst would obviously result in an enhanced performance of the process. In general, a piezoelectric material will exhibit a higher piezoelectric response when excited at its resonance frequency, or at a global resonance frequency of the whole mechanical system [25,26] where said piezoelectric material is being used (a piezocatalyst particle and a surrounding liquid in the present case). Hence, one would expect a higher piezocatalytic effect if a piezocatalyst was excited close to either its resonance frequency or a global resonance frequency of the system that could result in a high piezoelectric polarisation. However, the vast majority of research on piezocatalysis has only used low-power acoustic vibrations around 40 kHz [5-7,9-16,27,28] as the main method to mechanically excite piezocatalysts, far from their resonance frequencies (which should be in the MHz order of magnitude) and without consideration for global resonance frequencies of the whole mechanical system involved. Only recently the research community has started to explore the possibility of conducting piezocatalytical processes at different frequencies, but with a focus on the low range (<100 kHz) [17]. If piezocatalysts were truly excited at frequencies close to their resonance frequencies or the global resonance frequency of the system (i.e. frequencies where a significantly higher degree of bulk piezoelectric polarisation could be achieved), one would expect a remarkable enhancement of the piezocatalytic behaviour. If this was not the case, though, it would confirm the unviability of that proposed mechanism, shedding more light onto how piezocatalysis really works.

As previously reported by the authors [29] and more recently confirmed by other researchers [6], other phenomena such as sonochemistry (Fig. 1c) or sonocatalysis are also likely to occur when studying piezocatalysis whenever ultrasound is used to generate an acoustic field as the method to excite piezocatalysts, as this will also result in the occurrence of acoustic cavitation driving such phenomena. These phenomena are also severely influenced by both frequency and power of ultrasounds [30–33]. Therefore, the aim of this study is to evaluate and understand, from both piezocatalytic and sonochemical point of view, the effect that ultrasonic frequency and power have on the overall piezocatalytic process to find out whether bulk piezoelectric polarisation is really behind piezocatalysis.

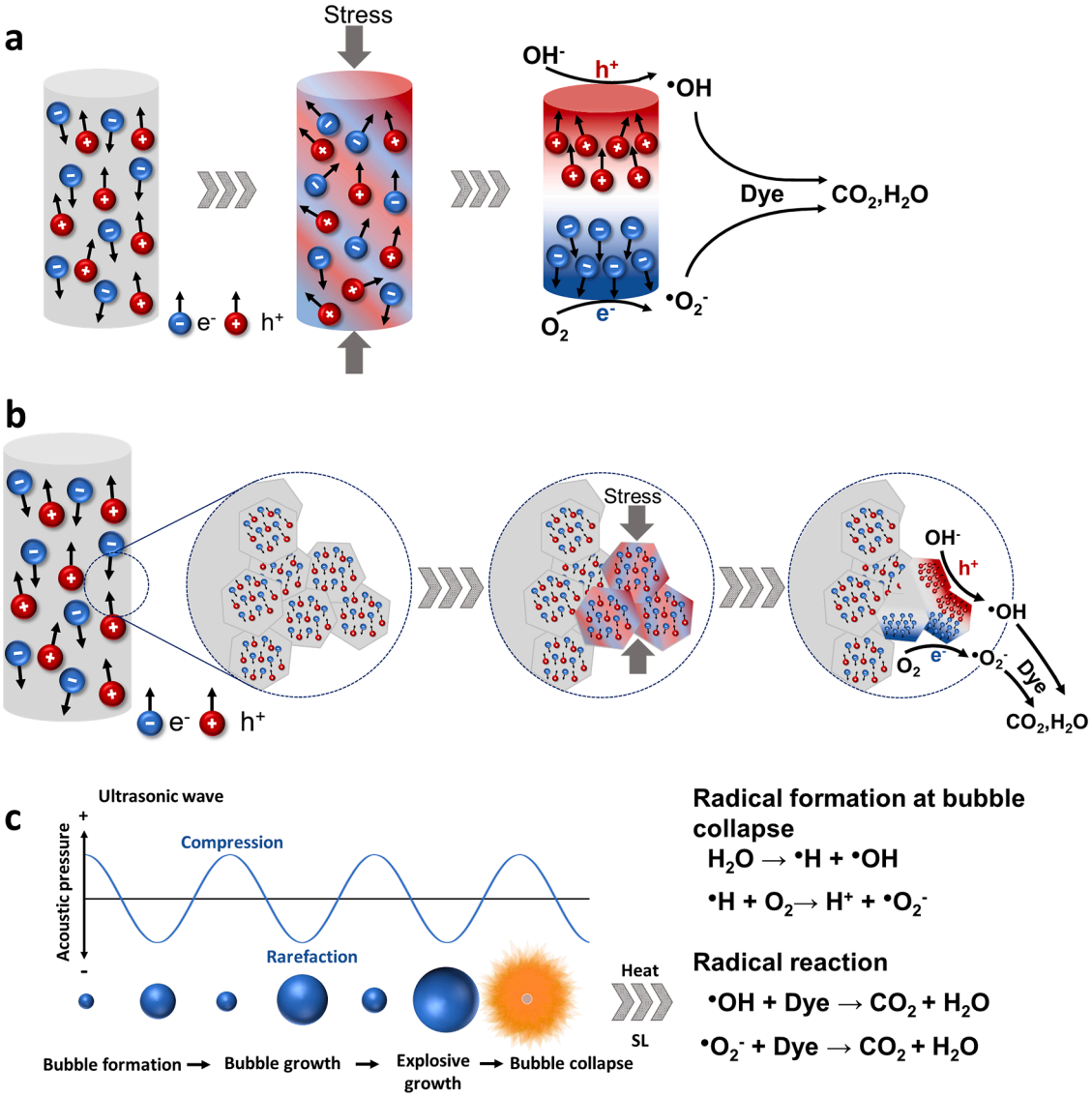

Fig. 1. Illustration of the different mechanisms for the overall piezocatalytic degradation of dyes: a) 'top-to-bottom' electric potential difference due to bulk polarisation of a piezoelectric particle under stress, b) electric potential difference due to localised polarisation within micro- and nano-structured features of piezocatalysts, c) bubble formation, growth and collapse under ultrasound and resulting chemical processes (i.e. sonochemistry).

2. Experimental

2.1. Catalyst preparation and characterisation

The piezoelectric material (poled potassium bismuth titanate-bismuth ferrite lead titanate, BF-KBT-PT) [34,35] and procedure that had been previously developed by the authors [29] were again employed to fabricate the piezocatalysts used in this study. The reasons for choosing this material are several: the source material, when poled, is highly piezoelectric (d_{33} and d_{31} values of 100 pC/N and −40 pC/N, respectively). Its high coercive stress allows for the maintenance of the piezoelectric effect even after applied stress such as grinding and sieving into fine particles to make the piezocatalysts (<63 μm)[29]. Focused ion beam-scanning electron microscopy (FIB-SEM, Zeiss Crossbeam 550) with an energy dispersive X-ray spectrometer (EDS) was used to analyse the surface structure and composition, whereas X-ray powder diffraction (XRPD) data was collected using a Bruker D8 X-ray powder diffractometer with CuKα-radiation to determine the crystalline structure of the BF-KBT-PT catalysts. The presence of the piezoelectric effect in the BF-KBT-PT piezocatalysts was proven empirically using a Berlincourt metre (APC International) and aligning the unelectroded particles in the metre in various orientations.

2.2. Finite element simulations

A finite element method model previously developed by the authors coupling the acoustic field in the liquid with the vibration of a single piezocatalytic particle and its piezoelectric response was used to simulate BF-KBT-PT piezocatalysts freely suspended in a liquid (i.e. piezocatalyst/water mechanical system) to investigate their piezoelectric response between 20 and 1150 kHz. A detailed explanation of the model, its simplifications and advantages over other models employed in the literature, as well as the material properties defined, can be found in a previous work by the authors [29].

2.3. Experimental setups and procedure

As opposed to the general trend in the field based on the use of small reactors up to 100 mL [4,7,8,14,19], all the experiments included in this study were conducted in reactors with substantially larger working volumes of 500 and 1000 mL containing 5 mg L^{-1} Rhodamine B (RhB) aqueous solutions. Reactor/ultrasonic transducer position and operating parameters were carefully set and controlled, and acoustic power calibrations of various powers at all frequencies were conducted by the standard calorimetric calibration method [36], to ensure reproducibility and comparability of experiments carried out in the different experimental setups. This included the use of a precise temperature control system (Grant LT ecocool 100 recirculating chiller) to provide a constant operating temperature of 30 ± 2 °C throughout all the RhB degradation experiments. Samples of the RhB aqueous solutions (3 mL) were taken every 10 min with a 0.22 μm PTFE-syringe-filter. Samples were then analysed by ultraviolet–visible spectroscopy (Shimadzu UV-3600 Plus) at the characteristic wavelength of 554 nm. In the piezocatalytic degradation experiments, 0.001 g mL^{-1} of BF-KBT-PT piezocatalysts were added to the RhB aqueous solution. To ensure adsorption-desorption equilibrium was reached, RhB aqueous solution containing the appropriate amount of catalyst were stirred at 200 rpm for 30 min. As previously reported, no adsorption nor photocatalytic degradation of RhB took place throughout the experiments [29].

Additional experiments to confirm previously reported radical initiated degradation routes [6,29] at high and low ultrasonic frequencies for sonochemical and piezocatalytic degradation of RhB were conducted in the presence and absence of BF-KBT-PT piezocatalysts and several radical and charge scavengers: 10 mM terephthalic acid (TA), 10 mM benzoquinone (BQ) and 2 mM ethylenediaminetetraacetic acid (EDTA) disodium salt dihydrate, all of high purity (99.5%, 99% and 99+%, respectively) from ACROS Organics. TA, BQ and EDTA were selected due to their role as chemical traps for $^{\bullet}OH$ [37], $^{\bullet}O_2^-$ [38] and h^+ [39], respectively.

2.3.1. Low ultrasonic frequency setups

An ultrasonic horn (Branson SFX 550) was employed for the experiments conducted at 20 kHz (Fig. 2a). The ultrasonic horn was centred and immersed to a depth of 4 cm into in a 1000 mL double-jacketed batch reactor. Depending on the experimental condition, the acoustic power was adjusted and calibrated as follows: 12.4 ± 0.4, 38.1 ± 0.7, 50.1 ± 0.3, 68.0 ± 0.3 and 89.8 ± 0.4 W L^{-1}.

An ultrasonic bath (Ultrawave QS12) was used for the experiments carried out at 32-38 kHz (Fig. 2b). A 1000 mL beaker was centred and immersed to a depth of 4 cm into the ultrasonic bath with a constant water level. The ultrasonic bath was operated at a full calibrated power of 12.2 ± 0.4 W L^{-1}. Prior to each experiment, the water in the ultrasonic bath was thoroughly degassed for 60 min ensuring a reproducible acoustic field inside the bath.

2.3.2. High ultrasonic frequency setup

An ultrasonic power multifrequency generator (Meinhard Ultrasonics) equipped with a 500 mL long-neck flask was used to conduct the experiments at 576, 864 and 1142 kHz (Fig. 2c). The power was adjusted and calibrated depending on the experimental conditions. The calibrated acoustic powers were 2.9 ± 0.4, 5.5 ± 0.4, 10.6 ± 0.3, 20.3 ± 0.7 and 33.7 ± 0.6 W L^{-1} at 576 kHz, 11.0 ± 0.6 W L^{-1} at 864 kHz and 10.0 ± 0.7 W L^{-1} at 1142 kHz.

2.3.3. Aluminium foil erosion experiments

The well-established aluminium foil erosion method [40–43] was performed to qualitatively evaluate the intensity of mechanical effects at different frequencies and power of 10-12 W L^{-1}. This method consisted of vertically suspending aluminium foil sheets within the reactor part of the different experimental setups used in this study. For this purpose, customised holders were designed and additive manufactured to secure the aluminium foil sheets within the reactors during the experiments. In all cases, the aluminium foil sheets were immersed in the sonicated solution for 5 min to allow for sufficient erosion of the foil.

3. Results and discussion

3.1. Catalyst characterisation

As reported in a previous work by the authors [29], FIB-SEM analysis revealed that the vast majority of BF-KBT-PT piezocatalysts exhibited a cuboid morphology with a particle size in the order of 63 μm or smaller (Fig. 3a). XRPD data (Fig. 3b) indicated peak splitting in the (200) phase; however, peak splitting of the (111) phase was not observed, confirming negligible lattice distortion of the rhombohedral phase due to the poled nature of the material [34]. XRPD data also confirmed the perovskite structure of BF-KBT-PT with no visible secondary phases [34]. Empiric piezoelectric analysis of BF-KBT-PT piezocatalysts in various random orientations (e.g. −35, −42, −47 or +143 pC/N) showed that the ground particles conserved their high piezoelectric nature (Fig. 3c).

3.2. Effect of ultrasonic frequency

3.2.1. FEM simulations

FEM simulations of a single BF-KBT-PT piezocatalyst suspended in water at ultrasonic frequencies ranging from 15 to 1150 kHz indicated the existence of six global resonance frequencies of the piezocatalyst/water mechanical system within the studied range (Fig. 4a): 123, 370, 618, 864, 1055 and 1111 kHz. In an ideal scenario, these are the frequencies the BF-KBT-PT piezocatalysts should be excited at, besides its resonance frequency (which would be in the MHz scale). However, in

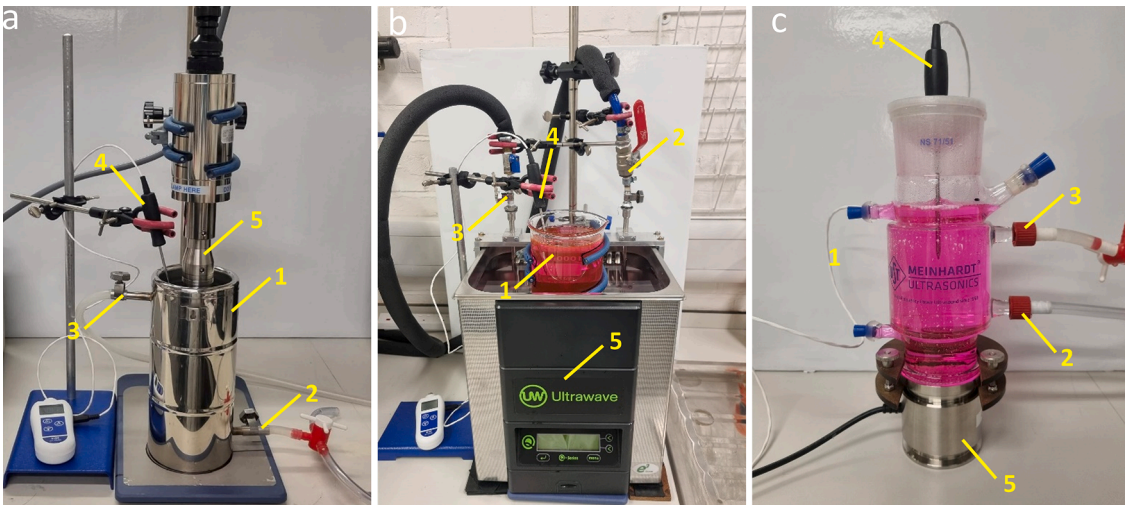

Fig. 2. Experimental setups used in the present study: a) 20 kHz ultrasonic horn setup, b) 32-38 kHz ultrasonic bath setup, c) 576, 864 and 1142 kHz multifrequency setup. Key components in all setups: 1) reactor, 2) cooling system inlet, 3) cooling system outlet, 4) thermocouple, 5) ultrasonic source.

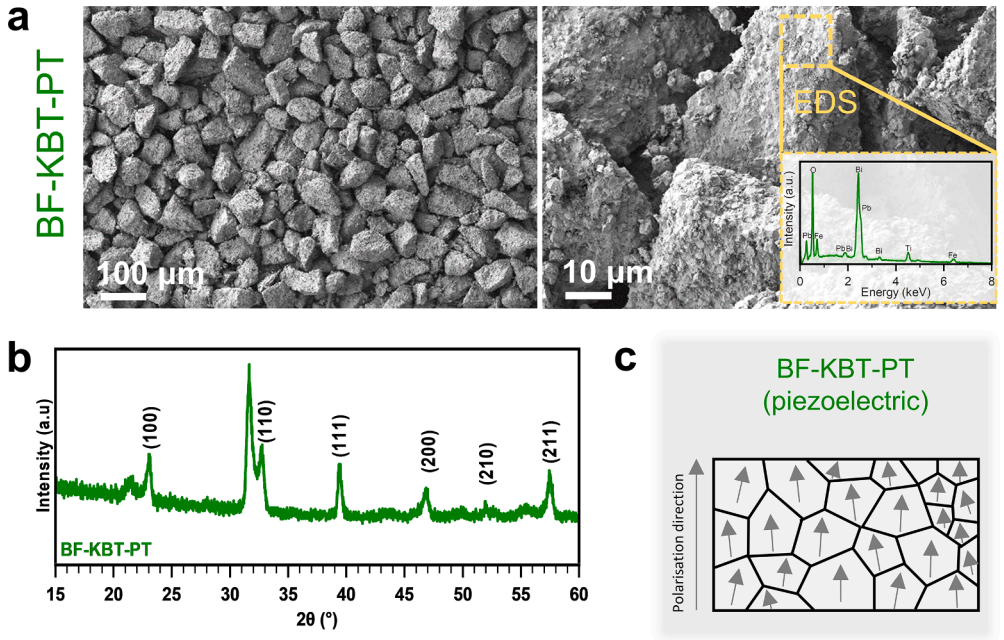

Fig. 3. Material characterisation of BF-KBT-PT piezocatalysts [29]: a) FIB-SEM and EDS, b) XRPD data. c) Schematic of aligned Weiss domains for piezoelectric BF-KBT-PT.

practice, the operating frequencies of ultrasonic systems depend upon the piezoceramics used to build the transducers that generate the acoustic field within the irradiated liquid, the liquid itself and the final geometry of the system [25,26,44]; operating frequencies are therefore close to the resonance frequency of the piezoceramics within the transducer that allow for its resonance in length mode [45]. For this reason, the simulated polarisation experienced by the piezocatalyst at the operating frequencies of the ultrasonic systems used in this study (20, 35, 576, 864 and 1142 kHz) were further investigated (Fig. 4b-f).

FEM simulations at 20, 35, 576, 864 and 1142 kHz indicated that, out of the five operating frequencies experimentally investigated in this study, 864 kHz (i.e. a global resonance frequency) should theoretically result in the BF-KBT-PT piezocatalyst achieving the greatest 'top-to-bottom' electric potential difference of 69.1 V. The minimum theoretical potential required for the redox reactions responsible of the piezocatalytic generation of $^{\bullet}OH$ and $^{\bullet}O_2^-$ radicals is 2.22 V (oxidation: $OH^- + h^+ \rightarrow {}^{\bullet}OH$, +1.89 V vs SHE [46]; Reduction: $O_2 + e^- \rightarrow {}^{\bullet}O_2^-$ [47]. Therefore, this theoretical result would in principle support the occurrence of bulk piezoelectric polarisation as a mechanism driving the piezocatalytic degradation of RhB at 864 kHz via $^{\bullet}OH$ and $^{\bullet}O_2^-$ radicals (Fig. 1a). At 576 and 1142 kHz, 'top-to-bottom' electric potential differences of 0.14 and 0.12 V, respectively, were observed. This would not be enough to overcome the minimum of 2.22 V by bulk polarisation, but other phenomena such as localised piezoelectric polarisation [48] (Fig. 1.b) or sonocatalysis [49] could still occur, resulting in the degradation of RhB by the same radicals, but to a lesser extent [29]. The latter would also apply to the low frequencies explored in this study, although to an even lesser extent, as the lowest 'top-to-bottom' electric potential difference of 0.08 V was observed for the simulations conducted at both 35 and 20 kHz.

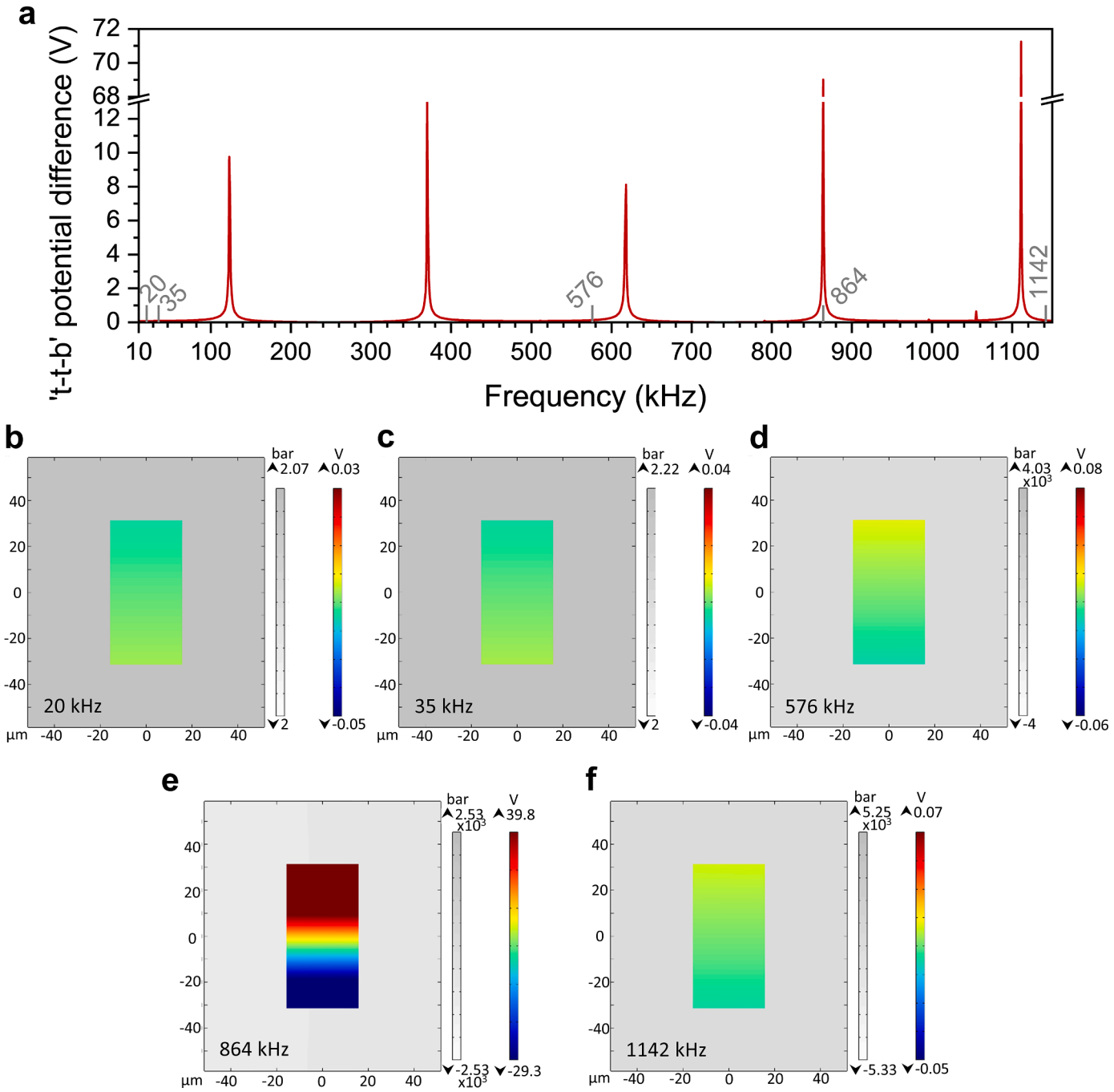

Fig. 4. a) 'Top-to-bottom' ('t-t-b') electric potential difference of a 63 μm BF-KBT-PT piezocatalyst suspended in water at ultrasonic frequencies ranging from 20 to 1150 kHz. b-f) 't-t-b' polarisation of a 63 μm BF-KBT-PT piezocatalyst suspended in water at different ultrasonic frequencies: 20, 35, 576, 864 and 1142 kHz, respectively.

3.2.2. RhB degradation experiments

Following the FEM simulations conducted at 20, 35, 576, 864 and 1142 kHz, one would expect to observe the greatest piezocatalytic effect at 864 kHz due to the greatest 'top-to-bottom' electric potential difference of 69.1 V observed at that global resonance frequency. However, RhB degradation experiments conducted at those same frequencies provided a completely different scenario (Fig. 5), even though the experiments indeed demonstrated the strong influence that frequency may have on the overall degradation of RhB. One reason for the disparity between the FEM simulations and the experimental results would be the simplifications made in the FEM model [29]: (i) use of 2D geometries (instead of 3D), (ii) use of linear acoustics not accounting for asymmetrical bubble collapses near the surface of the catalyst, (iii) the definition of perfectly smooth surfaces in the solid with no roughness that could result in localised piezoelectric polarisation and, especially, (iv) the simplified geometry of the domains used (i.e. small portion of liquid with a single piezocatalyst instead of the whole reactor with liquid and several hundreds or thousands of solid particles suspended in the liquid) . Another reason is related the acoustic pressure source defined in the FEM simulations (2 bar). Whilst 2 bar reflect a realistic acoustic pressure at low ultrasonic frequencies such as the 20 kHz ultrasonic horn or the 32-38 kHz ultrasonic bath [50–52], it may be too high for state-of-the-art systems operating at higher ultrasonic frequencies. This means that it is not possible, with state-of-the-art technology, to conduct

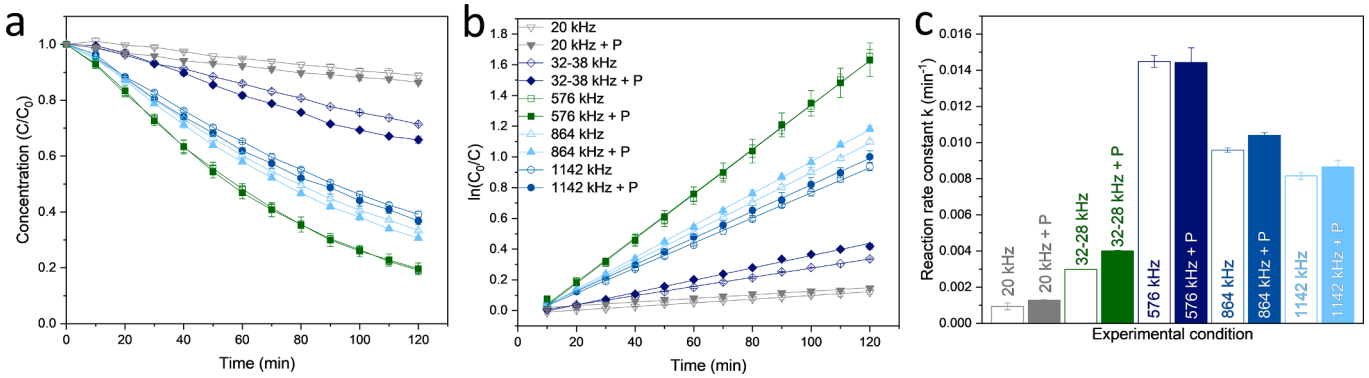

Fig. 5. RhB degradation experiments in the presence and absence of BF-KBT-PT piezocatalysts (P) at different frequencies and acoustic powers of 10-12 W $L-1$: a) evolution of C/C0 vs reaction time, b) pseudo first-order linear fit of ln(C0/C) vs reaction time, c) pseudo first-order degradation reaction rate constants.

experiments over a wide range of frequencies with exactly the same acoustic pressure source.

This situation, which indeed complicates the evaluation of the effect of frequency in piezocatalysis in terms of acoustic energy due to the differences in terms of reactor geometry, volume and ultrasonic source [53], can be overcome by estimating the acoustic power dissipated in the solution containing the piezocatalysts through calibration by calorimetry [36,54], a well-established method in sonochemistry research that enables the comparison by taking into account all those differences in the experimental setup [53]. For this reason, all the RhB degradation experiments displayed in Fig. 5 were conducted at a calibrated acoustic power around 10-12 W L^{-1}, as it was the maximum acoustic power that could be achieved by the 32-38 kHz ultrasonic bath; the dissipated acoustic powers in the different systems used at 20, 32–38, 576, 864 and 1142 kHz were 12.4 ± 0.4, 12.2 ± 0.4, 10.6 ± 0.3, 11.0 ± 0.6 and 10.0 ± 0.7 W L^{-1}, respectively.

RhB degradation experiments clearly showed two trends:

- At low frequencies, overall RhB degradation was rather low. In absence of the piezocatalyst (i.e. sonochemical generation of radicals only) [29], RhB degradations of around 11% and 29% were achieved at 20 and 32-38 kHz, respectively. The addition of the BF-KBT-PT piezocatalyst did result in a relative improvement of the overall degradation process, as RhB degradations of 14% (27% relative improvement) and 35% (21% relative improvement) were observed at 20 and 32-38 kHz, respectively.
- At higher frequencies, however, the overall degradation was significantly higher. In absence of the piezocatalyst, the greatest RhB degradation (81%) was observed at 576 kHz, whereas experiments conducted at 864 kHz and 1142 kHz yielded RhB degradations of 67% and 61%, respectively. In these cases, though, the addition of the BF-KBT-PT piezocatalyst did not result in a significant change in performance, as RhB degradations of 80% (0% relative improvement), 69% (3% relative improvement) and 63% (3% relative improvement) were observed at 576, 864 and 1142 kHz, respectively.

These results show that, when the ultrasonic frequency was varied from 20 to 1142 kHz while keeping the same acoustic power (around 10-12 W L^{-1}), the highest RhB was achieved at 576 kHz. This should not be a complete surprise, as it is believed that sonochemical radical formation is maximised at ultrasonic frequencies around 400 kHz [55–60]. Due to the shorter time length of the acoustic cycle, higher ultrasonic frequencies (>100 kHz) generally result in increased nucleation and a larger amount of cavitation bubbles that are smaller than at lower ultrasonic frequencies (i.e. 20-100 kHz) at the same acoustic power [30,31]. This results in enhanced formation of radicals [61] that contribute to the sonochemical degradation of RhB [29]. However, as also demonstrated by the present results, there is an upper limit of the applied ultrasonic frequency above which the RhB degradation diminishes, which is why RhB degradation at 864 and 1142 kHz was lower than that at 576 kHz. This is due to the bubbles forming at higher ultrasonic frequencies not being sufficiently large to undergo a violent collapse, hence why less radicals are formed to degrade RhB [30,53]. On the other hand, at lower ultrasonic frequencies (i.e. <100 kHz), cavitating bubbles are able to grow for longer time due to the longer time length of the acoustic cycle. As they grow larger, the bubbles undergo more violent collapses, resulting in less chemical effects like sonochemical formation of radicals [30,53], but more pronounced mechanical effects such as shock waves, micro-jetting and asymmetrical bubble collapse at the surface of solids [62].

To confirm the relevance of mechanical effects occurring at different frequencies used in this study, a qualitative evaluation of the acoustic field was conducted by immersing aluminium foil in the different experimental setups (Fig. 6). At low ultrasonic frequencies (<100 kHz), the aluminium foil experienced significant erosion caused by the mechanical effects of acoustic cavitation (Fig. 6a). This was particularly obvious for the foil immersed in the system operating at 32-38 kHz, where the greatest amount of erosion was observed. In fact, the erosion patterns clearly described the nature of the acoustic field established in the reactor, illustrating the clear existence of at least five pressure antinodes within the beaker where cavitating bubbles would concentrate. On the other hand, no noticeable erosion marks were observed by the naked eye on aluminium foil immersed in the multifrequency system operating at high frequencies (>100 kHz), a very clear indication of negligible mechanical effects (Fig. 6b). These results clearly link the occurrence of mechanical effects within the liquid being treated with the relative importance of the piezocatalytic contribution towards the degradation of RhB at different frequencies.

But why are mechanical effects generated by acoustic cavitation important in piezocatalysis? As previously stated, mechanical effects include phenomena such as shock waves, micro-jetting and, especially in this case, asymmetrical bubble collapse at the surface of solids. These phenomena result in piezocatalysts experiencing significantly high pressures (of the order of 100 bar), which would obviously lead to outstanding polarisations. The polarisation experienced by the piezocatalysts caused by the action of, for example, asymmetrical bubble collapses at their surface, would probably be far higher than the potential differences reported in the FEM simulations at low frequencies (<100 kHz); this polarisation would be enough to drive redox reactions at the surface of the piezocatalysts [63]. This is exactly the case of the present study, where the combination of a more violent collapse of cavitating bubbles with the poor sonochemical degradation of RhB via radical formation at low frequencies (<100 kHz) meant that, when BF-KBT-PT piezocatalysts were added to RhB aqueous solutions, a piezocatalytic contribution towards the degradation of RhB could be

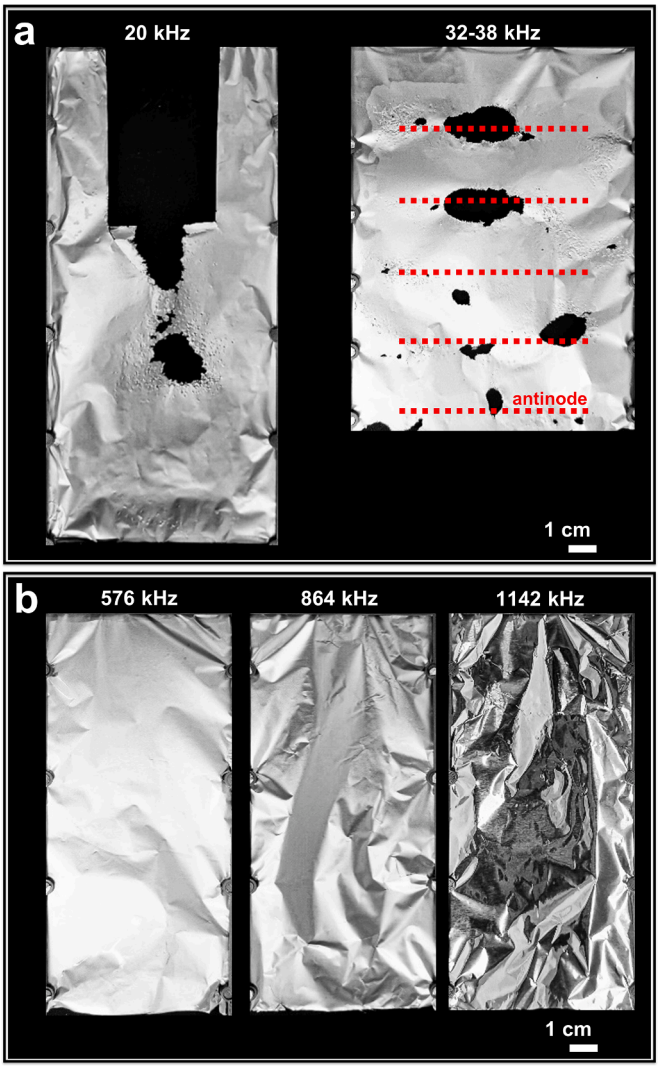

Fig. 6. Longitudinal view of aluminium foil erosion experiments (exposure time 5 min): a) low frequencies, b) high frequencies.

noticed. On the other hand, the superior sonochemical degradation of RhB via radical formation and the less violent collapse of cavitating bubbles at high ultrasonic frequencies (>100 kHz) [61] also explains why any potential piezocatalytic contribution is barely noticed in those conditions. In this case, though, the occurrence of mechanical effects that could cause a localised piezoelectric response [48] (Fig. 1b) would be more important than bulk piezoelectric polarisation resulting from exciting a piezocatalyst close to its resonance frequency (Fig. 1a). This was further confirmed by exploring the surface of the piezocatalysts after the experiments by FIB-SEM: in the particular case of the piezocatalysts used in experiments conducted at 32-38 kHz, smoother surfaces and erosion marks caused by asymmetric bubble collapses could be clearly seen (Fig. 7); a strong localised piezoelectric response would indeed be expected in the surroundings of those areas.

To summarise these findings, it can be stated that, with current ultrasonic transducer technology, one should focus in low ultrasonic frequencies to exploit the piezocatalytic degradation route to maximise the mechanical effects of acoustic cavitation; these would result in a localised piezoelectric response of the piezocatalyst (Fig. 1b). On the other hand, high frequencies would favour the sonochemical route (Fig. 1c), with no need to add a piezocatalyst at all.

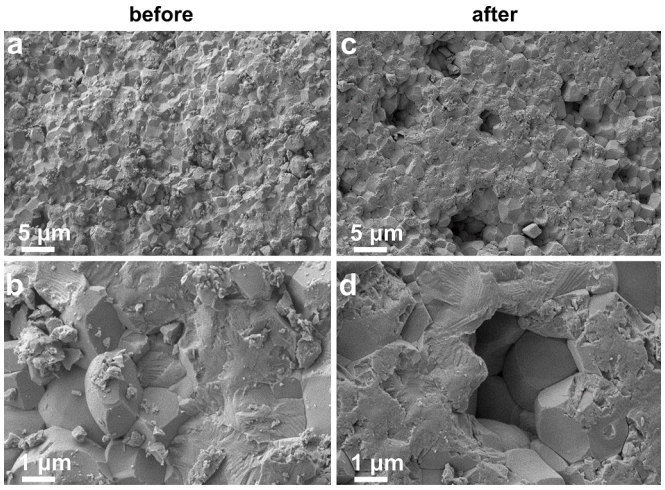

Fig. 7. FIB-SEM images of the surface of the BF-KBT-PT piezocatalyst used in experiments conducted at 32–38 kHz: a-b) before the experiment, c-d) after the experiment.

3.3. *Effect of ultrasonic power*

As demonstrated in the previous section, frequency is really important in both piezocatalytic and sonochemical degradation of RhB. Besides frequency, the other key parameter in ultrasonic systems is power. Therefore, to investigate the effect of ultrasonic power on both degradation mechanisms, additional experiments were conducted at 20 and 576 kHz. On the one hand, 20 kHz was chosen to investigate the effect of power at low ultrasonic frequencies for practical reasons: whereas the power output of the 20 kHz ultrasonic transducer could be further increased, the 32-38 kHz ultrasonic bath was already operating at its maximum power output. On the other hand, 576 kHz was chosen to investigate the effect of power at high ultrasonic frequencies due to the highest sonochemical degradation of RhB reported in the previous section.

Prior to the experiments, calorimetric calibrations were conducted at 20 and 576 kHz to determine five different acoustic power levels. At 20 kHz, the following acoustic powers were investigated based on the maximum output provided by the system: 12.4 ± 0.4, 38.1 ± 0.7, 50.1 ± 0.3, 68.0 ± 0.3 and 89.8 ± 0.4 W L^{-1}. At 576 kHz, the following acoustic powers were used, also based on the maximum output of the equipment: 2.9 ± 0.4, 5.5 ± 0.4, 10.6 ± 0.3, 20.3 ± 0.7 and 33.7 ± 0.6 W L^{-1}.

3.3.1. *Low ultrasonic frequency*

RhB degradation experiments conducted at 20 kHz (Fig. 8) revealed an increase in the overall degradation of RhB as the acoustic power was increased. RhB degradation in absence/presence of the BF-KBT-PT piezocatalyst was 11%/14% at 12 W L^{-1} (3% difference in overall degradation), 33%/37% at 38 W L^{-1} (4% difference in overall degradation) and 53%/64% at 50 W L^{-1} (11% difference in overall degradation), respectively, indicating a progressively growing contribution of piezocatalysis to the overall degradation of RhB. However, RhB degradation in the absence/presence of the BF-KBT-PT piezocatalyst was 79%/84% at 68 W L^{-1} (5% difference in overall degradation) and 92%/94% at 90 W L^{-1} (2% difference in overall degradation), indicating that, at certain point, further increasing the acoustic power would result in higher sonochemical degradation of RhB, but the contribution of the piezocatalyst towards the overall degradation would progressively decrease.

The apparent contradiction of these results can be explained with the effect of high ultrasonic power on the behaviour and distribution of cavitating bubbles at low frequencies, as illustrated by additional aluminium foil erosion experiments conducted in the 20 kHz setup at

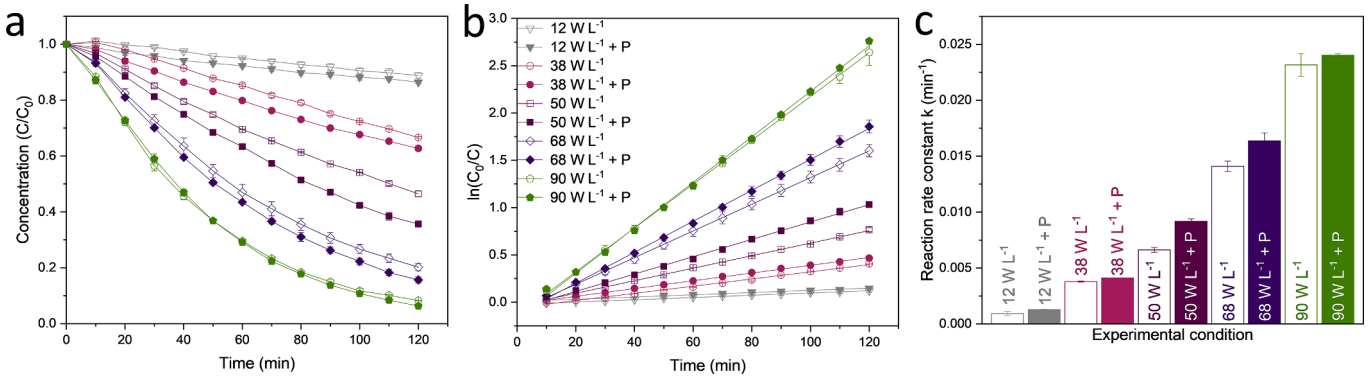

Fig. 8. RhB degradation experiments in the presence and absence of BF-KBT-PT piezocatalysts (P) at low frequency (20 kHz) and different acoustic powers: a) evolution of C/C0 vs reaction time. b) pseudo first-order linear fit of ln(C0/C) vs reaction time. c) pseudo first-order degradation reaction rate constants.

different acoustic powers (Fig. 9). As it is well known, there are upper and lower limits for acoustic power to result in 'efficient' cavitation activity [30,64]. Below the lower power threshold, the sound field is not efficient enough to induce bubble formation or nucleation; bubbles tend to succumb to surface tension effects and dissolve, leading to low cavitation activity [30,65]. This low cavitation activity would result in low sonochemical radical formation, but also low mechanical effects (Fig. 9a), hence the low sonochemical degradation and piezocatalytic contribution at 12 W L^{-1}. In between the upper and lower thresholds, the acoustic pressure influences not only the magnitude of the bubble collapse, but also the surface stability of the bubble as well as its oscillation. A more violent collapse results from the bubbles being exposed to higher negative pressures during the rarefaction phase of an ultrasonic wave, followed by higher pressures in the subsequent compression. This also leads to higher potential energy that is partially converted into radical formation, heat (i.e. higher collapse temperature), light (i.e. sonoluminescence) and sound emissions [58], with the subsequent increase in mechanical effects (Fig. 9b and c), hence the increase in sonochemical degradation and growing piezocatalytic contribution observed at 38 and, especially,50 W L^{-1}, where we can clearly see the piezocatalytic contribution of by the BF-KBT-PT particles. However, at excessive acoustic powers, an increase in bubble coalescence, degassing and liquid agitation takes place [30,31]. These phenomena may not have been enough to negatively affect the sonochemical degradation observed at 68 and 90 W L^{-1} (the overall degradation of RhB continued to increase), but it had a progressively negative effect on the mechanical effects that affect piezocatalysis (Fig. 9d and especially e), resulting in lower piezocatalytic contribution at 68 and 90 W L^{-1}. This did not mean that the acoustic field was weaker at those acoustic powers, though; in fact, the presence of a stronger pressure antinode could be noticed far from the emitter surface at those two powers. Therefore, with current ultrasonic transducer technology, low ultrasonic frequencies at moderate powers should be the aim to maximise the piezocatalytic degradation route, as high powers could result in a decrease in piezocatalytic activity.

Moreover, radical and charge scavenger experiments (Fig. 10) using TA, BQ and EDTA were conducted at 20 kHz and 50 W L^{-1} in the presence and absence of BF-KBT-PT piezocatalysts to further confirm the importance of radical initiated degradation routes in the degradation of RhB. TA showed a negligible effect on the sonochemical degradation of RhB at 20 kHz (Fig. 10a-c), indicating that $^{\bullet}$OH radicals were not being predominantly formed at such frequency and power. However, in the presence of BF-KBT-PT piezocatalysts, TA showed a more significant hindering effect on the overall degradation of RhB, suggesting the piezocatalytic formation of $^{\bullet}$OH in the presence of the piezocatalyst. BQ had a significant hindering effect on RhB degradation, whether in

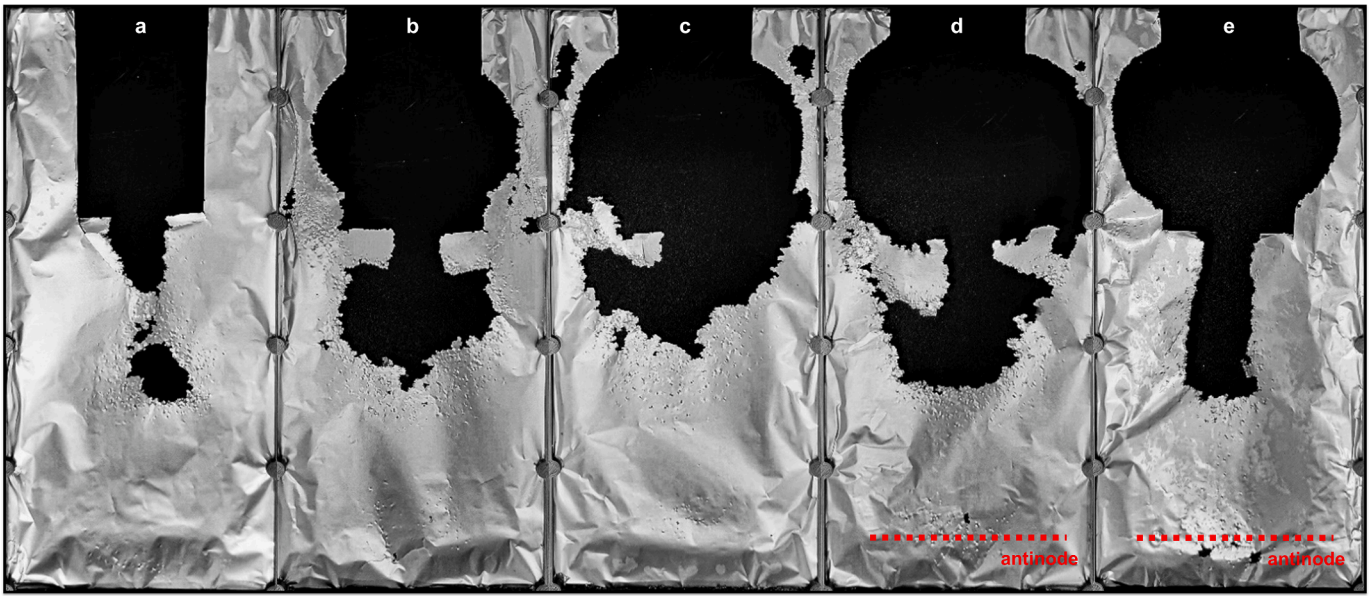

Fig. 9. Longitudinal view of aluminium foil erosion experiments (exposure time 5 min) conducted at low frequency (20 kHz) and different acoustic powers: a) 12 W $L-1$, b) 38 W $L-1$, c) 50 W $L-1$, d) 68 W $L-1$, e) 90 W $L-1$.

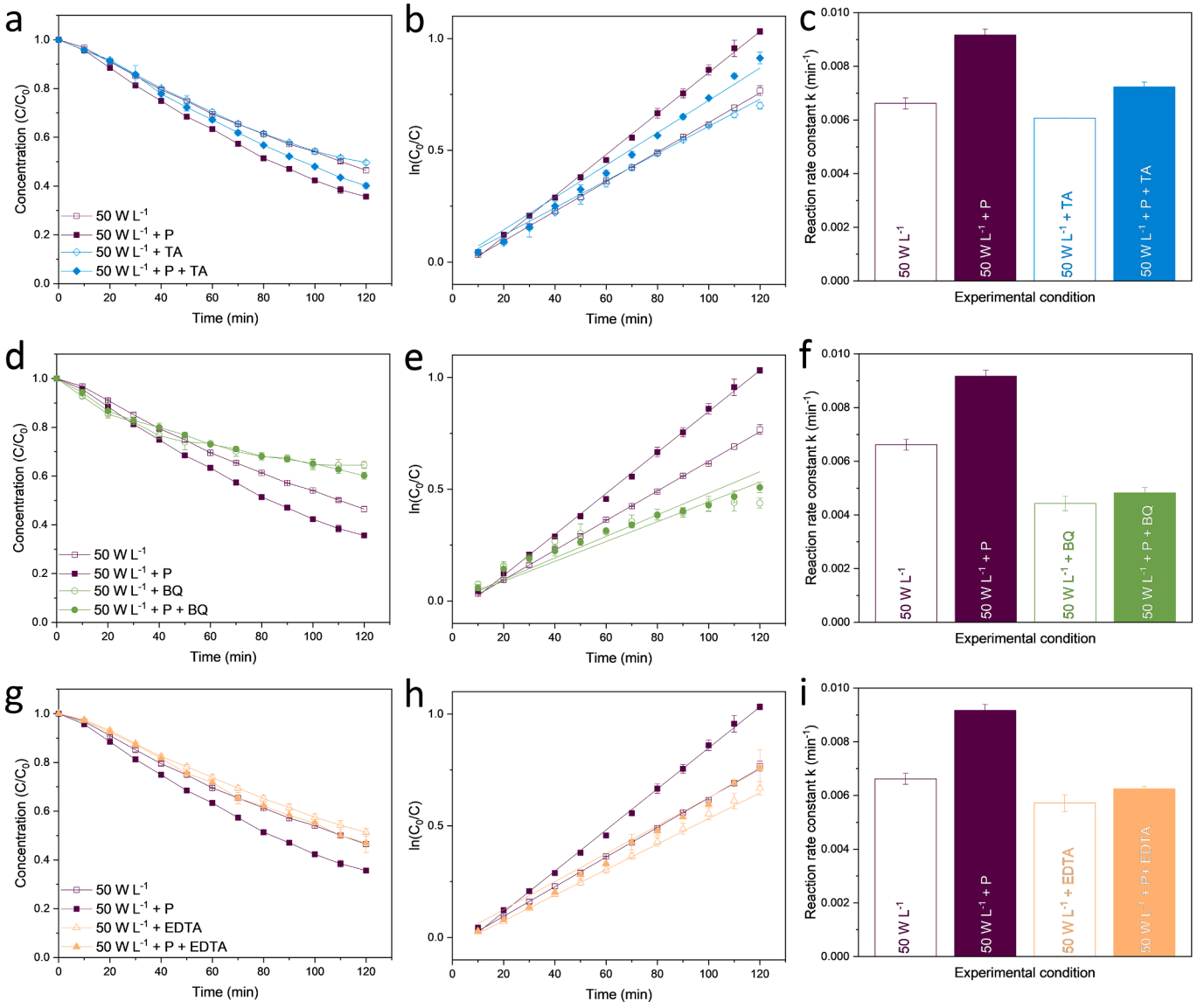

Fig. 10. RhB degradation experiments in the presence and absence of BF-KBT-PT piezocatalysts (P) at low frequency (20 kHz) and 50 W $L-1$ with different radical scavengers: a) evolution of C/C0 vs reaction time, b) pseudo first-order linear fit of ln(C0/C) vs reaction time, c) pseudo first-order degradation reaction rate constants in the presence of terephthalic acid (TA); d) evolution of C0/C vs reaction time, e) pseudo first-order linear fit of ln(C0/C) vs reaction time, f) pseudo first-order degradation reaction rate constants in the presence of benzoquinone (BQ); g) evolution of C0/C vs reaction time, h) pseudo first-order linear fit of ln(C0/C) vs reaction time, i) pseudo first-order degradation reaction rate constants in the presence of ethylenediaminetetraacetic acid (EDTA).

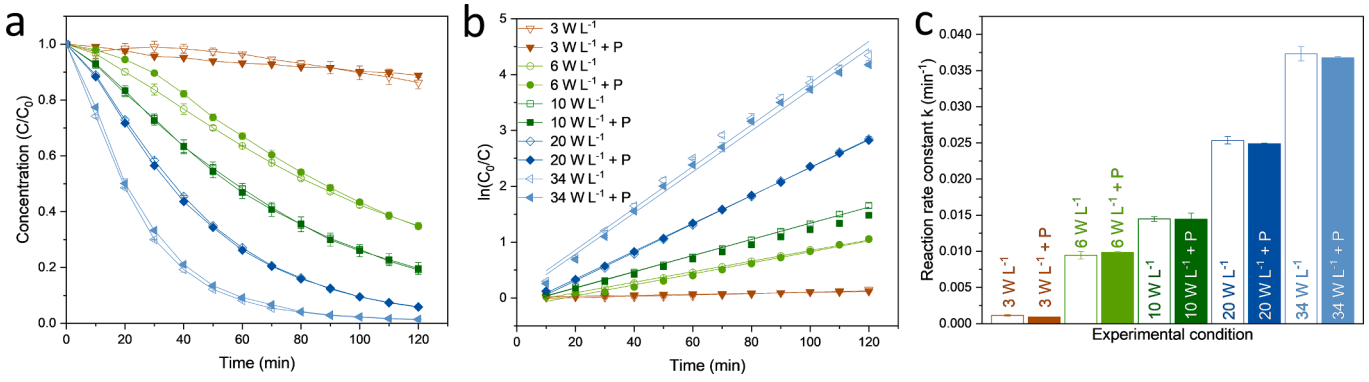

Fig. 11. RhB degradation experiments in the presence and absence of BF-KBT-PT piezocatalysts (P) at high frequency (576 kHz) with different acoustic powers: a) evolution of C/C0 vs reaction time. b) pseudo first-order linear fit of ln(C0/C) vs reaction time. c) pseudo first-order degradation reaction rate constants.

presence or absence of BF-KBT-PT piezocatalysts (Fig. 10D-f), demonstrating the importance of $^{\bullet}O_2^-$ radicals for the decomposition of RhB at low ultrasonic frequencies. The results also revealed that piezocatalytic degradation was significantly hindered using BQ to scavenger $^{\bullet}O_2^-$ radicals, indicating an enhanced production of $^{\bullet}O_2^-$ radicals in the presence of BF-KBT-PT piezocatalysts at the selected frequency and power. EDTA showed some minor decrease in the sonochemical degradation of RhB (Fig. 10g-i) due to its potential interaction with sonochemical formation of radicals [29,66]. However, the scavenging effect of EDTA on h^+ was clearly noticeable in the presence of BF-KBT-PT piezocatalysts, reducing the overall degradation of RhB close to the sonochemical decomposition. This demonstrates the importance of h^+ in the piezocatalytic degradation at lower ultrasonic frequencies.

3.3.2. *High ultrasonic frequency*

RhB degradation experiments conducted at 576 kHz (Fig. 11) also showed a progressive enhancement of the sonochemical degradation of RhB as the ultrasonic power was increased: overall RhB degradations of 14%, 65%, 80% and 94% were achieved at 3, 6, 10 and 20 W L^{-1}, respectively. Moreover, at the highest acoustic power used (34 W L^{-1}), 99% of RhB was degraded after 110 min; in other words, almost complete degradation of RhB was achieved in less than 2 h. As expected from the results from the previous section, the addition of the BF-KBT-PT piezocatalysts had little to no effect on the overall degradation, further indicating that only sonochemical degradation (Fig. 1c) with no piezocatalytic contribution was taking place at 576 kHz, no matter which acoustic power was being used. This should not be a complete surprise, though; near complete sonochemical degradation of RhB after 2-hour experiments at 300 kHz has been reported in the past, although at powers apparently higher (around 200 W L^{-1}) [67] than those reported in this study.

To better understand the observed degradation of RhB at higher ultrasonic frequencies, radical and charge scavenger experiments using TA, BQ and EDTA were again conducted at 576 kHz and 34 W L^{-1} (Fig. 12). TA showed some hindering effect on the degradation performance in the first 60 min of the experiments both in the absence and

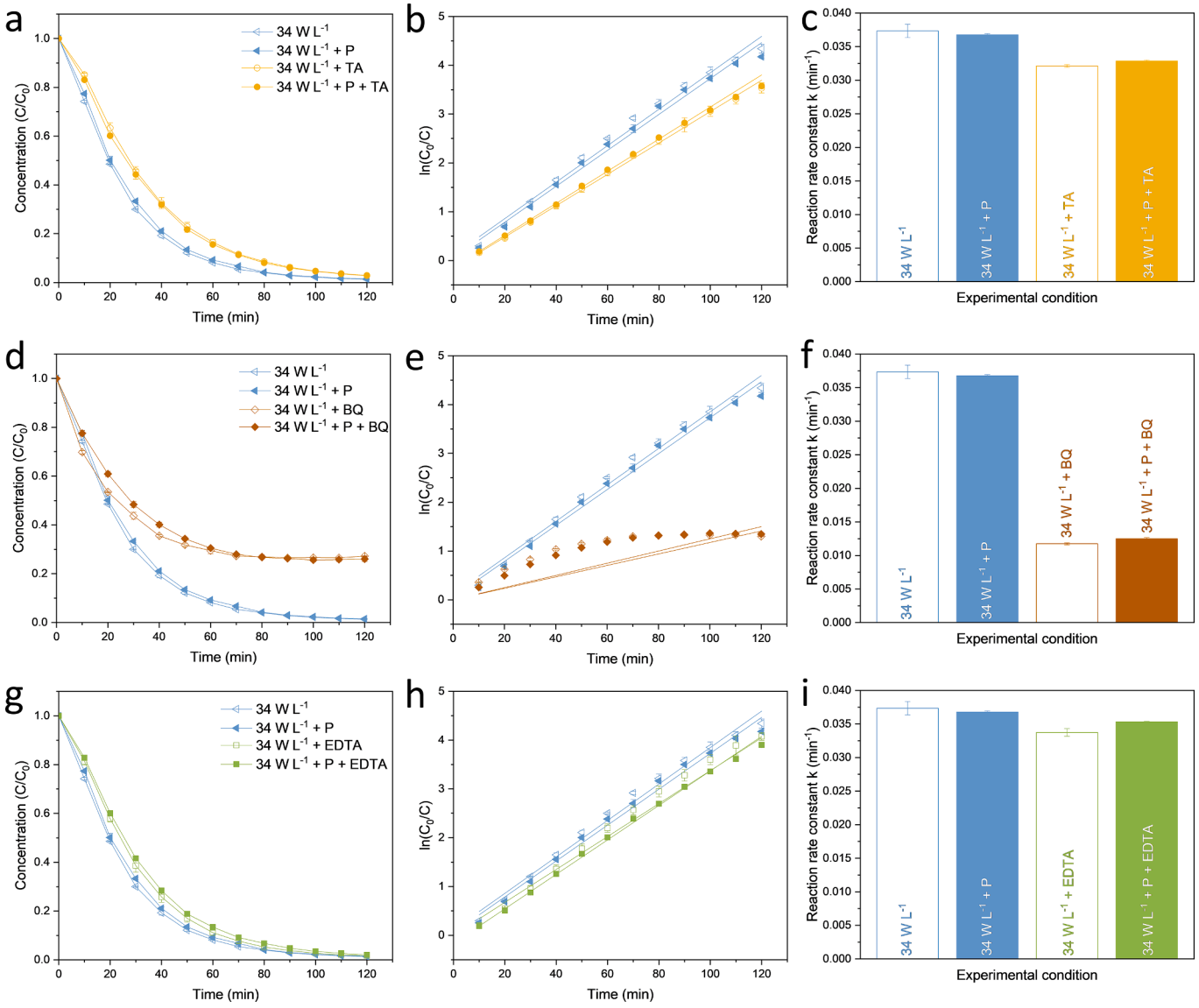

Fig. 12. RhB degradation experiments in the presence and absence of BF-KBT-PT piezocatalysts (P) at high frequency (576 kHz) and 34 W $L-1$ with different radical scavengers: a) evolution of C/C0 vs reaction time, b) pseudo first-order linear fit of ln(C0/C) vs reaction time, c) pseudo first-order degradation reaction rate constants in the presence of terephthalic acid (TA); d) evolution of C0/C vs reaction time, e) pseudo first-order linear fit of ln(C0/C) vs reaction time, f) pseudo first-order degradation reaction rate constants in the presence of benzoquinone (BQ); g) evolution of C0/C vs reaction time, h) pseudo first-order linear fit of ln(C0/C) vs reaction time, i) pseudo first-order degradation reaction rate constants in the presence of ethylenediaminetetraacetic acid (EDTA).

presence of BF-KBT-PT piezocatalysts (Fig. 12a-c). However, due to the significantly greater formation of $^{\bullet}OH$ radicals at 576 kHz compared to that at 20 kHz (in agreement with previous studies[68]), the added concentration of 10 mM TA was not enough to hinder the degradation of RhB at the end of the experiment (10 mM was around the saturation point in the solution). Nevertheless, the hindering effect was noticeable enough to confirm the contribution of $^{\bullet}OH$ radicals towards the degradation of RhB at high frequencies. The addition of BQ resulted in a significant hindering effect of the degradation of RhB (Fig. 12d-f) at 576 kHz, confirming the importance of $^{\bullet}O_2^-$ radicals on the decomposition of RhB at high frequencies. The addition of EDTA, however, had a very minor effect in the degradation of RhB (Fig. 12g-i), and the minor effect observed was likely due to the potential interaction of EDTA with the sonochemical formation of radicals [29,66]. The results in the presence of the BF-KBT-PT piezocatalysts are particularly revealing, confirming that h^+ were not involved in the degradation of RhB at 576 kHz. In other words, it further confirmed that there was no piezocatalysis taking place at high ultrasonic frequencies.

3.4. Overall discussion

The results from the experiments conducted at both low and high frequencies bring up an interesting discussion. At 20 kHz, whereas the presence of BF-KBT-PT piezocatalysts did enhance the overall degradation of RhB at 50 W L^{-1} (RhB degradation of 53%/64% in presence/absence of the piezocatalyst), further increasing the power to 90 W L^{-1} would result in a significantly higher RhB degradation with little contribution from the BF-KBT-PT piezocatalysts (RhB degradation of 92%/94% in the presence/absence of the piezocatalyst). In both cases, the piezocatalyst contribution would be strongly related to the mechanical effects caused by acoustic cavitation (e.g. shock waves, micro-jetting and asymmetrical bubble collapses near the surface of the piezocatalyst) that are maximised at low frequencies (<100 kHz). These mechanical effects might not be enough to generate by bulk polarisation (Fig. 1a) the minimum of 2.22 V necessary for the radical redox reactions to take place, but more than enough to cause localised piezoelectric polarisation (Fig. 1b) that would induce those reactions. Considering the energy requirements for ultrasound to generate acoustic cavitation and the resulting mechanical effects at low frequencies, though, one might prefer to explore less energy intensive options such as water-drive piezo-activation to achieve localised polarisation of piezocatalysts [69,70]. On the other hand, whereas no piezocatalysis was observed at high frequencies (>100 kHz) due to the significant decrease in the intensity and violence of those same mechanical effects, further tuning the frequency and increasing the power could result in the complete degradation of RhB at 576 kHz and 34 W L^{-1} through sonochemistry on its own (Fig. 1c). This would present straightforward advantages: there would be no need to add a catalyst to achieve the degradation (i.e. savings in materials, fabrication costs, separation processes after treatment, etc.), and there could be potential savings in energy consumption of the process, as full degradation was achieved at significantly lower acoustic powers than those used at 20 kHz.

Nevertheless, even with no piezocatalytic contribution to the overall process, the remarkable sonochemical degradation of RhB at 576 kHz and 34 W L^{-1} (pseudo first-order degradation reaction rate constant of 0.037 min^{-1}) outperforms the vast majority of the research on recent piezocatalytic degradation of RhB available in the literature (Table 1). As already indicated in their previous work [29] and more recently highlighted by other researchers [6,71], to achieve 'true' progress in piezocatalysis, expertise and practice from other fields (i.e. piezoelectricity, acoustics, sonochemistry and electrochemistry), as well as a systematic experimental approach with appropriate control experiments, must be incorporated into the research conducted in this area. If this is not followed, there is a strong risk that piezocatalysis may be, sooner rather than later, forgotten about without fully exploiting its potential.

Table 1
Comparison of pseudo first-order reaction rate constants for sonochemical and piezocatalytic degradation of RhB from this work with other piezocatalysis studies available in the literature.

Piezocatalyst	Frequency [kHz]	Acoustic power [W L^{-1}]	Rate constant [min^{-1}]	Ref
None	20	50.1 ± 0.3	0.007	this study
	20	89.8 ± 0.4	0.023	this study
	576	20.3 ± 0.7	0.025	this study
	576	33.7 ± 0.6	0.037	this study
BF-KBT-PT	20	50.1 ± 0.3	0.009	this study
	20	89.8 ± 0.4	0.024	this study
	576	20.3 ± 0.7	0.025	this study
	576	33.7 ± 0.6	0.037	this study
$BaTiO_3$	40	n/a (360 W)	0.013	[13]
$(Bi_{1/2}Na_{1/2})TiO_3$	40	n/a (100 W)	0.013	[14]
$Na_{0.5}Bi_{0.5}TiO_3$ (nanoparticles)	40	n/a (150 W)	0.022	[15]
$_{0.5}BNT–_{0.5}BFO$	40	n/a (120 W)	0.0204	[18]
$Bi_2Fe_4O_9$ (nanoplates)	40	n/a (200 W)	0.01615	[11]
$Ba_{0.95}Ca_{0.05}Ti_{0.9}Sn_{0.1}O_3$ (micron-sized powders)	40	n/a (100 W)	0.0245	[12]
$(K_{0.5}Na_{0.5})_{0.94}Li_{0.06}NbO_3$-PDMS	40	n/a (180 W)	~0.014	[9]
Bi- MOFs (bismuth-based)	40	n/a (300 W)	~0.025	[10]
Natural clay-modified MWCNT/kaolinite/PVDF membrane	30±5	n/a (50 W)	0.040	[19]
$Bi_2Fe_4O_9$ NSs	40	n/a (480 W)	0.0186	[20]
$BaTiO_3$@TiO_2 nanowires	28	n/a (n/a)	0.007	[17]
	45	n/a (200 W)	0.08	
	80	n/a (200 W)	0.002	
	100	n/a (200 W)	0.001	

4. Conclusion

The present study aimed to shed some light into the controversial discussion surrounding the piezocatalytic mechanisms by investigating the effect of ultrasonic frequency and power on the 'top-to-bottom' polarisation of piezocatalyst. The results indicated that the occurrence of mechanical effects (i.e. shock waves, micro-jetting and asymmetric collapse at the surface of the catalysts) predominant at lower ultrasonic powers (<100 kHz) would cause a localised piezoelectric response that would be more important for current piezocatalytic research rather than bulk piezoelectric polarisation resulting from exciting a piezocatalyst close to its resonance frequency.

The results also revealed that, whilst an increase in acoustic power would result in increased sonochemical degradation at both low and high ultrasonic frequencies, it did not necessarily result in an increased piezocatalytic contribution. Therefore, the use of lower ultrasonic frequencies with moderate powers should be encourage to maximise the piezocatalytic degradation route, whereas high powers and especially high ultrasonic frequencies would be favourable for the sonochemical degradation without the need to add a piezocatalyst. The latter could present straightforward advantages: savings in cost of materials, their

fabrication and post-treatment separation, as well as potential energy consumption.

Funding information

School of Engineering, The University of Edinburgh – Start Up fund. Carnegie Trust for the Universities of Scotland – RIG009799 grant. EPSRC – EP/P030564/1 grant.

CRediT authorship contribution statement

Franziska Bößl: Conceptualization, Methodology, Validation, Formal analysis, Investigation, Data curation, Writing – original draft, Visualization. **Valentin C. Menzel:** Methodology, Investigation. **Efthalia Chatzisymeon:** Resources, Writing – review & editing. **Tim P. Comyn:** Resources, Writing – review & editing. **Peter Cowin:** Resources. **Andrew J. Cobley:** Resources, Writing – review & editing. **Ignacio Tudela:** Conceptualization, Methodology, Resources, Writing – review & editing, Supervision, Project administration, Funding acquisition.

Declaration of Competing Interest

The authors declare that they have no known competing financial interests or personal relationships that could have appeared to influence the work reported in this paper.

Data availability

Data will be made available on request.

Acknowledgements

FB and IT acknowledge the University of Edinburgh for funding this research through its Start Up fund. IT would also like to thank the Carnegie Trust for the Universities of Scotland for its support through the Research Incentive Grant scheme (RIG009799). The authors also acknowledge the use of the Zeiss Crossbeam 550 FIB-SEM funded with EPSRC grant EP/P030564/1, and would also like to thank Dr James Cumby and Dr Thomas Glenn at the University of Edinburgh for their kind support in XRD and FIB-SEM analysis, respectively, as well as Mr Gordon Paterson for his help with some of the experimental setups used in this study.

References

[1] K. Wang, C. Han, J. Li, J. Qiu, J. Sunarso, S. Liu, The mechanism of piezocatalysis: energy band theory or screening charge effect? Angew. Chem. Int. Ed Engl. 61 (6) (2022), e202110429 https://doi.org/10.1002/anie.202110429.

[2] K.-S. Hong, H. Xu, H. Konishi, X. Li, Direct water splitting through vibrating piezoelectric microfibers in water, J. Phys. Chem. Lett. 1 (6) (2010) 997–1002, https://doi.org/10.1021/jz100027t.

[3] K.-S. Hong, H. Xu, H. Konishi, X. Li, Piezoelectrochemical Effect: a new mechanism for azo dye decolorization in aqueous solution through vibrating piezoelectric microfibers, The J. Phys. Chem. C 116 (24) (2012) 13045–13051, https://doi.org/10.1021/jp211455z.

[4] E. Lin, Z. Kang, J. Wu, R. Huang, N. Qin, D. Bao, BaTiO3 nanocubes/cuboids with selectively deposited Ag nanoparticles: efficient piezocatalytic degradation and mechanism, Appl. Catal. B: Environ. 285 (2021), https://doi.org/10.1016/j.apcatb.2020.119823.

[5] A. Zhang, Z. Liu, B. Xie, J. Lu, K. Guo, S. Ke, L. Shu, H. Fan, Vibration catalysis of eco-friendly Na0.5K0.5NbO3-based piezoelectric: an efficient phase boundary catalyst, Appl. Catal. B: Environ. 279 (2020), https://doi.org/10.1016/j.apcatb.2020.119353.

[6] H. Kalhori, A.H. Youssef, A. Ruediger, A. Pignolet, Competing contributions to the catalytic activity of barium titanate nanoparticles in the decomposition of organic pollutants, J. Environ. Chem. Eng. 10 (6) (2022), https://doi.org/10.1016/j.jece.2022.108571.

[7] W. Ma, M. Lv, F. Cao, Z. Fang, Y. Feng, G. Zhang, Y. Yang, H. Liu, Synthesis and characterization of ZnO-GO composites with their piezoelectric catalytic and antibacterial properties, J. Environ. Chem. Eng. 10 (3) (2022), https://doi.org/10.1016/j.jece.2022.107840.

[8] X. Zhou, Q. Sun, Z. Xiao, H. Luo, D. Zhang, Three-dimensional BNT/PVDF composite foam with a hierarchical pore structure for efficient piezo-photocatalysis, J. Environ. Chem. Eng. 10 (5) (2022), https://doi.org/10.1016/j.jece.2022.108399.

[9] X. Cheng, Z. Liu, Q. Jing, P. Mao, K. Guo, J. Lu, B. Xie, H. Fan, Porous (K0.5Na0.5)0.94Li0.06NbO3-polydimethylsiloxane piezoelectric composites harvesting mechanical energy for efficient decomposition of dye wastewater, J. Colloid Interface Sci. 629 (Pt A) (2023) 11–21, https://doi.org/10.1016/j.jcis.2022.08.131.

[10] S. Dong, L. Wang, W. Lou, Y. Shi, Z. Cao, Y. Zhang, J. Sun, Bi-MOFs with two different morphologies promoting degradation of organic dye under simultaneous photo-irradiation and ultrasound vibration treatment, Ultrason Sonochem. 91 (2022), 106223, https://doi.org/10.1016/j.ultsonch.2022.106223.

[11] Y. Du, T. Lu, X. Li, Y. Liu, W. Sun, S. Zhang, Z. Cheng, High-efficient piezocatalytic hydrogen evolution by centrosymmetric Bi2Fe4O9 nanoplates, Nano Energy 104 (2022), https://doi.org/10.1016/j.nanoen.2022.107919.

[12] J. He, C. Yu, Y. Hou, X. Su, J. Li, C. Liu, D. Xue, J. Cao, Y. Su, L. Qiao, T. Lookman, Y. Bai, Accelerated discovery of high-performance piezocatalyst in BaTiO3-based ceramics via machine learning, Nano Energy 97 (2022), https://doi.org/10.1016/j.nanoen.2022.107218.

[13] Z. Hu, W. Dong, Z. Dong, P. Li, Q. Bao, T. Cao, Facile fabrication of tetragonal phase single-crystalline BaTiO3 terrace-like dendrite by a simple solvothermal method and its piezocatalytic properties, Mater. Chem. Phys. 293 (2023), https://doi.org/10.1016/j.matchemphys.2022.126911.

[14] D.-.M. Liu, J.-.T. Zhang, C.-.C. Jin, B.-.B. Chen, J. Hu, R. Zhu, F. Wang, Insight into oxygen-vacancy regulation on piezocatalytic activity of (Bi1/2Na1/2)TiO3 crystallites: experiments and first-principles calculations, Nano Energy 95 (2022), https://doi.org/10.1016/j.nanoen.2022.106975.

[15] L. Shi, C. Lu, L. Chen, Q. Zhang, Y. Li, T. Zhang, X. Hao, Piezocatalytic performance of Na0.5Bi0.5TiO3 nanoparticles for degradation of organic pollutants, J. Alloys Compd. 895 (2022), https://doi.org/10.1016/j.jallcom.2021.162591.

[16] X. Zhou, B. Shen, J. Zhai, N. Hedin, Reactive oxygenated species generated on iodide-doped BiVO4/BaTiO3 heterostructures with Ag/Cu nanoparticles by coupled piezophototronic effect and plasmonic excitation, Adv. Funct. Mater. 31 (13) (2021), https://doi.org/10.1002/adfm.202009594.

[17] Q. Liu, D. Zhai, Z. Xiao, C. Tang, Q. Sun, C.R. Bowen, H. Luo, D. Zhang, Piezo-photoelectronic coupling effect of BaTiO3@TiO2 nanowires for highly concentrated dye degradation, Nano Energy 92 (2022), https://doi.org/10.1016/j.nanoen.2021.106702.

[18] Z. Liu, Y. Zheng, S. Zhang, J. Fu, Y. Li, Y. Zhang, W. Ye, (1−x) Bi0.5Na0.5TiO3–xBiFeO3 solid solutions with enhanced piezocatalytic dye degradation, Sep. Purif. Technol. 290 (2022), https://doi.org/10.1016/j.seppur.2022.120831.

[19] D. Mondal, S. Bardhan, N. Das, J. Roy, S. Ghosh, A. Maity, S. Roy, R. Basu, S. Das, Natural clay-based reusable piezo-responsive membrane for water droplet mediated energy harvesting, degradation of organic dye and pathogenic bacteria, Nano Energy 104 (2022), https://doi.org/10.1016/j.nanoen.2022.107893.

[20] C. Su, C. Li, R. Li, W. Wang, Insights into highly efficient piezocatalytic molecule oxygen activation over Bi2Fe4O9: active sites and mechanism, Chem. Eng. J. 452 (2023), https://doi.org/10.1016/j.cej.2022.139300.

[21] P.L. Wang, X.Y. Li, S.Y. Fan, X. Chen, M.C. Qin, D. Long, M.O. Tad, S.M. Liu, Impact of oxygen vacancy occupancy on piezo-catalytic activity of BaTiO3 nanobelt, Appl. Catal. B-Environ. 279 (2020), https://doi.org/10.1016/j.apcatb.2020.119340.

[22] B. Yuan, J. Wu, N. Qin, E. Lin, Z. Kang, D. Bao, Sm-doped Pb(Mg1/3Nb2/3)O3-xPbTiO3 piezocatalyst: exploring the relationship between piezoelectric property and piezocatalytic activity, Appl. Mater. Today 17 (2019) 183–192, https://doi.org/10.1016/j.apmt.2019.07.015.

[23] F. Bößl, I. Tudela, Piezocatalysis: can catalysts really dance? Current Opinion in Green and Sustain. Chem. 32 (2021) https://doi.org/10.1016/j.cogsc.2021.100537.

[24] J. Wu, Q. Xu, E. Lin, B. Yuan, N. Qin, S.K. Thatikonda, D. Bao, Insights into the role of ferroelectric polarization in piezocatalysis of nanocrystalline BaTiO3, ACS Appl. Mater. Interfaces 10 (21) (2018) 17842–17849, https://doi.org/10.1021/acsami.8b01991.

[25] O. Louisnard, J. Gonzalez-Garcia, I. Tudela, J. Klima, V. Saez, Y. Vargas-Hernandez, FEM simulation of a sono-reactor accounting for vibrations of the boundaries, Ultrason. Sonochem. 16 (2) (2009) 250–259, https://doi.org/10.1016/j.ultsonch.2008.07.008.

[26] I. Tudela, V. Sáez, M.D. Esclapez, P. Bonete, H. Harzali, F. Baillon, J. González-García, O. Louisnard, Study of the influence of transducer-electrode and electrode-wall gaps on the acoustic field inside a sonoelectrochemical reactor by FEM simulations, Chem. Eng. J. 171 (1) (2011) 81–91, https://doi.org/10.1016/j.cej.2011.03.064.

[27] Y. Chen, S. Lan, M. Zhu, Construction of piezoelectric BaTiO3/MoS2 heterojunction for boosting piezo-activation of peroxymonosulfate, Chinese Chem. Lett. 32 (6) (2021) 2052–2056, https://doi.org/10.1016/j.cclet.2020.11.016.

[28] K. Fan, C. Yu, S. Cheng, S. Lan, M. Zhu, Metallic Bi self-deposited BiOCl promoted piezocatalytic removal of carbamazepine, Surfaces and Interfaces 26 (2021), https://doi.org/10.1016/j.surfin.2021.101335.

[29] F. Bößl, T.P. Comyn, P.I. Cowin, F.R. García-García, I. Tudela, Piezocatalytic degradation of pollutants in water: importance of catalyst size, poling and excitation mode, Chem. Eng. J. Adv. 7 (2021), https://doi.org/10.1016/j.ceja.2021.100133.

[30] R.J. Wood, J. Lee, M.J. Bussemaker, A parametric review of sonochemistry: control and augmentation of sonochemical activity in aqueous solutions, Ultrason Sonochem. 38 (2017) 351–370, https://doi.org/10.1016/j.ultsonch.2017.03.030.
[31] E.A. Serna-Galvis, J. Lee, F. Hernández, A.M. Botero-Coy, R.A. Torres-Palma, Sonochemical advanced oxidation processes for the removal of pharmaceuticals in wastewater effluents, Removal and Degradation of Pharmaceutically Active Compounds in Wastewater Treatment (2020) 349–381.
[32] Z. Eren, N.H. Ince, Sonolytic and sonocatalytic degradation of azo dyes by low and high frequency ultrasound, J. Hazard Mater. 177 (1–3) (2010) 1019–1024, https://doi.org/10.1016/j.jhazmat.2010.01.021.
[33] M.H. Abdurahman, A.Z. Abdullah, N.F. Shoparwe, A comprehensive review on sonocatalytic, photocatalytic, and sonophotocatalytic processes for the degradation of antibiotics in water: synergistic mechanism and degradation pathway, Chem. Eng. J. 413 (2021), https://doi.org/10.1016/j.cej.2020.127412.
[34] J. Bennett, A.J. Bell, T.J. Stevenson, T.P. Comyn, Tailoring the structure and piezoelectric properties of BiFeO3-(K0.5Bi0.5)TiO3–PbTiO3 ceramics for high temperature applications, Appl. Phys. Lett. 103 (15) (2013), https://doi.org/10.1063/1.4824652.
[35] T. Stevenson, D.G. Martin, P.I. Cowin, A. Blumfield, A.J. Bell, T.P. Comyn, P. M. Weaver, Piezoelectric materials for high temperature transducers and actuators, J. Mater. Sci. Mater. Electron. 26 (12) (2015) 9256–9267, https://doi.org/10.1007/s10854-015-3629-4.
[36] R.F. Contamine, A.M. Wilhelm, J. Berlan, H. Delmas, Power measurement in sonochemistry, Ultrason. Sonochem. 2 (1) (1995) S43–S47, https://doi.org/10.1016/1350-4177(94)00010-p.
[37] N. Wang, L. Zhu, M. Wang, D. Wang, H. Tang, Sono-enhanced degradation of dye pollutants with the use of H2O2 activated by Fe3O4 magnetic nanoparticles as peroxidase mimetic, Ultrason. Sonochem. 17 (1) (2010) 78–83, https://doi.org/10.1016/j.ultsonch.2009.06.014.
[38] J.M. Monteagudo, H. El-Taliawy, A. Duran, G. Caro, K. Bester, Sono-activated persulfate oxidation of diclofenac: degradation, kinetics, pathway and contribution of the different radicals involved, J. Hazard Mater. 357 (2018) 457–465, https://doi.org/10.1016/j.jhazmat.2018.06.031.
[39] S. Farhadi, F. Siadatnasab, A. Khataee, Ultrasound-assisted degradation of organic dyes over magnetic CoFe2O4@ZnS core-shell nanocomposite, Ultrason. Sonochem. 37 (2017) 298–309, https://doi.org/10.1016/j.ultsonch.2017.01.019.
[40] D. Krefting, R. Mettin, W. Lauterborn, High-speed observation of acoustic cavitation erosion in multibubble systems, Ultrason. Sonochem. 11 (3–4) (2004) 119–123, https://doi.org/10.1016/j.ultsonch.2004.01.006.
[41] N. Bretz, J. Strobel, M. Kaltenbacher, R. Lerch, Numerical simulation of ultrasonic waves in cavitating fluids with special consideration of ultrasonic cleaning, IEEE Ultrason. Symposium 2005 (2005) 703–706, https://doi.org/10.1109/ultsym.2005.1602948.
[42] M.M. Chivate, A.B. Pandit, Quantification of cavitation intensity in fluid bulk, Ultrason. Sonochem. 2 (1) (1995) S19–S25, https://doi.org/10.1016/1350-4177(94)00007-f.
[43] G. Servant, J.L. Laborde, A. Hita, J.P. Caltagirone, A. Gerard, Spatio-temporal dynamics of cavitation bubble clouds in a low frequency reactor: comparison between theoretical and experimental results, Ultrason. Sonochem. 8 (3) (2001) 163–174, https://doi.org/10.1016/s1350-4177(01)00074-8.
[44] I. Tudela, V. Saez, M.D. Esclapez, M.I. Diez-Garcia, P. Bonete, J. Gonzalez-Garcia, Simulation of the spatial distribution of the acoustic pressure in sonochemical reactors with numerical methods: a review, Ultrason. Sonochem. 21 (3) (2014) 909–919, https://doi.org/10.1016/j.ultsonch.2013.11.012.
[45] S. Sherrit, M. Badescu, A.C. Noell, F. Kehl, M.F. Mora, N.J. Oborny, J.S. Creamer, P. A. Willis, Acoustic processing of fluidic samples for planetary exploration, Front. Space Technol. 3 (2022), https://doi.org/10.3389/frspt.2022.752335.
[46] V.K. Sharma, Oxidation of inorganic contaminants by ferrates (VI, V, and IV)–kinetics and mechanisms: a review, J. Environ. Manag. 92 (4) (2011) 1051–1073, https://doi.org/10.1016/j.jenvman.2010.11.026.
[47] W.H. Koppenol, D.M. Stanbury, P.L. Bounds, Electrode potentials of partially reduced oxygen species, from dioxygen to water, Free Radic. Biol. Med. 49 (3) (2010) 317–322, https://doi.org/10.1016/j.freeradbiomed.2010.04.011.
[48] J. Zhang, C. Wang, C. Bowen, Piezoelectric effects and electromechanical theories at the nanoscale, Nanoscale 6 (22) (2014) 13314–13327, https://doi.org/10.1039/c4nr03756a.
[49] P. Qiu, B. Park, J. Choi, B. Thokchom, A.B. Pandit, J. Khim, A review on heterogeneous sonocatalyst for treatment of organic pollutants in aqueous phase based on catalytic mechanism, Ultrason. Sonochem. 45 (2018) 29–49, https://doi.org/10.1016/j.ultsonch.2018.03.003.
[50] R. Chow, R. Mettin, B. Lindinger, T. Kurz, W. Lauterborn, The importance of acoustic cavitation in the sonocrystallisation of ice - high speed observations of a single acoustic bubble, IEEE Symposium on Ultrasonics 2003 (2003) 1447–1450, https://doi.org/10.1109/ultsym.2003.1293177.
[51] D.J. Flannigan, K.S. Suslick, Plasma line emission during single-bubble cavitation, Phys. Rev. Lett. 95 (4) (2005), 044301, https://doi.org/10.1103/PhysRevLett.95.044301.
[52] K. Yasui, Influence of ultrasonic frequency on multibubble sonoluminescence, J. Acoust. Soc. Am. 112 (4) (2002) 1405–1413, https://doi.org/10.1121/1.1502898.
[53] T.J. Mason, A.J. Cobley, J.E. Graves, D. Morgan, New evidence for the inverse dependence of mechanical and chemical effects on the frequency of ultrasound, Ultrason. Sonochem. 18 (1) (2011) 226–230, https://doi.org/10.1016/j.ultsonch.2010.05.008.
[54] T. Kimura, T. Sakamoto, J.-.M. Leveque, H. Sohmiya, M. Fujita, S. Ikeda, T. Ando, Standardization of ultrasonic power for sonochemical reaction, Ultrason. Sonochem. 3 (3) (1996) S157–S161, https://doi.org/10.1016/s1350-4177(96)00021-1.
[55] M. Ashokkumar, J. Lee, S. Kentish, F. Grieser, Bubbles in an acoustic field: an overview, Ultrason. Sonochem. 14 (4) (2007) 470–475, https://doi.org/10.1016/j.ultsonch.2006.09.016.
[56] M.A. Beckett, I. Hua, Impact of Ultrasonic Frequency on Aqueous Sonoluminescence and Sonochemistry, The J. Phys. Chem. A 105 (15) (2001) 3796–3802, https://doi.org/10.1021/jp003226x.
[57] J.-.W. Kang, H.-.M. Hung, A. Lin, M.R. Hoffmann, Sonolytic Destruction of Methyl tert-Butyl Ether by Ultrasonic Irradiation: The Role of O3, H2O2, Frequency, and Power Density, Environ. Sci. Technol. 33 (18) (1999) 3199–3205, https://doi.org/10.1021/es9810383.
[58] P. Kanthale, M. Ashokkumar, F. Grieser, Sonoluminescence, sonochemistry (H2O2 yield) and bubble dynamics: frequency and power effects, Ultrason. Sonochem. 15 (2) (2008) 143–150, https://doi.org/10.1016/j.ultsonch.2007.03.003.
[59] S. Koda, T. Kimura, T. Kondo, H. Mitome, A standard method to calibrate sonochemical efficiency of an individual reaction system, Ultrason. Sonochem. 10 (3) (2003) 149–156, https://doi.org/10.1016/S1350-4177(03)00084-1.
[60] C. Petrier, A. Jeunet, J.L. Luche, G. Reverdy, Unexpected frequency effects on the rate of oxidative processes induced by ultrasound, J. Am. Chem. Soc. 114 (8) (2002) 3148–3150, https://doi.org/10.1021/ja00034a077.
[61] G. Portenlanger, H. Heusinger, The influence of frequency on the mechanical and radical effects for the ultrasonic degradation of dextranes, Ultrason. Sonochem. 4 (2) (1997) 127–130, https://doi.org/10.1016/s1350-4177(97)00018-7.
[62] K.V. Tran, T. Kimura, T. Kondo, S. Koda, Quantification of frequency dependence of mechanical effects induced by ultrasound, Ultrason. Sonochem. 21 (2) (2014) 716–721, https://doi.org/10.1016/j.ultsonch.2013.08.018.
[63] J. Wu, N. Qin, D. Bao, Effective enhancement of piezocatalytic activity of BaTiO3 nanowires under ultrasonic vibration, Nano Energy 45 (2018) 44–51, https://doi.org/10.1016/j.nanoen.2017.12.034.
[64] K.S. Suslick, Sonoluminescence and sonochemistry, in: 1997 IEEE Ultrasonics Symposium Proceedings. An International Symposium (Cat. No.97CH36118), 1997, pp. 523–532, https://doi.org/10.1109/ultsym.1997.663076.
[65] T.J. Matula, J.R. Blake, Inertial cavitation and single–bubble sonoluminescence, Philosophical Trans. Royal Soc. London. Series A: Math. Phys. Eng. Sci. 357 (1751) (1999) 225–249, https://doi.org/10.1098/rsta.1999.0325.
[66] L. Parizot, T. Chave, M.-.E. Galvez, H. Dutilleul, P. Da Costa, S.I. Nikitenko, Sonocatalytic oxidation of EDTA in aqueous solutions over noble metal-free Co3O4/TiO2 catalyst, Appl. Catal. B: Environ. 241 (2019) 570–577, https://doi.org/10.1016/j.apcatb.2018.09.001.
[67] S. Merouani, O. Hamdaoui, F. Saoudi, M. Chiha, Sonochemical degradation of Rhodamine B in aqueous phase: effects of additives, Chem. Eng. J. 158 (3) (2010) 550–557, https://doi.org/10.1016/j.cej.2010.01.048.
[68] L. Milne, I. Stewart, D.H. Bremner, Comparison of hydroxyl radical formation in aqueous solutions at different ultrasound frequencies and powers using the salicylic acid dosimeter, Ultrason, Sonochem 20 (3) (2013) 948–989. https://doi.org/10.1016/j.ultsonch.2012.10.020.
[69] C. Yu, J. He, S. Lan, W. Guo, M. Zhu, Enhanced utilization efficiency of peroxymonosulfate via water vortex-driven piezo-activation for removing organic contaminants from water, Environ. Sci. Ecotechnol. 10 (2022), 100165, https://doi.org/10.1016/j.ese.2022.100165.
[70] S. Lan, B. Jing, C. Yu, D. Yan, Z. Li, Z. Ao, M. Zhu, Protrudent iron single-atom accelerated interfacial piezoelectric polarization for self-powered water motion triggered fenton-like reaction, Small 18 (2) (2022), e2105279, https://doi.org/10.1002/smll.202105279.
[71] M.M. Amer, R. Hommelsheim, C. Schumacher, D. Kong, C. Bolm, Electro-mechanochemical approach towards the chloro sulfoximidations of allenes under solvent-free conditions in a ball mill, Faraday Discuss 241 (2023) 79–90, https://doi.org/10.1039/d2fd00075j, 0.

4 Importance of energy band theory and screening charge effect

4.1 Introduction

The previous two chapters explored the concept of piezocatalysis focusing on the piezocatalytic mechanism following more traditional piezoelectric concepts: aiming to induce piezocatalytic activity entirely based on the piezoelectric polarisation (i.e. screening charge effects) through an optimum excitation method.

The piezoelectric polarisation experienced by the piezocatalyst was expected to exceed the difference between the reduction potentials of the redox reactions of interest. The results of the previous two chapters indicated that a localised piezoelectric response is more likely to achieve such high piezoelectric polarisations rather than a 'bulk' piezoelectric polarisation and are in accordance with other recent reports in the field of piezocatalysis [1-4].

However, in recent years a discussion emerged within the piezocatalytic community due to the introduction of another potential mechanism explaining the piezocatalytic phenomenon [5]. This mechanism is known as the energy band theory where the redox reactions at the catalyst surface are determined by the energy band levels of the valence and conduction bands [6-8]. The energy band levels of BF-KBT-PT had not been considered in the previous chapters and may have indeed been a reason why there is relatively subtle piezocatalytic contributions even at low ultrasonic frequencies and moderate acoustic powers (i.e. 20 kHz and 50 W L^{-1}). Therefore, the energy band levels for BF-KBT-PT were determined prior to this study, indicating that any observed piezocatalytic contribution in Chapter 2 and 3 would be primarily based on the screening charge effects rather than energy band theory.

To further investigate the importance of energy band theory and screening charge effects, two additional piezoelectric materials were used as piezocatalysts in this study. Zinc oxide nanoflowers were chosen for their well-known wide energy band gap and low piezoelectric properties [9-12], which suggested that any piezocatalytic contribution on the overall

degradation of RhB were likely to occur in accordance with the energy band mechanism rather than the screening charge effect. Barium titanate was chosen for its combination of very high piezoelectric properties and a wide energy band gap [13-16], which makes it an interesting candidate to potentially benefit from both mechanisms simultaneously.

By comparing the degradation performance of these three piezocatalysts, this study aimed to provide a clearer understanding of the importance of energy band theory and screening charge effects for the piezocatalytic process. Based on the findings in Chapter 2 and 3 it was decided to conduct this study only with the excitation method of combined ultrasound (32−38 kHz) and mechanical agitation (US+MA). This method proved to have the highest synergistic effect of sonochemistry and piezocatalysis while also exhibiting better energy efficiency compared to high power ultrasound at 20 kHz.

4.2 Discussion highlight and conclusions

The findings in this study suggest that both proposed mechanisms (i.e. energy band theory and screening charge effect) are likely to contribute to the overall piezocatalytic process, as the $BaTiO_3$ piezocatalyst achieving the best dye degradation could have generated superoxide and hydroxyl radicals via both mechanisms.

As expected from the literature, wide band gap values of 3.20 eV and 3.18 eV were determined for ZnO [9, 10, 17] and poled $BaTiO_3$ [13, 14], respectively. Poled BF-KBT-PT showed a narrow band gap of 2.16 eV. Band gap values for unpoled versions of BF-KBT-PT and $BaTiO_3$ were the same as for the poled versions of the materials, indicating that poling had no effect on the band gap values. A band alignment diagram was constructed (Fig. 4) with the help of XPS analysis to determine the valence band edge for all three piezocatalysts. The band alignment diagram in combination with the piezoelectric nature of the used piezocatalysts already provide a good indication of the potential reaction mechanisms likely to take place.

Based on these findings, ZnO should be able to generate superoxide and hydroxyl radicals via both piezocatalytic mechanism as well as via sonocatalysis. However, the poor piezocatalytic nature of ZnO would limit any piezocatalytic generation of radicals making sonocatalysis the most likely mechanism. In the case of BF-KBT-PT superoxide radicals could be generated by the sonocatalytic and both piezocatalytic mechanisms, whilst hydroxyl radicals should only be generated through the piezocatalytic screening charge mechanism due to energy band alignment. The highly piezoelectric nature and the energy band levels of $BaTiO_3$ would allow superoxide and hydroxyl generation via both piezocatalytic mechanisms. However, only superoxide radicals could be sonocatalytically generated with $BaTiO_3$.

Although the degradation experiments showed again that sonochemistry remained a significant contributor to the overall RhB degradation, the results clearly indicated that both piezocatalytic mechanisms seemed to take place simultaneously. It should therefore be beneficial to develop piezocatalyst with suitable energy band levels and high piezoelectric properties to optimise the piezocatalytic activity. Piezocatalysts with only one of these features might still exhibit some piezocatalytic behaviour, but this might be limited.

While this study provided some valuable insights into the mechanisms behind the piezocatalytic process there are still many unanswered questions. One of these is related to localised piezoelectric response in unpoled materials that do not possess piezoelectric properties, but showed some RhB degradation. Explaining these observations requires further research on micro- and nano-piezoelectricity. Another unsolved question is the superior performance of unpoled $BaTiO_3$ compared to unpoled BF-KBT-PT and even ZnO. A possible explanation could be the overpotentials required at the surfaces of the used catalyst being significantly lower for $BaTiO_3$. Further research is needed to fully understand these phenomena and transfer conventional electrocatalytical techniques to develop suitable piezocatalysts for more traditional electrochemical processes such as water electrolysis or CO_2 electroreduction.

Based on the findings in this study, it was decided to focus on $BaTiO_3$ as a core material in the subsequent chapter aiming to develop a bulky, easy-to-recover piezocatalyst to further enhance the piezocatalytic performance while reducing potential secondary pollution.

To gain a deeper understanding of the research outcomes and their significance, all results and a more comprehensive discussion can be found in *Importance of energy band theory and screening charge effect in piezo-electrocatalytical processes* published in *Electrochimica Acta*, which constitutes Chapter 4 of this thesis.

4.3 References

[1] W. Qian, K. Zhao, D. Zhang, C.R. Bowen, Y. Wang, Y. Yang
Piezoelectric Material-Polymer Composite Porous Foam for Efficient Dye Degradation via the Piezo-Catalytic Effect
ACS Appl Mater Interfaces, 11 (31) (2019), 27862-27869, 10.1021/acsami.9b07857

[2] G. Singh, M. Sharma, R. Vaish
Exploring the piezocatalytic dye degradation capability of lithium niobate
Advanced Powder Technology, 31 (4) (2020), 1771-1775, 10.1016/j.apt.2020.01.031

[3] K.P. Singh, G. Singh, R. Vaish
Utilizing the localized surface piezoelectricity of centrosymmetric $Sr_{1-x}Fe_xTiO_3$ ($x \leq 0.2$) ceramics for piezocatalytic dye degradation
Journal of the European Ceramic Society, 41 (1) (2021), 326-334, 10.1016/j.jeurceramsoc.2020.08.064

[4] N. Alfryyan, S. Kumar, S.B. Ahmed, I. Kebaili, I. Boukhris, P. Azad, M.S. Al-Buriahi, R. Vaish
Electric Poling Effect on Piezocatalytic $BaTiO_3$/Polymer Composites for Coatings
Catalysts, 12 (10) (2022), 10.3390/catal12101228

[5] K. Wang, C. Han, J. Li, J. Qiu, J. Sunarso, S. Liu
The Mechanism of Piezocatalysis: Energy Band Theory or Screening Charge Effect?
Angew Chem Int Ed Engl, 61 (6) (2022), e202110429, 10.1002/anie.202110429

[6] H. You, Z. Wu, L. Zhang, Y. Ying, Y. Liu, L. Fei, X. Chen, Y. Jia, Y. Wang, F. Wang, S. Ju, J. Qiao, C.H. Lam, H. Huang

Harvesting the Vibration Energy of $BiFeO_3$ Nanosheets for Hydrogen Evolution

Angew Chem Int Ed Engl, 58 (34) (2019), 11779-11784, 10.1002/anie.201906181

[7] P. Zhu, Y. Chen, J. Shi

Piezocatalytic Tumor Therapy by Ultrasound-Triggered and $BaTiO_3$ -Mediated Piezoelectricity

Adv Mater, 32 (29) (2020), e2001976, 10.1002/adma.202001976

[8] A. Zhang, Z. Liu, B. Xie, J. Lu, K. Guo, S. Ke, L. Shu, H. Fan

Vibration catalysis of eco-friendly $Na_{0.5}K_{0.5}NbO_3$-based piezoelectric: An efficient phase boundary catalyst

Applied Catalysis B: Environmental, 279 (2020), 10.1016/j.apcatb.2020.119353

[9] V. Srikant, D.R. Clarke

On the optical band gap of zinc oxide

Journal of Applied Physics, 83 (10) (1998), 5447-5451, Doi 10.1063/1.367375

[10] R. Anandhi, R. Mohan, K. Swaminathan, K. Ravichandran

Influence of aging time of the starting solution on the physical properties of fluorine doped zinc oxide films deposited by a simplified spray pyrolysis technique

Superlattices and Microstructures, 51 (5) (2012), 680-689, 10.1016/j.spmi.2012.02.006

[11] M.P. Bole, D.S. Patil

Effect of annealing temperature on the optical constants of zinc oxide films

Journal of Physics and Chemistry of Solids, 70 (2) (2009), 466-471, 10.1016/j.jpcs.2008.12.001

[12] E. Broitman, M.Y. Soomro, J. Lu, M. Willander, L. Hultman

Nanoscale piezoelectric response of ZnO nanowires measured using a nanoindentation technique

Phys Chem Chem Phys, 15 (26) (2013), 11113-8, 10.1039/c3cp50915j

[13] H. Fan, H. Li, B. Liu, Y. Lu, T. Xie, D. Wang

Photoinduced charge transfer properties and photocatalytic activity in Bi_2O_3/$BaTiO_3$ composite photocatalyst

ACS Appl Mater Interfaces, 4 (9) (2012), 4853-7, 10.1021/am301199v

[14] S. Das, S. Ghara, P. Mahadevan, A. Sundaresan, J. Gopalakrishnan, D.D. Sarma

Designing a Lower Band Gap Bulk Ferroelectric Material with a Sizable Polarization at Room Temperature

ACS Energy Letters, 3 (5) (2018), 1176-1182, 10.1021/acsenergylett.8b00492

[15] H. Takahashi, Y. Numamoto, J. Tani, S. Tsurekawa

Piezoelectric Properties of $BaTiO_3$ Ceramics with High Performance Fabricated by Microwave Sintering

Japanese Journal of Applied Physics, 45 (9B) (2006), 7405-7408, 10.1143/jjap.45.7405

[16] P. Zheng, J.L. Zhang, Y.Q. Tan, C.L. Wang

Grain-size effects on dielectric and piezoelectric properties of poled $BaTiO_3$ ceramics

Acta Materialia, 60 (13-14) (2012), 5022-5030, 10.1016/j.actamat.2012.06.015

[17] Y. Natsume, H. Sakata, T. Hirayama

Low-temperature electrical conductivity and optical absorption edge of ZnO films prepared by chemical vapour deposition

Physica Status Solidi (a), 148 (2) (1995), 485-495, 10.1002/pssa.2211480217

Electrochimica Acta 462 (2023) 142730

Contents lists available at ScienceDirect

Electrochimica Acta

journal homepage: www.journals.elsevier.com/electrochimica-acta

Importance of energy band theory and screening charge effect in piezo-electrocatalytical processes

Franziska Bößl [a,*], Valentin C. Menzel [a], Karina Jeronimo [b], Ayushi Arora [c], Yishu Zhang [c], Tim P. Comyn [d], Peter Cowin [d], Caroline Kirk [c], Neil Robertson [c], Ignacio Tudela [a,1,*]

[a] School of Engineering, Institute for Materials and Processes, Edinburgh Electrochemical Engineering Group (e3 Group), The University of Edinburgh, Sanderson Building, Robert Stevenson road, Edinburgh EH9 3FB, UK
[b] School of Engineering, Institute for Integrated Micro and Nano systems, Scottish Microelectronics Centre, University of Edinburgh, Alexander Crum Brown Road, Edinburgh EH9 3FF, UK
[c] School of Chemistry, The University of Edinburgh, Joseph Black Building, David Brewster road, Edinburgh EH9 3FJ, UK
[d] Ionix Advanced Technologies Ltd., 3 M Buckley Innovation Centre, Firth Street, Huddersfield HD1 3BD, UK

ARTICLE INFO

Keywords:
Piezo-electrocatalysis
Piezocatalysis
Energy band theory
Screen charge effect
Sonocatalysis
Sonochemistry

ABSTRACT

The present study tries to shed more light on the controversial discussion around the 'true' mechanism behind piezo-electrocatalysis: energy band theory or screening charge effects. For this purpose, piezo-electrocatalysts made of three different materials with different energy band levels and piezoelectric properties, ZnO, $BaTiO_3$ and BF-KBT-PT, were used to degrade Rhodamine B in aqueous solutions where combined ultrasound and mechanical agitation was used as the excitation method. The results suggest that both mechanisms may actually play an important role in the overall process, as the largest overall dye degradation was achieved with the piezo-electrocatalyst most likely to generate radicals via both piezo-electrocatalytic mechanisms.

1. Introduction

Over the last decade, a new concept known as *piezocatalysis* [1–5], *piezo-electrocatalysis* [6–10] or *piezo-electrochemistry* [11–16] has attracted a wide attention of the catalysis community. Piezo-electrocatalysis is based on the occurrence of redox reactions at the surface of a piezoelectric material driven by its polarisation under applied mechanical stress. To some extent, it could be considered that piezo-electrocatalysts behave as miniaturised electrochemical devices that combine a power source and electrodes. Due to this advantage and the long-term aim to harness redundant mechanical vibrations in industrial systems [5], piezo-electrocatalysis is seen as an intriguing concept with the potential to drive electrochemical reactions without the use of more traditional energy sources such as light and electricity.

However, despite the rising numbers of reports exploring piezo-electrocatalysis (mostly focused on the development of novel piezo-electrocatalyst materials), the mechanism behind the reported catalytic activity remains controversial. Over the years, the research community has proposed two main potential mechanisms, i.e. screening charge effect and energy band theory, and the way the academic debate has developed over time is that either one *or* the other is the 'true' mechanism behind piezo-electrocatalysis [2].

The screening charge effect mechanism implies that redox reactions over the surface of piezo-electrocatalysts rely entirely on the piezoelectric polarisation generated by the deformation of the piezo-electrocatalyst [1,4,14,17,18]. In this mechanism, the piezoelectric potential experienced by the piezo-electrocatalyst should exceed the difference between the reduction potentials of the redox reactions of interest. In other words, the piezoelectric potential will determine its ability to drive specific electrochemical reactions in certain regions of the surface, which would act as either cathode or anode. This screening charge effect mechanism has recently moved away from 'bulk' piezoelectric polarisation towards a more localised piezoelectric response [19–24]. Under ultrasound, asymmetrical collapse of cavitating bubbles near the piezo-electrocatalyst [25], amongst other mechanical effects caused by cavitation, would lead to localised high pressures of several hundreds of bars [26] that could result in superficial piezoelectric polarisation of micro- and nano-features of the catalysts [19–25,27,28].

The energy band mechanism is analogous to photocatalysis where redox reactions, which take place over the surface of piezo-

* Corresponding authors.
E-mail addresses: (F. Bößl), (I. Tudela).
[1] ISE member

https://doi.org/10.1016/j.electacta.2023.142730
Received 12 March 2023; Received in revised form 19 May 2023; Accepted 10 June 2023
Available online 16 June 2023

electrocatalysts, are determined by the energy band levels of the valence and conduction bands [3,29–31]. Based on this theory, the piezoelectric polarisation of the piezo-electrocatalyst is considered an indirect promoter of electrochemical reactions by adjusting the band structure and controlling internal charge flow to the surface of the piezo-electrocatalyst [2]. If energy band theory was the dominant mechanism behind piezo-electrocatalysis, one would expect superior piezo-electrocatalytic performance when using a piezo-electrocatalyst having a wide enough energy band gap to drive targeted electrochemical reactions. The electrochemical potential derived from the excitation of electrons to higher energy levels must not only be sufficient for those redox reactions to occur, but also should be enough to overcome kinetic and concentration overpotentials, as well as ohmic losses. Further to this, the band configuration and electronic states of the piezo-electrocatalyst have to be appropriate for the reduction and oxidation reactions of interest to occur.

The preliminary study presented here followed a simple approach to explore the importance of energy band theory and screening charge effect in piezo-electrocatalysis by investigating the performance of different piezo-electrocatalysts on the degradation of Rhodamine B (RhB) under combined ultrasound and mechanical agitation. The piezo-electrocatalysts consisted of three different piezoelectric materials, allowing for the two mechanisms to be studied in isolation and combination through the different energy band levels and piezoelectric characteristics of these materials:

- Zinc oxide (ZnO) was chosen due to its wide energy band gap [32–34] and weaker piezoelectric performance [35–38] in comparison with the properties of the other piezo-electrocatalysts used in this study. For this material, any piezo-electrocatalytic effect on the overall degradation of RhB would most likely occur in accordance to the energy band mechanism rather than the screening charge effect.
- Potassium bismuth titanate-bismuth ferrite lead titanate (BF-KBT-PT) was chosen due to its very high piezoelectric properties [27,39,40] and narrow energy band gap. This implied that any piezo-electrocatalytic contribution to the overall degradation of RhB would be solely caused by the screening charge mechanism.
- Barium titanate ($BaTiO_3$) was chosen due to its combination of very high piezoelectric properties and a wide energy band gap [4,41–44]. This would make $BaTiO_3$ an interesting option, as it could potentially benefit from both mechanisms simultaneously; higher piezo-electric contribution towards the degradation of RhB would therefore be expected from this piezo-electrocatalyst.

In the case of BF-KBT-PT and $BaTiO_3$, the performance of both poled (highly piezoelectric) and unpoled (non-piezoelectric) versions of the same materials were investigated to get a better picture of the importance of the piezoelectric nature in the overall performance of the piezo-electrocatalysts.

2. Experimental

2.1. Catalyst preparation and characterisation

2.1.1. Catalysts preparation

ZnO nanoflowers were synthesised via a hydrothermal method previously described by the authors [38]. Equimolar concentrations (20 mM) of $Zn(NO_3)_2{\cdot}6H_2O$ and hexamethylenetetramine were added to de-ionized water and magnetically stirred for 10 min. The solution was then sealed and kept in an oven at 90 °C for 18 h. The resulting solution was cooled down to room temperature, washed and centrifuged three times with ethanol. The remaining white sediment in ethanol (i.e. ZnO nanoflowers) was left to dry at room temperature overnight.

Commercial $BaTiO_3$ piezoceramic discs (Steiner & Martins, Inc.) with high piezoelectric properties (d_{33} and d_{31} values of 160 pC/N and 30 pC/N, respectively, measured according to IEEE standards [45,46]) were used to fabricate P and UP versions of the $BaTiO_3$ piezo-electrocatalysts. The $BaTiO_3$ piezoceramic discs (i.e. poled materials with aligned ferroelectric domains) were ground into fine particles (<63 μm) following the method described by the authors in a previous study [27], to fabricate the P $BaTiO_3$ piezo-electrocatalysts. To obtain the unpoled version (non-piezoelectric; d_{33} and d_{31} values of 0 pC/N) of this material, the commercial $BaTiO_3$ piezoceramics were depoled by heating them above their Curie temperature for several hours and cooling them down to room temperature to produce UP $BaTiO_3$ piezo-electrocatalysts (i.e. unpoled materials with randomly orientated ferroelectric domains).

ZnO and both P and UP $BaTiO_3$ piezo-electrocatalysts were compared with P and UP BF-KBT-PT piezo-electrocatalysts already evaluated under the same experimental conditions in a previous study by the authors [27], except for their energy band information. P and UP BF-KBT-PT piezo-electrocatalysts had been prepared from poled and depoled piezoceramic discs of the same material, with the poled discs exhibiting a strong piezoelectric behaviour (d_{33} and d_{31} values of 100 pC/N and −40 pC/N, respectively) while the unpoled discs exhibited no piezoelectricity at all (d_{33} and d_{31} values of 0 pC/N) [27].These discs were also ground into fine particles (<63 μm) to fabricate P and UP BF-KBT-PT piezo-electrocatalysts.

2.1.2. Catalyst characterisation

The morphology, surface structure and composition of all piezo-electrocatalysts was analysed using a focused ion beam-scanning electron microscopy (FIB-SEM, Zeiss Gemini 2 crossbeam 550) equipped with an energy dispersive X-ray spectrometer (EDS). X-ray powder diffraction (XRPD) data for all piezo-electrocatalysits was obtained with a Bruker D2 PHASER diffractometer equipped with Cu Kα radiation to confirm the identity of the crystalline phases of the materials. Data were collected over the 2θ range from 5 to 60° and a scanning speed of 0.2 steps/second. Energy band gaps were determined by ultraviolet–visible diffuse reflectance spectroscopy (UV–Vis DRS) using a JASCO V-670 spectrophotometer equipped with an integrating sphere attachment. Direct and indirect band gaps were quantified using Kubleka-Munk theory and corresponding Tauc plots. The valence band maximum of all the materials used in this study was estimated by X-ray photoelectron spectrometry (XPS) in a Scienta XPS system equipped with monochromatic source.

2.2. Experimental setups and procedures

RhB degradation experiments were conducted under the same conditions defined in a previous study by the authors [27], where combined ultrasound and mechanical agitation was used as the mean to excite the piezo-electrocatalysts. For this purpose, a SciQuip Basic 20 overhead stirrer was centred and immersed into a 1000 mL beaker acting as the reactor; the beaker was also centred and immersed to a 4 cm depth into a 32–38 kHz Ultrawave QS12 ultrasonic bath with constant water level. At full ultrasonic power and mechanical agitation of 200 rpm, the experimental setup was calibrated by calorimetry [47], resulting in a dissipated acoustic power of 14.3 ± 0.7 W L^{-1}. Prior to each experiment, the water in the ultrasonic bath was thoroughly degassed for 60 min to ensure a reproducible acoustic field inside the bath. The temperature in the reactor was kept at 30 ± 2 °C throughout all the experiments by a precise temperature control system (Grant LT ecocool 100 recirculating chiller).

120 min control (i.e. no piezo-electrocatalyst) and piezo-electrocatalytic RhB degradation experiment were performed on 1000 mL of 5 mg L^{-1} aqueous solutions at pH = 4.5. In each experiment, 3-mL aliquots of the RhB solution were sampled every 10 min with a 0.22 μm PTFE-syringe-filter. In the particular case of ZnO piezo-electrocatalysts, samples were also centrifuged to remove the nanoflowers from the solution. Ultraviolet–visible spectroscopy at the characteristic wavelength of 554 cm was conducted in a Shimadzu UV-3600 Plus spectrophotometer to analyse the solution samples. In all piezo-

electrocatalytic experiments, 1 g L^{-1} of piezo-electrocatalysts were added to the RhB solutions to be treated. Prior to each experiment, though, adsorption-desorption equilibrium was ensured by mechanically stirring the catalysts at 200 rpm for 30 min in the RhB solution (no RhB adsorption was observed in all cases).

3. Results and discussion

3.1. Piezo-electrocatalyst characterisation

FIB-SEM and EDS analysis provided interesting details on the morphology and surface structure of the piezo-electrocatalysts used in this study, and confirmed the composition of the different materials used. The ZnO piezo-electrocatalysts generally presented a flower-like structure formed by nanorods growing radially from the centre of the particles (Fig. 1a, left). As expected from previous work [38], the individual nanorods were several microns long with an average length ranging from 3 to 6 μm, and a diameter of several hundreds of nanometers with an average diameter around 180–220 nm (Fig. 1a, centre). EDS confirmed that the ZnO piezo-electrocatalysts were free from any impurities (Fig. 1a, right). P and UP BF-KBT-PT piezo-electrocatalysts presented identical cuboid morphology with sizes of the order of several tens of microns (Fig. 1b and c, left) where smaller debris originating from the catalyst fabrication process (i.e. grinding of piezoceramic discs) could be noticed over the surface (Fig. 1b and c, centre); both versions of BF-KBT-PT also presented identical composition (Fig. 1b and c, right).

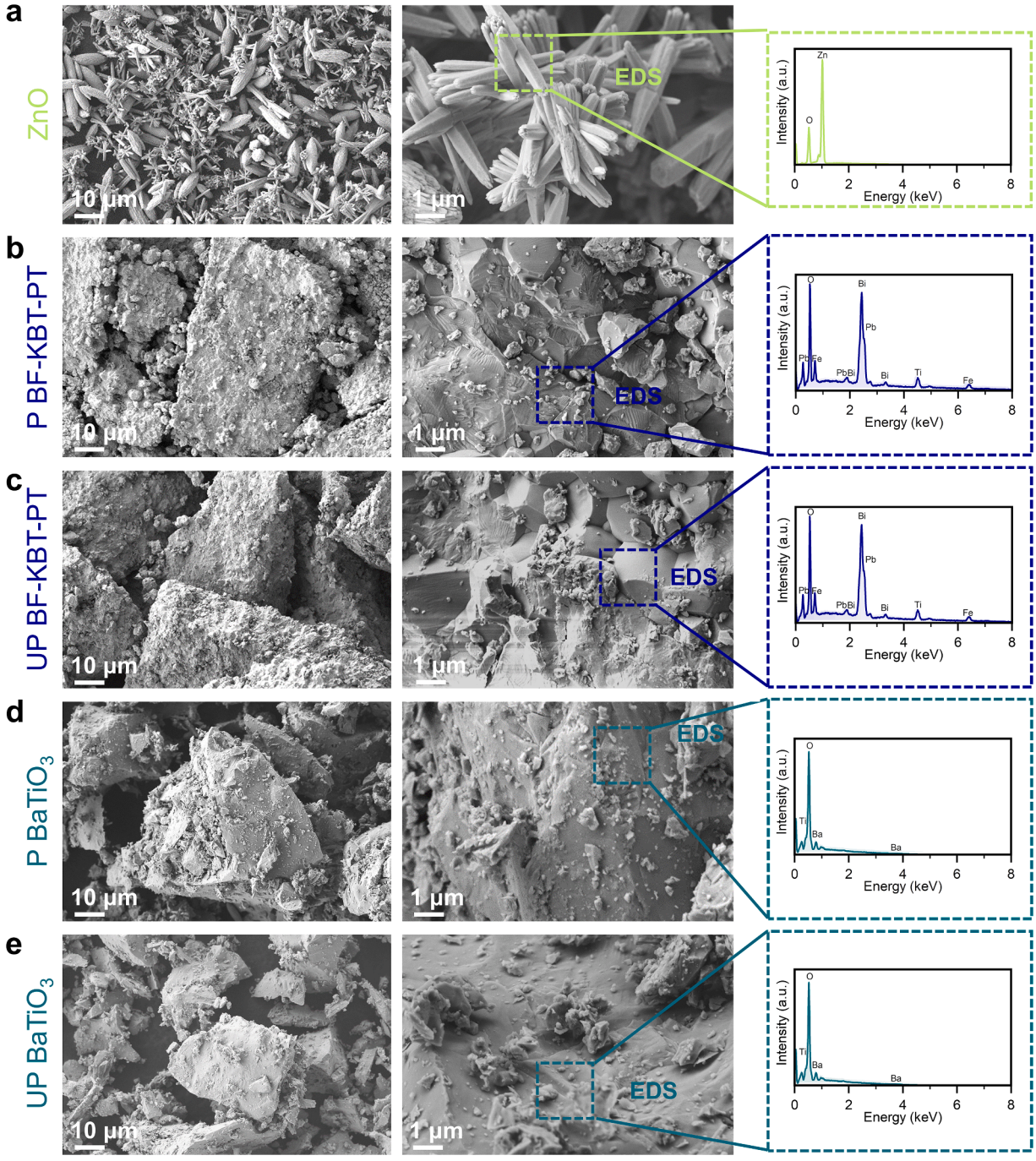

Fig. 1. FIB-SEM and EDS analysis of the different piezo-electrocatalysts used in this study: (a) ZnO, (b) P BF-KBT-PT, (c) UP BF-KBT-BT, (d) P $BaTiO_3$, and (e) P $BaTiO_3$.

This confirmed that, in terms of shape, surface structure and composition, P and UP BF-KBT-PT piezo-electrocatalysts were virtually the same material. The same trend was confirmed for P and UP $BaTiO_3$ piezo-electrocatalysts, which also presented a cuboid morphology with sizes of the same order of several tens of microns (Fig. 1d and e, left) where smaller debris were again noticed over the surface (Fig. 1d and e, centre); no difference was observed in terms of material composition between the P and UP piezo-electrocatalysts (Fig.1d and e, right).

XRPD analysis was used to confirm the phase(s) present in the piezo-electrocatalysts used in this study (Fig. 2). XRPD data collected on the ZnO sample matched well to the standard International Centre for Diffraction Data (ICDD) Powder Diffraction File (PDF) [36–1451], confirming the piezo-electrocatalyst sample was the hexagonal wurtzite polymorph of ZnO. The three main characteristic peaks observed at 32°, 34° and 36° were clearly identified, confirming good crystallinity of the prepared ZnO piezo-electrocatalysts. XRPD data of both P and UP BF KBT-PT piezo-electrocatalysts indicated phase co-existence due to peak splitting in most of the reflections [39], especially in the case of the (110) planes, as reported before by the authors [27,39]. Lattice distortion of the rhombohedral phase was considered negligible due to no observed peak splitting in of the 111 reflection and only minor peak splitting of the 200 reflection, which is characteristic of tetragonal materials [39]. Minor differences in signal intensities were observed for the P and UP BF-KBT-PT piezo-electrocatalysts were noticed. However, the relative heights of both samples were the same for both versions of BF-KBT-PT, confirming their identical phase structure. The XRPD data collected on the P and UP $BaTiO_3$ piezo-electrocatalyst samples matched well to the standard International Centre for Diffraction Data (ICDD) Powder Diffraction File (PDF) [74–1959] for tetragonal $BaTiO_3$. Both P and UP $BaTiO_3$ piezo-electrocatalysts showed the presence of only the perovskite $BaTiO_3$ phase, with no other peaks observed showing no impurity phases were present. Peak splitting was observed in both the P and UP $BaTiO_3$ at around 45°, where the 200 peak in the cubic polymorph splits into (002) and (200), indicating the tetragonal polymorph of $BaTiO_3$ is present [1,48].

The Kubelka-Munk function was applied to collected UV–Vis DRS data (Fig. 3a) to produce Tauc plots that allowed the energy band gaps of all piezo-electrocatalysts to be estimated: ZnO (Fig. 3b), P versions of BF-KBT-PT and $BaTiO_3$ (Fig. 3c), and UP versions of BF-KBT-PT and $BaTiO_3$ (Fig. 3d). The value of the band gap for ZnO was quite high (3.20 eV), as expected from the literature [33,34]. Similar band gaps values (3.18 eV) were obtained for P and UP $BaTiO_3$, which were also in agreement with values from the literature [41,42], confirming that the energy band gap value did not depend on whether the piezo-electrocatalyst was poled or unpoled. The same trend was observed for the P and UP BF-KBT-PT piezo-electrocatalysts, although in this case, both versions of this material exhibited a significantly lower energy band gap (2.16 eV) than the other materials studied in this work. XPS data was used to estimate values of the valence band edge for all piezo-electrocatalysts used in this study (Fig. 3e). The values of the valence band edge for both P and UP versions of the same material (either BF-KBT-PT or $BaTiO_3$) were nearly identical, as was the case for the energy band gap levels.

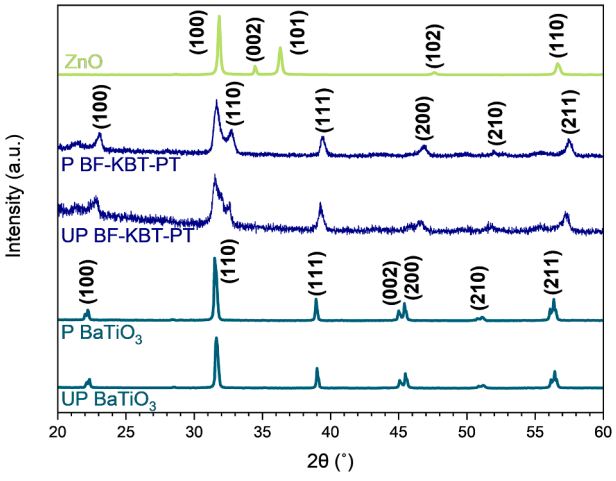

Fig. 2. XRPD data collected on the different piezo-electrocatalysts used in this study: ZnO, P and UP BF-KBT-PT, and P and UP $BaTiO_3$.

Valence band edge values obtained from XPS data were used to estimate the valence band maximum (VBM) vs SHE (Standard Hydrogen Electrode) of all the piezo-electrocatalysts after taking into account the electronic energy of SHE (−4.44 eV) [49] and the work function of the XPS system (4.5 eV). VBM values were then used, along with the band gap values obtained from the application of the Kubelka-Munk function to the UV–Vis DRS data, to estimate the conduction band minimum (CBM) vs SHE for all the piezo-electrocatalysts. VBM and CBM values were also used to construct the band alignment diagram for all the piezo-electrocatalysts used in the present study (Fig. 4). The standard equilibrium potential of those redox reactions responsible for the generation of superoxide ($^{\bullet}O_2^-$) and hydroxyl ($^{\bullet}OH$) radicals at the surface of piezo-electrocatalyst [1,13], which are responsible for the degradation of RhB [25,27], were also included in the diagram, along with the equilibrium potential for the hydrogen evolution reaction (HER) and oxygen evolution reaction (OER) at pH = 4.5 (i.e. the pH of the RhB solutions used in this study):

- Reduction reactions
  - $O_2 + e^- \leftrightarrow {}^{\bullet}O_2^-$ (−0.33 V vs SHE) [50]
  - $2\,H^+ + 2\,e^- \leftrightarrow H_2$ (−0.27 V vs SHE)
- Oxidation reactions
  - $OH^- + h^+ \leftrightarrow {}^{\bullet}OH$ (1.89 V vs SHE) [51]
  - $2\,H_2O \leftrightarrow O_2 + 4\,H+ + 4\,e^-$ (0.96 V vs SHE)

It should be noted that, as the VBM values were obtained from XPS measurements, they are intrinsically true under vacuum. However, that may not be fully representative of the 'real' conditions in the experiments (i.e. RhB solution at pH = 4.5). Ideally, Mott-Schottky plots obtained for electrodes fabricated with the catalysts (e.g. by drop casting) and immersed in the working solution should be used to estimate the flatband potential, which could then be considered as the conduction band in the case of an n-type semiconductor or the valence band in the case of a p-type semiconductor. This was not an option in this study due to the nature of most of the piezo-electrocatalysts used in the study (i.e. P and UP versions of both $BaTiO_3$ and BF-KBT-PT had a size of several tens of microns and a cuboid shape), which made it impossible to prepare electrodes with smooth and uniform surfaces where full coverage of the substrate was achieved. Nevertheless, in the case of the P and UP $BaTiO_3$ piezo-electrocatalysts, if it is considered that the isoelectric point of diluted suspensions of $BaTiO_3$ in deionised water is reached at pH ≈ 6.5 [52], it is reasonable to believe that the bandgaps depicted for both piezo-electrocatalysts in Fig. 4 would be, to some extent, displaced to more positive potentials in the experimental conditions used here. The ZnO piezo-electrocatalysts would be in a similar situation, provided that the isoelectric point of ZnO nanoparticles in water is reached at pH ≈ 10.3 [53]. The case of P and UP BF-KBT-PT piezo-electrocatalysts is slightly more complex, given that it is a ternary system ($BiFeO_3$, $K_{0.5}Bi_{0.5}TiO_3$ and $PbTiO_3$) [39]. Whereas the isoelectric point for $BiFeO_3$ is reached at pH ≈ 2.8 [54], the isoelectric point of $PbTiO_3$ is reached at pH ≈ 11.5 [55]; however, no isoelectric point data is available for $K_{0.5}Bi_{0.5}TiO_3$. Therefore, it was deemed reasonable to assume that the bandgaps depicted for both P and UP BF-KBT-PT piezo-electrocatalysts in Fig. 4 would not be significantly displaced to either more positive or negative potentials.

3.2. Reaction mechanisms

The material characterisation previously included confirmed that P

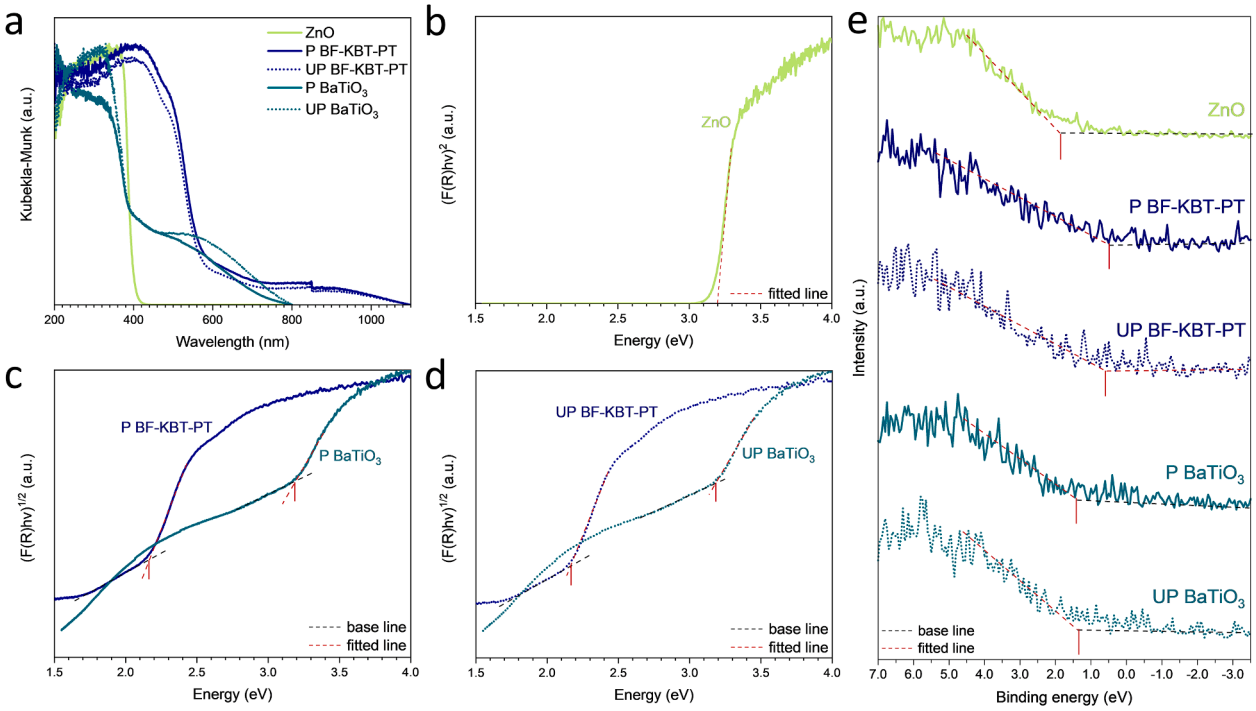

Fig. 3. (a) Application of Kubelka-Munk to UV–Vis DRS data, (b–d) corresponding Tauc plots, and (e) XPS data collected on all piezo-electrocatalysts used in this study: ZnO, P and UP BF-KBT-PT, and P and UP $BaTiO_3$.

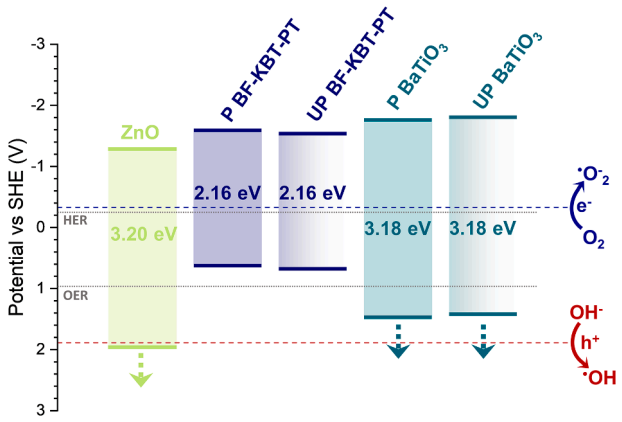

Fig. 4. Band alignment diagram for all piezo-electrocatalysts used in this study: ZnO, P and UP BF-KBT-PT, and P and UP $BaTiO_3$. Arrows indicate direction of the displacement of bandgaps in RhB degradation experiments.

and UP $BaTiO_3$, as well as P and UP BF-KBT-PT, were virtually identical except for their poled or unpoled nature. The knowledge of the piezoelectric nature of all piezo-electric materials used in this study, along with their energy band levels, would already give a strong indication of which reaction mechanisms are likely to occur for each piezo-electrocatalyst, and which one is likely to deliver the highest piezo-electrocatalytic contribution towards the overall degradation of RhB. To discuss this, though, the possible piezo-electrocatalytic mechanisms that could be taking place must also be further explained at the same time (Fig. 5).

The screening charge mechanism [2] would be based on the localised superficial piezoelectric response of micro- and nano-scale features of the surface of piezo-electrocatalysts [28] under periodic mechanical stress (Fig. 5a), which would be caused in this case by acoustic cavitation (i.e. asymmetrical bubble collapse near to the surface) [25]. Without any applied external force, the surfaces of poled piezo-electrocatalysts remain electrically neutral as bound charges are balanced by screening charges from the electrolyte [56] (e.g. charged adsorbates) [57]. However, under a mechanical strain (e.g. that resulting from the acoustic cavitation phenomena caused by ultrasound), the charge balance is disrupted, leading to a redistribution of bound charges where electrons and holes travel to different surfaces of the piezo-electrocatalyst, which become oppositely polarised. As a result, more screening charges of opposite sign in the electrolyte will be attracted and adsorbed onto the polarised surfaces, balancing again the bound charges in those surfaces. Once the mechanical strain becomes weaker, bound charges will start to leave those polarised surfaces, which will obviously become less polarised, resulting in an excess of screening charges. This excess of screening charges would then be released from the surface until a charge balance in those surfaces is reached again; these charges could then take part in redox reactions with the surrounding electrolyte near the piezo-electrocatalyst surface. These same steps would then occur again and again in a cyclic way as the piezo-electrocatalysts are subject to ultrasound and the action of acoustic cavitation and its mechanical effects. Worth noting here is that screening charges may be sourced from many sources such as electrons, holes, anions and cations, cationic vacancies and polar molecules, indicating that there is still much research to do in order to identify how this could affect this mechanism [2]. In any case, it is obvious that the piezoelectric properties of the material will be important for this mechanism to make a greater impact on the degradation of RhB, which is why P versions of the materials with high piezoelectric properties (i.e. BF-KBT-PT and $BaTiO_3$) would be more likely to experience this mechanism. Nevertheless, localised piezoelectric polarisation at the domain level could be enough for piezo-electrocatalytical processes to occur at the surface of non-piezoelectric ferroelectric materials [20]. This also means that, as well as ZnO (which is significantly less piezoelectric than P BF-KBT-PT and $BaTiO_3$), UP versions of the BF-KBT-PT and $BaTiO_3$ piezo-electrocatalysts could also experience enough localised piezoelectric activity to drive those same redox reactions, but in a lesser extent.

The mechanism based on energy band theory is strongly related to

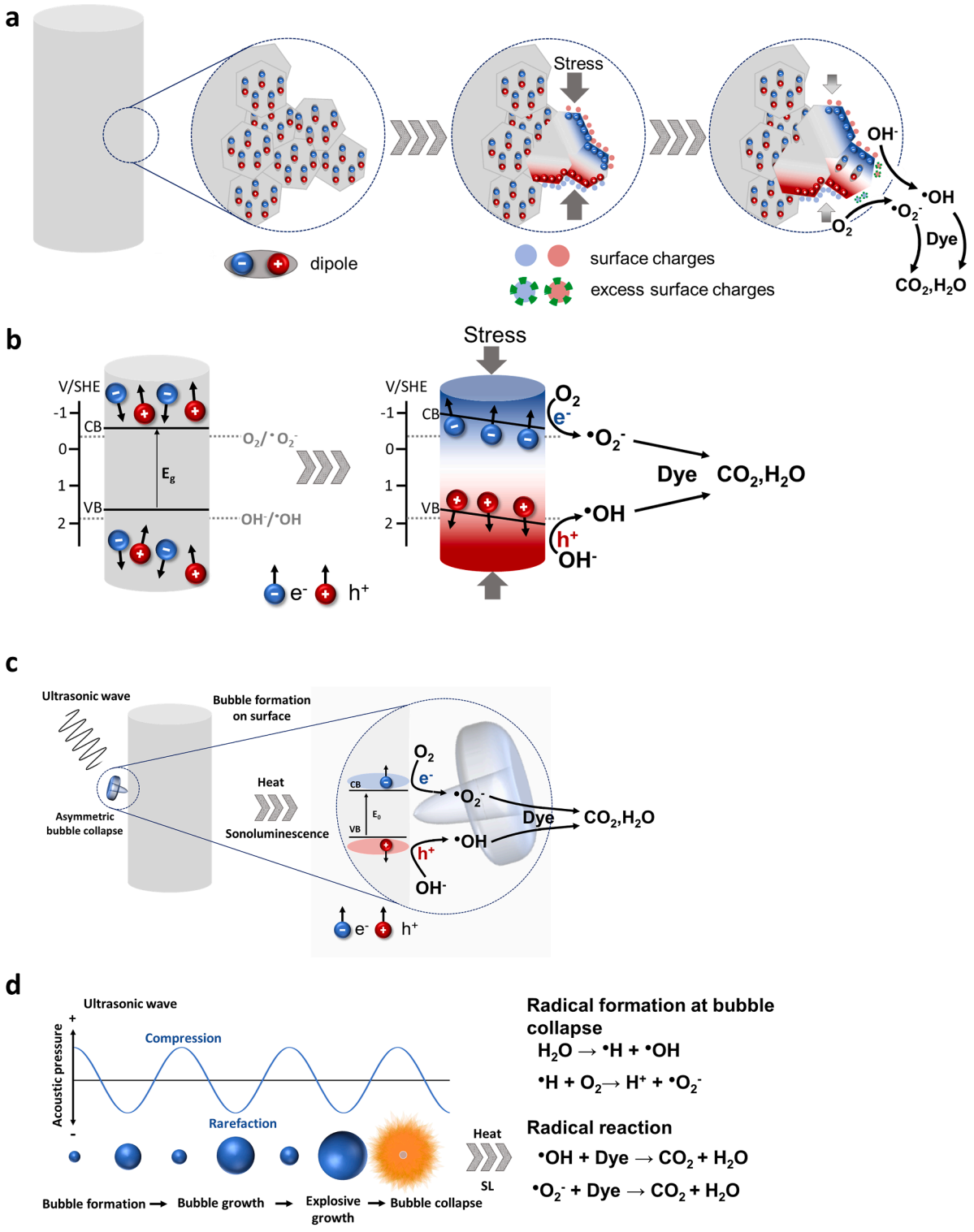

Fig. 5. Illustration of different mechanisms for overall dye degradation: (a) Screening charge effects via localised piezoelectric response, (b) Energy band theory mechanism, (c) Sonocatalytic mechanisms, (d) Sonochemical mechanism.

photocatalysis, as electrons would be excited from the valence band (VB) to the conduction band (CB), leading to the generation of reactive species (i.e. electrons and holes) driving redox reactions. However, in piezo-electrocatalysis, this excitation would rely on mechanical energy rather than light. It is still under debate whether this excitation is a result of direct excitation due to the high pressures of collapsing bubbles or a thermally induced indirect excitation [2]. In any case, the piezopotential generated within the piezoelectric material would lead to an improvement in the redox capability of the piezo-electrocatysts due to the bending/tilting of the energy bands (Fig. 5b). This would enable the alignment of the valence and conduction bands over/under the equilibrium potentials of the anodic/cathodic redox reactions of interest [2], which in this case are those involved in the generation of superoxide and hydroxyl radicals (Fig. 4). Obviously, this means that those materials highly piezoelectric in nature, which also exhibit wide band gaps and suitable VBM and CBM values likely to be bended/tilted beyond the

equilibrium potentials, would be likely to induce the generation of radicals via the energy band mechanism. In the present study, P $BaTiO_3$ piezo-electrocatalysts would be very likely to degrade RhB via superoxide and hydroxyl radicals generated by this mechanism due to their wide bang gap and VBM relatively close to the potential required to generate hydroxyl radicals. In a first instance, ZnO might also seem in a very strong position to also experience this due to its energy band levels. However, the degradation should not be as high as one might initially expect due to its relative poor piezoelectric nature. In the case of P BF-KBT-PT piezo-electrocatalysts, their band gap is rather narrow, and although their CBM would enable the generation of superoxide radicals, the generation of hydroxyl radicals via this mechanism would be highly unlikely due to their VBM, despite their strong piezoelectric nature. A similar situation would be expected for the UP versions of BF-KBT-PT and $BaTiO_3$, with the addition that these piezo-electrocatalysts are not intrinsically piezoelectric; therefore, no superoxide and hydroxyl radicals should be generated by the energy band mechanism.

Besides the piezo-electrocatalytic mechanisms just discussed (based on the screening charge effect and energy band theory), there is another potential mechanism that must always be considered whenever semiconductors such as the piezoelectric materials used in this study are suspended in a liquid solution irradiated with ultrasound: sonocatalysis (Fig. 5b). Sonocatalysis is even more similar to photocatalysis, where the excitation of the electrons would be caused either thermally or by sonoluminescence due to the action of cavitating bubbles collapsing nearby the surface of the material [58]. The band alignment diagram (Fig. 4) again indicates that the generation of superoxide radicals via sonocatalysis would be likely to occur in all of the materials studied here. However, the generation of hydroxyl radicals should only take place sonocatalytically in the ZnO piezo-electrocatalysts, and not on the other materials.

The previous paragraphs can be summarise as follows:

- In the case of ZnO piezo-electrocatalysts, it would be expected that, based on its energy band characteristics and piezoelectric properties, both superoxide and hydroxyl radicals were generated by piezo-electrocatalysis via the energy band and screening charge mechanisms, as well as sonocatalytically. However, both piezo-electrocatalytical mechanisms would be limited due to the material's relatively poor piezoelectric nature, which is why sonocatalysis may be the predominant mechanism in this case [59]. Although it is already well known that ZnO piezo-electrocatalysts suspended in aqueous solutions under ultrasound generate superoxide radicals, hydroxyl radicals and holes [60,61], it is expected that the contribution of ZnO piezo-electrocatalysts to the overall degradation of RhB may not be the greatest of all the piezo-electrocatalysts used in this study.
- In the case of P $BaTiO_3$, its energy band levels and highly piezoelectric nature should result in significant generation of superoxide and hydroxyl radicals via both piezo-electrocatalytical mechanisms, which would obviously enhance the overall degradation of RhB; many studies have indeed confirmed the generation of superoxide radicals, hydroxyl radicals and holes under ultrasound with this material [62–64]. Whereas superoxide radicals could also be generated via sonocatalysis, this would not be the case for the generation of hydroxyl ions.
- In the case of P BF-KBT-PT piezo-electrocatalysts, whereas superoxide radicals could also be generated via the sonocatalytical and both piezo-electrocatalytical mechanisms, the hydroxyl radical could only be generated via the piezo-electrocatalytical screening charge mechanism due to its energy band alignment. The authors already demonstrated the capability of P BF-KBT-PT to generate superoxide radicals, hydroxyl radicals and holes, as well as their critical role on the degradation of RhB, under identical conditions [25,27]; however, it would be expected, that its performance would be lower than that of P $BaTiO_3$ piezo-electrocatalysts as the latter could also benefit from the piezo-electrocatalytic energy band mechanism.
- The UP versions of the BF-KBT-PT and $BaTiO_3$ should exhibit lower catalytic effect than their P counterparts due to their non-piezoelectric nature. For this reason, if any piezo-electrocatalytic degradation of RhB was observed with these materials, it would most likely be caused by localised screen charge effect at the domain level.

It should be noted, however, that there is an additional mechanism for the formation of the superoxide and hydroxyl radicals [25] involved in the degradation of RhB, which does not require the presence of any catalyst. That mechanism is based on sonochemistry (Fig. 5d), where the production of radicals is driven by the extreme high temperatures (order of 5000 K) and pressures (order of 1000 atm) reached at the centre of cavitating bubbles after their collapse once they have reached a certain size [65]. This mechanism is therefore expected to play a significant role in the overall degradation of RhB under the experimental conditions of this study, as already demonstrated in the past by the authors [27].

3.3. Degradation experiments

Fig. 6 displays the normalised concentration of RhB during different degradation experiments conducted under combined ultrasound and mechanical stirring, in the absence (MA + US; i.e. sonochemical degradation own its own) and presence of the ZnO, BF-KBT-PT and $BaTiO_3$ piezoelectro-catalysts (both P and UP versions in the case of BF-KBT-PT and $BaTiO_3$). First order kinetics derived from Langmuir-Hinshelwood theory were used to estimate the overall degradation reaction rates in absence and presence of the different piezo-electrocatalysts:

$$\frac{C}{C_0} = e^{-kt} \tag{1}$$

where t was time, C was the concentration of RhB at time t, C_0 was the initial concentration of RhB and k was the kinetic degradation rate constant. The overall degradation efficiency (DE) was calculated using the following expression:

$$DE = \left(1 - \frac{C}{C_0}\right) \times 100 \tag{2}$$

As expected, significant degradation of RhB was already achieved in absence of a piezo-electrocatalyst (MA + US) via sonochemistry on its own (DE = 50% after 60 min). The addition of the UP versions of BF-KBT-PT and $BaTiO_3$ piezo-electrocatalysts resulted in a relatively small enhancement of the degradation of RhB (DE values of 54% and 61%, respectively); this enhancement would mostly rely on the piezo-electrocatalytic screening charge mechanism, as discussed in the previous section. The P versions of the same materials, P BF-KBT-PT and P $BaTiO_3$, delivered a further enhancement of the degradation of RhB. In the case of P BF-KBT-PT, there was a relative improvement of 22% compared to sonochemistry on its own (DE = 61%). This indicates that, even though the piezo-electrocatalytic screening charge mechanism would be taking place in the presence of both UP and P versions of BF-KBT-PT, this mechanism was significantly enhanced by the highly piezoelectric nature of P BF-KBT-PT, highlighting the importance of the piezoelectric properties of the material in piezo-electrocatalysis. This was even more remarkable in the case of P $BaTiO_3$, where an outstanding improvement of 50% was achieved compared to sonochemistry on its own (DE = 73%). In this case, however, this improvement would not be caused by the piezo-electrocatalytic screening charge mechanism on its own, but also by the piezo-electrocatalytic energy band mechanism, as discussed in the previous section. This indicates that developing piezo-electrocatalysts highly piezoelectric in nature *with* suitable energy band alignments should be the aim, as both piezo-

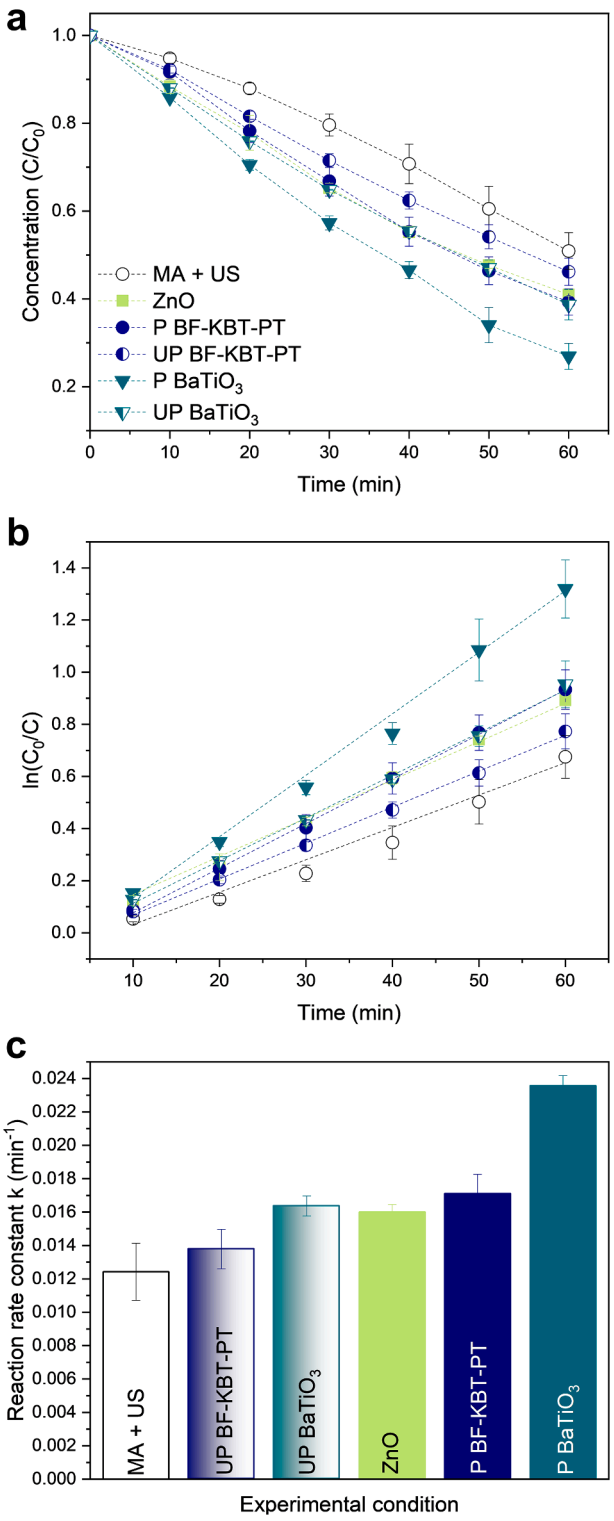

Fig. 6. RhB degradation experiments under combined ultrasound and mechanical agitation in absence and presence of piezoelectric ZnO, BF-KBT-PT and $BaTiO_3$: (a) evolution of C/C_0 vs reaction time, (b) First-order linear fit of $\ln(C_0/C)$ vs reaction time, (c) First-order degradation reaction rate constants.

electrocatalytic mechanisms (i.e. based on energy band theory and the screening charge effect) are likely to occur simultaneously. The results for ZnO further strengthens this latter idea, as a rather disappointing relative improvement of 18% was achieved in comparison to sonochemistry on its own (DE = 59%). As discussed in the previous section, ZnO piezo-electrocatalysts should generate superoxide and hydroxyl radicals both piezo-electrocatalytically and sonocatalytically. However, their poor piezoelectric nature would significantly reduce the piezo-electrocatalytical performance, even though both energy band and screening charge effect mechanisms are likely to occur.

The results agree with the hypothesis and discussion previously made in Section 3.2, strongly suggesting that both energy band and screening charge effect mechanisms are likely to occur simultaneously in piezo-electrocatalysis. To benefit from this, piezo-electrocatalysts must exhibit suitable energy band levels with a large enough band gap, as well as high piezoelectric properties (i.e. P $BaTiO_3$ piezo-electrocatalysts). A piezoelectric material that presents either one feature (i.e. suitable energy band levels with large band gap but poor piezoelectric properties like the ZnO piezoelectricatalysts) or the other (i.e. highly piezoelectric nature but small band gap like the P BF-KBT-PT piezo-electrocatalysts) may still drive redox reactions via piezo-electrocatalysis at its surface; however, its performance will be significantly lower.

This preliminary study sheds some light onto the 'true' mechanisms behind piezo-electrocatalysis, which will be extremely helpful in the future development of this research area. However, there are still many questions that need answering. For example, in the case of unpoled materials whose piezo-electric nature is mostly non-existent, RhB degradation was still occurring. The assumption is that the localised piezoelectric response at the domain level is responsible for this, but micro- and nano- piezoelectricity is a field still in its infancy, which means that more work is required to better understand this phenomenon. Furthermore, UP $BaTiO_3$ piezo-electrocatalysts worked significantly better than the UP BF-KBT-PT ones; in fact, they appeared to perform slightly better than the ZnO piezo-electrocatalysts. A potential reason for this could be that, for the reactions of interest in this study (e.g. generation of superoxide and hydroxyl radicals to degrade RhB), the overpotential required at the surface of $BaTiO_3$ may be significantly lower than that at the surface of BF-KBT-PT or ZnO. The authors are currently exploring this, although more work is required to respond to this question due to the challenging task of transferring traditional electroanalytical techniques into this area. This would enable the design of suitable piezo-electrocatalysts for more 'established' electrochemical processes such as water electrolysis [66–68] or CO_2 electroreduction [69,70], accounting not just for the piezoelectric aspect, but also for the electrochemical one.

4. Conclusion

The present study sheds more light on the 'true' mechanisms behind piezo-electrocatalysis. P $BaTiO_3$ piezo-electrocatalysts that were likely to generate superoxide and hydroxyl radicals via the two proposed mechanisms, either energy band theory or screening charge effect, were shown to deliver the largest overall degradation of RhB. This indicates that research should move from the debate on whether one mechanism *or* the other is behind piezo-electrocatalysis, to the more likely prospect that *both* mechanisms are occurring simultaneously, according to the results from this preliminary study. This opens a new opportunity in the development of piezo-electrocatalysts for different applications, where special attention must be paid to the piezoelectric nature of the materials used, as well as their energy band levels.

Besides piezo-electrocatalysis, other phenomena such as sonochemistry and (potentially) sonocatalysis were taking place during the experiments, which means that the contribution towards the overall process via their corresponding mechanisms should never be discarded in this field. Accounting for non-piezoelectricity-related mechanisms is still not usual in piezo-electrocatalysis research as previously discussed by the authors [23,25,27] and recently highlighted by other research groups [71,72]. It is hoped the results from this research will further contribute to change this perception.

CRediT authorship contribution statement

Franziska Bößl: Conceptualization, Methodology, Validation, Formal analysis, Investigation, Data curation, Writing – original draft, Visualization. **Valentin C. Menzel:** Methodology, Validation. **Karina Jeronimo:** Methodology, Resources. **Ayushi Arora:** Investigation. **Yishu Zhang:** Investigation. **Tim P. Comyn:** Resources, Writing – review & editing. **Peter Cowin:** Resources. **Caroline Kirk:** Investigation, Resources, Writing – review & editing. **Neil Robertson:** Resources, Writing – review & editing. **Ignacio Tudela:** Conceptualization, Methodology, Resources, Writing – review & editing, Supervision, Project administration, Funding acquisition.

Declaration of Competing Interest

The authors declare that they have no known competing financial interests or personal relationships that could have appeared to influence the work reported in this paper.

Data availability

Data will be made available on request.

Acknowledgements

FB and IT acknowledge the University of Edinburgh for funding this research through its Start Up fund. The authors acknowledge the use of the Zeiss Crossbeam 550 FIB-SEM funded with EPSRC grant EP/P030564/1, and would like to thank Dr Thomas Glenn and Dr Fraser Laidlaw at the University of Edinburgh for their kind support in FIB-SEM analysis. The authors would also like to thank Dr Stephen Francis at the University of St Andrews for his support with XPS analysis.

References

[1] J. Wu, Q. Xu, E. Lin, B. Yuan, N. Qin, S.K. Thatikonda, D. Bao, Insights into the role of ferroelectric polarization in piezocatalysis of nanocrystalline $BaTiO_3$, ACS Appl. Mater. Interfaces 10 (21) (2018) 17842–17849, https://doi.org/10.1021/acsami.8b01991.

[2] K. Wang, C. Han, J. Li, J. Qiu, J. Sunarso, S. Liu, The mechanism of piezocatalysis: energy band theory or screening charge effect? Angew. Chem. Int. Ed. Engl. 61 (6) (2022), e202110429 https://doi.org/10.1002/anie.202110429.

[3] H. You, Z. Wu, L. Zhang, Y. Ying, Y. Liu, L. Fei, X. Chen, Y. Jia, Y. Wang, F. Wang, S. Ju, J. Qiao, C.H. Lam, H. Huang, Harvesting the vibration energy of $BiFeO_3$ nanosheets for hydrogen evolution, Angew. Chem. Int. Ed. Engl. 58 (34) (2019) 11779–11784, https://doi.org/10.1002/anie.201906181.

[4] E. Lin, Z. Kang, J. Wu, R. Huang, N. Qin, D. Bao, $BaTiO_3$ nanocubes/cuboids with selectively deposited Ag nanoparticles: efficient piezocatalytic degradation and mechanism, Appl. Catal. B 285 (2021), https://doi.org/10.1016/j.apcatb.2020.119823.

[5] J. Wang, Y. Liang, Z. Wang, B. Huo, C. Liu, X. Chen, H. Xu, D. Li, Z. Zhu, Y. Wang, F. Meng, High efficiently degradation of organic pollutants via low-speed water flow activation of Cu2O@MoS2/PVDF modified pipeline with piezocatalysis performance, Chem. Eng. J. 458 (2023), https://doi.org/10.1016/j.cej.2023.141409.

[6] S.L. Guo, S.N. Lai, J.M. Wu, Strain-induced ferroelectric heterostructure catalysts of hydrogen production through piezophototronic and piezoelectrocatalytic system, ACS Nano 15 (10) (2021) 16106–16117, https://doi.org/10.1021/acsnano.1c04774.

[7] Y.T. Lin, S.N. Lai, J.M. Wu, Simultaneous piezoelectrocatalytic hydrogen-evolution and degradation of water pollutants by quartz microrods@few-layered mos_2 hierarchical heterostructures, Adv. Mater. 32 (34) (2020), e2002875, https://doi.org/10.1002/adma.202002875.

[8] N. Liu, R. Wang, S. Gao, R. Zhang, F. Fan, Y. Ma, X. Luo, D. Ding, W. Wu, High-performance piezo-electrocatalytic sensing of ascorbic acid with nanostructured wurtzite zinc oxide, Adv. Mater. 33 (51) (2021), e2105697, https://doi.org/10.1002/adma.202105697.

[9] J. Ma, S. Jing, Y. Wang, X. Liu, L.Y. Gan, C. Wang, J.Y. Dai, X. Han, X. Zhou, Piezo-electrocatalysis for CO_2 reduction driven by vibration, Adv. Energy Mater. 12 (27) (2022), https://doi.org/10.1002/aenm.202200253.

[10] X. Xiong, Y. Wang, J. Ma, Y. He, J. Huang, Y. Feng, C. Ban, L.Y. Gan, X. Zhou, Oxygen vacancy engineering of zinc oxide for boosting piezo-electrocatalytic hydrogen evolution, Appl. Surf. Sci. 616 (2023), https://doi.org/10.1016/j.apsusc.2023.156556.

[11] X. Ning, A. Hao, Y. Cao, N. lv, D. Jia, Boosting piezocatalytic performance of Ag decorated ZnO by piezo-electrochemical synergistic coupling strategy, Appl. Surf. Sci. 566 (2021), https://doi.org/10.1016/j.apsusc.2021.150730.

[12] H. You, Y. Jia, Z. Wu, X. Xu, W. Qian, Y. Xia, M. Ismail, Strong piezo-electrochemical effect of multiferroic BiFeO3 square micro-sheets for mechanocatalysis, Electrochem. Commun. 79 (2017) 55–58, https://doi.org/10.1016/j.elecom.2017.04.017.

[13] K.S. Hong, H. Xu, H. Konishi, X. Li, Piezoelectrochemical effect: a new mechanism for azo dye decolorization in aqueous solution through vibrating piezoelectric microfibers, J. Phys. Chem. C 116 (24) (2012) 13045–13051, https://doi.org/10.1021/jp211455z.

[14] K.S. Hong, H. Xu, H. Konishi, X. Li, Direct water splitting through vibrating piezoelectric microfibers in water, J. Phys. Chem. Lett. 1 (6) (2010) 997–1002, https://doi.org/10.1021/jz100027t.

[15] M.B. Starr, X. Wang, Coupling of piezoelectric effect with electrochemical processes, Nano Energy 14 (2015) 296–311, https://doi.org/10.1016/j.nanoen.2015.01.035.

[16] W. Qian, W. Yang, Y. Zhang, C.R. Bowen, Y. Yang, Piezoelectric materials for controlling electro-chemical processes, Nanomicro Lett. 12 (1) (2020) 149, https://doi.org/10.1007/s40820-020-00489-z.

[17] P. Wang, X. Li, S. Fan, X. Chen, M. Qin, D. Long, M.O. Tadé, S. Liu, Impact of oxygen vacancy occupancy on piezo-catalytic activity of $BaTiO_3$ nanobelt, Appl. Catal. B 279 (2020), https://doi.org/10.1016/j.apcatb.2020.119340.

[18] S. Lan, Y. Chen, L. Zeng, H. Ji, W. Liu, M. Zhu, Piezo-activation of peroxymonosulfate for benzothiazole removal in water, J. Hazard. Mater. 393 (2020), 122448, https://doi.org/10.1016/j.jhazmat.2020.122448.

[19] W. Qian, K. Zhao, D. Zhang, C.R. Bowen, Y. Wang, Y. Yang, Piezoelectric material-polymer composite porous foam for efficient dye degradation via the piezo-catalytic effect, ACS Appl. Mater. Interfaces 11 (31) (2019) 27862–27869, https://doi.org/10.1021/acsami.9b07857.

[20] G. Singh, M. Sharma, R. Vaish, Exploring the piezocatalytic dye degradation capability of lithium niobate, Adv. Powder Technol. 31 (4) (2020) 1771–1775, https://doi.org/10.1016/j.apt.2020.01.031.

[21] N. Alfryyan, S. Kumar, S.B. Ahmed, I. Kebaili, I. Boukhris, P. Azad, M.S. Al-Buriahi, R. Vaish, Electric poling effect on piezocatalytic $BaTiO_3$/polymer composites for coatings, Catalysts 12 (10) (2022), https://doi.org/10.3390/catal12101228.

[22] Q. Zhou, N. Li, D. Chen, Q. Xu, H. Li, J. He, J. Lu, Efficient removal of Bisphenol A in water via piezocatalytic degradation by equivalent-vanadium-doped SrTiO3 nanofibers, Chem. Eng. Sci. 247 (2022), https://doi.org/10.1016/j.ces.2021.116707.

[23] F. Bößl, I. Tudela, Piezocatalysis: can catalysts really dance? Curr. Opin. Green Sustain. Chem. 32 (2021) https://doi.org/10.1016/j.cogsc.2021.100537.

[24] K.P. Singh, G. Singh, R. Vaish, Utilizing the localized surface piezoelectricity of centrosymmetric Sr1-xFexTiO3 ($x \leq 0.2$) ceramics for piezocatalytic dye degradation, J. Eur. Ceram. Soc. 41 (1) (2021) 326–334, https://doi.org/10.1016/j.jeurceramsoc.2020.08.064.

[25] F. Bößl, V.C. Menzel, E. Chatzisymeon, T.P. Comyn, P.I. Cowin, I. Tudela, Effect of frequency and power on the piezocatalytic and sonochemical degradation of dyes in water, Chem. Eng. J. Adv. (2023), https://doi.org/10.1016/j.ceja.2023.100477.

[26] P.T. Thuy Phuong, Y. Zhang, N. Gathercole, H. Khanbareh, N.P. Hoang Duy, X. Zhou, D. Zhang, K. Zhou, S. Dunn, C. Bowen, Demonstration of enhanced piezo-catalysis for hydrogen generation and water treatment at the ferroelectric curie temperature, iScience 23 (5) (2020), 101095, https://doi.org/10.1016/j.isci.2020.101095.

[27] F. Bößl, T.P. Comyn, P.I. Cowin, F.R. García-García, I. Tudela, Piezocatalytic degradation of pollutants in water: importance of catalyst size, poling and excitation mode, Chem. Eng. J. Adv. 7 (2021), https://doi.org/10.1016/j.ceja.2021.100133.

[28] J. Zhang, C. Wang, C. Bowen, Piezoelectric effects and electromechanical theories at the nanoscale, Nanoscale 6 (22) (2014) 13314–13327, https://doi.org/10.1039/c4nr03756a.

[29] P. Zhu, Y. Chen, J. Shi, Piezocatalytic tumor therapy by ultrasound-triggered and $BaTiO_3$ -mediated piezoelectricity, Adv. Mater. 32 (29) (2020), e2001976, https://doi.org/10.1002/adma.202001976.

[30] A. Zhang, Z. Liu, B. Xie, J. Lu, K. Guo, S. Ke, L. Shu, H. Fan, Vibration catalysis of eco-friendly $Na_{0.5}K_{0.5}NbO_3$-based piezoelectric: an efficient phase boundary catalyst, Appl. Catal. B 279 (2020), https://doi.org/10.1016/j.apcatb.2020.119353.

[31] J. Wu, N. Qin, D. Bao, Effective enhancement of piezocatalytic activity of $BaTiO_3$ nanowires under ultrasonic vibration, Nano Energy 45 (2018) 44–51, https://doi.org/10.1016/j.nanoen.2017.12.034.

[32] V. Srikant, D.R. Clarke, On the optical band gap of zinc oxide, J. Appl. Phys. 83 (10) (1998) 5447–5451, https://doi.org/10.1063/1.367375.

[33] R. Anandhi, R. Mohan, K. Swaminathan, K. Ravichandran, Influence of aging time of the starting solution on the physical properties of fluorine doped zinc oxide films deposited by a simplified spray pyrolysis technique, Superlattices Microstruct. 51 (5) (2012) 680–689, https://doi.org/10.1016/j.spmi.2012.02.006.

[34] Y. Natsume, H. Sakata, T. Hirayama, Low-temperature electrical conductivity and optical absorption edge of ZnO films prepared by chemical vapour deposition, Phys. Status Solidi (A) 148 (2) (1995) 485–495, https://doi.org/10.1002/pssa.2211480217.

[35] M.P. Bole, D.S. Patil, Effect of annealing temperature on the optical constants of zinc oxide films, J. Phys. Chem. Solids 70 (2) (2009) 466–471, https://doi.org/10.1016/j.jpcs.2008.12.001.

[36] E. Broitman, M.Y. Soomro, J. Lu, M. Willander, L. Hultman, Nanoscale piezoelectric response of ZnO nanowires measured using a nanoindentation

technique, Phys. Chem. Chem. Phys. 15 (26) (2013) 11113–11118, https://doi.org/10.1039/c3cp50915j.
[37] T. Abu Ali, J. Pilz, P. Schäffner, M. Kratzer, C. Teichert, B. Stadlober, A.M. Coclite, Piezoelectric properties of zinc oxide thin films grown by plasma-enhanced atomic layer deposition, Phys. Status Solidi (A) 217 (21) (2020), https://doi.org/10.1002/pssa.202000319.
[38] K. Jeronimo, V. Koutsos, R. Cheung, E. Mastropaolo, PDMS-ZnO piezoelectric nanocomposites for pressure sensors, Sensors 21 (17) (2021), https://doi.org/10.3390/s21175873 (Basel).
[39] J. Bennett, A.J. Bell, T.J. Stevenson, T.P. Comyn, Tailoring the structure and piezoelectric properties of $BiFeO_3$-$K_{0.5}Bi_{0.5}TiO_3$-$PbTiO_3$ ceramics for high temperature applications, Appl. Phys. Lett. 103 (15) (2013), https://doi.org/10.1063/1.4824652.
[40] T. Stevenson, D.G. Martin, P.I. Cowin, A. Blumfield, A.J. Bell, T.P. Comyn, P. M. Weaver, Piezoelectric materials for high temperature transducers and actuators, J. Mater. Sci. Mater. Electron. 26 (12) (2015) 9256–9267, https://doi.org/10.1007/s10854-015-3629-4.
[41] H. Fan, H. Li, B. Liu, Y. Lu, T. Xie, D. Wang, Photoinduced charge transfer properties and photocatalytic activity in Bi_2O_3/$BaTiO_3$ composite photocatalyst, ACS Appl. Mater. Interfaces 4 (9) (2012) 4853–4857, https://doi.org/10.1021/am301199v.
[42] S. Das, S. Ghara, P. Mahadevan, A. Sundaresan, J. Gopalakrishnan, D.D. Sarma, Designing a lower band gap bulk ferroelectric material with a sizable polarization at room temperature, ACS Energy Lett. 3 (5) (2018) 1176–1182, https://doi.org/10.1021/acsenergylett.8b00492.
[43] H. Takahashi, Y. Numamoto, J. Tani, S. Tsurekawa, Piezoelectric properties of $BaTiO_3$ ceramics with high performance fabricated by microwave sintering, Jpn. J. Appl. Phys. 45 (9B) (2006) 7405–7408, https://doi.org/10.1143/jjap.45.7405.
[44] P. Zheng, J.L. Zhang, Y.Q. Tan, C.L. Wang, Grain-size effects on dielectric and piezoelectric properties of poled $BaTiO_3$ ceramics, Acta Mater. 60 (13–14) (2012) 5022–5030, https://doi.org/10.1016/j.actamat.2012.06.015.
[45] IEEE standard on piezoelectricity, 176–1987, 1988.
[46] IEEE standard for relaxor-based single crystals for transducer and actuator applications, 1859–2017, 2017.
[47] R.F. Contamine, A.M. Wilhelm, J. Berlan, H. Delmas, Power measurement in sonochemistry, Ultrason. Sonochem. 2 (1) (1995) S43–S47, https://doi.org/10.1016/1350-4177(94)00010-p.
[48] Y. Mao, S. Mao, Z.G. Ye, Z. Xie, L. Zheng, Solvothermal synthesis and Curie temperature of monodispersed barium titanate nanoparticles, Mater. Chem. Phys. 124 (2–3) (2010) 1232–1238, https://doi.org/10.1016/j.matchemphys.2010.08.063.
[49] S. Trasatti, The absolute electrode potential: an explanatory note (Recommendations 1986), Pure Appl. Chem. 58 (7) (1986) 955–966, https://doi.org/10.1351/pac198658070955.
[50] V.K. Sharma, Oxidation of inorganic contaminants by ferrates (VI, V, and IV)–kinetics and mechanisms: a review, J. Environ. Manag. 92 (4) (2011) 1051–1073, https://doi.org/10.1016/j.jenvman.2010.11.026.
[51] W.H. Koppenol, D.M. Stanbury, P.L. Bounds, Electrode potentials of partially reduced oxygen species, from dioxygen to water, Free Radic. Biol. Med. 49 (3) (2010) 317–322, https://doi.org/10.1016/j.freeradbiomed.2010.04.011.
[52] M.C. Blanco López, B. Rand, F.L. Riley, The isoelectric point of BaTiO3, J. Eur. Ceram. Soc. 20 (2) (2000) 107–118, https://doi.org/10.1016/s0955-2219(99)00137-5.
[53] F. Yuan, H. Peng, Y. Yin, Y. Chunlei, H. Ryu, Preparation of zinc oxide nanoparticles coated with homogeneous Al_2O_3 layer, Mater. Sci. Eng. B 122 (1) (2005) 55–60, https://doi.org/10.1016/j.mseb.2005.04.016.
[54] M.A. Abbasi, A. Rehman, Z. Ali, M. Atif, Z. Ali, W. Khalid, Congo red removal by lanthanum-doped bismuth ferrite nanostructures, J. Phys. Chem. Solids 170 (2022), https://doi.org/10.1016/j.jpcs.2022.110964.
[55] J. Moon, J.A. Kerchner, J. LeBleu, A.A. Morrone, J.H. Adair, Oriented lead titanate film growth at lower temperatures by the sol-gel method on particle-seeded substrates, J. Am. Ceram. Soc. 80 (10) (2005) 2613–2623, https://doi.org/10.1111/j.1151-2916.1997.tb03164.x.
[56] Y. Wang, X. Wen, Y. Jia, M. Huang, F. Wang, X. Zhang, Y. Bai, G. Yuan, Y. Wang, Piezo-catalysis for nondestructive tooth whitening, Nat. Commun. 11 (1) (2020) 1328, https://doi.org/10.1038/s41467-020-15015-3.
[57] O. Copie, N. Chevalier, G. Le Rhun, C.L. Rountree, D. Martinotti, S. Gonzalez, C. Mathieu, O. Renault, N. Barrett, Adsorbate screening of surface charge of microscopic ferroelectric domains in sol-gel $PbZr_{0.2}Ti_{0.8}O_3$ thin films, ACS Appl. Mater. Interfaces 9 (34) (2017) 29311–29317, https://doi.org/10.1021/acsami.7b08925.
[58] P. Qiu, B. Park, J. Choi, B. Thokchom, A.B. Pandit, J. Khim, A review on heterogeneous sonocatalyst for treatment of organic pollutants in aqueous phase based on catalytic mechanism, Ultrason. Sonochem. 45 (2018) 29–49, https://doi.org/10.1016/j.ultsonch.2018.03.003.
[59] S. Chakma, V.S. Moholkar, Investigation in mechanistic issues of sonocatalysis and sonophotocatalysis using pure and doped photocatalysts, Ultrason. Sonochem. 22 (2015) 287–299, https://doi.org/10.1016/j.ultsonch.2014.06.008.
[60] F. Peng, H. Li, W. Xu, H. Min, Z. Li, F. Li, X. Huang, W. Wang, C. Lu, A discovery of field-controlling selective adsorption for micro ZnO rods with unexpected piezoelectric catalytic performance, Appl. Surf. Sci. 545 (2021), https://doi.org/10.1016/j.apsusc.2021.149032.
[61] Y. Bai, J. Zhao, Z. Lv, K. Lu, Enhanced piezocatalytic performance of ZnO nanosheet microspheres by enriching the surface oxygen vacancies, J. Mater. Sci. 55 (29) (2020) 14112–14124, https://doi.org/10.1007/s10853-020-05053-z.
[62] C. Yu, M. Tan, Y. Li, C. Liu, R. Yin, H. Meng, Y. Su, L. Qiao, Y. Bai, Ultrahigh piezocatalytic capability in eco-friendly $BaTiO_3$ nanosheets promoted by 2D morphology engineering, J. Colloid Interface Sci. 596 (2021) 288–296, https://doi.org/10.1016/j.jcis.2021.03.040.
[63] D. Liu, C. Jin, F. Shan, J. He, F. Wang, Synthesizing $BaTiO_3$ nanostructures to explore morphological influence, kinetics, and mechanism of piezocatalytic dye degradation, ACS Appl. Mater. Interfaces 12 (15) (2020) 17443–17451, https://doi.org/10.1021/acsami.9b23351.
[64] X. Xu, Z. Wu, L. Xiao, Y. Jia, J. Ma, F. Wang, L. Wang, M. Wang, H. Huang, Strong piezo-electro-chemical effect of piezoelectric BaTiO3 nanofibers for vibration-catalysis, J. Alloy. Compd. 762 (2018) 915–921, https://doi.org/10.1016/j.jallcom.2018.05.279.
[65] J. González-García, V. Sáez, I. Tudela, M.I. Díez-Garcia, M. Deseada Esclapez, O. Louisnard, Sonochemical treatment of water polluted by chlorinated organocompounds. A review, Water 2 (1) (2010) 28–74, https://doi.org/10.3390/w2010028.
[66] Y. Long, H. Xu, J. He, C. Li, M. Zhu, Piezoelectric polarization of BiOCl via capturing mechanical energy for catalytic H_2 evolution, Surf. Interfaces 31 (2022), https://doi.org/10.1016/j.surfin.2022.102056.
[67] J. He, Z. Yi, Q. Chen, Z. Li, J. Hu, M. Zhu, Harvesting mechanical energy induces piezoelectric polarization of MIL-100(Fe) for cocatalyst-free hydrogen production, Chem. Commun. (Camb.) 58 (76) (2022) 10723–10726, https://doi.org/10.1039/d2cc03976a.
[68] Y. Zhang, H. Khanbareh, S. Dunn, C.R. Bowen, H. Gong, N.P.H. Duy, P.T. T. Phuong, High efficiency water splitting using ultrasound coupled to a $BaTiO_3$ nanofluid, Adv Sci (Weinh.) 9 (9) (2022), e2105248, https://doi.org/10.1002/advs.202105248.
[69] J. He, X. Wang, S. Lan, H. Tao, X. Luo, Y. Zhou, M. Zhu, Breaking the intrinsic activity barriers of perovskite oxides photocatalysts for catalytic CO_2 reduction via piezoelectric polarization, Appl. Catal. B 317 (2022), https://doi.org/10.1016/j.apcatb.2022.121747.
[70] P.T.T. Phuong, D.V.N. Vo, N.P.H. Duy, H. Pearce, Z.M. Tsikriteas, E. Roake, C. Bowen, H. Khanbareh, Piezoelectric catalysis for efficient reduction of CO_2 using lead-free ferroelectric particulates, Nano Energy 95 (2022), https://doi.org/10.1016/j.nanoen.2022.107032.
[71] H. Kalhori, A.H. Youssef, A. Ruediger, A. Pignolet, Competing contributions to the catalytic activity of barium titanate nanoparticles in the decomposition of organic pollutants, J. Environ. Chem. Eng. 10 (6) (2022), https://doi.org/10.1016/j.jece.2022.108571.
[72] M.M. Amer, R. Hommelsheim, C. Schumacher, D. Kong, C. Bolm, Electro-mechanochemical approach towards the chloro sulfoximidations of allenes under solvent-free conditions in a ball mill, Farady Discuss. 241 (0) (2023) 79–90, https://doi.org/10.1039/d2fd00075j.

5 Additive manufactured PVDF-based materials for piezocatalytic and sono-adsorption removal of pollutants

5.1 Introduction

The previous three chapters tried to shed more light onto the 'true' mechanism behind piezocatalysis and highlighted that the piezocatalytic process is far more complex than what has generally been reported in the literature. The piezocatalytic studies in Chapters 2-4 with larger scale reactors (i.e. >500 mL) demonstrated the predominant occurrence of other phenomena such as sonolysis and sonocatalysis and with this emphasising on an important aspect that has so far not fully been considered in piezocatalytic research. Besides the consideration of other phenomena taking place simultaneously, there are other potential issues surrounding piezocatalytic research that have not received a lot of attention yet.

Piezocatalysis research has primarily focused on developing and fabricating micro- and nanoscale piezocatalysts [1-4], which may pose a risk of becoming secondary pollutants that require complex separation techniques [5-7]. Such secondary pollution caused by micro- and nanosized piezocatalysts can be addressed by using support materials to fabricate bulky catalyst composites that can be easily recovered from the treated wastewater [8]. However, the choice of composite material is critical in piezocatalysis as it can affect the overall piezoelectric properties of the catalysts and subsequently influence their performance. Therefore, careful consideration must be given to the selection of support materials to ensure optimal piezocatalytic performance.

Polyvinylidene fluoride (PVDF) is polymer known for its unique piezoelectric properties upon poling [9]. This characteristic makes it an ideal candidate as a support material in piezocatalytic composites that incorporate piezocatalysts like $BaTiO_3$ [10]. Besides this, PVDF is a polymer with remarkable chemical and mechanical stability [9] and only soluble in a few organic solvents such as triethyl phosphate (TEP) [11]. The ability of PVDF to dissolve in selected

organic solvents enables its use in Additive Manufacturing (AM) techniques such as Direct Ink Writing (DIW) [9].

The present study tried to combine these advantageous properties of PVDF, both in terms of piezoelectric nature and AM processability, with the $BaTiO_3$ piezocatalysts that exhibited the best piezocatalytic behaviour in Chapter 4. The aim was to develop a bulky, easy-to-separate piezocatalyst for the removal of RhB from an aqueous solution. In this regard, an AM DIW method was developed to fabricate poled PVDF-$BaTiO_3$ composites via in-situ poling during 3D-printing.

5.2 Discussion highlights and conclusions

The development of an additive manufacturing method for PVDF-$BaTiO_3$ composite was driven by the disintegration of $BaTiO_3$ piezocatalysts during the second half of the RhB degrading studies. However, the RhB degradation experiments provided interesting results. At the beginning, RhB degradation with P PVDF-$BaTiO_3$ appeared to be higher compared to experiments without a catalyst, but ultimately, the degradation in the presence of P PVDF-$BaTiO_3$ composites was similar to that without a catalyst and lower than with $BaTiO_3$ piezocatalysts. Moreover, observations such as the deviation from first-order RhB degradation kinetics and the lack of significant effects from poling indicated the occurrence of different physico-chemical phenomena. To understand these results, additional experiments were conducted with additive manufactured PVDF slabs ($_{AM}$PVDF) and as-supplied PVDF powder ($_{P}$PVDF). $_{AM}$PVDF initially achieved higher RhB degradation, but the rate slowed down in the second half of the experiments. $_{P}$PVDF showed similar overall RhB degradation, but a lower rate in the first half compared to $_{AM}$PVDF. It was noticed that already around 4% of RhB was adsorbed onto the $_{AM}$PVDF slabs during the adsorption-desorption equilibrium period. These results suggested that PVDF, rather than $BaTiO_3$ particles, was responsible for the removal of RhB in the experiments with PVDF-$BaTiO_3$ composites.

In order to better understand the adsorption of RhB on $_{AM}$PVDF and its potential enhancement by ultrasound, additional experiments were conducted using different amounts of $_{AM}$PVDF under mechanical agitation with and without ultrasound. The results clearly showed an increase in the removal of RhB with an increasing amount of $_{AM}$PVDF. Whilst in absence of ultrasound 1g L^{-1} of $_{AM}$PVDF only removed around 13% after 2 hours, the same amount of $_{AM}$PVDF already removed 27% of RhB within 10 minutes under sonication. This demonstrated the importance of ultrasound for the enhanced adsorption of RhB onto $_{AM}$PVDF. However, the most remarkable removal of RhB in this study was achieved with 4 g L^{-1} $_{AM}$PVDF. Within 10 minutes of sonication already 80% of RhB were removed from the solution. After 40 minutes RhB was virtually removed.

Based on the experimental observations, a simple model was developed to better understand how ultrasound is enhancing the adsorption of RhB onto $_{AM}$PVDF. The developed model assumed that diffusion inside the $_{AM}$PVDF slabs was the main mass transport mechanism due to the effects of ultrasound such as acoustic streaming and shockwaves on reducing the film resistance at the adsorbent's surface. A strong feature of the model is that it only relied on an unknown parameter, the Henry law constant *H*; nevertheless, the model also had to consider that adsorption was further enhancing the sonochemical degradation of RhB to fully agree with the experimental results. This feature of the model, which might sound rather intriguing in first instance, should not be a surprise when one takes into account that the sonochemical degradation followed first order kinetics and that the predicted concentration in the adsorbed phase was roughly 400 times that of the bulk liquid; this would easily explain the previously reported synergistic effect between sonochemical and adsorption processes [12, 13]. Although some deviations were noticed, in particular at short times likely due to the residual film resistance and the simplification of the kinetics of the adsorption-enhanced sonochemical RhB degradation, the overall fit of the proposed model was very reasonable. Furthermore, when adding a film resistance this model would also be able to predict RhB adsorption of $_{AM}$PVDF in absence of ultrasound.

Whilst previous studies have relied on empirical models to analyse their experimental data that potentially can lead to misinterpretations of the underlying mass transport mechanism [14], the present work highlighted the importance of a different approach to model sono-adsorption processes by developing and implementing a phenomenological model that accounts for the most meaningful physico-chemical phenomena in the system. Without this new approach, the synergic effect between ultrasound and adsorption would have again been overlooked.

In conclusion, this study did not only show an innovative approach to additively manufacture easy-to-recover PVDF-$BaTiO_3$ piezocatalysts, but also shed light on the occurrence of another concurrent phenomena in piezocatalysis: adsorption. Based on these findings, it is suggested to consciously consider and optimise concurrent phenomena such as sonochemistry and sono-adsorption in piezocatalytic research. By embracing and exploring these synergistic effects, the field of piezocatalysis could unlock new opportunities for advancements and applications in environmental remediation.

To gain a deeper understanding of the research outcomes and their significance, all results and a more comprehensive discussion can be found in *Sono-adsorption and adsorption-enhanced sonochemical degradation of dyes in water by additive manufactured PVDF-based materials* published in *Ultrasonics Sonochemistry*, which constitutes Chapter 5 of this thesis.

5.3 References

[1] F. Bößl, I. Tudela
Piezocatalysis: Can catalysts really dance?
Current Opinion in Green and Sustainable Chemistry, 32 (2021), 10.1016/j.cogsc.2021.100537

[2] N. Liu, R. Wang, S. Gao, R. Zhang, F. Fan, Y. Ma, X. Luo, D. Ding, W. Wu
High-Performance Piezo-Electrocatalytic Sensing of Ascorbic Acid with Nanostructured Wurtzite Zinc Oxide
Adv Mater, 33 (51) (2021), e2105697, 10.1002/adma.202105697

[3] P.T.T. Phuong, D.-V.N. Vo, N.P.H. Duy, H. Pearce, Z.M. Tsikriteas, E. Roake, C. Bowen, H. Khanbareh

Piezoelectric catalysis for efficient reduction of CO_2 using lead-free ferroelectric particulates

Nano Energy, 95 (2022), 10.1016/j.nanoen.2022.107032

[4] Y. Zheng, X. Wu, Y. Zhang, Y. Li, W. Shao, J. Fu, Q. Lin, J. Tan, S. Gao, W. Ye, H. Huang

Highly efficient harvesting of vibration energy for complex wastewater purification using $Bi_5Ti_3FeO_{15}$ with controlled oxygen vacancies

Chemical Engineering Journal, 453 (2023), 10.1016/j.cej.2022.139919

[5] Y. Liu, M. Tourbin, S. Lachaize, P. Guiraud

Nanoparticles in wastewaters: Hazards, fate and remediation

Powder Technology, 255 (2014), 149-156, 10.1016/j.powtec.2013.08.025

[6] V. Nogueira, I. Lopes, T. Rocha-Santos, F. Goncalves, R. Pereira

Toxicity of solid residues resulting from wastewater treatment with nanomaterials

Aquat Toxicol, 165 (2015), 172-8, 10.1016/j.aquatox.2015.05.021

[7] C.M. Vineeth Kumar, V. Karthick, V.G. Kumar, D. Inbakandan, E.R. Rene, K.S.U. Suganya, A. Embrandiri, T.S. Dhas, M. Ravi, P. Sowmiya

The impact of engineered nanomaterials on the environment: Release mechanism, toxicity, transformation, and remediation

Environ Res, 212 (Pt B) (2022), 113202, 10.1016/j.envres.2022.113202

[8] S.D. Aguilar, D.R. Ramos, J.A. Santaballa, M. Canle

Preparation, characterization and testing of a bulky non-supported photocatalyst for water pollution abatement

Catalysis Today, 413-415 (2023), 10.1016/j.cattod.2022.12.023

[9] S. Mohammadpourfazeli, S. Arash, A. Ansari, S. Yang, K. Mallick, R. Bagherzadeh

Future prospects and recent developments of polyvinylidene fluoride (PVDF) piezoelectric polymer; fabrication methods, structure, and electro-mechanical properties

RSC Adv, 13 (1) (2022), 370-387, 10.1039/d2ra06774a

[10] J. Shi, W. Zeng, Z. Dai, L. Wang, Q. Wang, S. Lin, Y. Xiong, S. Yang, S. Shang, W. Chen, L. Zhao, X. Ding, X. Tao, Y. Chai

Piezocatalytic Foam for Highly Efficient Degradation of Aqueous Organics

Small Science, 1 (2) (2020), 10.1002/smsc.202000011

[11] J.E. Marshall, A. Zhenova, S. Roberts, T. Petchey, P. Zhu, C.E.J. Dancer, C.R. McElroy, E. Kendrick, V. Goodship

On the Solubility and Stability of Polyvinylidene Fluoride

Polymers (Basel), 13 (9) (2021), 10.3390/polym13091354

[12] Y. Iida, T. Kozuka, T. Tuziuti, K. Yasui

Sonochemically enhanced adsorption and degradation of methyl orange with activated aluminas

Ultrasonics, 42 (1-9) (2004), 635-9, 10.1016/j.ultras.2004.01.092

[13] S. Nikolaou, J. Vakros, E. Diamadopoulos, D. Mantzavinos

Sonochemical degradation of propylparaben in the presence of agro-industrial biochar

Journal of Environmental Chemical Engineering, 8 (4) (2020), 10.1016/j.jece.2020.104010

[14] S. Brandani

Kinetics of liquid phase batch adsorption experiments

Adsorption, 27 (3) (2020), 353-368, 10.1007/s10450-020-00258-9

Ultrasonics Sonochemistry 100 (2023) 106602

Contents lists available at ScienceDirect

Ultrasonics Sonochemistry

journal homepage: www.elsevier.com/locate/ultson

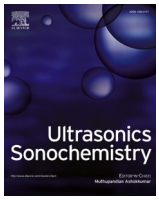

Synergistic sono-adsorption and adsorption-enhanced sonochemical degradation of dyes in water by additive manufactured PVDF-based materials

Franziska Bößl [a,b,*], Stefano Brandani [a], Valentin C. Menzel [a,b], Matilda Rhodes [c], Mayra S. Tovar-Oliva [a,b], Caroline Kirk [c], Ignacio Tudela [a,b,*]

[a] School of Engineering, Institute for Materials and Processes, The University of Edinburgh, Sanderson Building, Robert Stevenson Road, Edinburgh EH9 3FB, UK
[b] Edinburgh Electrochemical Engineering Group (e3 Group), The University of Edinburgh, Sanderson Building, Robert Stevenson Road, Edinburgh EH9 3FB, UK
[c] School of Chemistry, The University of Edinburgh, Joseph Black Building, David Brewster Road, Edinburgh EH9 3FJ, UK

ARTICLE INFO

Keywords:
Sono-adsorption
Sonochemistry
Piezocatalysis
Additive manufacturing
Composite materials

ABSTRACT

The present study proposes the first mechanistic model accounting for the most meaningful physico-chemical phenomena taking place in liquid phase adsorption processes under ultrasound. Initially, this study was aimed at developing an easy-to-make and easy-to-recover piezocatalyst for the degradation of RhB in water by combining the high piezocatalytical performance of $BaTiO_3$ with a compatible piezoelectric support such as PVDF, manufactured by a customised additive manufacturing – direct ink writing system with in-situ poling. However, initial results showed that the resulting PVDF-$BaTiO_3$ composite slabs performed worse than $BaTiO_3$ piezocatalysts on their own, and that poling did not have any effect on their performance (82% RhB removal after 2 h when using either poled or unpoled PVDF-$BaTiO_3$ composite slabs compared to 92% RhB removal after 2 h in presence of $BaTiO_3$ piezocatalysts). Further investigation with pure PVDF materials demonstrated that, instead of piezocatalysis, synergistic ultrasound-assisted adsorption and sonochemical degradation were taking place, enabling the removal of >95% of the dye within 40 min of ultrasound treatment in the presence of 4 g L^{-1} of additive manufactured PVDF slabs. The results of this study and their evaluation with the mechanistic model proposed for liquid phase adsorption under ultrasound suggest that the adsorption of RhB on additive manufactured PVDF slabs was enhanced by the structure, higher specific surface ratio and higher volume of mesopores achieved through the 3D-printing process, as well as the minimisation of film resistance to mass transport due to ultrasound. Moreover, adsorption on additive manufactured PVDF enhanced the sonochemical degradation of the dye due to its high concentration in the adsorbed phase. This study demonstrates that adsorption processes, especially in the presence of PVDF materials, may be significantly more important in piezocatalysis than what has been reported to date, to the point that the synergistic combination of sono-adsorption and sonochemical degradation in presence of additive-manufactured PVDF slabs may be enough to achieve high removal rates of dyes in water.

1. Introduction

Harvesting excess system vibrations and turning them into energy is an attractive principle that has been intensively studied in the field of piezoelectric energy (re-)generation [1–4]. The emerging field of piezocatalysis takes this concept one step further and directly utilises vibrations to catalyse various chemical reactions. In piezocatalysis, piezoelectric materials suspended in liquid media are excited by a mechanical field (e.g. ultrasound), generating an electro-mechanical response that enables the occurrence of redox chemical processes such as the degradation of organic pollutants via radicalary reactions [5–7], water splitting [8–10] or even CO_2 reduction [11–13] at the surface of the piezoelectric material. For this reason, piezocatalysis has attracted significant attention in recent years due to its potential, where many processes using catalysts such as barium titanate ($BaTiO_3$) [14–16], zinc oxide [17–19] or complex metal oxides [20–22] have been explored.

* Corresponding authors at: School of Engineering, Institute for Materials and Processes, The University of Edinburgh, Sanderson Building, Robert Stevenson Road, Edinburgh EH9 3FB, UK.
E-mail addresses: (F. Bößl), (I. Tudela).

https://doi.org/10.1016/j.ultsonch.2023.106602
Received 30 June 2023; Received in revised form 28 August 2023; Accepted 14 September 2023
Available online 19 September 2023

Piezocatalytic processes are, however, far more complex than what has generally been reported in the literature; despite very recent efforts by the authors that have shed more light onto it [23], the 'true' mechanism behind this phenomenon is still under debate [24]. Moreover, the very few studies trying to bring piezocatalysis from very small lab reactors (i.e. <100 mL) into larger scales (i.e. >500 mL) have highlighted the occurrence of other phenomena such as sonolysis and sonocatalysis [25,26], illustrating that, for piezocatalysis to make a real impact, knowledge from other research areas besides piezoelectricity such as electrochemistry and sonochemistry must be accounted for [27].

Wastewater from the dye industry is considered as one of the most complex organic contaminant mixtures [28,29] that can have a significant impact on water bodies, even at low concentrations [30,31]. Dyes such as Methylene Blue, Methylene Orange or Rhodamine B (RhB) have become popular degradation targets in piezocatalysis [5–7] due to their toxicity [31] and ability to promote oligotrophic water conditions [30]. In this regard, the vast majority of piezocatalysis research has focused on the development and fabrication of micro- and nano-sized piezocatalysts [7,11,18,27]. However, there is a significant risk for these micro- and nano-sized piezocatalysts to become pollutants themselves, leading to secondary pollution that would require additional complex separation steps to the overall pollution removal process [32–35]. A potential solution would be the use of support materials, allowing for the fabrication of bulky composite catalysts that could be easily removed from treated wastewater [36]. However, in the case of piezocatalysis, the type of support material would need to be carefully considered; otherwise, the piezoelectric nature of the catalysts would be affected and the piezocatalytic performance could be significantly reduced.

Polyvinylidene fluoride (PVDF) is one of the few polymers that exhibit a piezoelectric response after being poled [37], allowing for its use as a support material in piezocatalytic composites containing piezocatalysts such as $BaTiO_3$ [38] or $LiNbO_3$ ceramics [39], as well as a piezocatalyst on its own [40]. As a polymer exhibiting high chemical and mechanical stability [37], PVDF is soluble in just a few organic solvents like dimethylformamide, dimethyl sulfoxide, N-methylpyrrolidone or triethyl phosphate (TEP) [41], which allows PVDF to be used in additive manufacturing processes such as direct ink writing [37].

In the study presented here, these advantageous properties of PVDF, both in terms of piezoelectric nature and additive manufacturing processibility, were combined with a well-known piezocatalyst, $BaTiO_3$ [23], to create a bulky, easy-to-separate piezoelectric composite material. This was achieved by developing a direct ink writing method to fabricate poled PVDF-$BaTiO_3$ composites via *in-situ* poling during 3D-printing. However, the use of the 3D-printed poled PVDF-$BaTiO_3$ composite in the degradation of RhB revealed the competing contribution of yet another simultaneous phenomenon that had rarely been associated to piezocatalysis before: ultrasound-assisted adsorption, also known as *sono-adsorption* [42,43]. To better understand this, a mechanistic model accounting for the main physico-chemical phenomena occurring in adsorption experiments under ultrasound was proposed, to the best of the author's knowledge, for the very first time. The model indicated that adsorption of RhB on additive manufactured PVDF slabs benefited from the minimisation of film resistance to mass transport due to ultrasound. This adsorption further enhanced the ongoing sonochemical degradation of RhB via radicalary reactions [25,26] due to the high concentration of the dye in the adsorbed phase. The present study therefore highlights how this overlooked phenomenon in piezocatalysis could be further exploited, in combination with sonochemical degradation, to achieve outstanding dye removal rates. This removes the need to employ micro- and nano-size piezocatalysts fabricated via complex synthesis methods whose use would require additional costly separation approaches.

2. Experimental

2.1. Material preparation and characterisation

2.1.1. Material preparation

Poled $BaTiO_3$ piezoelectic particles were fabricated from commercial piezoceramic discs (Steiner & Martins, Inc.) with high piezoelectric properties (d_{33} = 160 pC/N, d_{31} = 30 pC/N) and suitable energy band levels (3.18 eV band gap) [23]. The $BaTiO_3$ piezoceramic discs were ground into fine particles (<63 μm) following the same procedure previously described by the authors [23,25]. Depending on the experiments, the poled $BaTiO_3$ piezoelectric particles were used as piezocatalysts on their own or as fillers in additive manufactured PVDF-$BaTiO_3$ composites.

PVDF powder with a molecular weight of 94.1 g (Fluorochem Ltd.) was used to fabricate all the additive manufactured PVDF-based materials used in this study; these materials were manufactured using a customised additive manufacturing – direct ink writing setup previously developed by the authors based on a Prusa Research MK3S + printer [44]. In this case, additional modifications were introduced to achieve in-situ electrical poling-assisted direct ink writing of PVDF-based materials (Fig. 1):

- To ensure the safe operation of the in-situ electrical poling system, the 3D-printing setup was installed within a custom-made enclosure (Fig. 1a) equipped with a magnetic switch installed on its door, which would automatically shut down the external power supply to prevent any unintentional access to the running setup. An emergency switch-off system was also mounted on the right side of the enclosure to halt the power supply in case of an unexpected emergency (Fig. 1b).
- A glass plate was mounted onto the Prusa heat bed to insulate the applied voltage (Fig. 1c). Copper tape was applied on top of the glass plate to create a conductive printing surface. To prevent short circuits between the print surface and nozzle, Kapton tape was applied to the copper layer as an insulator (Fig. 1c). These modifications allowed for an efficient operation of the in-situ electrical poling by mitigating the risk of electrical damage to the 3D-printer.
- The external power supply was connected to the 3D-printer using cables and power inlets that were also mounted in the custom-made enclosure (Fig. 1b). The positive voltage cable was connected to the printing surface through a soldered connection with the copper layer (Fig. 1c), whilst the negative voltage cable was connected to the metal nozzle with a solder tag (Fig. 1d).

Manufacturing of all additive manufactured PVDF-based materials started by mixing 0.5 g of PVDF powder with 2.1 mL triethyl phosphate (TEP, Sigma-Aldrich). The mixture was then manually stirred for two minutes until a translucent, smooth and viscous paste was obtained. This PVDF-TEP paste was further mixed for another two minutes at 90 °C to allow for the solvation of most of the PVDF with TEP. In the case of PVDF-$BaTiO_3$ composites, 0.5 g of the $BaTiO_3$ piezoelectric particles were added and mixed until a homogeneous paste was obtained again. In all cases, the resulting PVDF-based paste was added into a 10 mL luer lock syringe equipped with a metal blunt syringe tip (0.25 mm internal tip diameter) acting as the nozzle. In the case of poled PVDF-$BaTiO_3$ composites, in-situ poling was achieved by applying an electrical field of around 13 MV m^{-1}.

2.1.2. Material characterisation

A focused ion beam-scanning electron microscope (FIB-SEM, Zeiss Gemini 2 crossbeam 550) equipped with an energy dispersive X-ray spectrometer (EDS) was used to determine the morphology, surface structure and composition of all materials used in this study. In addition, X-ray powder diffraction (XRPD) data was obtained with a Bruker D2 PHASER diffractometer equipped with Cu Kα radiation to confirm the

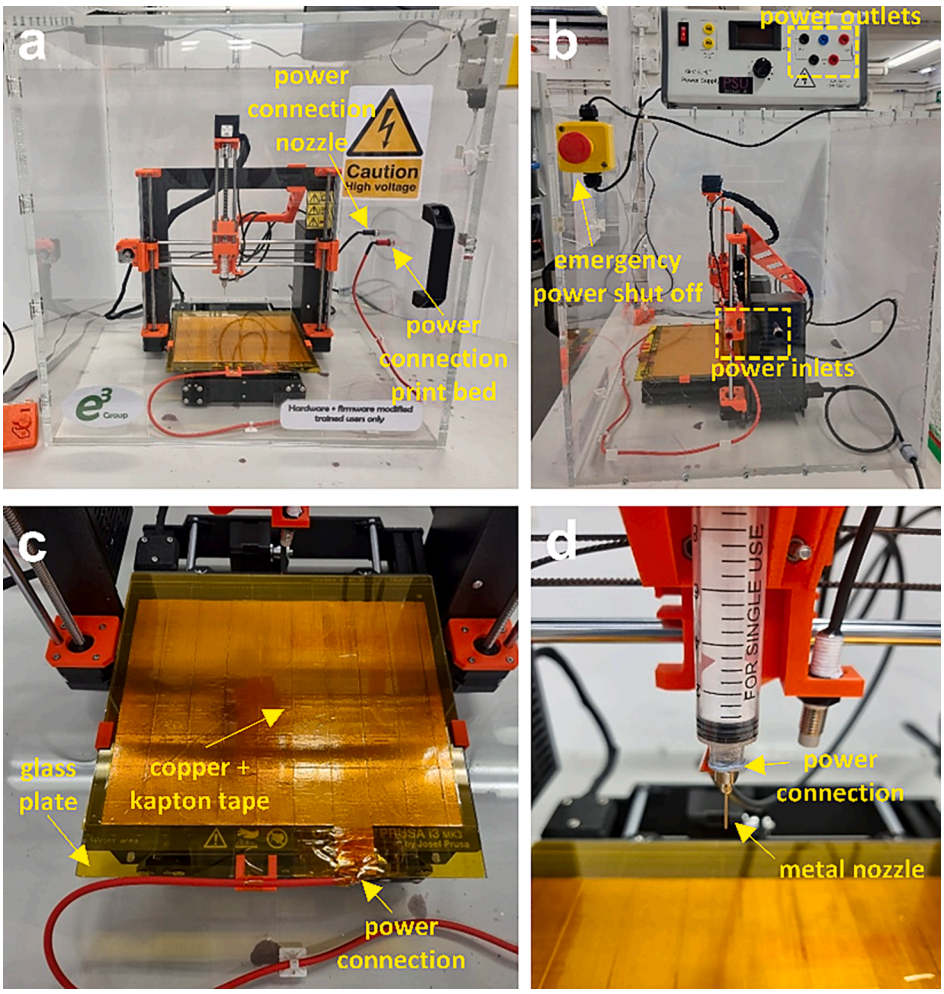

Fig. 1. Additive manufacturing – direct ink writing setup modified for in-situ electrical poling during printing: (a) 3D-printer inside custom-made enclosure for safe operation; (b) external power supply and enclosure with power inlets and emergency switch-off system; (c) modified print bed (glass plate, copper layer and Kapton tape) connected to positive power supply cable via a soldered connection; (d) metal nozzle connected to negative power supply cable via a solder tag.

identity of the crystalline phases of the materials; data were collected over the 2θ range from 5 to 60° and a scanning speed of 0.2 steps/second. Specific surface area (SSA) and pore size distribution in pure PVDF materials (both additive manufactured and in powder form) were determined by nitrogen adsorption/desorption isotherms with an automated sorption analyser (Quantachrome Autosorb-iQ). For this latter purpose, samples were degassed at 100 °C for 6 h prior to recording adsorption/desorption isotherms at −196.15 °C; Brunauer–Emmett–Teller (BET) and DFT theory were applied to calculate SSA and pore size distribution, respectively.

2.2. Experimental setups and procedure

The same experimental parameters used in previous studies by the authors [23,25] were again defined for the RhB removal experiments conducted within this study. In all experiments, an overhead stirrer (SciQuip Basic 20) operating at 200 rpm was centred and immersed into a 1 L beaker acting as the reactor. The beaker was also centred and immersed 4 cm into an ultrasonic bath (Ultrawave QS12) operating at 32–38 kHz and 14.3 ± 0.7 W g L^{-1} after being calibrated by the standard calorimetric method [45]. Prior to each experiment, the water inside the ultrasonic bath was thoroughly degassed for 60 min to ensure a reproducible acoustic field inside the bath.

1 L of aqueous solutions containing 5 mg g L^{-1} of RhB were treated in all experiments. Temperature was controlled and kept at 30 ± 2 °C throughout the experiments by a temperature control system (Grant LT ecocool100). 3 mL aliquots of the treated RhB solution were taken every 10 min with a 0.22 μm PTFE-syringe-filter; samples were then analysed by ultraviolet–visible spectroscopy (Shimadzu UV-3600 Plus) at the characteristic wavelength of 554 nm. 1 g g L^{-1} of catalysts were added to the aqueous RhB solution in all 'piezocatalysis' experiments; prior to each experiment, though, the RhB solution was stirred for 30 min at 200 rpm to ensure adsorption–desorption equilibrium. In the case of the sono-adsorption experiments, adsorbent concentration was varied depending on the experimental condition (1–4 g g L^{-1}).

3. Results and discussion

3.1. Material characterisation

As previously reported by the authors [23], $BaTiO_3$ piezocatalysts generally presented a cuboid morphology with sizes in the order of several tens of microns and a rough surface structure (Fig. 2a, left), where very small debris produced during the fabrication of the piezocatalysts (i.e. grinding of commercial piezoceramic discs) were observed (Fig. 2a, centre). All additive manufactured PVDF-based materials, i.e. poled (P) and unpoled (UP) PVDF-$BaTiO_3$ composites and pure PVDF ($_{AM}$PVDF), generally presented an elongated slab morphology with a length of approximately 10 mm and a width of approximately 1.5 mm (Fig. 2b–d, left). The thickness of these additive manufactured PVDF-

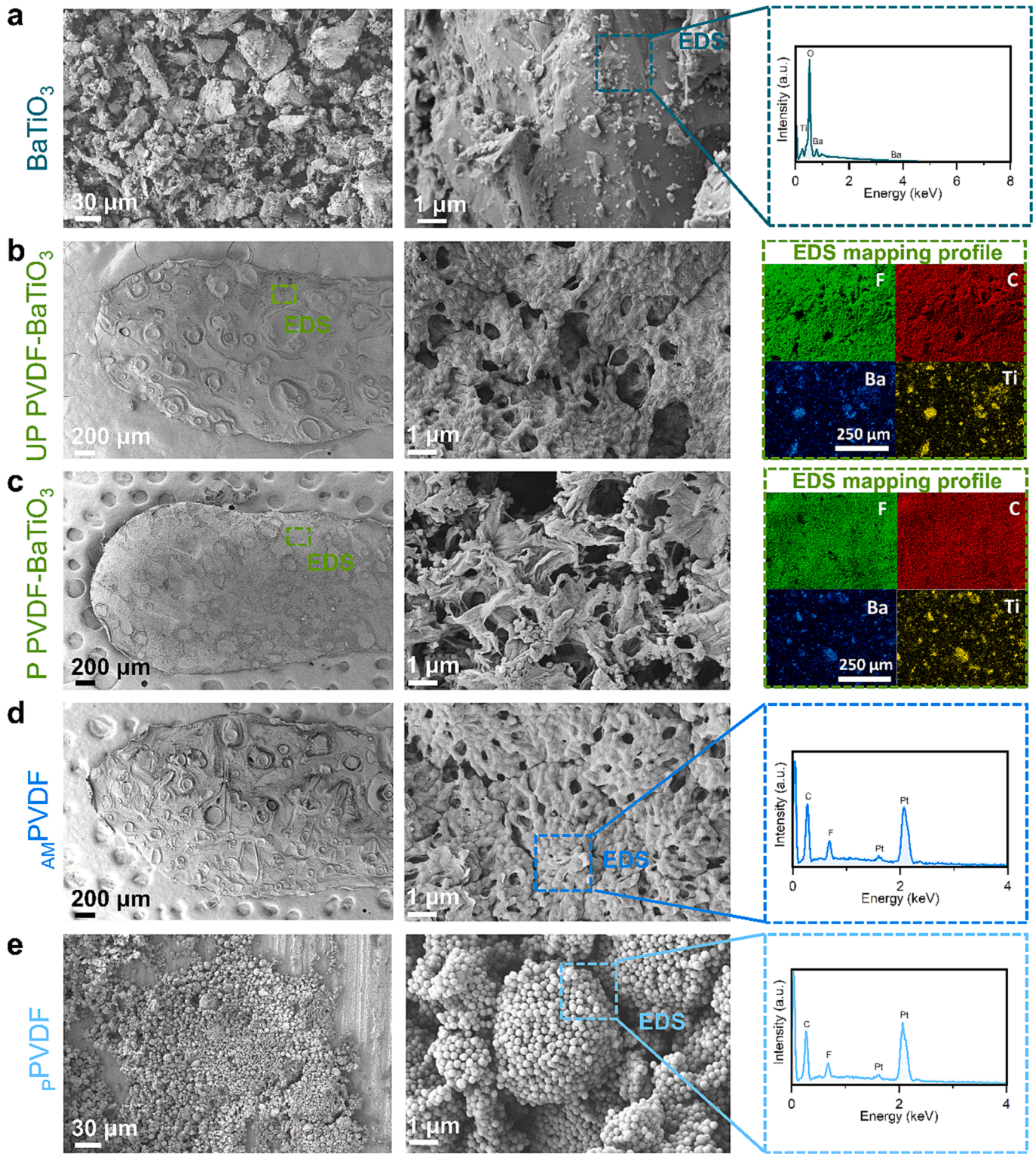

Fig. 2. FIB-SEM and EDS analysis for (a) $BaTiO_3$ piezocatalyst, (b) additive manufactured poled (P) PVDF-$BaTiO_3$ composite, (c) additive manufactured unpoled (UP) PVDF-$BaTiO_3$ composite, (d) additive manufactured pure PVDF ($_{AM}$PVDF), (e) pure PVDF powder (pPVDF). PVDF-based samples were covered with a Pt film to increase their conductivity and improve the quality of the images.

based slabs was approximately 0.12 mm. A closer look at the surface of the additive manufacture PVDF-based materials revealed a porous surface structure in all of them (Fig. 2b–d, centre); however, the P PVDF-$BaTiO_3$ slabs appeared to have a more irregular surface than both UP PVDF-$BaTiO_3$ and $_{AM}$PVDF slabs, which were not subjected to poling during the printing process. Pure PVDF powder as received ($_{P}$PVDF) presented a very fine granular morphology in the nanoscale; nanoparticles were forming compact aggregates of several microns or even larger (Fig. 2e, left and centre). In all cases, EDS analysis confirmed the composition of the $BaTiO_3$ piezocatalysts (Fig. 2a, right), pure PVDF 'catalysts' (Fig. 2d and e, right) and PVDF-$BaTiO_3$ composites (Fig. 2b and c, right).

XRPD analysis was used to confirm the phase(s) present in the materials used in this study (Fig. 3). As reported by the authors in a previous study [23], XRPD data collected on the $BaTiO_3$ piezocatalysts matched well to the standard International Centre for Diffraction Data Powder Diffraction File [74-1959] for tetragonal $BaTiO_3$. Only the perovskite $BaTiO_3$ phase was observed, as no peaks related to any impurity phases were noticed. Peak splitting was clearly observed at around 45°, indicating the presence of tetragonal polymorph $BaTiO_3$ where the (200) peak in the cubic polymorph would split into (002) and (200) [46,47]. In the case of $_P$PVDF and $_{AM}$PVDF, peaks were clearly noticed at around 18.4°, 19.9° and 27.8°, which indicate the presence of (020), (021) and (111) crystal planes characteristic of PVDF in its non-piezoelectric α phase [48]. A shoulder on the left of the (020) peak was also noticed in both cases; this shoulder would indicate the existence of (100) crystal planes at around 17.7°, which are again characteristic of α-PVDF [48]. Additional peaks were also noticed in the case of $_{AM}$PVDF at around 35.7°, 39.0° and 57.4° suggesting the presence of (200), (002) and (022) crystal planes, which are again characteristic of α-PVDF [48]. Regarding the composite materials, both UP and P PVDF-$BaTiO_3$ exhibited the same features previously discussed for tetragonal $BaTiO_3$, including the peak splitting at around 45° characteristic of tetragonal polymorph $BaTiO_3$. Subtle peaks that could be associated to α-PVDF and β-PVDF could also be noticed, especially in the case of P PVDF-$BaTiO_3$; however, these latter results are inconclusive. The reason for this would be the high content of $BaTiO_3$ in the composites (50%), as ferroelectric ceramic content higher than 20% could distort the results of characterisation tests due to their dominant influence on the recorded data [49].

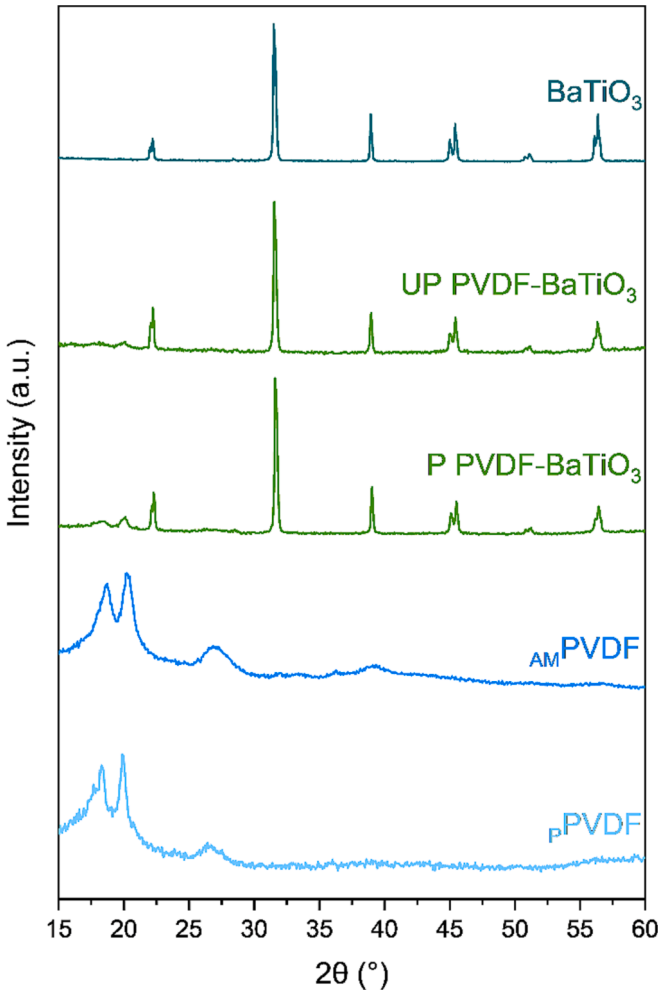

Fig. 3. XRPD data collected on the different materials used in this study: $BaTiO_3$ piezocatalysts, unpoled (UP) and poled (P) additive manufactured PVDF-$BaTiO_3$ composites, and pure PVDF in additive manufactured slab ($_{AM}$PVDF) and powder ($_P$PVDF) form.

3.2. Degradation of RhB by additive manufactured PVDF-$BaTiO_3$

Fig. 4a displays how the normalised concentration of RhB changed over time during different experiments under combined ultrasound and mechanical agitation on their own (MA + US, i.e. sonochemical degradation), as well as in the presence of $BaTiO_3$ piezocatalysts and different PVDF-based materials (P and UP PVDF-$BaTiO_3$ composites, $_{AM}$PVDF and $_P$PVDF). For the vast majority of experimental studies on piezocatalysis and sonochemistry reported in the literature, a time constant can be defined by approximating the dynamic response of the concentration of RhB with an exponential decay. This time constant generally corresponds with an apparent first order kinetic constant, which constitutes a suitable way to quantitatively compare experiments conducted under similar conditions. This apparent first order RhB degradation kinetics would follow the following expression:

$$\frac{C}{C_0} = e^{-kt} \tag{1}$$

where t was the irradiation time, C the RhB concentration at time t, C_0 the initial concentration of RhB and k the apparent first-order degradation reaction rate constant. The degradation efficiency (DE) was determined by the following expression:

$$DE = \left(1 - \frac{C}{C_0}\right) \times 100 \tag{2}$$

As already reported by the authors in previous studies [23,25], the combination of mechanical agitation and ultrasound in absence of a piezocatalyst (US + MA) was enough to achieve a significant degradation of RhB after two hours (DE = 83%). RhB degradation would take place in this case via chemical reactions involving superoxide and hydroxyl radicals [25]; these radicals would be generated by the remarkably high temperatures (order of 5,000 K) and pressures (order of 1,000 atm) reached at the centre of cavitating bubbles formed by the acoustic field established in the sonicated liquid after their collapse [50].

The presence of $BaTiO_3$ piezocatalysts, as reported in previous work by the authors [23], further enhanced the degradation of the dye within the same time (DE = 92%). This enhancement would also be mainly caused via the same chemical reactions involving superoxide and hydroxyl radicals [51–53]; in this case, though, the superoxide and hydroxyl radicals would be caused by redox reactions occurring at the surface of the piezocatalysts under the action of a mechanical field (e.g. ultrasound in water) [24,27]. Unfortunately, the continuous action of cavitation phenomena (e.g. shockwaves and, more importantly, asymmetrical bubble collapse over the surface of particles) [25] caused significant erosion over the surface of the $BaTiO_3$ piezocatalysts, which broke down into significantly smaller particles. This led to the 0.22 μm PTFE-syringe-filters used to prepare the aliquots for the ultraviolet–visible spectroscopy analysis starting to clog in the later stages of the experiments. Such disintegration of the $BaTiO_3$ piezocatalysts, although did not seem to hinder its piezocatalytic performance, would potentially constitute a source of secondary pollution due to the overall environmental impact and recovery challenges associated to it [32–35], as previously mentioned in the introduction.

The disintegration of the $BaTiO_3$ piezocatalysts in the second half of the two-hour RhB degradation experiments was precisely what drove the development of the additive manufacturing process to fabricate fully piezoelectric PVDF-$BaTiO_3$ composites. In these composites, the PVDF would not only act as a support material to produce bulkier composite catalysts that would be easy to recover from treated wastewater [36], but it should also enhance the overall performance of the piezocatalyst

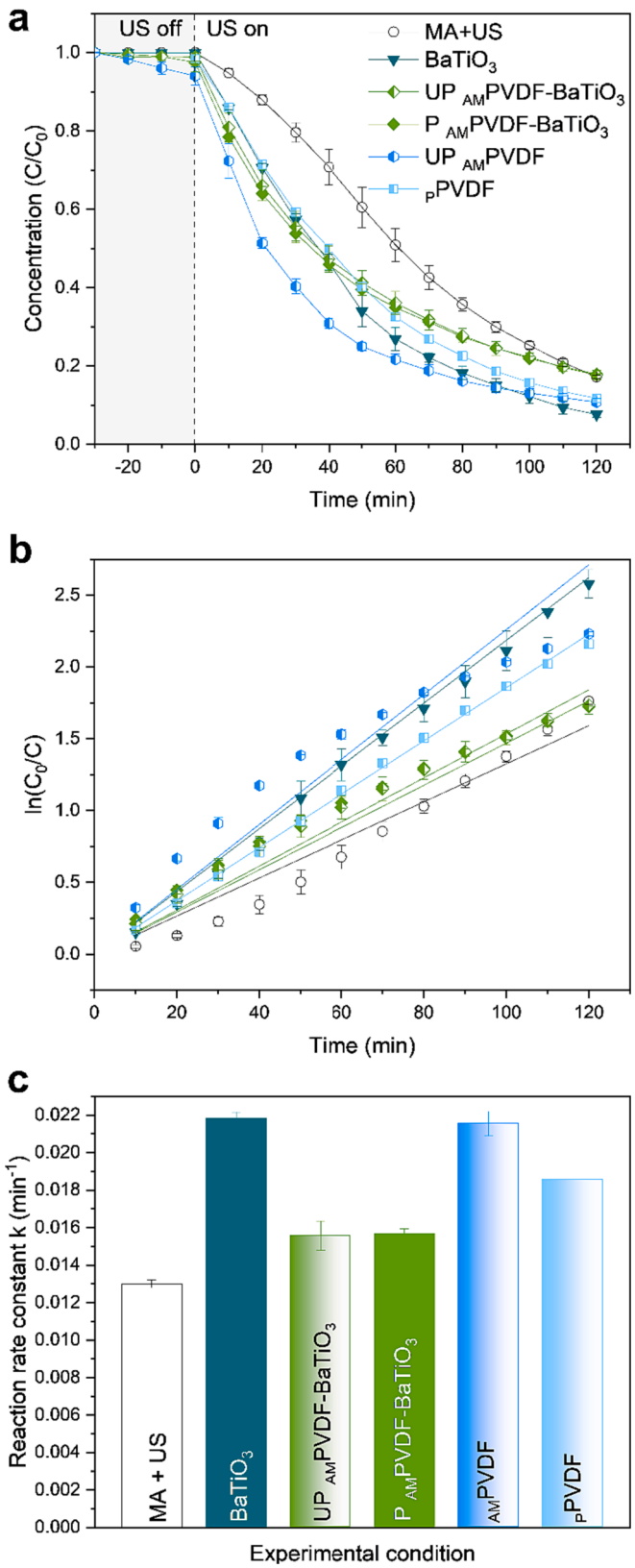

Fig. 4. RhB degradation experiments under combined ultrasound and mechanical agitation in absence/presence of $BaTiO_3$ piezocatalysts, additive manufactured P and UP PVDF-$BaTiO_3$ composites, $_{AM}$PVDF and $_{P}$PVDF: (a) evolution of C_0/C vs reaction time. (b) first-order linear fit of $\ln(C_0/C)$ vs reaction time. (c) Apparent first-order degradation reaction rate constants.

[38,39] as the PVDF itself would also be piezoelectric due to in-situ poling during 3D-printing. The RhB degradation experiments, however, provided rather intriguing results for several reasons. On one hand, RhB 'degradation' seemed to increase compared to that of experiments conducted in absence of a catalyst (MA + US) and presence of $BaTiO_3$ in the very early stages of the experiments. However, at the very end, RhB 'degradation' in presence of the additive manufactured PVDF-$BaTiO_3$ composites was very similar to that of experiments conducted in absence of a catalyst (MA + US), and noticeably lower than that of experiments in the presence of the $BaTiO_3$ piezocatalysts. It is true that the concentration of catalyst used (1 g L^{-1}) remained the same; in practical terms, this means that less $BaTiO_3$ was effectively being used in the experiments in presence of the PVDF-$BaTiO_3$ composites, as the amount of $BaTiO_3$ in the composites was 50%. In addition, as the $BaTiO_3$ particles in the composites were embedded into the PVDF support, their vibration could be restrained, which would limit their piezoelectric behaviour under ultrasound. On the other hand, $BaTiO_3$ piezocatalysts on their own would vibrate freely under ultrasound, which would lead to a higher piezocatalytic effect. Surprisingly, poling did not have any significant effect on the results obtained with the composites (nearly identical results were obtained with both P and UP PVDF-$BaTiO_3$); it could be expected that, even if restrained, the $BaTiO_3$ in the composites would have benefited from the vibration of the PVDF in the case of P PVDF-$BaTiO_3$. However, it did not happen. This, along with the fact that the experimental data obtained with the additive manufactured PVDF-$BaTiO_3$ composites was diverging from first-order RhB degradation kinetics (Fig. 4b), suggested the occurrence of different physico-chemical phenomena in the presence of the PVDF-$BaTiO_3$ composites instead of piezocatalysis.

To shed more light onto these different physico-chemical phenomena occurring in presence of the PVDF-$BaTiO_3$ composites, additional experiments using additive manufactured PVDF slabs ($_{AM}$PVDF) and as-supplied PVDF powder ($_{P}$PVDF) were conducted; worth noting at this point that both $_{AM}$PVDF and $_{P}$PVDF were unpoled (i.e. non-piezoelectric). In the first 60 min, $_{AM}$PVDF apparently achieved an even higher RhB 'degradation' compared to that of $BaTiO_3$ piezocatalysts. However, the 'degradation' of RhB seemed to significantly slow down in the second half of the experiments, resulting in an even greater deviation from first-order RhB degradation kinetics (Fig. 4b); even then, high RhB 'degradation' was observed after two hours (DE = 90%). Very similar RhB 'degradation' was observed in presence of $_{P}$PVDF at the end of the two-hour experiments; however, the rate achieved throughout the first half in presence of $_{P}$PVDF was clearly lower than that in presence of $_{AM}$PVDF. Moreover, contrary to every other piezocatalyst evaluated by the authors in the present work and previous studies (i.e. $BaTiO_3$, ZnO and BF-KBT-PT) [23,25,26], around 4% of the RhB seemed to be adsorbed onto the $_{AM}$PVDF slabs during the 30-minute period set to achieve adsorption–desorption equilibrium prior to turning the ultrasonic system on. Overall, these results further indicated that, rather than the piezoelectric $BaTiO_3$ particles, PVDF was the material behind the 'degradation' of RhB in the PVDF-$BaTiO_3$ composite coatings. Moreover, piezoelectricity had not influence on this; rather than piezocatalysis, the enhancement in the 'degradation' of RhB observed in the presence of all the PVDF-based materials used in this study would be caused by adsorption. Therefore, from now on, rather than 'degradation' another term such as 'removal' would be better suited to cover both the sonochemical degradation of RhB and its adsorption on PVDF.

To confirm that adsorption was the physico-chemical phenomenon behind the enhancement of the removal of RhB compared to its sonochemical degradation in absence of any particles, additional research was conducted aiming at desorbing some of the adsorbed RhB from any of the PVDF materials (Fig. 5). As $_{AM}$PVDF was the material that would have adsorbed the most of RhB in the previous experiments, 1 g of $_{AM}$PVDF slabs were left in 1 L of deionised water for a single week to observe any desorption without noticing any significant signs of RhB being desorbed. However, a change in pH caused by adding enough

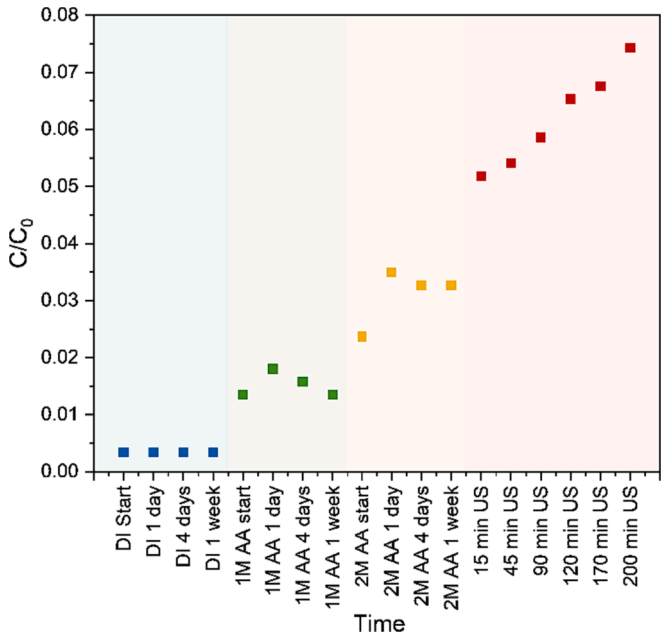

Fig. 5. Desorption of RhB from 1 g of $_{AM}$PVDF initially immersed in 1 L of deionised (DI) water. After one week, acetic acid (AA) was added to make up an AA 1 M solution. After another week, more AA was added to make up an AA 2 M solution. Ultrasound (US) was then applied three weeks after the experiment started.

acetic acid (AA) to bring the concentration of the solution up to 1 M AA resulted in a noticeable amount of RhB being desorbed, although this amount was rather small even after another week. Further addition of AA to bring the concentration up to 2 M AA resulted in roughly doubling the amount of RhB desorbed after an additional week; nevertheless, the total amount of RhB desorbed was still low, and the desorption process was still rather slow. This situation completely changed when that same 2 M AA solution containing the $_{AM}$PVDF slabs with adsorbed RhB was immersed in the same ultrasonic bath used in the previous experiments. Under sonication, a clear increase in the amount of RhB desorbed was rapidly observed; the desorbed amount of RhB continued to increase while the solution was being sonicated. These results confirmed that adsorption was indeed taking place; moreover, the fact that RhB desorption was significantly accelerated once the solution was sonicated also confirmed that adsorption was somehow influenced by ultrasound.

3.3. Sono-adsorption of RhB on additive manufactured PVDF

To better understand the adsorption of RhB on $_{AM}$PVDF and how ultrasound may enhance the process, additional experiments with different concentrations of $_{AM}$PVDF were conducted under mechanical agitation (MA) with and without ultrasound (US). Prior to that, though, it is worth understanding why the $_{AM}$PVDF slabs seemed to remove more RhB than $_{P}$PVDF in the experiments displayed in Fig. 4, even though the same amount of adsorbent (1 g L^{-1}) was used in both cases. On one hand, $_{P}$PVDF (Fig. 6a) appeared to be hydrophobic, as it formed large agglomerates over the surface of the RhB solution during the experiments (Fig. 6b). Aggregated PVDF nanoparticles in $_{P}$PVDF had already been observed by FIB-SEM (Fig. 2e); one would have expected that combined ultrasound and mechanical agitation would have contributed to disaggregating these PVDF nanoparticles [54], but agglomeration was even more pronounced during the experiments due to their hydrophobic nature. This meant that not all of the $_{P}$PVDF could be effectively used in the removal of RhB (Fig. 6c). On the other hand, $_{AM}$PVDF (Fig. 6d) seemed more hydrophilic (Fig. 6e), making them easier to wet and adsorb RhB during the experiments (Fig. 6f). Nitrogen adsorption/desorption isotherms provided another reason for the enhanced removal of RhB with $_{AM}$PVDF (Fig. 5g). For both $_{AM}$PVDF and $_{P}$PVDF, type II isotherms with type H3 hysteresis loops were obtained, as one would expect from nonporous ($_{P}$PVDF) or macroporous ($_{AM}$PVDF) adsorbents [55]; however, the macroporous nature of $_{AM}$PVDF (Fig. 6i) resulted in a significantly higher specific surface area (SSA values estimated by the multi-point BET method were 24.21 m^2 g^{-1} and 66.57 m^2 g^{-1} for $_{P}$PVDF and $_{AM}$PVDF, respectively). Moreover, despite their macroporous nature, $_{AM}$PVDF slabs also presented a greater volume of mesopores (Fig. 6h), which would further contribute to the superior adsorption performance of $_{AM}$PVDF compared to $_{P}$PVDF.

The hydrophilic nature, significantly higher SSA and greater volume of mesopores of $_{AM}$PVDF are intrinsically linked to the additive manufacturing – direct ink writing process devised to fabricate them. The solvent used, TEP, enabled a partial dissolution of the PVDF powder that, once the 3D-printing was carried out and TEP fully evaporated, resulted in the highly porous network observed in $_{AM}$PVDF (Fig. 2d, centre and 6i), but also in both P and UP PVDF-$BaTiO_3$ composites (Fig. 2b and c, centre), leading to a higher SSA and greater volume of mesopores. The size and shape achieved by direct ink writing also contributed to a more practical but long-term important outcome: the recovery after wastewater treatment. $_{AM}$PVDF slabs (and both P and UP PVDF-$BaTiO_3$ composites) were extremely easy to recover from the RhB solution after the experiments with a sieve or simply by hand. $_{P}$PVDF, on the other hand, required vacuum filtration to be fully recovered from the treated solution.

The results from experiments with different concentrations of $_{AM}$PVDF conducted under mechanical agitation (MA) with and without ultrasound (US) are displayed in Fig. 7. In absence of ultrasound, around 13% of the RhB was absorbed in the presence of 1 g L^{-1} of $_{AM}$PVDF (MA $_{AM}$PVDF 1 g) at the end of the experiments. This already confirmed the importance of ultrasound in enhancing the adsorption of RhB on $_{AM}$PVDF previously reported (MA + US $_{AM}$PVDF 1 g). Moreover, increasing the concentration of $_{AM}$PVDF resulted in significantly faster removal of RhB; whilst 1 g L^{-1} of $_{AM}$PVDF under ultrasound resulted in the removal of 27% of RhB within 10 min of sonication (MA + US $_{AM}$PVDF 1 g), 46% and 80% of RhB was removed within the same period in presence of 2 g L^{-1} (MA + US $_{AM}$PVDF 2 g) and 4 g L^{-1} (MA + US $_{AM}$PVDF 4 g) of $_{AM}$PVDF, respectively. In fact, virtually all the RhB was removed from the solution after 40 min of sonication when using 4 g L^{-1} of $_{AM}$PVDF (MA + US $_{AM}$PVDF 4 g). It must be noted, to be consistent with all the experiments conducted for the present study and previous work by the authors [23,25,26], the 30-minute period allowing adsorption–desorption equilibrium to be reached before sonication started was kept in all experiments included in Fig. 7, even though 30 min would not be enough to reach such equilibrium as RhB adsorption on $_{AM}$PVDF was clearly occurring. Nevertheless, this approach actually helped to better demonstrate the critical effect of ultrasound on the adsorption of RhB on $_{AM}$PVDF, as illustrated by the significant drop in the concentration of RhB observed right after sonication started in all cases (MA + US $_{AM}$PVDF 1 g, 2 g and 4 g).

3.4. Sono-adsorption and adsorption-assisted sonochemical degradation: A mechanistic model

To better understand the results shown in Fig. 7, a mechanistic model was developed for the adsorption experiments conducted in presence of $_{AM}$PVDF under ultrasound. The aim was to capture the main transport phenomena occurring in the system while making a series of feasible assumptions to arrive at a model with the least number of adjustable parameters. The model was derived from basic principles of chemical engineering: a mass balance in a batch reactor accounting for adsorption and sonochemical degradation where diffusion in the pores of the particles is the main mass transport mechanism based on the physicochemical phenomena occurring in the process.

As mechanical effects of acoustic cavitation generated by ultrasound

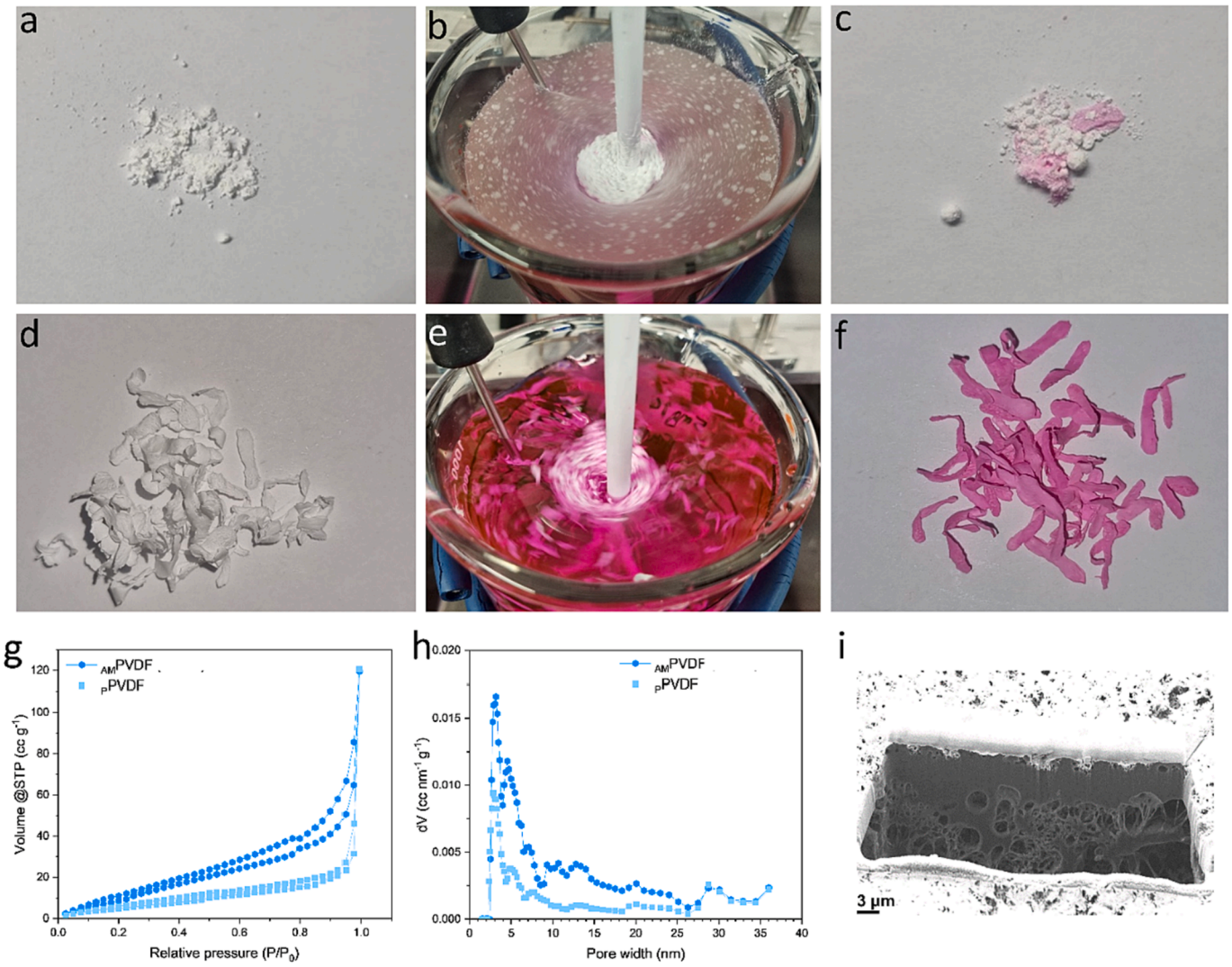

Fig. 6. a) $_{P}$PVDF before use, b) $_{P}$PVDF during RhB removal experiments, c) recovered $_{P}$PVDF after RhB removal experiments, d) $_{AM}$PVDF before use, e) $_{AM}$PVDF during RhB removal experiments, f) recovered after RhB removal experiments, g) Nitrogen sorption isotherms at −196.15 °C, h) pore size distribution of powder and additive manufactured PVDF, i) FIB-SEM cross-section of $_{AM}$PVDF.

such as the asymmetrical collapse of bubbles at the surface of solids [26] are likely to disrupt any film boundary layer on the external surface of the particles, it is reasonable to assume that mass transport is controlled by diffusion in the pores of the particles. The shape of the particles (Fig. 6d and f) has a high aspect ratio, thus a 1-D slab geometry was assumed. It is possible to define the concentration in the particles as

$$Q = \varepsilon_P C_P + (1-\varepsilon_P) q \tag{3}$$

where C_P is the fluid concentration in the pores; q is the adsorbed phase concentration; and ε_P is the porosity, which was estimated to be 0.75 based on the density of PVDF and that of the $_{AM}$PVDF slabs (approximately 400 kg m^{-3}).

Assuming that adsorption is fast at the pore level, it is possible to introduce the Henry law constant $H = q/C_P$, and obtain the mass balance equation inside the particles given by [56]

$$\frac{\partial Q}{\partial t} - \frac{\varepsilon_P}{\tau}\frac{D_m}{\varepsilon_P + (1-\varepsilon_P)H}\frac{\partial^2 Q}{\partial x^2} + R_{USP} = 0 \tag{4}$$

where τ is the tortuosity, which is calculated as the inverse of the porosity; D_m is the molecular diffusivity of RhB (4.2×10^{-10} m^2/s) [57]; and R_{USP} represents the degradation kinetics occurring within the particles resulting from the presence of ultrasounds. This term could, for example, be due to radicals generated in the bulk fluid diffusing inside the particles and reacting with RhB.

The assumption of a linear isotherm is in part justified by the fact that most of the experimental results lie at relatively low concentrations of RhB as a result of its combined sonochemical degradation and adsorption onto $_{AM}$PVDF. This is only a rough approximation at higher concentrations, for example in the case of adsorption in absence of ultrasound.

Equation (3) is coupled to the boundary condition at the centre of the particle:

$$\left(\frac{\partial Q}{\partial x}\right)_{x=0} = 0 \tag{5}$$

which can be seen either as a condition of symmetry or zero flux at the centre.

At the surface of the particles, equilibrium is assumed as no external film resistance is present:

$$(Q)_{x=l_P} = [\varepsilon_P + (1-\varepsilon_P)H]C \tag{6}$$

where C is the measured concentration in the bulk fluid and l_P is the half-thickness of the particles.

To close the problem, the mass balance in the cell is given by

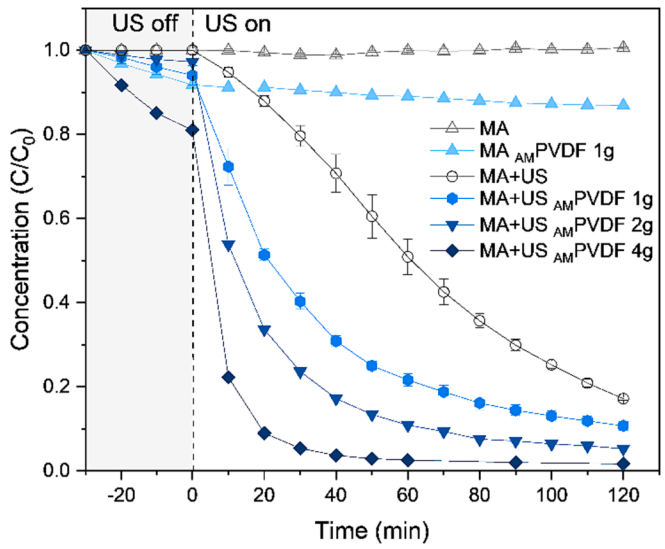

Fig. 7. Evolution of C_0/C vs reaction time in RhB removal experiments under combined ultrasound and mechanical agitation in absence/presence of $_{AM}$PVDF at different concentrations.

$$V_L\frac{dC}{dt}+\frac{V_S}{l_P}\frac{\varepsilon_P}{\tau}\frac{D_m}{\varepsilon_P+(1-\varepsilon_P)H}\left(\frac{\partial Q}{\partial x}\right)_{x=l_P}+V_L R_{US}=0 \quad (7)$$

where V_L is the volume of the liquid (i.e. water), V_S is the volume of the adsorbent (i.e. $_{AM}$PVDF), and R_{US} is the degradation rate of RhB per unit volume in the bulk liquid in the presence of ultrasound. This term was set to be equal to the degradation rate measured in the absence of any particles and assuming the apparent first-order degradation kinetics (equation (1))

$$R_{US}=k_{US}C \quad (8)$$

where $k_{US}=2.1\times10^{-4}\ s^{-1}$ (experiments labelled as MA + US in Figs. 4 and 7).

The model equations were implemented in gPROMS, where the initial concentration was used for each experiment, and only the data obtained under the presence of ultrasound were used. The simulations were used to regress the Henry law constant, H, either assuming that there is no degradation occurring inside the particles, i.e. $R_{USP}=0$, or assuming that $R_{USP}=k_{US}Q$, i.e. that the same kinetic constant applies in the solid particles, but the concentration is that of RhB in the particles. This would be consistent, for example, with RhB degradation by radicalary reactions occurring in large excess of radicals.

Fig. 8a displays the concentration of RhB calculated from the model with $R_{USP}=0$ and $H=50113$. It is clear that the model without any internal degradation reaction severely underestimated the removal capability of $_{AM}$PVDF under ultrasound.

Fig. 8b displays the concentration of RhB predicted by the model with $R_{USP}=k_{US}Q$ and $H=1655$. For comparison purposes, the experimental data obtained with ultrasound in the absence of any particles (MA + US) and with 1 g L^{-1} of PVDF in absence of ultrasound (MA $_{AM}$PVDF 1 g), along with the predicted concentrations in both cases. In the case of MA + US, the curve shown is that obtained using the first-order degradation reaction kinetics with $k_{US}=2.1\times10^{-4}\ s^{-1}$. In the case of MA $_{AM}$PVDF 1 g, the calculated concentration was obtained assuming that adsorption would indeed occur but there would be an external film resistance present, this requires only a change the boundary condition (Eq (4)). Here a value of a film coefficient of 0.9×10^{-6} m s^{-1} was used. This estimated external film resistance is in fact of the same order of magnitude as 3×10^{-6} m s^{-1}, predicted using a Sherwood number of 2 (theoretical value for a sphere in a stagnant fluid) and an equivalent spherical particle with the same surface-to-volume

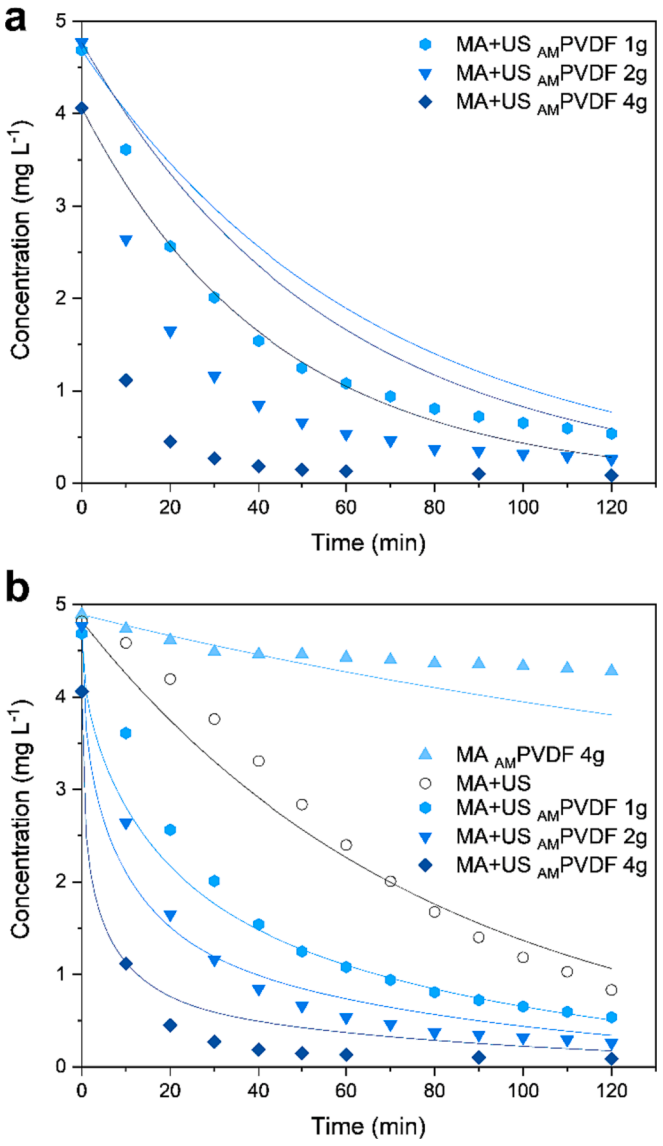

Fig. 8. (a) RhB removal experiments with ultrasound in the presence of $_{AM}$PVDF at different concentrations. Continuous lines depict the predicted concentration of RhB calculated using ultrasound-assisted adsorption combined with sonochemical first-order RhB degradation kinetics (equations (3), 4, 6 and 7). (b) RhB removal experiments with and without ultrasound in the presence/absence of $_{AM}$PVDF at different concentrations. Continuous lines depict the predicted concentration of RhB calculated using sonochemical first-order RhB degradation kinetics (MA + US), ultrasound-assisted adsorption combined with adsorption-enhanced sonochemical first-order RhB degradation kinetics (equations (3), 4, 7 and 8) (MA + US $_{AM}$PVDF 1 g, 2 g and 4 g) and adsorption kinetics with film resistance (MA $_{AM}$PVDF 1 g).

ratio. The deviations in this case could be caused by the likely nonlinearity of the system in absence of ultrasound due to the higher concentrations of RhB and the fact that the geometry is far from that of a sphere. Given the low density of the $_{AM}$PVDF slabs, mechanical agitation was likely to have resulted in their complete fluidization, which is why the film resistance should not be too far from that in a stagnant film.

The experimental data and the predicted concentration of RhB with the model shown in Fig. 8b illustrate the soundness of the physical mechanisms proposed following the nature of the experiments, with and without ultrasound. In the case of the ultrasound-assisted adsorption experiments (MA + US $_{AM}$PVDF 1 g, 2 g and 4 g), it is clear the presence of the adsorbent particles further enhanced the sonochemical degradation of RhB (MA + US) by locally increasing the concentration of RhB

within and in the surroundings of the $_{AM}$PVDF slabs (for an *H* value of 1655, the concentration of RhB in the adsorbed phase would be 400 times greater than the concentration in the bulk of the liquid). This should not entirely be a surprise; taking into account the first-order kinetics nature of the sonochemical degradation of RhB, it would be safe to assume that, if sonochemical degradation was occurring in the vicinity of the surface of $_{AM}$PVDF or inside its pores, it would benefit from the extremely high concentration in the adsorbed phase. Moreover, there are several studies in the literature demonstrating a synergistic relationship between sonochemical and adsorption processes [58,59], indicating that further enhancing the sonochemical degradation of RhB by adsorption on $_{AM}$PVDF would be possible. It must be mentioned that some deviations were noticed, especially at short times, which most likely be caused by the existence of a residual film resistance and nonlinear equilibrium. Nevertheless, the fact all the curves can be matched reasonably well using a single parameter supports the conclusion that the structure of the model represents the main physical processes at play. Therefore, the addition of the $_{AM}$PVDF slabs to the sonicated solutions not only results in sono-adsorption of RhB onto $_{AM}$PVDF, but also in its adsorption-enhanced sonochemical degradation, leading to the complete removal of RhB in less than one hour (>95% removal after 40 min of treatment under ultrasound).

3.5. Sono-adsorption, ultrasound-assisted sonochemistry or piezocatalysis?

During the present study, the journey that started with the aim to build on $BaTiO_3$ piezocatalysts to fabricate PVDF-$BaTiO_3$ composite piezocatalysts by additive manufacturing with in-situ poling ended with the observation of sono-adsorption and adsorption-enhanced sonochemical degradation in presence of additive manufactured PVDF slabs that led to the removal of >95% of RhB in 1 L of solution within 40 min of treatment under ultrasound. Surprisingly enough, the observation of sono-adsorption in piezocatalysis research has been routinely overlooked or dismissed as a physical phenomenon that could be relevant to piezocatalysis, even in those cases where one could see adsorption occurring before sonication started [40,60–63]. Some of the studies where adsorption of dyes can be clearly noticed involved PVDF-based materials [38,64,65]. In this regard, whilst allocating 30 min to reach adsorption–desorption equilibrium or saturation prior to piezocatalytic experiments may be enough for $BaTiO_3$ (e.g. this study) or BF-KBT-PT [25], it could lead to incorrect assumptions in the case of PVDF-based piezocatalysts, as demonstrated by the present research with $_{AM}$PVDF (Fig. 8).

One of the reasons why ultrasound-assisted adsorption may have been overlooked by the piezocatalysis research community is the generalised unawareness of other ultrasound-related phenomena such as sonochemistry or sonocatalysis that may occur concurrently with piezocatalytic processes [11,23,25–27,66,67]. In this regard, ultrasound-assisted adsorption and desorption has been known for a while; some early work on this topic were published over two decades ago [68,69]. However, the effect of ultrasound on adsorption processes did not receive much attention until recent years, where the number of publications on sono-adsorption for environmental remediation applications has flourished [42,43,70–78]. In all of these studies, though, experimental sono-adsorption data was routinely fitted to empirical models such as pseudo-first order adsorption kinetics, pseudo-second order adsorption kinetics, Elovich chemisorption kinetics and intra-particle diffusion that may lead to the incorrect interpretation of the mass transport mechanisms behind the overall adsorption process [56]. Moreover, the only study to date that has treated with certain rigour adsorption occurring concurrently with piezocatalysis also used these empirical approaches to characterise it [65]. The present study demonstrates that a different approach is both necessary and possible to model sono-adsorption processes by developing and implementing, to the best of the author's knowledge, the very first mechanistic model accounting for the most meaningful physico-chemical phenomena within the system. In fact, the synergistic relation between ultrasound and adsorption, and how adsorption would also enhance the sonochemical degradation of RhB, would have been completely overlooked if only empirical approaches had been followed to evaluate the experiments.

To finalise this discussion, it is perhaps worth providing additional food for thought to the research community interested in further developing the field of piezocatalysis, especially if ultrasound is used as the means to 'excite' piezocatalysts. In a previous study, the authors already demonstrated that, by tuning frequency and power, sonochemical degradation on its own could deliver RhB degradation rates outstandingly higher than those reported in most of the piezocatalytic studies published at the time [26]. In the work here presented, the use of easy-to-manufacture and easy-to-recover $_{AM}$PVDF adsorbents instead of complex piezocatalysts (complex in terms of material design, fabrication methods and recovery approaches) led to a removal of >90% and >95% of RhB after 20 and 40 min, respectively, under ultrasound. This RhB removal efficiency is superior to that reported in most of the research dealing with piezocatalytical degradation of RhB to date (Table 1). Moreover, the very few studies that have reported higher RhB removal in shorter times indeed used PVDF as one of the materials of the piezocatalysts, meaning that sono-adsorption of RhB on PVDF may have been very likely to occur and influence the overall degradation/removal process to some extent.

4. Conclusion

What started as a journey to fabricate highly piezoelectric 'bulky' PVDF-$BaTiO_3$ piezocatalysts that were both easy to manufacture and easy to recover ended with different physico-chemical phenomena, sono-adsorption and adsorption-enhanced sonochemistry, which led to a complete removal of RhB present in water in less than one hour of treatment under ultrasound.

Whereas the customised additive manufacturing – direct ink writing method developed as part of this study allowed for the production of piezoelectric PVDF-$BaTiO_3$ composite slabs due to its *in-situ* poling capabilities, the resulting particles were less successful than $BaTiO_3$ on its own in removing RhB after two hours of treatment under ultrasound (82% RhB removal after 2 h when using either poled or unpoled PVDF-$BaTiO_3$ composite slabs compared to 92% RhB removal after 2 h in presence of $BaTiO_3$ piezocatalysts). However, the same 3D-printing method (with no need for *in-situ* poling) delivered PVDF slabs with suitable internal structure and wettability, as well as higher specific surface ratio and volume of mesopores, which performed successfully as an adsorbent for the adsorption of RhB. The adsorption of RhB on additive manufactured PVDF was outstandingly enhanced by the presence of ultrasound, to the point that >95% of RhB in water was removed within 40 min of ultrasound treatment when using 4 g L^{-1} of additive manufactured PVDF. The reasons for this enhancement would be the minimisation of the film resistance at the surface of the adsorbent, with diffusion inside particles becoming the main mass transport mechanism, as well as the adsorption-enhanced sonochemical degradation of RhB, as suggested by the very first mechanistic model for liquid phase adsorption processes under ultrasound proposed in this work.

The results indicate that sono-adsorption may be likely to occur concurrently in piezocatalysis processes, especially in the case of PVDF-based materials. Moreover, it demonstrates the potential of sono-adsorption on its own (or in combination to 'classical' sonochemical degradation) to achieve outstanding removal of pollutants in water at faster rates than those obtained with piezocatalysis. This opens new doors to optimise phenomena such as sonochemistry and sono-adsorption that may occur concurrently along with piezocatalysis to further develop this field.

Table 1
Comparison of RhB removal efficiencies of $_{AM}$PVDF and other reported piezocatalysts containing PVDF.

Material	Setup	Frequency [kHz]	Acoustic power (Electric input power)	Removal efficiency [%]	Removal time [min]	Other information (concentration, geometry, etc.)	Ref
$_{AM}$PVDF	MA + US	32–38	14.3 ± 0.7 (200 W)	>90 >95	20 40	4 g L^{-1}	this study
$Bi_{0.5}Na_{0.5}$ TiO_3/PVDF	US	45	– (200 W)	76.6	180	1 g L^{-1}	[79]
PVDF–$BaTiO_3$	US	–	– (180 W)	~85	80	2.5 cm × 2.5 cm × 2 mm foam	[38]
PVDF/$ZnSnO_3$	US	33 ± 3	– (120 W)	>95	20	No information	[80]
MOFs/Bi_2WO_6–PVDF membranes	US	–	– (180 W)	87	80	1 g L^{-1} (powder), 2 × 2 cm membrane	[65]
MoS_2-PVDF films	US	–	– (100 W)	90	20	2 cm × 2 cm × 50 μm	[81]
Ag@$LiNbO_3$/ PVDF Composite Film	US	40	– (70)	~80	120	Circular films with a diameter of 2.5 cm	[39]
MWCNT-kaolinite-PVDF membrane	US	30 ± 5	– (50 W)	96	45	1 cm × 1 cm membrane	[82]
t-$BaTiO_3$ / Ag / β-PVDF	US	40	– (120 W)	~70	120	No information	[64]

CRediT authorship contribution statement

Franziska Bößl: Conceptualization, Methodology, Validation, Formal analysis, Investigation, Data curation, Writing – original draft, Visualization. **Stefano Brandani:** Software, Formal analysis, Writing – review & editing. **Valentin C. Menzel:** Methodology, Investigation. **Matilda Rhodes:** Investigation, Writing – review & editing. **Mayra S. Tovar-Oliva:** Investigation. **Caroline Kirk:** Investigation, Resources, Writing – review & editing. **Ignacio Tudela:** Conceptualization, Methodology, Resources, Writing – review & editing, Supervision, Project administration, Funding acquisition.

Declaration of Competing Interest

The authors declare that they have no known competing financial interests or personal relationships that could have appeared to influence the work reported in this paper.

Data availability

Data will be made available on request.

Acknowledgements

FB and IT acknowledge the University of Edinburgh for funding this research through its Start Up fund. VCM and IT thank the Engineering and Physical Sciences Research Council (EPSRC) in UK for its support through a PhD studentship (grant EP/R513209/1, project reference 2275546). IT would also like to thank the Carnegie Trust for the Universities of Scotland for its support through the Research Incentive Grant scheme (RIG009799). FB and IT would also like to thank Jamie Graham for his support on building the additive manufacturing setup with *in-situ* poling, and Ross E. Mathieson for his suggestions on keeping the high-voltage elements of the setup safe. The authors acknowledge the use of the Zeiss Crossbeam Cryo FIB/SEM acquired with EPSRC grant EP/P030564/1 and Fraser Laidlaw for help with image acquisition.

References

[1] W. Chen, Q. Zheng, Y.A. Lv, Y. Chen, Q. Fan, X. Zhou, H. Li, Q. Yu, H. Liu, Piezoelectric energy harvesting and dissipating behaviors of polymer-based piezoelectric composites for nanogenerators and dampers, Chem. Eng. J. 465 (2023) 142755, https://doi.org/10.1016/j.cej.2023.142755.
[2] S.D. Mahapatra, P.C. Mohapatra, A.I. Aria, G. Christie, Y.K. Mishra, S. Hofmann, V. K. Thakur, Piezoelectric Materials for Energy Harvesting and Sensing Applications: Roadmap for Future Smart Materials, Adv. Sci. 8 (2021), e2100864, https://doi.org/10.1002/advs.202100864.
[3] N. Sezer, M. Koç, A comprehensive review on the state-of-the-art of piezoelectric energy harvesting, Nano Energy 80 (2021) 105567, https://doi.org/10.1016/j.nanoen.2020.105567.
[4] M. Venkatesan, W.-C. Chen, C.-J. Cho, L. Veeramuthu, L.-G. Chen, K.-Y. Li, M.-L. Tsai, Y.-C. Lai, W.-Y. Lee, W.-C. Chen, C.-C. Kuo, Enhanced piezoelectric and photocatalytic performance of flexible energy harvester based on $CsZn_{0.75}Pb_{0.25}I_3$/CNC–PVDF composite nanofibers, Chem. Eng. J. 433 (2022) 133620, doi:10.1016/j.cej.2021.133620.
[5] Z. Liu, Y. Zheng, S. Zhang, J. Fu, Y. Li, Y. Zhang, W. Ye, (1–x) $Bi_{0.5}Na_{0.5}TiO_3$–x$BiFeO_3$ solid solutions with enhanced piezocatalytic dye degradation, Sep. Purif. Technol. 290 (2022) 120831, https://doi.org/10.1016/j.seppur.2022.120831.
[6] J. Wang, Y. Liang, Z. Wang, B. Huo, C. Liu, X. Chen, H. Xu, D. Li, Z. Zhu, Y. Wang, F. Meng, High efficiently degradation of organic pollutants via low-speed water flow activation of Cu_2O@MoS_2/PVDF modified pipeline with piezocatalysis performance, Chem. Eng. J. 458 (2023) 141409, https://doi.org/10.1016/j.cej.2023.141409.
[7] Y. Zheng, X. Wu, Y. Zhang, Y. Li, W. Shao, J. Fu, Q. Lin, J. Tan, S. Gao, W. Ye, H. Huang, Highly efficient harvesting of vibration energy for complex wastewater purification using $Bi_5Ti_3FeO_{15}$ with controlled oxygen vacancies, Chem. Eng. J. 453 (2023) 139919, https://doi.org/10.1016/j.cej.2022.139919.
[8] J. Dai, N. Shao, S. Zhang, Z. Zhao, Y. Long, S. Zhao, S. Li, C. Zhao, Z. Zhang, W. Liu, Enhanced Piezocatalytic Activity of $Sr_{0.5}Ba_{0.5}Nb_2O_6$ Nanostructures by Engineering Surface Oxygen Vacancies and Self-Generated Heterojunctions, ACS Appl. Mater. Interfaces 13 (2021) 7259–7267, https://doi.org/10.1021/acsami.0c21202.
[9] W. Feng, J. Yuan, L. Zhang, W. Hu, Z. Wu, X. Wang, X. Huang, P. Liu, S. Zhang, Atomically thin ZnS nanosheets: Facile synthesis and superior piezocatalytic H_2 production from pure H_2O, Appl. Catal. B (2020), 119250, https://doi.org/10.1016/j.apcatb.2020.119250.
[10] Y. Ma, B. Wang, Y. Zhong, Z. Gao, H. Song, Y. Zeng, X. Wang, F. Huang, M.-R. Li, M. Wang, Bifunctional $RbBiNb_2O_7$/poly(tetrafluoroethylene) for high-efficiency piezocatalytic hydrogen and hydrogen peroxide production from pure water, Chem. Eng. J. 446 (2022), https://doi.org/10.1016/j.cej.2022.136958.
[11] P.T.T. Phuong, D.-V.-N. Vo, N.P.H. Duy, H. Pearce, Z.M. Tsikriteas, E. Roake, C. Bowen, H. Khanbareh, Piezoelectric catalysis for efficient reduction of CO_2 using lead-free ferroelectric particulates, Nano Energy 95 (2022) 107032, https://doi.org/10.1016/j.nanoen.2022.107032.
[12] Z. Ren, F. Chen, Q. Zhao, G. Zhao, H. Li, W. Sun, H. Huang, T. Ma, Efficient CO_2 reduction to reveal the piezocatalytic mechanism: From displacement current to active sites, Appl. Catal. B 320 (2023) 122007, https://doi.org/10.1016/j.apcatb.2022.122007.
[13] Y. Zhang, P.T. Thuy Phuong, N.P. Hoang Duy, E. Roake, H. Khanbareh, M. Hopkins, X. Zhou, D. Zhang, K. Zhou, C. Bowen, Polarisation tuneable piezocatalytic activity of Nb-doped PZT with low Curie temperature for efficient CO_2 reduction and H_2 generation, Nanoscale Adv. 3 (2021) 1362–1374, https://doi.org/10.1039/D1NA00013F.
[14] Q. Tang, J. Wu, D. Kim, C. Franco, A. Terzopoulou, A. Veciana, J. Puigmartí-Luis, X.Z. Chen, B.J. Nelson, S. Pané, Enhanced Piezocatalytic Performance of BaTiO3 Nanosheets with Highly Exposed 001 Facets, Adv. Funct. Mater. 32 (2022) 2202180, https://doi.org/10.1002/adfm.202202180.
[15] Y. Wang, Q. Tang, R. Wu, S. Sun, J. Zhang, J. Chen, M. Gong, C. Chen, X. Liang, Ultrasound-triggered piezocatalysis for selectively controlled NO gas and chemodrug release to enhance drug penetration in pancreatic cancer ACS, Nano 17 (4) (2023) 3557–3573, https://doi.org/10.1021/acsnano.2c09948.

[16] J. Wu, N. Qin, D. Bao, Effective enhancement of piezocatalytic activity of $BaTiO_3$ nanowires under ultrasonic vibration, Nano Energy 45 (2018) 44–51, https://doi.org/10.1016/j.nanoen.2017.12.034.

[17] K.-S. Hong, H. Xu, H. Konishi, X. Li, Direct water splitting through vibrating piezoelectric microfibers in water, J. Phys. Chem. Lett. 1 (2010) 997–1002, https://doi.org/10.1021/jz100027t.

[18] N. Liu, R. Wang, S. Gao, R. Zhang, F. Fan, Y. Ma, X. Luo, D. Ding, W. Wu, High-Performance Piezo-Electrocatalytic Sensing of Ascorbic Acid with Nanostructured Wurtzite Zinc Oxide, Adv. Mater. 33 (2021), e2105697, https://doi.org/10.1002/adma.202105697.

[19] X. Xiong, Y. Wang, J. Ma, Y. He, J. Huang, Y. Feng, C. Ban, L.-Y. Gan, X. Zhou, Oxygen vacancy engineering of zinc oxide for boosting piezo-electrocatalytic hydrogen evolution, Appl. Surf. Sci. 616 (2023) 156556, https://doi.org/10.1016/j.apsusc.2023.156556.

[20] D. Liu, X. Sun, L. Tan, J. Zhang, C.-C. Jin, F. Wang, High-performance piezocatalytic hydrogen evolution by $Bi_{0.5}Na_{0.5}TiO_3$ cubes decorated with cocatalysts, Ceram. Int. 49 (12) (2023) 20343–20350, https://doi.org/10.1016/j.ceramint.2023.03.158.

[21] C. Su, C. Li, R. Li, W. Wang, Insights into highly efficient piezocatalytic molecule oxygen activation over $Bi_2Fe_4O_9$: Active sites and mechanism, Chem. Eng. J. 452 (2023) 139300, https://doi.org/10.1016/j.cej.2022.139300.

[22] C. Wang, C. Hu, F. Chen, H. Li, Y. Zhang, T. Ma, H. Huang, Polar Layered Bismuth-Rich Oxyhalide Piezoelectrics $Bi_4O_5X_2$ (X=Br, I): Efficient Piezocatalytic Pure Water Splitting and Interlayer Anion-Dependent Activity, Adv. Funct. Mater. 33 (2023) 2301144, https://doi.org/10.1002/adfm.202301144.

[23] F. Bößl, V.C. Menzel, K. Jeronimo, A. Arora, Y. Zhang, T.P. Comyn, P. Cowin, C. Kirk, N. Robertson, I. Tudela, Importance of energy band theory and screening charge effect in piezo-electrocatalytical processes, Electrochim. Acta 462 (2023) 142730, https://doi.org/10.1016/j.electacta.2023.142730.

[24] K. Wang, C. Han, J. Li, J. Qiu, J. Sunarso, S. Liu, The mechanism of piezocatalysis: energy band theory or screening charge effect? Angew. Chem. 134 (2022), e202110429 https://doi.org/10.1002/ange.202110429.

[25] F. Bößl, T.P. Comyn, P.I. Cowin, F.R. García-García, I. Tudela, Piezocatalytic degradation of pollutants in water: Importance of catalyst size, poling and excitation mode, Chem. Eng. J. Adv. 7 (2021) 100133, https://doi.org/10.1016/j.ceja.2021.100133.

[26] F. Bößl, V.C. Menzel, E. Chatzisymeon, T.P. Comyn, P. Cowin, A.J. Cobley, I. Tudela, Effect of frequency and power on the piezocatalytic and sonochemical degradation of dyes in water, Chem. Eng. J. Adv. 14 (2023) 100477, https://doi.org/10.1016/j.ceja.2023.100477.

[27] F. Bößl, I. Tudela, Piezocatalysis: Can catalysts really dance?, Curr. Opin. Green Sustain. Chem. 32 (2021) 100537, doi:10.1016/j.cogsc.2021.100537.

[28] R. Al-Tohamy, S.S. Ali, F. Li, K.M. Okasha, Y.A. Mahmoud, T. Elsamahy, H. Jiao, Y. Fu, J. Sun, A critical review on the treatment of dye-containing wastewater: Ecotoxicological and health concerns of textile dyes and possible remediation approaches for environmental safety, Ecotoxicol. Environ. Saf. 231 (2022), 113160, https://doi.org/10.1016/j.ecoenv.2021.113160.

[29] D.A. Yaseen, M. Scholz, Textile dye wastewater characteristics and constituents of synthetic effluents: a critical review, Int. J. Environ. Sci. Technol. 16 (2018) 1193–1226, https://doi.org/10.1007/s13762-018-2130-z.

[30] M. Davarazar, M. Kamali, C. Venâncio, A. Gabriel, T.M. Aminabhavi, I. Lopes, Activation of persulfate using copper oxide nanoparticles for the degradation of Rhodamine B containing effluents: Degradation efficiency and ecotoxicological studies, Chem. Eng. J. 453 (2023) 139799, https://doi.org/10.1016/j.cej.2022.139799.

[31] A. Tkaczyk, K. Mitrowska, A. Posyniak, Synthetic organic dyes as contaminants of the aquatic environment and their implications for ecosystems: A review, Sci. Total Environ. 717 (2020), 137222, https://doi.org/10.1016/j.scitotenv.2020.137222.

[32] Y. Liu, M. Tourbin, S. Lachaize, P. Guiraud, Nanoparticles in wastewaters: Hazards, fate and remediation, Powder Technol. 255 (2014) 149–156, https://doi.org/10.1016/j.powtec.2013.08.025.

[33] V. Nogueira, I. Lopes, T. Rocha-Santos, F. Goncalves, R. Pereira, Toxicity of solid residues resulting from wastewater treatment with nanomaterials, Aquat. Toxicol. 165 (2015) 172–178, https://doi.org/10.1016/j.aquatox.2015.05.021.

[34] T.A. Saleh, Nanomaterials: Classification, properties, and environmental toxicities, Environ. Technol. Innov. 20 (2020) 101067, https://doi.org/10.1016/j.eti.2020.101067.

[35] C.M. Vineeth Kumar, V. Karthick, V.G. Kumar, D. Inbakandan, E.R. Rene, K.S.U. Suganya, A. Embrandiri, T.S. Dhas, M. Ravi, P. Sowmiya, The impact of engineered nanomaterials on the environment: Release mechanism, toxicity, transformation, and remediation, Environ. Res. 212 Part B (2022) 113202, doi:10.1016/j.envres.2022.113202.

[36] S.D. Aguilar, D.R. Ramos, J.A. Santaballa, M. Canle, Preparation, characterization and testing of a bulky non-supported photocatalyst for water pollution abatement, Catal. Today 413–415 (2023) 113992, https://doi.org/10.1016/j.cattod.2022.12.023.

[37] S. Mohammadpourfazeli, S. Arash, A. Ansari, S. Yang, K. Mallick, R. Bagherzadeh, Future prospects and recent developments of polyvinylidene fluoride (PVDF) piezoelectric polymer; fabrication methods, structure, and electro-mechanical properties, RSC Adv. 13 (2023) 370–387, https://doi.org/10.1039/d2ra06774a.

[38] J. Shi, W. Zeng, Z. Dai, L. Wang, Q. Wang, S. Lin, Y. Xiong, S. Yang, S. Shang, W. Chen, L. Zhao, X. Ding, X. Tao, Y. Chai, Piezocatalytic foam for highly efficient degradation of aqueous organics, Small Sci 1 (2021), 2000011, https://doi.org/10.1002/smsc.202000011.

[39] G. Singh, M. Sharma, R. Vaish, Flexible Ag@$LiNbO_3$/PVDF composite film for piezocatalytic dye/pharmaceutical degradation and bacterial disinfection, ACS Appl. Mater. Interfaces 13 (2021) 22914–22925, https://doi.org/10.1021/acsami.1c01314.

[40] W. Ma, B. Yao, W. Zhang, Y. He, Y. Yu, J. Niu, Fabrication of PVDF-based piezocatalytic active membrane with enhanced oxytetracycline degradation efficiency through embedding few-layer E-MoS_2 nanosheets, Chem. Eng. J. 415 (2021) 129000, https://doi.org/10.1016/j.cej.2021.129000.

[41] J.E. Marshall, A. Zhenova, S. Roberts, T. Petchey, P. Zhu, C.E.J. Dancer, C. R. McElroy, E. Kendrick, V. Goodship, On the solubility and stability of polyvinylidene fluoride, Polymers 13 (2021) 1354, https://doi.org/10.3390/polym13091354.

[42] W. Hamza, N. Fakhfakh, N. Dammak, H. Belhadjltaeif, M. Benzina, Sono-assisted adsorption of organic compounds contained in industrial solution on iron nanoparticles supported on clay: Optimization using central composite design, Ultrason. Sonochem. 67 (2020), 105134, https://doi.org/10.1016/j.ultsonch.2020.105134.

[43] S. Sivalingam, S. Sen, Sono-assisted Adsorption of As(V) from Water by Rice-Husk-Ash-Derived Iron-Modified Mesoporous Zeolite Y: A Cradle-to-Cradle Solution to a Problematic Solid Waste Material, Ind. Eng. Chem. Res. 58 (2019) 14073–14087, https://doi.org/10.1021/acs.iecr.9b01785.

[44] V.C. Menzel, X. Yi, F. Bößl, C. Kirk, N. Robertson, I. Tudela, Additive manufacturing of polyaniline electrodes for electrochemical applications, Addit. Manuf. 54 (2022) 102710, https://doi.org/10.1016/j.addma.2022.102710.

[45] R.F. Contamine, A.M. Wilhelm, J. Berlan, H. Delmas, Power measurement in sonochemistry, Ultrason. Sonochem. 2 (1995) S43–S47, https://doi.org/10.1016/1350-4177(94)00010-p.

[46] Y. Mao, S. Mao, Z.-G. Ye, Z. Xie, L. Zheng, Solvothermal synthesis and Curie temperature of monodispersed barium titanate nanoparticles, Mater. Chem. Phys. 124 (2010) 1232–1238, https://doi.org/10.1016/j.matchemphys.2010.08.063.

[47] J. Wu, Q. Xu, E. Lin, B. Yuan, N. Qin, S.K. Thatikonda, D. Bao, Insights into the Role of Ferroelectric Polarization in Piezocatalysis of Nanocrystalline $BaTiO_3$, ACS Appl. Mater. Interfaces 10 (2018) 17842–17849, https://doi.org/10.1021/acsami.8b01991.

[48] D.M. Esterly, B.J. Love, Phase transformation to β-poly(vinylidene fluoride) by milling, J. Polym. Sci. B 42 (2004) 91–97, https://doi.org/10.1002/polb.10613.

[49] R. Gregorio, M. Cestari, F.E. Bernardino, Dielectric behaviour of thin films of β-PVDF/PZT and β-PVDF/$BaTiO_3$ composites, J. Mater. Sci. 31 (1996) 2925–2930, https://doi.org/10.1007/bf00356003.

[50] J. González-García, V. Sáez, I. Tudela, M.I. Díez-Garcia, M. Deseada Esclapez, O. Louisnard, Sonochemical Treatment of Water Polluted by Chlorinated Organocompounds. A Review, Water 2 (2010) 28–74, https://doi.org/10.3390/w2010028.

[51] D. Liu, C. Jin, F. Shan, J. He, F. Wang, Synthesizing $BaTiO_3$ nanostructures to explore morphological influence, kinetics, and mechanism of piezocatalytic dye degradation, ACS Appl. Mater. Interfaces 12 (2020) 17443–17451, https://doi.org/10.1021/acsami.9b23351.

[52] C. Yu, M. Tan, Y. Li, C. Liu, R. Yin, H. Meng, Y. Su, L. Qiao, Y. Bai, Ultrahigh piezocatalytic capability in eco-friendly $BaTiO_3$ nanosheets promoted by 2D morphology engineering, J. Colloid Interface Sci. 596 (2021) 288–296, https://doi.org/10.1016/j.jcis.2021.03.040.

[53] X. Xu, Z. Wu, L. Xiao, Y. Jia, J. Ma, F. Wang, L. Wang, M. Wang, H. Huang, Strong piezo-electro-chemical effect of piezoelectric $BaTiO_3$ nanofibers for vibration-catalysis, J. Alloy. Compd. 762 (2018) 915–921, https://doi.org/10.1016/j.jallcom.2018.05.279.

[54] I. Tudela, Y. Zhang, M. Pal, I. Kerr, A.J. Cobley, Ultrasound-assisted electrodeposition of thin nickel-based composite coatings with lubricant particles, Surf. Coat. Technol. 276 (2015) 89–105, https://doi.org/10.1016/j.surfcoat.2015.06.030.

[55] M. Thommes, K. Kaneko, A.V. Neimark, J.P. Olivier, F. Rodriguez-Reinoso, J. Rouquerol, K.S.W. Sing, Physisorption of gases, with special reference to the evaluation of surface area and pore size distribution (IUPAC Technical Report), Pure Appl. Chem. 87 (2015) 1051–1069, https://doi.org/10.1515/pac-2014-1117.

[56] S. Brandani, Kinetics of liquid phase batch adsorption experiments, Adsorption 27 (2020) 353–368, https://doi.org/10.1007/s10450-020-00258-9.

[57] P.O. Gendron, F. Avaltroni, K.J. Wilkinson, Diffusion coefficients of several rhodamine derivatives as determined by pulsed field gradient-nuclear magnetic resonance and fluorescence correlation spectroscopy, J. Fluoresc. 18 (2008) 1093–1101, https://doi.org/10.1007/s10895-008-0357-7.

[58] Y. Iida, T. Kozuka, T. Tuziuti, K. Yasui, Sonochemically enhanced adsorption and degradation of methyl orange with activated aluminas, Ultrasonics 42 (2004) 635–639, https://doi.org/10.1016/j.ultras.2004.01.092.

[59] S. Nikolaou, J. Vakros, E. Diamadopoulos, D. Mantzavinos, Sonochemical degradation of propylparaben in the presence of agro-industrial biochar, J. Environ. Chem. Eng. 8 (2020) 104010, https://doi.org/10.1016/j.jece.2020.104010.

[60] T. Cheng, W. Gao, H. Gao, S. Wang, Z. Yi, X. Wang, H. Yang, Piezocatalytic degradation of methylene blue, tetrabromobisphenol A and tetracycline hydrochloride using $Bi_4Ti_3O_{12}$ with different morphologies, Mater. Res. Bull. 141 (2021) 111350, https://doi.org/10.1016/j.materresbull.2021.111350.

[61] W. Ma, B. Yao, W. Zhang, Y. He, Y. Yu, J. Niu, C. Wang, A novel multi-flaw MoS_2 nanosheet piezocatalyst with superhigh degradation efficiency for ciprofloxacin, Environ. Sci. Nano 5 (2018) 2876–2887, https://doi.org/10.1039/c8en00944a.

[62] S. Masimukku, Y.-C. Hu, Z.-H. Lin, S.-W. Chan, T.-M. Chou, J.M. Wu, High efficient degradation of dye molecules by PDMS embedded abundant single-layer tungsten disulfide and their antibacterial performance, Nano Energy 46 (2018) 338–346, https://doi.org/10.1016/j.nanoen.2018.02.008.

[63] S. Zhang, H. Yu, X. Zhu, X. Sang, Y. Li, J. Fu, Q. Li, Y. Zhang, W. Ye, Highly efficient piezocatalytic activity of poly(tetrafluoroethylene) for large-scale organic wastewater purification, ACS Appl. Polym. Mater. 5 (2023) 3585–3594, https://doi.org/10.1021/acsapm.3c00243.
[64] H. Jiao, J. Jin, K. Zhao, X.R. Zhou, X. Zhang, S. Song, J. Wang, Y. Tang, G. Cui, Synthesis and piezoelectric photocatalytic, mechanical, and electrical properties of porous t-$BaTiO_3$/Ag/β-PVDF composite material, J. Thermoplast. Compos. Mater. 36 (2023) 2031–2049, https://doi.org/10.1177/08927057221088466.
[65] Z. Kang, M. Chen, E. Lin, J. Wu, K. Ke, N. Qin, D. Bao, Functionalized MIL-53 and its derivatives modified Bi_2WO_6 as effective piezocatalysts and membranes for adsorption and decomposition of organic pollutants, Sep. Purif. Technol. 306 (2023) 122618, https://doi.org/10.1016/j.seppur.2022.122618.
[66] H. Kalhori, I.C. Amaechi, A.H. Youssef, A. Ruediger, A. Pignolet, Catalytic activity of $BaTiO_3$ nanoparticles for wastewater treatment: piezo- or sono-driven? ACS Appl. Nano Mater. 6 (2023) 1686–1695, https://doi.org/10.1021/acsanm.2c04568.
[67] H. Kalhori, A.H. Youssef, A. Ruediger, A. Pignolet, Competing contributions to the catalytic activity of barium titanate nanoparticles in the decomposition of organic pollutants, J. Environ. Chem. Eng. 10 (2022) 108571, https://doi.org/10.1016/j.jece.2022.108571.
[68] M. Breitbach, D. Bathen, Influence of ultrasound on adsorption processes, Ultrason. Sonochem. 8 (2001) 277–283, https://doi.org/10.1016/s1350-4177(01)00089-x.
[69] M. Breitbach, D. Bathen, H. Schmidt-Traub, Effect of ultrasound on adsorption and desorption processes, Ind. Eng. Chem. Res. 42 (2003) 5635–5646, https://doi.org/10.1021/ie030333f.
[70] M.H. Calimli, M.S. Nas, H. Burhan, S.D. Mustafov, Ö. Demirbas, F. Sen, Preparation, characterization and adsorption kinetics of methylene blue dye in reduced-graphene oxide supported nanoadsorbents, J. Mol. Liq. 309 (2020) 113171, https://doi.org/10.1016/j.molliq.2020.113171.
[71] M. Eloussaief, W. Hamza, N. Fakhfakh, A. Tlili, N. Kallel, S. Lambert, H. Zaitan, M. Benzina, Characterization of iron-modified natural clay for textile dye retention by sono-adsorption technology, Arab. J. Geosci. 15 (2022) 1109, https://doi.org/10.1007/s12517-022-10400-2.
[72] R. Foroutan, R. Mohammadi, B. Ramavandi, Elimination performance of methylene blue, methyl violet, and Nile blue from aqueous media using AC/$CoFe_2O_4$ as a recyclable magnetic composite, Environ. Sci. Pollut. Res. Int. 26 (2019) 19523–19539, https://doi.org/10.1007/s11356-019-05282-z.
[73] A. Gupta, H. Viltres, N.K. Gupta, Sono-adsorption of organic dyes onto $CoFe_2O_4$/Graphene oxide nanocomposite, Surf. Interfaces 20 (2020) 100563, https://doi.org/10.1016/j.surfin.2020.100563.
[74] W. Hamza, N. Dammak, H.B. Hadjltaief, M. Eloussaief, M. Benzina, Sono-assisted adsorption of Cristal Violet dye onto Tunisian Smectite Clay: characterization, kinetics and adsorption isotherms, Ecotoxicol. Environ. Saf. 163 (2018) 365–371, https://doi.org/10.1016/j.ecoenv.2018.07.021.
[75] A. Hassani, R. Darvishi Cheshmeh Soltani, M. Kıranşan, S. Karaca, C. Karaca, A. Khataee, Ultrasound-assisted adsorption of textile dyes using modified nanoclay: Central composite design optimization, Korean J. Chem. Eng. 33 (2015) 178–188, https://doi.org/10.1007/s11814-015-0106-y.
[76] A. Hayoune, H. Akkari, T. Mekhalif, F. Martin, Sono-assisted adsorption of methylene blue dye from aqueous medium using magnetic Algerian Halloysite clay (Fe_3O_4-HKDD3), Int. J. Environ. Anal. Chem. (2022) 1–15, https://doi.org/10.1080/03067319.2021.2020770.
[77] S. Jorfi, R. Darvishi Cheshmeh Soltani, M. Ahmadi, A. Khataee, M. Safari, Sono-assisted adsorption of a textile dye on milk vetch-derived charcoal supported by silica nanopowder, J. Environ. Manage. 187 (2017) 111–121, https://doi.org/10.1016/j.jenvman.2016.11.042.
[78] V. Kumar, P. Saharan, A.K. Sharma, A. Umar, I. Kaushal, A. Mittal, Y. Al-Hadeethi, B. Rashad, Silver doped manganese oxide-carbon nanotube nanocomposite for enhanced dye-sequestration: Isotherm studies and RSM modelling approach, Ceram. Int. 46 (2020) 10309–10319, https://doi.org/10.1016/j.ceramint.2020.01.025.
[79] X. Zhou, Q. Sun, Z. Xiao, H. Luo, D. Zhang, Three-dimensional BNT/PVDF composite foam with a hierarchical pore structure for efficient piezo-photocatalysis, J. Environ. Chem. Eng. 10 (2022) 108399, https://doi.org/10.1016/j.jece.2022.108399.
[80] T.D. Raju, S. Veeralingam, S. Badhulika, Polyvinylidene fluoride/$ZnSnO_3$ nanocube/Co_3O_4 nanoparticle thermoplastic composites for ultrasound-assisted piezo-catalytic dye degradation, ACS Appl. Nano Mater. 3 (2020) 4777–4787, https://doi.org/10.1021/acsanm.0c00771.
[81] B. Bagchi, N.A. Hoque, N. Janowicz, S. Das, M.K. Tiwari, Re-usable self-poled piezoelectric/piezocatalytic films with exceptional energy harvesting and water remediation capability, Nano Energy 78 (2020), 105339, https://doi.org/10.1016/j.nanoen.2020.105339.
[82] D. Mondal, S. Bardhan, N. Das, J. Roy, S. Ghosh, A. Maity, S. Roy, R. Basu, S. Das, Natural clay-based reusable piezo-responsive membrane for water droplet mediated energy harvesting, degradation of organic dye and pathogenic bacteria, Nano Energy 104 Part, B (2022) 107893, https://doi.org/10.1016/j.nanoen.2022.107893.

6 Overall conclusions and future work

6.1 Overall conclusions and thesis contributions

In conclusion, this PhD study provided valuable insights into the complex phenomenon of piezocatalysis and its interactions with other ultrasound-assisted phenomena. The results obtained in this PhD thesis indicated that piezocatalysis does indeed exist, although its effects on the overall degradation process are likely to depend on the reactor size used, as well as its operation in terms of frequency and power. In some instances, piezocatalytic effects observed in this study employing larger-scale reactors appeared to be negligible compared to the dominant role of sonochemical effects in the overall degradation process. These findings challenge the promising results reported in the literature using smaller-scale reactors and highlight the inherent difficulties in scaling up ultrasound-assisted processes.

The study also investigated the underlying mechanisms of piezocatalysis and found that the previously assumed bulk piezoelectric mechanism is unlikely to occur. Instead, the evidence found in this thesis indicates that a localised piezoelectric response is more likely to contribute to the piezocatalytic process. Additionally, it was observed that other ultrasound-assisted phenomena occur simultaneously and contribute to the overall degradation process. Therefore, it is essential to consider and optimise these concurrent phenomena such as sonochemistry, sonocataysis and sono-adsorption in piezocatalytic research.

The present PhD thesis also revealed that ultrasonic frequency and power have an effect on the piezocatalytic process, but not as initially assumed. Lower ultrasonic frequencies combined with moderate ultrasonic powers were found to enhance piezocatalytic contributions, where mechanical effects are strong enough to induce local piezoelectric responses without hindering each other. On the other hand, higher frequencies were found to favour the sonochemical degradation, which aligns with previous research in the field of sonochemistry. Based on these findings, it can be assumed that the piezocatalytic process

relies on strong mechanical effects, in particularly cavitation bubble collapse. The likely dependency on cavitation bubble collapse could limit the potential of piezocatalysis for future industrial applications, due to the limited number of commercial applications that could fully utilise those cavitation effects. Moreover, the high energy consumption required for these strong cavitation effects could also raise further questions about the practicality, economic viability and effectiveness of piezocatalysis in future industrial applications.

Therefore, another potential mechanism that could explain the piezocatalytic phenomenon was investigated. Based on reports in the literature, the energy band theory was identified as another potential mechanism explaining the piezocatalytic process. Contrary to the initial assumption in the literature, that only one of the proposed mechanisms can be at play [1], the preliminary study conducted in Chapter 4 found that both mechanisms, screening charge effects (i.e. localised piezoelectric response) and energy band theory, are likely to contribute simultaneously to the generation of radicals involved in the piezocatalytic process. Therefore, it is believed to be advantageous to develop piezocatalysts that can generate radicals via both mechanisms in order to optimise their piezocatalytic performance. Although the generation of radicals was enhanced with a piezocatalyst benefiting from both mechanisms, the overall piezocatalytic contributions still remained smaller compared to the dominant sonochemical effects in a larger-scale reactor. Nevertheless, these findings contributed to further understanding and optimising the piezocatalytic phenomenon.

The last part of this PhD thesis, tried to develop a piezocatalyst that incorporates the beneficial characteristics of generating radicals from two potential mechanism, while also trying to reduce a potential secondary pollution from micro- and nano-particles. The utilisation of bulkier PVDF-based piezocatalysts revealed another concurrent ultrasound-assisted phenomenon, known as ultrasound-enhanced adsorption. The results presented in Chapter 5 revealed interesting synergistic effects between ultrasound and adsorption that could benefit the sonochemical and piezocatalytic removal of dyes. These findings shed light on the potential of harnessing multiple ultrasound-assisted phenomena simultaneously, rather than focusing solely on a

single phenomenon. This could pave the way for a more effective and sustainable removal of dyes.

In summary, this PhD research has provided valuable insights in the complexity of piezocatalysis and other concurrent ultrasound-assisted phenomena. While piezocatalysis may indeed exist, its significance is lower in larger-scale reactors compared to sonochemical effects, which highlights the need to carefully consider control experiments to distinguish between concurrent phenomena. The findings not only highlight challenges in scaling up ultrasound-assisted processes and emphasise to consider both potential piezocatalytic mechanisms in the design and optimisation of piezocatalysts, but also suggest to take advantage of the synergistic effects of concurrent phenomena. Without considering and overcoming the limitations of the piezocatalytic process highlighted in this PhD project there will not be any meaningful future application of this technology.

To sum up, the future of piezocatalysis holds both challenges and opportunities as highlighted by the contributions of this PhD project. The critical insights gained from this research revealed the complexity of scaling up piezocatalysis to larger-scale reactors. To unlock the full potential of piezocatalysis future development must focus enhancing piezocatalytic efficiency in larger-scale reactors, improving energy efficiency as well as combining piezocatalysis with other technologies. Piezocatalysis may find its place in combined treatment processes, working in synergy with other established methods to create more efficient and sustainable wastewater treatment process.

6.2 Future work

To fully comprehend the piezocatalytic phenomenon and further enhance its potential as an industrial relevant process, future research should focus on larger-scale investigations. These studies would help gaining a more comprehensive understanding of the piezocatalytic process

under real-world conditions. The objective should be to overcome the limitations of piezocatalysis in larger scale-reactors as highlighted throughout this thesis. In this regard it is essential to identify operating conditions where the piezocatalytic effect is amplified to outperform concurrent sonochemical effects and thereby establishing piezocatalysis as an efficient technology.

Besides this, future research should also focus on trying to make piezocatalysis more energy-efficient. Efforts should be directed towards reducing the high energy consumption associated with moderate ultrasonic powers. In this regard, it would be worth exploring pulses in piezocatalytic processes. By employing pulses in sonochemistry it was already possible to significantly decrease energy consumption while maintaining a consistent acoustic performance [2, 3]. This approach could therefore also offer promising opportunities to optimise the energy efficiency of piezocatalytic systems and thereby contributing to the development of more sustainable and cost-effective green technology.

Researchers should also explore alternative methods to induce equivalent mechanical forces required for piezocatalytic reactions. Additionally, it is important to identify industrial processes or systems where such mechanical forces can be harnessed for piezocatalysis. By leveraging these industrial systems, the energy consumption of piezocatalytic processes can be significantly reduced and consequentially making piezocatalysis more economically viable and environmentally sustainable.

Furthermore, research should shift away from radical-dependent degradation processes and explore more traditional electrochemical-induced reactions. This shift would enable researchers to showcase the true potential of piezocatalysis as a distinct and innovative green technology. By investigating electrochemical-induced reactions it would be possible to explore new pathways and mechanisms for organic pollutant degradation and thereby revealing further opportunities for piezocatalysis. An example to investigate the potential of piezocatalysis of non-radicallary dependant processes could be the degradation of trichloroacetic acid, which is known to be hardly degraded by sonochemistry [4, 5]. Such investigations would also provide

direct evidence of the advantages piezocatalysis could offer over traditional sonochemical techniques.

Building upon the findings in chapter 5, future research should also delve into the area of sono-adsorption to investigate its potential for organic pollutant removal. Further research is needed to fully understand the synergic effects of ultrasound and adsorption processes and how this can benefit environmental remediation. The effects of high-frequency and high-power ultrasound should be explored as the formation of small-sized cavitation bubbles may lead to significantly enhanced pollutant removal efficiencies.

In light of the promising results from preliminary desorption experiments conducted in Chapter 5, which demonstrated the effective desorption of RhB from $_{AM}$PVDF, a logical avenue for future work lies in the exploration of the cyclic adsorption capabilities of this adsorbent material. The cyclic adsorption process has the potential to significantly enhance the overall adsorption capacity of $_{AM}$PVDF for RhB at even higher initial concentrations. This would make ultrasound-assisted dye adsorption a more efficient and sustainable method for dye removal. This research direction would not only further extend the understanding of $_{AM}$PVDF performance in adsorption-desorption cycles but also holds promise for practical applications, particularly in larger scale and potentially industrial wastewater treatment and environmental remediation. Further investigations into the optimisation of cyclic adsorption parameters and the reusability of the adsorbent will be invaluable in advancing this area of study.

6.3 References

[1] K. Wang, C. Han, J. Li, J. Qiu, J. Sunarso, S. Liu
The Mechanism of Piezocatalysis: Energy Band Theory or Screening Charge Effect?
Angew Chem Int Ed Engl, 61 (6) (2022), e202110429, 10.1002/anie.202110429

[2] J. Lee, K. Yasui, T. Tuziuti, T. Kozuka, A. Towata, Y. Iida

Spatial distribution enhancement of sonoluminescence activity by altering sonication and solution conditions

J Phys Chem B, 112 (48) (2008), 15333-41, 10.1021/jp8060224

[3] G.J. Price, M. Ashokkumar, F. Grieser

Sonoluminescence quenching of organic compounds in aqueous solution: frequency effects and implications for sonochemistry

J Am Chem Soc, 126 (9) (2004), 2755-62, 10.1021/ja0389624

[4] M.D. Esclapez, V. Saez, D. Milan-Yanez, I. Tudela, O. Louisnard, J. Gonzalez-Garcia

Sonoelectrochemical treatment of water polluted with trichloroacetic acid: from sonovoltammetry to pre-pilot plant scale

Ultrason Sonochem, 17 (6) (2010), 1010-20, 10.1016/j.ultsonch.2009.11.009

[5] M.D. Esclapez, I. Tudela, M.I. Díez-García, V. Sáez, P. Bonete

Towards the complete dechlorination of chloroacetic acids in water by sonoelectrochemical methods: Effect of the cathode material on the degradation of trichloroacetic acid and its degradation by-products

Applied Catalysis B: Environmental, 166-167 (2015), 66-74, 10.1016/j.apcatb.2014.10.061

Appendix

Chapter 2 Supplementary Material

Attached is the supplementary material of Chapter 2 that was previously published in *Chemical Engineering Journal Advances* as part of *Piezocatalytic degradation of pollutants in water: Importance of catalyst size, poling and excitation mode* by F. Bößl, T. P. Comyn, P. I. Cowin, F. R. García-García and I. Tudela.

Piezocatalytic degradation of pollutants in water: importance of catalyst size, poling and excitation mode

Authors: Franziska Bößl[a,b,*], Tim P. Comyn[c], Peter Cowin[c], Francisco R. García-García[b], Ignacio Tudela[a,b,**]

[a] Edinburgh Electrochemical Engineering Group (e^3 Group), The University of Edinburgh, Edinburgh EH9 3FB, UK
[b] Institute for Materials and Processes, School of Engineering, The University of Edinburgh, Edinburgh EH9 3FB, UK
[c] Ionix Advanced Technologies Ltd., 3M Buckley Innovation Centre, Firth Street, Huddersfield HD1 3BD, UK

Corresponding authors.
E-mail addresses: , *

Supplementary Material

1. FEM Model

Fig. S1 depicts the liquid and solid domains defined for all FEM simulations, as well as the different boundary conditions. The main difference in all the different simulations presented in this study is the particle size, which was modified appropriately to reflect the different particle sizes used in the experiments. The frequency in the simulations was 35 kHz to replicate the conditions of the experiments conducted in the ultrasonic bath. The liquid domain was defined as water, while the piezocatalysts were defined as poled BF-KBT-PT. A realistic acoustic pressure source of 2 bar [1-3] in the liquid was defined to reflect the nature of the ultrasonic field 'exciting' the piezocatalyst.

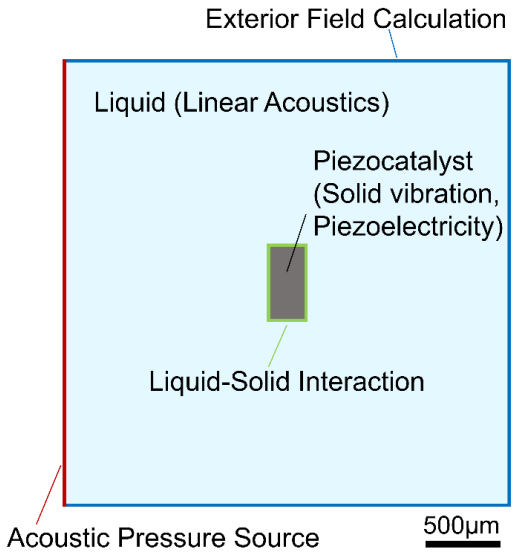

Figure S1. Schematic representing liquid and solid domains and boundary conditions in the present FEM model.

1.1. Linear acoustics in the liquid

The propagation of an acoustic linear wave in the liquid with no attenuation can be described by the Helmholtz equation:

$$\nabla^2 p_t + \left(\frac{\omega}{c_l}\right)^2 p_t = 0 \quad (1)$$

where p_t is the acoustic pressure, ω the angular frequency and c_l the speed of sound in the liquid.

1.2. Boundary acoustic conditions of the liquid

A constant acoustic pressure $\boldsymbol{p_0}$ is specified in the liquid boundary defined as the source of acoustic pressure to establish the acoustic field:

$$p_t = p_0 \quad (2)$$

where p_0 is the amplitude of a harmonic pressure source.

For the remaining liquid boundaries, a condition of 'exterior field calculation' using the Kirchhoff-Helmholtz Integral Equation [4] was defined to reflect the *continuity* of the acoustic field beyond the liquid domain and ensure the wave is propagated beyond those same boundaries [5]

1.3. Vibration of the solid

The vibrations of the piezocatalyst were calculated using elasto-dynamic theory by assuming elastic deformation where volume forces were neglected and a mono-harmonic vibration was assumed:

$$\nabla \cdot \bar{\bar{\Sigma}} = -\rho_s \omega^2 U_s \quad (3)$$

where U_s is the complex displacement field in the solid, $\bar{\bar{\Sigma}}$ the elastic stress tensor and ρ_s the density of the solid.

1.4. Piezoelectric response of the solid

The piezoelectric characteristics of the piezocatalyst were accounted for by relating its stress with the electric displacement and electric field. This piezoelectric effect can be described by the following stress-charge relations:

$$\bar{\bar{\Sigma}} = c_E \bar{\bar{\xi}} - e^T \boldsymbol{E} \quad (4)$$

$$\boldsymbol{D} = \boldsymbol{e}\bar{\bar{\Sigma}} + \epsilon_0 \, \epsilon_{rS} \boldsymbol{E} \quad (5)$$

where $\bar{\bar{\xi}}$ is the strain tensor, $\boldsymbol{E}$ the electric field, $\boldsymbol{D}$ the electric displacement, ϵ_0 electrical permittivity of free space and c_E, $\boldsymbol{e}$ and ϵ_{rS} are the piezoelectric elasticity matrix, coupling

matrix and relative permittivity, respectively.

The electrostatics of the piezocatalyst was defined by the following equations:

$$\nabla \cdot \boldsymbol{D} = \rho_V \quad (6)$$

$$\boldsymbol{E} = -\nabla \mathrm{V} \quad (7)$$

where $\nabla \cdot \boldsymbol{D}$ is the electric charge density, ρ_V the electric charge concentration and E the electric field due to the electric potential V.

1.5. Liquid- solid interaction boundary

The stress exerted on the solid was defined as the normal pressure stress exerted by the liquid:

$$\bar{\bar{\Sigma}} \cdot \boldsymbol{n} = -p_t \cdot \boldsymbol{n} \quad (8)$$

where p_t is the acoustic pressure field in the liquid calculated on the interface and $\boldsymbol{n}$ the normal pointing outwards of the liquid.

1.6. Solid domain properties

The schematic below (Fig. S2) describes the piezoelectric and mechanical characteristics of the solid domain (i.e. piezocatalyst) in the FEM simulations, as well as the sources of the values for the properties.

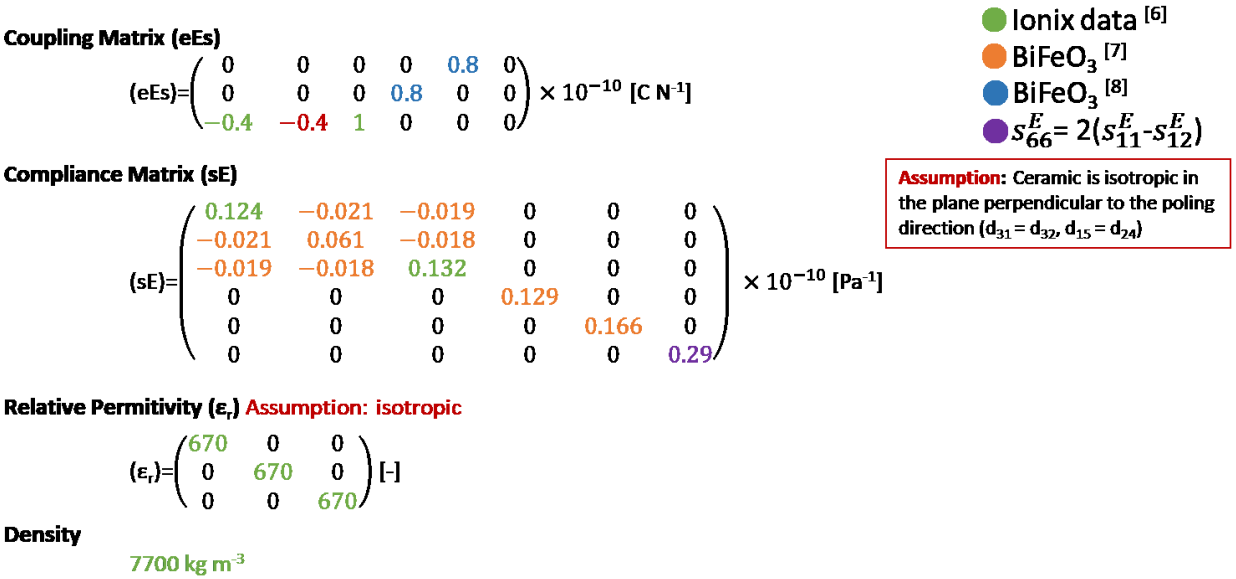

Figure S2. Schematic describing the piezoelecto-mechanical properties of the solid domain in the present FEM model.

2. Porosity and adsorption characterisation of piezocatalysts

Nitrogen adsorption isotherms were conducted on the different poled piezocatalysts (P63, P125, P250 and P500) in a Quantachrome Autosorb-iQ to confirm their non-porous, non-adsorbent nature. This was confirmed by the results obtained, which indicated that type VI isotherm with step-wise multilayer adsorption on a uniform and non-porous surface was occurring (Fig. S3).

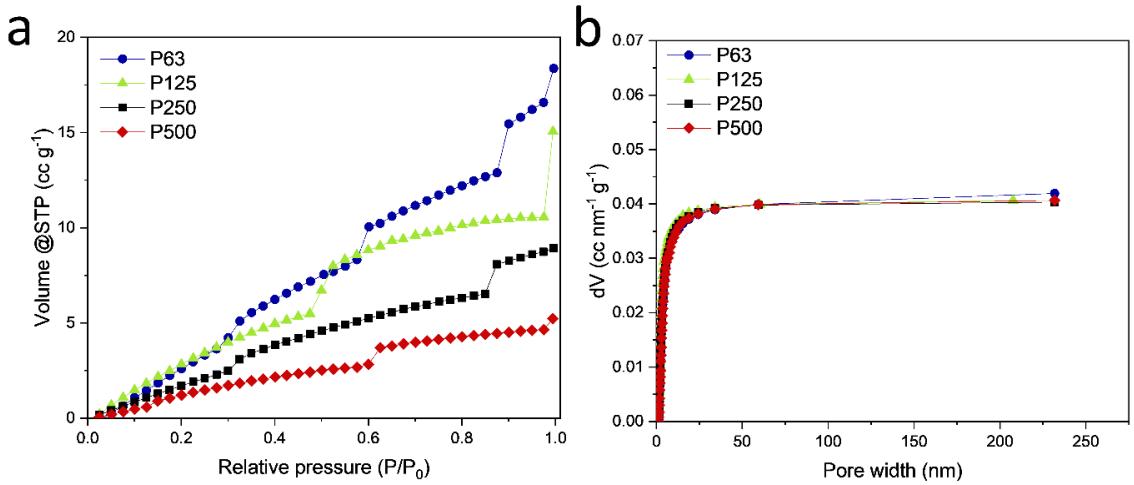

Figure S3. Nitrogen adsorption isotherm analysis on different piezocatalysts used in this study: a) BET adsorption isotherms, b) DFT pore size distribution.

3. Experimental set-up

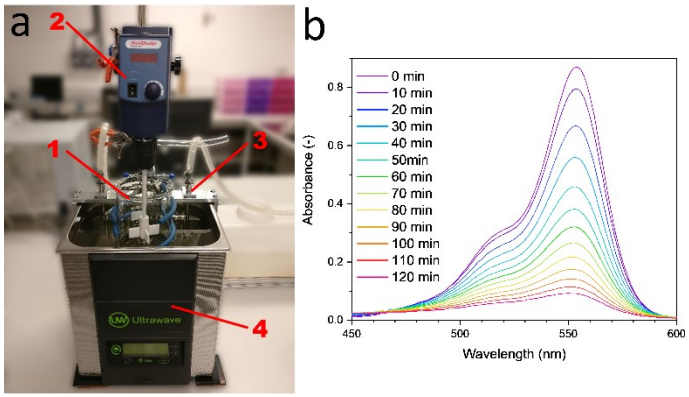

Figure S4. a) Experimental set-up used in the present study: (1) reactor (1000 mL beaker), (2) overhead stirrer (when required), (3) coil part of circulating water cooling system, and (4) ultrasonic bath. b) UV–vis absorption spectra of RhB aqueous solution at set intervals.

References:

[1] K. Yasui, Influence of ultrasonic frequency on multibubble sonoluminescence, J. Acoust. Soc. Am. 112 (2002) 1405–1413. https://doi.org/10.1121/1.1502898.

[2] R. Chow, R. Mettin, B. Lindinger, T. Kurz, W. Lauterborn, The importance of acoustic cavitation in the sonocrystallisation of ice - high speed observations of a single acoustic bubble, IEEE Symposium on Ultrasonics 2003, Honolulu, HI, USA, 2003, pp. 1447–1450. https://doi.org/10.1109/ULTSYM.2003.1293177.

[3] D.J. Flannigan, K.S. Suslick, Plasma line emission during single-bubble cavitation, Phys. Rev. Lett. 95 (2005) 44301. https://doi.org/10.1103/PhysRevLett.95.044301.

[4] S. Ise, A principle of sound field control based on the kirchhoff-helmholtz integral equation and the theory of inverse systems, Acta Acust. united Ac. 85 (1999) 78–87.

[5] D. Stephens, C.J. Miller, P.E. Slaboch, J. Brown, J.M. Celestina, Supersonic Engine Inlet Tone Noise Radiation, AIAA 2019-2493, 25th AIAA/CEAS Aeroacoustics Conference, Delft, The Netherlands, 2019. https://doi.org/10.2514/6.2019-2493.

[6] Ionix Data Sheet, https://ionixadvancedtechnologies.co.uk/

[7] M. de Jong, W. Chen, H. Geerlings, M. Asta, K. A. Persson. A database to enable discovery and design of piezoelectric properties. Scientific Data 2 (2015) 50053. https://doi.org/10.1038/sdata.2015.53

[8] Jin, Y., Lu, X., Zhang, J. et al. Studying the Polarization Switching in Polycrystalline $BiFeO_3$ Films by 2D Piezoresponse Force Microscopy. Sci Rep 5, 12237 (2015). https://doi.org/10.1038/srep12237